COMPLETENESS AND DIVERSITY PATTERNS OF PALAEOZOIC CHONDRICHTHYANS

by

LISA SCHNETZ

A thesis submitted to the University of Birmingham for the degree of

DOCTOR OF PHILOSOPHY

Department of Earth Sciences

School of Geography, Earth and Environmental Sciences

College of Life and Environmental Sciences

University of Birmingham

June 2022

UNIVERSITY OF
BIRMINGHAM

University of Birmingham Research Archive

e-theses repository

This unpublished thesis/dissertation is copyright of the author and/or third parties. The intellectual property rights of the author or third parties in respect of this work are as defined by The Copyright Designs and Patents Act 1988 or as modified by any successor legislation.

Any use made of information contained in this thesis/dissertation must be in accordance with that legislation and must be properly acknowledged. Further distribution or reproduction in any format is prohibited without the permission of the copyright holder.

Abstract

Chondrichthyans, the cartilaginous fishes, are a highly successful clade of vertebrates that have occupied the aquatic realm for over 450 million years. Of these, the Palaeozoic represents a key time interval in terms of their origin and early diversification, yet much of their early macroevolutionary patterns remains unresolved because of the limitations of their fossil record. Their early fossil record is poor because their mostly cartilaginous skeletons are rarely well preserved and this, in turn, has restricted the data available for estimates of their evolutionary history. In this thesis, multiple statistical methods for quantifying the skeletal completeness and estimating diversity trends are combined to critically assess the quality of the Palaeozoic chondrichthyan fossil record. A novel metric is presented to quantify levels of soft tissue preservation next to skeletal completeness in the stem-chondrichthyan acanthodians which are known to preserve notoriously little skeletal features. The results identify a complex array of natural and human-driven biases that greatly influences our understanding of the Palaeozoic chondrichthyan fossil record. Variation in completeness impacts on the utility of characters for assessing phylogenetic relationships of the various chondrichthyan groups, specifically the stem-chondrichthyan lineages. An extensive assessment of early chondrichthyan diversity patterns give greater insight on their environmental and biological drivers but also highlight the impact sampling biases may have on them. Together, the quantified macroevolutionary patterns of completeness and diversity draw a more comprehensive picture of the evolutionary history and nature of the early chondrichthyan fossil record.

Acknowledgements

This thesis is the result of almost four years of work and none of it would have been possible without the continuous help and support of so many wonderful and kind people. First and foremost, my sincerest thanks go to my main supervisor Ivan Sansom. I am so extremely grateful to have been given the opportunity to work on this PhD project with him and to have received constant faith, support and guidance throughout (and the chance to somewhat annoy him with door knocks on a regular basis). I am also incredibly grateful to my second supervisor Richard Butler and my external supervisor Mike Coates for their efforts and commitment to my work and to Mike for some of the most helpful as well as entertaining comments and observations I have ever received on a manuscript.

However, I am most grateful to my wonderful colleagues at the Earth Sciences department at the University of Birmingham who have really made this experience an unforgettable one. Procrastination would have never been so sweet without the commitment of my fellow PhD students Alastair, Bridget, Emma, Gemma, Hazel, Iacopo, Jake, JP, Kerys, Luke, Marie and Matt. I am also very grateful to former Birmingham PhD students Andy, Dan, Davey and Kate and former Birmingham postdocs Terry, Gemma and Chris for their support in the first two years of my PhD. I would like to thank the milk fund and its presidents Luke and JP for their dedication to providing us with the best coffee on Fridays. Special thanks go to my PhD cohort buddies Luke Meade, Nicola Kirby and Struan Henderson with whom I shared some interesting workshops and fun conference visits. I am so thankful to Dan Cashmore and Emma Dunne

for helping and sharing their knowledge and resources with me, especially in terms of coding, and Richard Dearden for his enthusiasm on chondrichthyans, and I have learned so much from them.

I would also like to thank my friends back home in Austria for their support through the years, even though we were for the most part over thousand kilometres apart. Special thanks go to Iris Feichtinger whose joint passion for chondrichthyans has allowed for countless conversations and ideas.

Finally, none of this would have been possible without the unconditional love and support of my family, especially my parents Ulrike and Markus and my sister Hanna, and I am deeply thankful for it.

TABLE OF CONTENTS

1 INTRODUCTION **1**

1.1 A tale of chondrichthyans 2

1.2 Palaeozoic chondrichthyan groups 7

1.3 What is a chondrichthyan? 9

1.4 Objectives 11

2 SKELETAL AND SOFT TISSUE COMPLETENESS OF THE ACANTHODIAN FOSSIL RECORD **13**

2.1 Introduction 13

2.2 Methods 17

2.2.1 Dataset 17

2.2.2 Completeness metrics 18

2.2.3 Acanthodian completeness data 23

2.2.4 Statistical analyses 27

2.3 Results 28

2.3.1 Changes in acanthodian completeness through time 28

2.3.2 Correlations with taxonomic richness 33

2.3.3 Differences between skeletal and soft tissue completeness metrics 33

2.3.4 Acanthodian subgroups 35

2.3.5 Comparison to other vertebrate groups 37

2.3.6 Geographic comparisons 39

2.3.7 Depositional and environmental comparisons 41

2.3.8 Sea level correlations 45

2.4 Discussion 46

2.4.1 Completeness metrics comparisons 47
2.4.2 Taxonomic group comparisons 49
2.4.3 Vertebrate group comparisons 50
2.4.4 Geographical impacts 51
2.4.5 Environmental and ecological biases 53
2.4.6 Impact on phylogenetic assessments 58
2.5 Conclusions 60

3 THE COMPLETENESS OF THE PALAEOZOIC CHONDRICHTHYAN FOSSIL RECORD 62

3.1 Introduction 62
3.2 Methods 66
3.2.1 Completeness metrics 66
3.2.2 Chondrichthyan completeness data 69
3.2.3 Statistical analyses 73
3.3 Results 74
3.3.1 Chondrichthyan completeness through time 74
3.3.2 Correlations with taxonomic richness 77
3.3.3 Taxonomic groups 78
3.3.4 Comparisons with the completeness of other vertebrate groups 78
3.3.5 Acanthodian versus non-acanthodian chondrichthyan completeness 80
3.3.6 Geographical completeness 81
3.3.7 Sea level correlations 82
3.3.8 Depositional and environmental variation 83
3.4 Discussion 88
3.4.1 Comparisons with other vertebrate groups 90
3.4.2 Completeness variation between chondrichthyan orders 91
3.4.3 Geographical controls on chondrichthyan completeness 92
3.4.4 Palaeoenvironmental and Palaeoecological biases 94
3.5 Conclusions 97

4 PATTERNS OF CHONDRICHTHYAN DIVERSITY DURING THE PALAEOZOIC 98

4.1 Introduction 98

4.2 Methods 101

4.2.1 Dataset 101

4.2.2 Subsets and explanation of phylogenetic concepts used 102

4.2.3 Sampling and Diversity 104

4.3 Results 105

4.4 Discussion 116

4.4.1 Patterns of Palaeozoic chondrichthyan diversity 116

4.4.2 Environmental influences and the impact of biases on Palaeozoic chondrichthyan diversity 121

4.4.3 Comparisons with invertebrate diversity trends 123

4.5 Conclusions 124

5 SUMMARY AND PERSPECTIVES 126

5.1 Future work and directions 128

REFERENCES 130

APPENDICES 169

A SKELETAL AND SOFT TISSUE COMPLETENESS OF THE ACANTHODIAN FOSSIL RECORD 169

A.1 Justification for the acanthodian body exemplars 169

A.2 Scoring acanthodian completeness 172

A.3 Figures and tables 174

B THE COMPLETENESS OF THE PALAEOZOIC CHONDRICHTHYAN FOSSIL RECORD 196

B.1 Characteristics of the different chondrichthyan body exemplars 196

B.2 Chondrichthyan completeness scores 199

B.3 Figures and tables 201

C PATTERNS OF CHONDRICHTHYAN DIVERSITY DURING THE

PALAEOZOIC **217**

C.1 Figures and tables 218

LIST OF FIGURES

1.1 Simplified timeline of early chondrichthyan history, including acanthodian and non-acanthodian discoveries. 4

1.2 Strict consensus tree showing the phylogenetic affiliations of early chondrichthyans from Frey *et al.* 2020. 6

2.1 Skeletal (A) and soft tissue (B) reconstruction of *Acanthodes* 21

2.2 Changes in acanthodian completeness and raw taxonomic richness through time. 30

2.3 Relative percentage distributions of the different body regions used in the dataset. 35

2.4 Distribution of completeness between different acanthodian subgroups. 36

2.5 Distribution of acanthodian SCM2 values compared to other vertebrate groups. 38

2.6 Distribution of acanthodian SCM2 and STCM2 scores between the northern and southern hemispheres. 39

2.7 Distribution of acanthodian completeness between different continents. 41

2.8 Changes in acanthodian completeness through time based on freshwater versus marine occurrences together with sea level changes. 42

2.9 Changes in acanthodian completeness through time based on Benthic Assemblage (BA) zones. 45

3.1 Chondrichthyan skeletal proportions 67

3.2 Changes in Palaeozoic chondrichthyan completeness and raw taxonomic richness through time. 75

3.3 Distribution of original chondrichthyan SCM2 values compared to the subsets. 77

3.4 Comparisons of chondrichthyan SCM2 values with other vertebrate groups 79
3.5 Geographical distribution of chondrichthyan SCM2 81
3.6 Chondrichthyan completeness through time based on freshwater versus marine occurrences plotted against sea level changes. 83
3.7 Changes in chondrichthyan completeness through time based on Benthic Assemblage (BA) zones. 85

4.1 Chondrichthyan raw genus richness, local richness and sampling proxies in the Palaeozoic. 106
4.2 Chondrichthyan subsampled genus diversity and origination/extinction rates in the Palaeozoic. 108
4.3 Coverage-based rarefaction curves for all investigated intervals of the Palaeozoic. 109
4.4 Squares diversity for acanthodian and non-acanthodian chondrichthyans through the Palaeozoic. 111
4.5 Subsampled and raw richness estimates of chondrichthyan subgroups . 112
4.6 Subsampled and raw richness estimates of Chondrichthyan subclasses based on systematics 113
4.7 Local richness (alpha diversity) from the Ordovician to the Permian divided into freshwater and marine occurrences. 114
4.8 Local richness (alpha diversity) divided into benthic assemblage zones (BA) from the Ordovician to the Permian. 115
4.9 Comparisons of chondrichthyan diversity curves in the Devonian and Carboniferous. 117
4.10 Simplified timeline of major events shaping chondrichthyan diversity. . . 125

A.1 Illustrations of the acanthodian taxa used for the acanthodian body exemplars. 174
A.2 Changes in median acanthodian SCM2 and STCM2 through time. . . . 175
A.3 Distribution of acanthodian SCM1/SCM2 values compared to STCM1/ STCM2 values. 180
A.4 Distribution of completeness between different acanthodian subgroups. 182
A.5 Distribution of acanthodian completeness values compared to other vertebrate groups. 187

A.6 Distribution of acanthodian SCM2 and STCM2 between freshwater and marine deposits. 191
A.7 Distribution of acanthodian completeness between the different Benthic Assemblage (BA) zones. 194

B.1 Changes in median chondrichthyan skeletal completeness through time. 201
B.2 Distribution of chondrichthyan SCM2 between the different subgroups. . 204
B.3 Distribution of subset chondrichthyan SCM2 values compared to other vertebrate groups. 211
B.4 Distribution of chondrichthyan SCM2 and STCM2 between freshwater and marine deposits. 215
B.5 Distribution of chondrichthyan skeletal completeness between the different Benthic Assemblage (BA) zones. 216

C.1 Relative genus abundance of chondrichthyans for each stage of the Palaeozoic. 218
C.2 Chondrichthyan local richness (alpha diversity) in the Palaeozoic after removing the three highest collections. 219
C.3 Chondrichthyan subsampled genus diversity with Holocephali/ Euchondrocephali excluded. 221

LIST OF TABLES

2.1 Results of pairwise comparisons between BA and total acanthodian SCM2 using GLS. 43

2.2 Results of pairwise comparisons between BA and total acanthodian STCM2 using GLS. 44

2.3 Results of pairwise comparisons for sea level trends in different time series using GLS excluding the Permian outliers. 46

3.1 Results of pairwise comparisons for sea level trends with chondrichthyan completeness using GLS. 83

3.2 Results of pairwise comparisons between BA and total chondrichthyan SCM2 using GLS. 84

3.3 Mann-Whitney-Wilcoxon test results of comparisons of the distribution and median SCM2 values of chondrichthyans from different environments 87

4.1 Results of GLS pairwise comparisons of different diversity estimates. . . 111

A.1 Results of comparisons of the distribution and median of acanthodian total SCM2/STCM2 with the three subsets. 176

A.2 Results of model-fitting analyses testing the best explanations of observed acanthodian SCM2. 177

A.3 Results of model-fitting analyses testing the best explanations of observed acanthodian STCM2. 178

A.4 Results of model-fitting analyses testing the best explanations of observed acanthodian taxonomic richness. 179

A.5 Results of comparisons of the distribution and median of different acanthodian completeness metrics. 180

A.6 Results of comparisons of the distribution and median SCM2 values of different acanthodian subgroups. 181
A.7 Results of comparisons of SCM2 values of a subset of different acanthodian subgroups without isolated fin spine-based taxa. 183
A.8 Results of comparisons of the distribution and median SCM2 values of a subset of different acanthodian subgroups without isolated scale and fin spine-based taxa. 183
A.9 Results of comparisons of the distribution and median SCM2 values of a subset of different acanthodian subgroups without isolated scale-based taxa. 184
A.10 Results of comparisons of STCM2 values of different acanthodian subgroups. 184
A.11 Results of comparisons of STCM2 values of a subset of different acanthodian subgroups without isolated scale and fin spine-based taxa. . . . 185
A.12 Results of comparisons of STCM2 values of a subset of different acanthodian subgroups without isolated scale-based taxa. 185
A.13 Results of comparisons of STCM2 values of a subset of different acanthodian subgroups without isolated fin spine-based taxa. 186
A.14 Results of comparisons of acanthodian SCM2 values in comparison to other vertebrate groups. 186
A.15 Results of the comparisons of acanthodian STCM2 values in comparison to other vertebrate groups. 188
A.16 Results of the comparisons of SCM2 values of the acanthodian subset without isolated fin spine and scale-based taxa in comparison to other vertebrate groups. 188
A.17 Results of comparisons of the distribution of acanthodian SCM2 values between continents. 189
A.18 Results of comparisons of the distribution of acanthodian STCM2 values for different continents. 190
A.19 Results of comparisons of the distribution of SCM2 and STCM2 values for freshwater versus marine acanthodians. 191
A.20 Results of comparisons of the distribution of acanthodian SCM2 values from different environments. 192

A.21 Results of comparisons of the distribution of acanthodian STCM2 values from different environments. 193

A.22 Results of pairwise comparisons for sea level trends in different time series using GLS. 195

B.1 Results of comparisons of the distribution and median of original chondrichthyan SCM2 with the two subsets and a dataset combining acanthodian and chondrichthyan SCM2 values. 201

B.2 Results of pairwise comparisons for completeness metric trends (original SCM2 and subsets) using GLS. 202

B.3 Results of model-fitting analyses testing the best explanations of observed chondrichthyan SCM2. 202

B.4 Results of model-fitting analyses testing the best explanations of observed chondrichthyan taxonomic richness. 203

B.5 Results of comparisons of the distribution and median SCM2 values of different chondrichthyan subgroups. 205

B.6 Results of comparisons of chondrichthyan SCM2 values in comparison to other vertebrate groups. 210

B.7 Results of the comparisons of SCM2 values of the chondrichthyan subset without isolated tooth-based taxa in comparison to other vertebrate groups. 212

B.8 Results of the comparisons of SCM2 values of the chondrichthyan subset without isolated tooth, fin spine and scale-based taxa in comparison to other vertebrate groups. 212

B.9 Results of the comparisons of SCM2 values of total chondrichthyan SCM2 values (combined with the acanthodian SCM2 values) in comparison to other vertebrate groups. 213

B.10 Results of comparisons of the distribution of chondrichthyan SCM2 values between continents. 214

B.11 Results of pairwise comparisons of chondrichthyan SCM2 values without tooth based taxa for sea level trends using GLS. 215

B.12 Results of pairwise comparisons of both acanthodian and chondrichthyan SCM2 values for sea level trends using GLS. 216

C.1 Diversity dynamic metrics for Palaeozoic chondrichthyans through time. 220

CHAPTER 1

INTRODUCTION

The quality of the fossil record through time and space shapes our understanding of the evolution and diversity of organisms. However, it has also long been recognised that the fossil record, no matter which group of organisms, is incomplete and shaped by an unevenness in spatial and temporal sampling of fossils (e.g., Raup 1972; Sepkoski *et al.* 1981; Kidwell & Holland 2002). Incompleteness and unevenness of the fossil record through time have a direct impact on assessing past macroevolutionary patterns, predominantly patterns of palaeodiversity, and remain a widely discussed topic in palaeontology to date (e.g., Benton & Emerson 2007; Alroy *et al.* 2008; Close *et al.* 2018; Benson *et al.* 2021). Considerable improvements have been made to capturing, analysing, and interpreting the quality of the fossil record in recent years but, ultimately, all rely on the underlying data available, and these are the organisms that became fossilised and provide glimpses into the past. Indeed, the skeletal components of an organism's remains are for the most part considered the key unit of palaeontological research. The fossilized skeleton is widely used to reconstruct anatomy, ecomorphology and phylogenetic relationships. However, preservation of these structures differs from taxon to taxon and, together with natural and sampling constraints, limits our knowledge on their evolutionary patterns.

Hard structures such as biomineralized tissues (e.g., bones and teeth or shells)

more likely are preserved than soft tissues that do not biomineralize during an organism's life (e.g., skin, muscles, or organs) (Allison & Briggs 1993; Schweitzer 2011). The environment a carcass is deposited in can have a major influence on whether and how it becomes fossilised (e.g., stagnant lake compared to a fast-flowing river) (Newell 1959; Benson & Butler 2011; Purnell *et al.* 2018). Geological processes through time can aid or hinder preservation of fossils, and time itself can play a denominating factor: the more ancient a rock becomes, the more likely it is that it has been subjected to weathering, erosion, subduction, metamorphism or burial and with it the fossils it might contain (Raup 1972; Smith 2001; Smith & McGowan 2007; Smith *et al.* 2012). Aside from natural constraints, human-driven influences often play an equally important role in shaping (and biasing) the fossil record of organisms. Spatial sampling of fossils has been heavily influenced by historical research interests, leading to an unequal representation of geographical regions (e.g., Bernard *et al.* 2010; Cashmore & Butler 2019; Cashmore *et al.* 2020). A bias towards heightened collection effort in certain regions means that fossil occurrences in other regions will be underrepresented, and thus estimates of any global macroevolutionary pattern will be skewed by these spatial biases (e.g., Alroy *et al.* 2008; Vilhena & Smith 2013; Close *et al.* 2020; Benson *et al.* 2021).

Thus, understanding and quantifying how these constraints influence our perception of the fossil record through geological time is of paramount importance when reconstructing the evolutionary histories of organisms. This thesis focuses on disentangling the drivers and biases influencing the completeness and diversity of the fossil record, using a clade that has rarely featured in discussions of the quality of the fossil record despite its ecological importance and evolutionary persistence: the chondrichthyans.

1.1 A tale of chondrichthyans

The Chondrichthyes or cartilaginous fishes are a highly successful group of jawed vertebrates (gnathostomes) that play a key ecological role in our modern-day

freshwater and marine environments (e.g., Cailliet *et al.* 2005). Living chondrichthyans include the familiar Elasmobranchii (sharks, rays, and skates) and the less well-known sister group Holocephali (the chimaeras or rat and elephant fish) (Weigmann 2016). Their evolutionary history, however, reaches back far further than recent times. Chondrichthyans have inhabited this planet's waters for more than 450 million years and survived at least four of the five major mass extinctions in Earth's history. Chondrichthyans diverged from their sister group osteichthyans (bony fishes), which include the tetrapods, at least 423 million years ago in the Palaeozoic era (Zhu et al 2009; Brazeau & Friedman 2015).

Chondrichthyans, indeed, first evolved at some point in the Palaeozoic, albeit the precise timing of their appearance is not certain: chondrichthyan-like dermal scales from the Middle and Upper Ordovician (467 to 453 million years ago) suggest a potential initial radiation of the clade within that time period (Karatajūtė-Talimaa 1992; Sansom *et al.* 2001; Sansom *et al.* 2012; Andreev *et al.* 2015; Andreev *et al.* 2016) but some uncertainty remains due to the limitations of using scale characteristics for phylogenetic analyses (Sansom & Andreev 2017, see below for a further discussion). The oldest universally accepted chondrichthyan remains (the informal 'euchondrichthyans' sensu Pradel *et al.* 2014), consisting of isolated teeth and body fossils, are considerably younger and found in Lower Devonian (419 to 393 million years) strata (Young 1982; Mader 1986; Maisey & Anderson 2001; Miller *et al.* 2003; Botella *et al.* 2009; Ginter *et al.* 2010; Maisey *et al.* 2019) (Figure 1.1). Thus, there is a roughly 30-million-year gap in their fossil record that was initially unaccounted for, however, evidence is accumulating to explain this phenomenon.

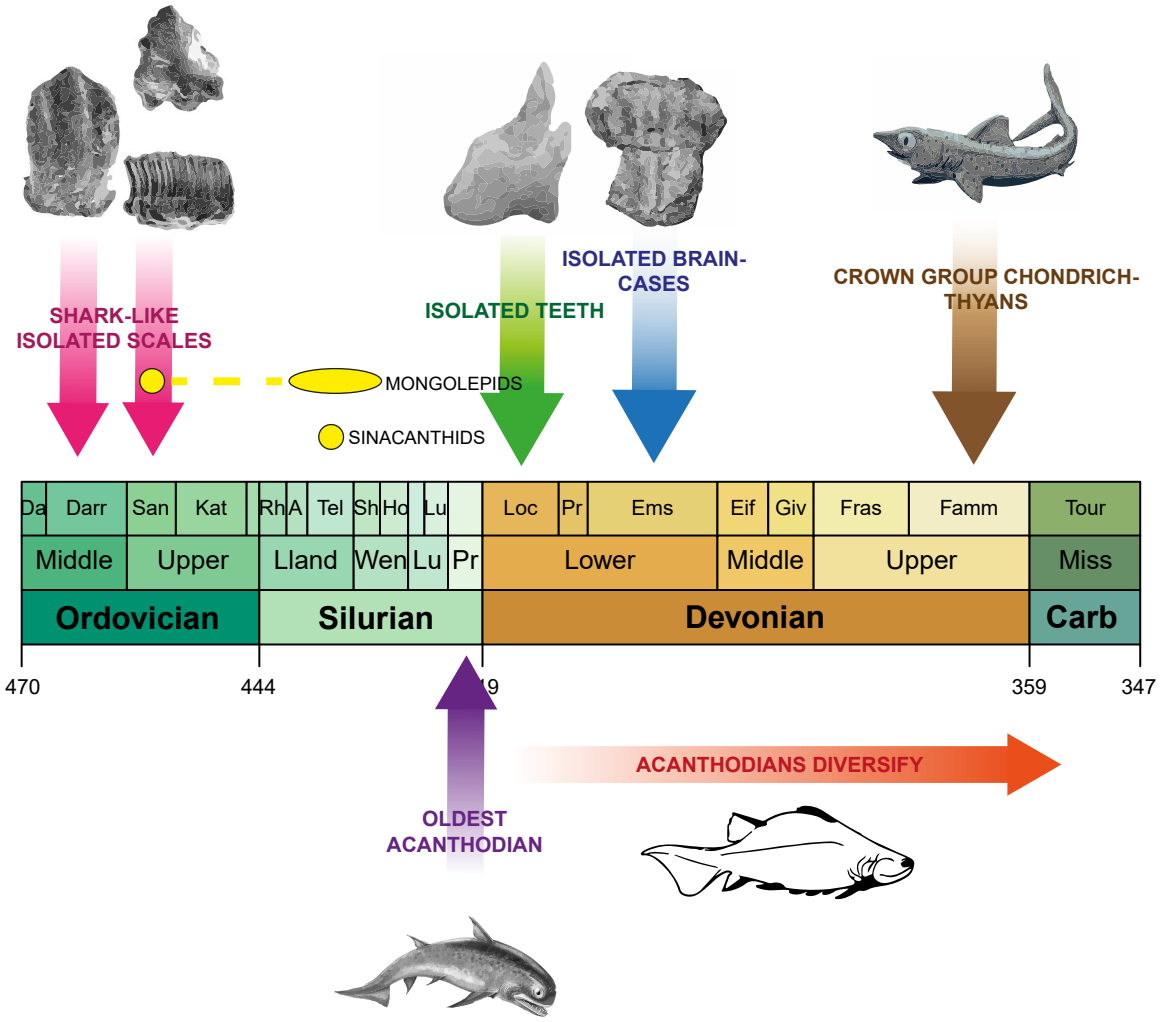


Figure 1.1: Simplified timeline of early chondrichthyan history, including acanthodian and non-acanthodian discoveries. *Nerepisacanthus* reconstruction by Danielle Dufault in Burrow & Rudkin 2014; *Ptomacanthus* in Brazeau 2012; *Ferromirum* reconstruction in Frey *et al.* 2020; *Pucapampella* braincase in Maisey & Anderson 2001; *Leonodus* teeth in Botella *et al.* 2009; *Tantalepis* scales in Sansom *et al.* 2012; *Solinalepis* scales in Andreev *et al.* 2016.

At the centre of this evidence is a small extinct group of spinose fusiform fishes that are known from the Silurian through to the Permian: the acanthodians (Denison 1979; Burrow 2021). They comprise a peculiar collection of predominantly small fishes whose skeletons fossilize poorly and preserve little internal anatomy. Initially, they were described based on isolated spines in the mid-19th century (Agassiz 1833-1844) and the multitude of mostly paired bony spines associated with their fins remains their most

prominent feature, albeit it is no longer considered a taxonomically defining character for the group (Brazeau & Friedman 2014). After their initial discovery, acanthodians were assigned to different lineages of jawed vertebrates for the next 150 years, including chondrichthyans (e.g., Ørvig 1957; Nelson 1969; Jarvik 1977), osteichthyans (Miles 1973a; Miles 1973b; Maisey 1986) and occasionally placoderms (Watson 1937; Romer 1966), following a multitude of competing hypotheses. Their integrity as a monophyletic group, however, remained largely intact throughout despite lacking strong morphologically informative evidence (Maisey 1986; Janvier 1996; Brazeau & Friedman 2014).

In recent years, a suite of fossil discoveries and (re-) descriptions of early gnathostomes together with the application of wider phylogenetic analyses have put a renewed focus on the inter- and intrarelationships of acanthodians. One site in particular, the Man On The Hill (MOTH) locality from the Lower Devonian Lochkovian of Canada, has yielded an array of articulated spinose fishes with both acanthodian-like and chondrichthyan-like features, blurring the lines between the two groups (e.g. Hanke *et al.* 2001; Hanke & Wilson 2006; Hanke & Wilson 2010; Hanke & Davis 2012). To make matters more complicated, paired fin spines, a trait previously considered to be a synapomorphy of the monophyletic acanthodians, were discovered in both stem-osteichthyans (Zhu *et al.* 1999; Zhu *et al.* 2009; Choo *et al.* 2017) and in the early Devonian chondrichthyan *Doliodus problematicus* (Miller *et al.* 2003). Finally, the traditional acanthodian monophyly was shattered in the form of a description of the braincase of the 'acanthodian' *Ptomacanthus* together with a phylogenetic analysis, placing the acanthodians as a grade scattered on the stems of both osteichthyans and chondrichthyans (Brazeau 2009). Subsequent phylogenetic analyses have continued to reject their monophyly and have further positioned an overwhelming proportion of acanthodians along the chondrichthyan stem (Davis *et al.* 2012; Zhu *et al.* 2013; Long *et al.* 2015; Brazeau & de Winter 2015; King *et al.* 2016; Qiao *et al.* 2016; Zhu *et al.* 2016; Coates *et al.* 2018; Dearden *et al.* 2019; Frey *et al.* 2020; King & Rücklin 2020) (Figure 1.2). Consequently, the seeming gap in the chondrichthyan fossil record

has mostly been filled by the addition of acanthodian-grade stem chondrichthyans and other putative early chondrichthyans.

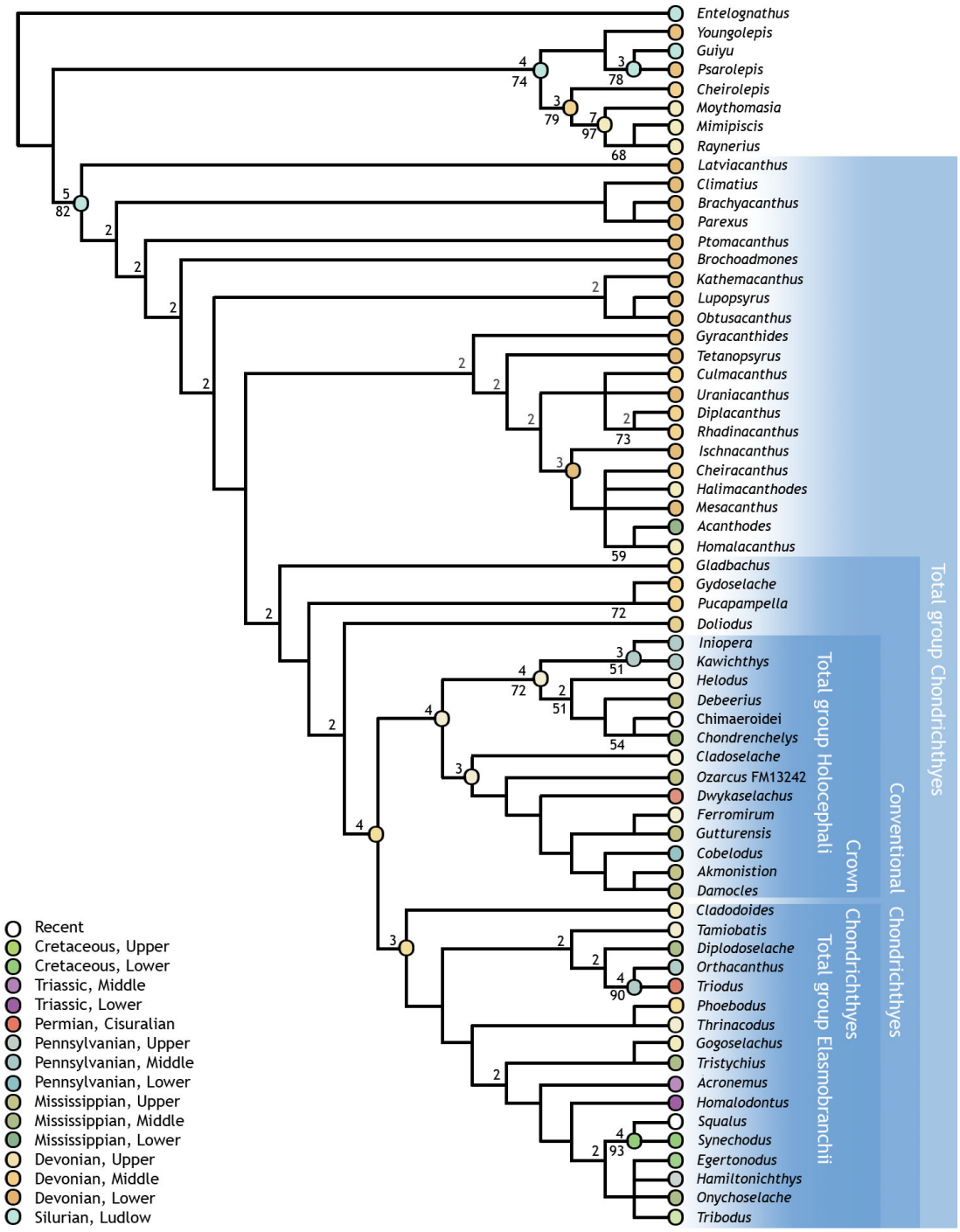


Figure 1.2: Strict consensus tree showing the phylogenetic affiliations of early chondrichthyans from Frey *et al.* 2020.

1.2 Palaeozoic chondrichthyan groups

Earliest representatives of major living chondrichthyan orders can be found in Mesozoic rocks (252-66 million years ago) (Grogan & Lund 2004), while the last common ancestor to crown chondrichthyans is dated back as far as the Middle (Frey *et al.* 2020) to Late Devonian (Janvier & Pradel 2015). The Palaeozoic indeed contains a diverse multitude of chondrichthyan forms. Members of the stem-group include the acanthodian grade and a small number of shark-like fishes, also termed conventional chondrichthyans, from the Lower to Middle Devonian, *Pucapampella*, *Doliodus*, *Gydoselache* and *Gladbachus* (e.g., Dearden *et al.* 2019; Frey *et al.* 2020; King & Rücklin 2020). Two shark-like orders from Upper Ordovician and lower Silurian assemblages, the Sinacanthida and Mongolepidida may also be part of the chondrichthyan stem (Karatajūtė-Talimaa *et al.* 1990; Karatajūtė-Talimaa 1995; Zhu 1998; Sansom *et al.* 2000; Sansom *et al.* 2005). They are known from isolated spines and scales, respectively, which has made their taxonomic placement difficult, but recent reassessments have further strengthened their status as some of the earliest total-group chondrichthyan fossils (Andreev *et al.* 2016; Andreev *et al.* 2020).

The Palaeozoic further saw the rise of several prominent chondrichthyan groups, with most of them being placed within the chondrichthyan crown-group in the most recent phylogenetic analyses: within the total-group Elasmobranchii, this includes the Carboniferous-Triassic xenacanth sharks with their elongated bodies and affinity to freshwater environments, the Devonian-Permian ctenacanth sharks with their ornamented dorsal fin spines, the hybodontiforms which existed from the Devonian to the late Cretaceous and are considered the closest group to the Neoselachii (extant sharks and rays), and the marine Devonian-Carboniferous phoebodontiforms (Janvier 1996; Underwood 2006; Coates *et al.* 2018; Dearden *et al.* 2019; Frey *et al.* 2019; Frey *et al.* 2020). The total-group Holocephali contains prominent Palaeozoic members such as the Carboniferous iniopterygians, the widely distributed symmoriiforms from

the Devonian-Permian and the Devonian-Permian helodontids (Janvier 1996; Coates *et al.* 2018; Dearden *et al.* 2019; Frey *et al.* 2020). These recent analyses also recover the well-known Devonian shark *Cladoselache* as a stem-holocephalan symmoriiform.

Another group of early chondrichthyans that had their heyday in the Palaeozoic are the eugeneodontids with their characteristic tooth series that advance into extreme symphyseal whorls in the edestoids such as *Helicoprion* (Tapanila *et al.* 2020). Finally, the petalodontids are known from the Carboniferous and Permian intervals. While they are mainly characterised by their petal-shaped teeth, forms such as *Belantsea*, *Janassa* or *Siksika* are famously known for their distinctive non-shark-like body shapes. Both groups are not included in the more recent phylogenetic analyses of early chondrichthyans but have been associated with holocephalans rather than elasmobranchs (Janvier 1996; Grogan *et al.* 2012).

Thus, the Palaeozoic saw the origin and subsequent rise of abundant and diverse forms of chondrichthyans that lay the groundwork for their roughly 450-million-year perseverance into recent times. Considerable advances in disentangling the early history and origins of chondrichthyans have been made in recent years but all highlight one overwhelming problem: the limitations of dealing with an incomplete and sparse fossil record. Unfortunately, chondrichthyans, amongst all jawed vertebrates, are particularly prone to this as their endoskeleton is predominantly cartilaginous (Zangerl 1981). It lacks extensive mineralisation and fossilizes poorly compared to bone. Accordingly, their fossil record predominantly consists of isolated teeth and dermal scales that contain hypermineralized tissues (e.g., Donoghue 2002; Lübke *et al.* 2015). However, interpretations of stem-chondrichthyan conditions to-date heavily rely on braincases or body fossils which are sparse in their early record, found only from the Devonian on (Brazeau & Friedman 2015). Discoveries such as the fairly complete neurocrania of the stem-chondrichthyan *Pucapampella* (Maisey 2001; Maisey & Anderson 2001; Maisey *et al.* 2019) and a partial body fossil of *Doliodus* (Miller *et al.* 2003; Maisey *et al.* 2009) have greatly aided in disentangling some of the uncertainties sur-

rounding early chondrichthyan anatomies but ultimately highlight the reliance on the levels of completeness in the early chondrichthyan fossil record for inferring their early history and evolution.

1.3 What is a chondrichthyan?

In the light of recent reconsiderations of acanthodians and further investigations into the chondrichthyan stem- and total-group, the question of what constitutes a chondrichthyan becomes increasingly complex. 'Conventionally defined' chondrichthyans are predominantly established by one hallmark feature, tessellated calcified cartilage (TCC) (Zhu *et al.* 2013; Pradel *et al.* 2014; Brazeau & Friedman 2014), which is a main structural component of their endoskeletons (Dean & Summers 2006). It is often used as a single defining character of chondrichthyans in phylogenetic analyses, but recent investigations suggest that a more complex character and state distribution is warranted (Maisey *et al.* 2021). Potential evolutionary precursors of TCC in sinacanthids and some acanthodians could render the division of stem-chondrichthyans into putative/conventional based on the absence/presence of TCC obsolete and suggest that a greater diversity of tesseral architecture should be accounted for in future analyses (Maisey 2013; Maisey *et al.* 2021).

A second traditional character considered to represent a chondrichthyan synapomorphy is the presence of pelvic claspers, a pair of copulatory organs modified from the pelvic fins. Claspers are not unique to chondrichthyans but are also present in ptyctodont, antiarch and arthrodire placoderms, suggesting they potentially were widespread in placoderms (Denison 1978, Ahlberg *et al.* 2009; Long *et al.* 2015). However, the placoderm claspers are generally considered to have been independently derived (Denison 1978) and are not considered homologous compared to chondrichthyans as suggested by their absence in osteichthyans and acanthodians (Brazeau & Friedman 2014).

Finally, a third characteristic that has been traditionally used to define both

extant chondrichthyans and the total-group chondrichthyans is the presence of neck canals in their dermal scales (Reif 1978; Maisey 1984; Maisey 1986; Lund & Grogan 1997; Sansom *et al.* 2012). However, neck canals seemingly are more broadly distributed amongst early crown-group gnathostomes, with the presence of them documented in some stem-osteichthyans and actinopterygians (Gross 1968, Gross 1973; Qu *et al.* 2013a; Qu *et al.* 2013b). Furthermore, while neck canals are present in *Solinalepis*, they are absent in the other Ordovician chondrichthyan-like scale taxa (Karatajūtė-Talimaa 1992; Sansom *et al.* 2001; Sansom *et al.* 2012; Andreev *et al.* 2015; Andreev *et al.* 2016).

While TCC may be considered the only undisputed chondrichthyan character trait of the three by some, further attempts by Brazeau & Friedman (2014) and subsequently Dearden (2018) and Dearden *et al.* (2021) have been made to reassess chondrichthyan clade characters and conduct a list of derived characters that permit a confident placement in the total-group Chondrichthyes. These in-depth investigations highlight the state of flux some of these characters are in. Brazeau and Friedman (2014) retained the acanthodians as somewhat separate from the total-group chondrichthyans (and understandably so given their phylogenetic assumptions), while Dearden (2018) investigated total-group chondrichthyan characters with all acanthodians as stem-chondrichthyans in mind. As a consequence, prismatic TCC and pelvic claspers are only retained as a character of the total-group crown-wards of the acanthodian-grade taxa. The presence of neck canals is not considered a synapomorphy of chondrichthyans by either investigation and warrants a more through exporation.

Isolated scales are, as explained previously, the earliest remains of potential chondrichthyan origin but have also been found and described throughout the later Palaeozoic. However, compared to body fossils or even isolated teeth, they contain relatively little information to use to infer characters for phylogenetic placement and current phylogenetic analyses use a limited range of these characters to infer chondrichthyan and broader gnathostome relationships (Andreev *et al.* 2015; Sansom &

Andreev 2017). These limitations have often been overcome in past studies by using compound character sets to place an isolated scale within the chondrichthyan total-group based on overall similarity (e.g., Sansom *et al.* 2012, Andreev *et al.* 2016), an approach that has been criticised (Brazeau & Friedman 2014; Dearden 2018). If these characters are considered individually, many fail to identify an isolated scale as chondrichthyan. As a consequence, Brazeau & Friedman (2014) accept a single synapomorphy based on the growth pattern of chondrichthyan scales, which is further divided into two unique character traits by Dearden (2018). Thus, neither analysis confidently places the Ordovician scale-based taxa within the chondrichthyan total-group. Dearden (2018) also rejects the definite assignment of the Silurian-early Devonian scale-based elegestolepids based on the lack of sufficient characters. By contrast, reinvestigations and revisions of current phylogenetic data matrices using both scale and body characters by Sansom and Andreev (2017) indicate a placement of the Ordovician taxa within the chondrichthyan total-group but may not satisfy the criticisms regarding distinct characters.

To conclude, 'what is a chondrichthyan' is not as easy of a question to answer as one might think, especially within the context of fossil taxa. Considerable advances have been made to identify potential characters that define a chondrichthyan but are still far from resolved. Additionally, characters might become obsolete upon the discoveries of new fossils and reinvestigations of old ones as understanding of the evolution of character shifts.

1.4 Objectives

The aim of this thesis is to examine patterns and drivers of completeness and diversity in the fossil record of Palaeozoic chondrichthyans using a plethora of integrative and quantitative approaches to gain a better understanding of early chondrichthyan history. I compile an extensive dataset using data from museum collection visits augmented with literature review to quantify completeness and diversity of chondrichthyans

from the Ordovician to the Permian, the key interval in their origination and first radiation. Within this thesis, I highlight the limitations of previous completeness studies and expand them to a fish group while accounting for a different body plan and skeletal composition. This thesis uses the latest advances in analytical methods estimating diversity from an incomplete fossil record to thoroughly examine the earliest history of chondrichthyans and identify the drivers behind it.

In Chapter 2, I quantify the skeletal completeness of the stem-chondrichthyan acanthodian fossil record and introduce a new metric to quantify soft-tissue completeness alongside skeletal completeness.

In Chapter 3, I assess skeletal completeness patterns of the entire Palaeozoic chondrichthyan clade and compare acanthodian with non-acanthodian chondrichthyan completeness.

In Chapter 4, I use the data collected in Chapters 2 and 3 to dive into total-group chondrichthyan diversity, origination and extinction dynamics throughout the Palaeozoic and discuss the implications for the observed patterns. I compare diversity estimates using different methods of sampling standardisation to test if there is a clear signal in Palaeozoic chondrichthyan diversity patterns or if sampling biases mask most of them.

CHAPTER 2

SKELETAL AND SOFT TISSUE COMPLETENESS OF THE ACANTHODIAN FOSSIL RECORD

This chapter is a slightly modified version of a manuscript published in the journal Palaeontology*, entitled:*

SCHNETZ, L., BUTLER, R. J., COATES, M. I. and SANSOM, I. J. in press. Skeletal and soft tissue completeness of the acanthodian fossil record. Palaeontology.

My contribution to this work involved conducting all aspects of the research, including data collection, data analysis, interpretation of results and manuscript writing. I co-designed the methodology in collaboration with my co-authors. I. Sansom provided environmental data for Benthic Assemblage zone (BA) assignments. My co-authors provided feedback on the interpretations of the results and earlier versions of the manuscript. The editorial "we" is used here to reflect these contributions.

2.1 Introduction

Within the past 15 years, an array of new approaches to examining and estimating the quality of the fossil record based on specimen completeness have emerged.

Initially, these assessed the quality of preservation of a fossil skeleton on the basis of four to five broad categories (e.g., one bone, more than one bone, one specimen and more than one specimen) (Benton *et al.* 2004; Fountaine *et al.* 2005; Smith 2007; Benton 2008a). Subsequent expansion included categorizing completeness within different skeletal regions rather than just for the entire skeleton (Beardmore *et al.* 2012a; Beardmore *et al.* 2012b). The most widely used approach in recent years follows Mannion & Upchurch (2010) who proposed two completeness metrics to accurately quantify the completeness of individual specimens and species, initially applying this to sauropodomorph dinosaurs. These metrics are the skeletal completeness metric (SCM), which measures absolute proportions of the preserved skeleton of a given species, and the character completeness metric (CCM), which measures the proportion of potential phylogenetically informative characters preserved. Several studies have subsequently used this methodology to assess completeness based on individual specimen data for the fossil record of different terrestrial (Brocklehurst *et al.* 2012; Walther & Fröbisch 2013; Brocklehurst & Fröbisch 2014; Dean *et al.* 2016; Gardner *et al.* 2016; Verrière *et al.* 2016; Davies *et al.* 2017; Brown *et al.* 2019; Cashmore & Butler 2019; Mannion *et al.* 2019; Cashmore *et al.* 2020) and marine vertebrate groups (Cleary *et al.* 2015; Tutin & Butler 2017; Driscoll *et al.* 2018).

Comparisons of completeness metrics with changes in taxonomic diversity, geography, sampling effort, preservation and environmental deposition have revealed a number of correlations and highlighted different biases. Environmental factors such as changes in sea level can correlate with changes in completeness, diversity and abundance of a group and reveal underlying ecological mechanisms such as habitat preferences (Mannion & Upchurch 2010; Cleary *et al.* 2015; Tutin & Butler 2017). In some groups, an uneven sampling both on a geographical and historical level has led to a substantial bias in the completeness of their fossil record as more effort is directed towards particular taxa or localities of interest by researchers (see e.g. Cleary *et al.* 2015; Driscoll *et al.* 2018; Cashmore & Butler 2019; Cashmore *et al.* 2020). This is

likely to yield a higher number of and potentially more complete fossils compared to taxa or localities that are not considered as important, thus resulting in a significant bias within the group. However, these increasingly sophisticated studies of tetrapod record quality have not yet been applied to the fossil record of fishes, especially those with little or no bone and which therefore might be subject to considerable preservation bias.

Acanthodii are a grade of extinct fishes from the Palaeozoic. They first emerged in the early Silurian, diversified in the Devonian, declined in the Carboniferous and disappeared from the fossil record in the Permian (Moy-Thomas 1971; Nicol 1982; Janvier 1996; Mutter & Richter 2007; Burrow & Rudkin 2014; Dearden *et al.* 2019). Acanthodians were globally distributed in both freshwater and marine habitats and are thought to have been microphagous for the most part while some of the tooth-bearing groups likely were predators (Denison 1979). The most prominent characteristic of acanthodians are the numerous bony fin spines located in front of all paired and midline fins, except the caudal fin (Denison 1979). These fin spines could grow to extreme sizes in certain taxa, and are sometimes the only skeletal part that is preserved. Notably, possession of a pre-anal fin spine remains the only putative synapomorphy of a monophyletic Acanthodii (Brazeau & Friedman 2014). Acanthodians show little diversity in range of body shape, inferred function and ecomorphology compared to other major groups of fishes (Denison 1979; Blais 2017).

A slew of proposals have considered the monophyletic or paraphyletic status of the acanthodians and their assignment to the chondrichthyans or the osteichthyans as sister group or stem lineage (e.g., Nelson 1969; Miles 1973a; Miles 1973b; Jarvik 1977; Denison 1979; Maisey 1986; Long 1986; Janvier 1996; Hanke & Wilson 2004; Brazeau 2009; Burrow & Turner 2010; Davis *et al.* 2012; Zhu *et al.* 2013; Brazeau & Friedman 2014). Recent phylogenetic analyses have stabilised an increasing proportion of acanthodians as stem-chondrichthyans, rejecting their status as a clade, while debates around the position of other stem-gnathostomes such as placoderms

are ongoing (Brazeau 2009; Davis *et al.* 2012; Zhu *et al.* 2013; Long *et al.* 2015; Brazeau & de Winter 2015; King *et al.* 2016; Qiao *et al.* 2016; Zhu *et al.* 2016; Coates *et al.* 2018; Dearden *et al.* 2019; Frey *et al.* 2020; King & Rücklin 2020). Fossil discoveries from the Lower Devonian (Lochkovian) Man On The Hill (MOTH) locality of Canada provided some of the earliest articulated acanthodians, including taxa with both acanthodian-like features and characteristics more usually associated with conventional chondrichthyans (e.g. Hanke *et al.* 2001; Hanke & Wilson 2006; Hanke & Wilson 2010; Hanke & Davis 2012). Further instances of this are becoming evident in chondrichthyans from multiple localities in North America, Antarctica, Australia and Asia, but exemplified most notably by the early Devonian chondrichthyan *Doliodus problematicus* from New Brunswick, Canada, demonstrating a widespread distribution of paired fin spines, previously considered to be an acanthodian synapomorphy (Young 1982; Janvier 1996; Zhu *et al.* 1999; Miller *et al.* 2003; Zhu *et al.* 2009).

In general, acanthodian species have been diagnosed by characteristics of the dermal skeleton and/or specific isolated skeletal characters because the rarely preserved endoskeleton (Brazeau 2009; Davis *et al.* 2012; Brazeau & Friedman 2014; Coates *et al.* 2018; Dearden *et al.* 2019) often includes little anatomical detail (Sansom *et al.* 2011; Chevrinais *et al.* 2015) and the micromeric dermal skeleton is commonly disintegrated post-mortem. However, ascertaining the potential taphonomic filters in the nature and quality of the fossil record of these predominantly cartilaginous vertebrates has not been attempted to date. Quantifying the completeness of the acanthodian fossil record might therefore yield novel insights into the impact that ecological, geographical and sampling biases may have on it, contributing to our understanding of the macroevolutionary patterns of this group.

In this chapter, we quantify the completeness of the acanthodian fossil record for the first time using modified versions of previously developed completeness metrics (Mannion & Upchurch 2010; Beardmore *et al.* 2012a; Beardmore *et al.* 2012b). This also provides the first quantitative completeness analyses for a non-tetrapod ver-

tebrate group. We statistically compare the variations in completeness of the acanthodian fossil record through time with taxonomic diversity, geographical distribution and depositional environment. We aim to improve our understanding of the hypotheses concerning origin and early evolution of the acanthodian grade by identifying biases and filters that influence data set quality. In turn, these results are likely to provide a more informed perspective on the potential biases introduced by missing data (Sansom & Wills 2013) on hypotheses of early chondrichthyan evolution, and the sequential assembly of what are now understood as conventional chondrichthyan conditions (Coates *et al.* 2018).

2.2 Methods

2.2.1 Dataset

Despite these recent reconsiderations of acanthodian interrelationships, a detailed and thorough systematic revision of the Acanthodii has yet to be tackled and is beyond the scope of the present chapter. We therefore adhere to the conventional definition and consider all species formally assigned to the Acanthodii as acanthodians for this chapter (a more detailed explanation is given in the taxonomic groups section below). The Paleobiology Database (PBDB; `https://www.paleobiodb.org`) included only 56 total occurrences limited to 26 taxa from 22 geological formations in 36 collections (as of 12 May 2020). These data are evidently unsuitable and would considerably skew any completeness estimates. Therefore, unlike most previous completeness studies that used published literature and the PBDB (Mannion & Upchurch 2010; Brocklehurst *et al.* 2012; Dean *et al.* 2016; Gardner *et al.* 2016; Verrière *et al.* 2016; Davies *et al.* 2017; Tutin & Butler 2017; Brown *et al.* 2019; Cashmore & Butler 2019; Mannion *et al.* 2019; Cashmore *et al.* 2020), primary data were gathered from museum collections. These were then augmented via reference to peer-reviewed literature (illustrations and text). Where applicable, taxonomic information on museum catalogues was checked for validity and corrected to the currently accepted taxonomic

name and systematic position. Together with the completeness scores, information on the lithostratigraphy (e.g., geological formation), geographical locality and chronostratigraphic age were recorded for subsequent analyses. Additionally, palaeoenvironmental information was extracted from published sources where detailed lithostratigraphy descriptions for specimen occurrence were available. The final dataset contains an unprecedented survey of over 1600 acanthodian specimens in 300 species and 121 genera, plus two acanthodian specimens in open nomenclature, and is up to date as of June 2021. We additionally generated 3 subsets excluding isolated scale-based taxa, isolated fin spine-based taxa as well as excluding both isolated scale and fin spine-based taxa from the dataset and ran some of the analyses multiple times using each subset. This allows us to compare and contrast how isolated skeletal remains that are commonly used in acanthodian species identification impact on acanthodian completeness.

2.2.2 Completeness metrics

Background. Several methods have been proposed to quantify the quality of the fossil record, with different levels of precision (e.g. Benton & Storrs 1994; Fountaine *et al.* 2005; Benton 2008b; Mannion & Upchurch 2010; Beardmore *et al.* 2012a; Beardmore *et al.* 2012b). The two most commonly used metrics for estimating the completeness of a fossil vertebrate skeleton are the character completeness metric (CCM) and the skeletal completeness metric (SCM) by Mannion and Upchurch (2010). CCM quantifies the proportion of potential phylogenetic characters preserved from different parts of the skeleton in a given species based on calculating the percentage of characters attributed to each body region from published phylogenies. SCM measures the absolute proportion of the overall skeleton preserved in a given species based on dividing the skeleton into different regions and estimating how much of it is represented. Both of these metrics were established in two variants, CCM1/SCM1, which establishes the completeness of a single most complete specimen for a given species or taxon, and

CCM2/SCM2, which estimates completeness using all specimens of a given species or taxon (a composite of all investigated specimens). The latter has been preferred for both CCM and SCM in subsequent studies because it takes into account that the most complete specimen might still be missing skeletal information available in other specimens of the same species (Brocklehurst *et al.* 2012; Dean *et al.* 2016; Verrière *et al.* 2016; Cashmore & Butler 2019; Cashmore *et al.* 2020). Another completeness metric (Beardmore *et al.* 2012a; Beardmore *et al.* 2012b) estimates preservation of a fossil based upon both disarticulation and completeness. Rather than scoring total numbers of individual bones, this method divides the body into equally weighted skeletal regions and uses an index of 0-4 to score the levels of completeness in each region.

Acanthodian 'problems' and this chapter. Previous studies have shown a significant positive correlation of CCM and SCM in different vertebrate clades, thus suggesting that these metrics capture similar signals in fossil record quality (Mannion & Upchurch 2010; Tutin & Butler 2017). CCM is generally scored using an assumption that if one skeletal element is complete, all phylogenetic characters of that element can be assessed. While this correlation may hold true for the three-dimensionally preserved bones of the previously studied tetrapod groups, it is likely problematic for acanthodians with fragile cartilaginous skeletons that are prone to fragmentation and erosion, with consequent loss of character information. Acanthodians are often small in size (usually less than 20cm total length; Denison 1979) and embedded in matrix, hiding potential informative characters from view. Additionally, the composition of the matrix may preclude them from using methods such as acid digestion and lack appropriate resolution for CT scanning. For example, several acanthodian species from the MOTH locality are known from full body specimens but mostly lack detailed skeletal features of neurocranial, jaw or branchial arch elements (e.g., Hanke 2002; Hanke & Wilson 2006; Hanke & Davis 2008; Hanke & Davis 2012). Thus, considering the similarity in signal for CCM and SCM observed in other groups (Mannion & Upchurch 2010; Tutin & Butler 2017), the clear connection between SCM and natural taphonomic and environmental

processes, and the problem of character loss on cartilaginous skeletons, we follow the protocol by Cashmore & Butler (2019) in assessing fossil record quality using SCM rather than CCM in this study.

Completeness metrics in this chapter. We calculated acanthodian completeness based on two different metrics. We used the SCM as a base to calculate the completeness of skeletal characters within the fossil record of acanthodians but divide the skeleton into anatomical regions as implemented by Beardmore *et al.* (2012a, 2012b). Contrary to the original application of the SCM, assessing the relative percentage of the total skeleton made up by any individual bone within fossil fish specimens proved to not be feasible and the total number of elements within a skeletal region in acanthodians (such as the vertebral column or branchial arches) are rarely known. Therefore, following Beardmore's Skeletal Completeness, values between 0 (absent) and 4 (more than 75% complete) were assigned to nine different skeletal regions. Detailed information on the scoring system and descriptions for each individual skeletal region is accessible in the supplementary material. Using this method, an isolated scale would receive a score of 1, while an acanthodian with more than 75% of the body covered in scales is given a score of 4. We divided the acanthodian skeleton into braincase, upper jaw, lower jaw, hyoid and gill arches, pectoral girdle, vertebrae, teeth, fine spines and scales (Figure 2.1).

The absence or minimal presence of endoskeletal bone together with the mode of preservation in most acanthodians results in different challenges for assessing the quality of their fossil record compared to the other vertebrate groups that have previously been investigated. To account for this difference in preservation and thus estimating their completeness, we developed a novel completeness metric, the Soft Tissue Completeness Metric (STCM). Its framework is based upon Beardmore's non-weighted method. Preservation of muscles, vasculature or nerve fibres in vertebrate fossils can occur under exceptional conditions (Arsenault *et al.* 2004; Trinajstic *et al.* 2007; Conway Morris & Caron 2012). Thus far, reports of acanthodian soft tissues

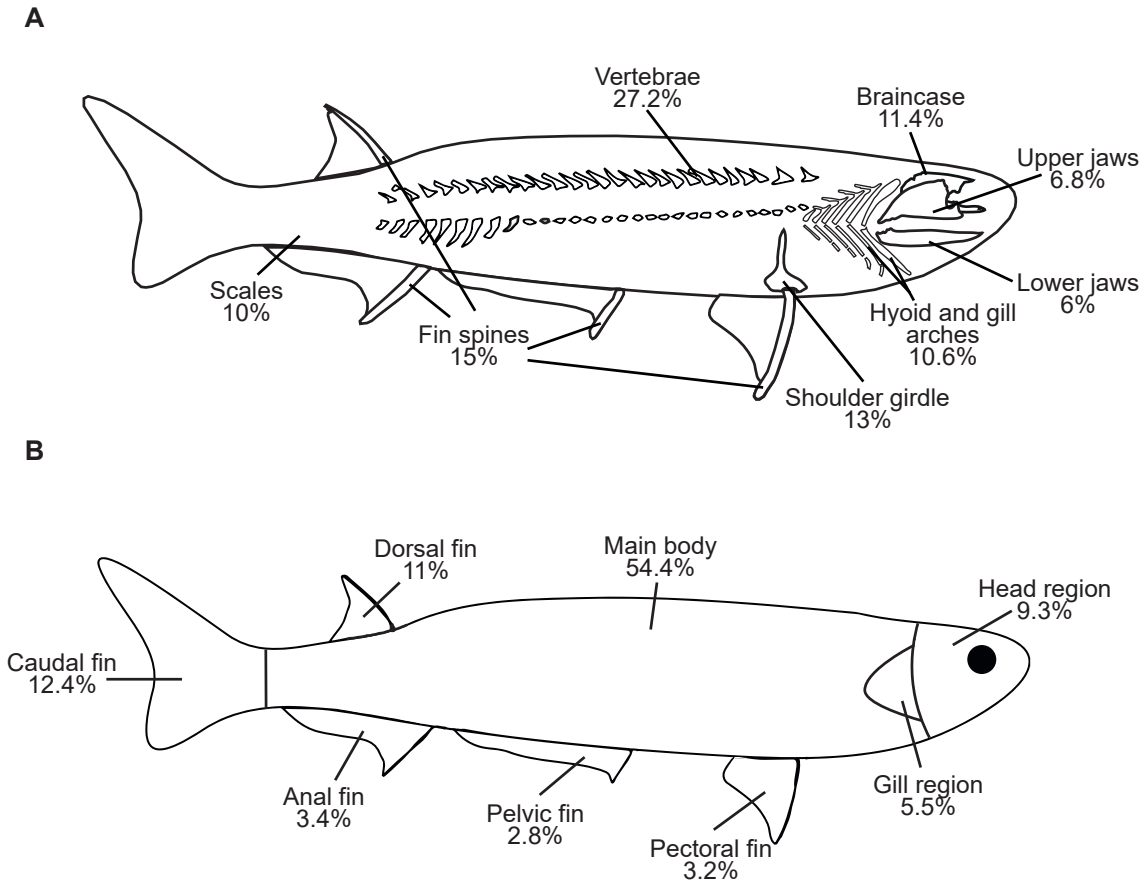


Figure 2.1: Skeletal and soft tissue reconstruction of *Acanthodes* based on the vertebral column of *Acanthodes sulcatus* (Miles 1970), the general reconstruction of *Acanthodes lopatini* (Beznosov 2009) and braincase, jaws, hyoid and gill arches of *Acanthodes confusus* sensu Heidtke (2011) (noted as *Acanthodes bronni* in Miles 1973b; Davis *et al.* 2012) to illustrate the relative body proportions of acanthodians. Relative proportions of the different regions were calculated by assessing the surface areas of the reconstructions.

are limited to traces of the internal organs (such as kidney, liver and heart), eyes, and integument outline (Davidson & Trewin 2005; Chevrinais *et al.* 2015). Here, we include the integument outline as a soft tissue component of acanthodians, represented by different head, main body and fin imprints. Soft tissue regions were implemented based on the acanthodian body and preservation potential and divided into head, gill region, main body, dorsal fin, pectoral fin, intermediate fin, pelvic fin, anal fin and caudal fin. Scores of 0 to 4 were attributed as above. To account for the differences that both skeletal and soft tissue regions contribute to the overall body, we determined rel-

ative proportions of the different regions by assessing their surface areas (Figure 2.1). For this, 2D reconstructions from literature (see supplements) were used to generate proportion scores for each of the regions using the vector graphics software Inkscape (`https://inkscape.org/`).

Different kinds of acanthodians are known to encompass varying sets or complements of skeletal parts, such as the presence or absence of teeth, or the distribution of fins and parts of fins, including an absence of specific fins and fin spines (see e.g., Denison 1979 for a range of different body exemplars) which may result in biased scores. In order to account for this, we calculated both skeletal and soft tissue proportions for representatives of eight acanthodian taxa: *Diplacanthus crassisimus* Duff, 1842 (diplacanthid-exemplar), *Acanthodes* Agassiz, 1833 (acanthodid-exemplar A), *Acanthodopsis* Hancock & Atthey, 1868 (Acanthodopsis-exemplar), *Traquairichthys pygmaeus* Fritsch, 1895 (acanthodid-exemplar B), Ischnacanthiformes Berg, 1940 (ischnacanthid-exemplar), *Mesacanthus mitchelli* Egerton, 1861 (mesacanthid-exemplar), *Climatius reticulatus* Agassiz, 1845 (climatiid-exemplar), *Tetanopsyrus lindoei* Gagnier, Hanke & Wilson, 1999 (Tetanopsyrus-exemplar) and an averaged acanthodian-exemplar based on all the measurements (for more details, see supplementary information). The averaged acanthodian-exemplar exhibits all skeletal and soft tissue body regions defined in this study (including teeth, intermediate fin spines, anal fin, etc.), averaged from the measurements of the representatives of the eight acanthodian taxa. These proportions were then used to correct the initial 0 to 4 scores for each individual skeletal and soft tissue region before calculating the final SCM and STCM scores (ranging between 0 and 100%). Body exemplars were attributed to each acanthodian taxon based on best anatomical fit (where possible) and taxonomic similarity. The averaged acanthodian-exemplar is used primarily for taxa that are known exclusively from isolated fragmentary material and could not be assigned to a higher taxonomic level (Incerti sedis). Acanthodian body fossils are predominantly preserved in lateral compression. Therefore, we follow Cleary *et al.* (2015), Brown *et al.* (2019) and Cashmore

& Butler (2019) and report completeness based on the side visible (assuming a similar preservation of the other side). For other orientations such as dorsoventrally flattened specimens, completeness was calculated based on the skeletal features visible on the respective orientation (either dorsal or ventral) alone. If fossils were split into part and counterparts, both sides were examined to infer completeness. Using the skeletal and soft tissue completeness metrics, we are able to compare completeness of two contrasting modes of preservation and account for the problems of limited preservation of skeletal material resulting from the absence of bone.

2.2.3 Acanthodian completeness data

Time series. Stage-level time bins were used to conduct the temporal analyses and time series starting from the Rhuddanian (basal stage of the Silurian) and ending with the Capitanian (Guadalupian, middle Permian). Chronological ages, time bin lengths and stage midpoints were established in accordance with the latest information from the International Commission on Stratigraphy (IUGS) stratigraphic charts (v2020/03; Cohen *et al.* 2013). Stage bin length varies substantially in the Palaeozoic, ranging from 1.8 Ma (Gorstian) to 15.8 Ma (Visean). An epoch-level time bin had to be used for the Pridoli (Silurian) as there are currently no officially recognized stages within this epoch. A finer resolution than stage-level (such as substage) proved impossible for the acanthodian fossil record as the required stratigraphic information is not available for the majority of taxa. We recognize that this might result in a bias towards stretching out single spot occurrences to the lower and upper boundaries of the stage. However, stage-level analyses generally provide the norm for macroevolutionary and macroecological studies of the fossil record through deep time and are suitable for our completeness studies. Mean and median completeness scores for both SCM and STCM were calculated for all species for each time bin. Sampled-in-bin occurrences of specimens were used to determine the temporal range of individual taxa.

Taxonomic groups. In this chapter, we are following the phylogenetic analysis by Dear-

den *et al.* (2019), subsequently corroborated by Frey *et al.* (2020), which places the acanthodians as a grade on the stem-group chondrichthyans. We exclude *Pucapampella* and all taxa more closely related to the chondrichthyan crown except for *Brochoadmones* and *Lupopsyrus* which were traditionally described as acanthodians and have an acanthodian-like body plan (Hanke & Wilson 2006; Hanke & Davis 2012) but fall outside the acanthodian grade sensu Dearden *et al.* (2019). See supplementary material for a full list of included genera and species. Two very incomplete acanthodian specimens were included in the analyses because they extend the acanthodian occurrence range into the Middle Permian (Mutter & Richter 2007). These specimens were recorded as separate taxa because of their contrasting skeletal composition (isolated scale versus isolated fin spine fragments), but taxonomic information beyond classification as members of the Acanthodii is lacking. This assignment as operational taxonomic units (OTUs) is consistent with procedures used in a previous study (Cashmore & Butler 2019). The traditional separation of acanthodians into three orders, the Climatiiformes, Ischnacanthiformes and Acanthodiformes, has been rejected (e.g., Janvier 1996; Gagnier & Wilson 1996; Hanke & Wilson 2004; Brazeau 2009; Burrow & Turner 2010). Diplacanthiformes and Tchunacanthida were recovered as distinct orders of acanthodians alongside this traditional tripartite division (Karatajūtė-Talimaa & Smith 2003; Hanke *et al.* 2001; Burrow & Turner 2010; Burrow *et al.* 2016). However, the Climatiiformes/Climatiidae now form a grade capturing a section of the chondrichthyan stem, exclusive of *Pucapampella* and more crownward taxa, and exclusive of the acanthodid stem, which forms a monophyletic sister group (acanthodids + ischnacanthids + diplacanthids) to all other chondrichthyans (Coates *et al.* 2018, Dearden *et al.* 2019). While the position of the diplacanthiforms has been resolved in these most recent analyses, the Tchunacanthida have not been reassigned and formally remain as a distinct order of acanthodians. To compare SCM and STCM scores between the major subgroups, acanthodians were subdivided into Acanthodiformes, Ischnacanthiformes, Diplacanthiformes, Climatiidae, Tchunacanthida and Incerti sedis taxa. As

there has not been any formal reassessment of the Climatiidae family up-to-date, we follow the currently accepted taxonomic recognition of this group as a taxon-rich delimitable grade and use them as subgroup for our analysis. The Tchunacanthida are included here as they have been formally erected as a distinct order of acanthodians by Karatajūtė-Talimaa & Smith (2003) but it should be noted that the described material is limited to isolated scales from four sampled horizons of northern Asia. The Incerti sedis subgroup is most likely polyphyletic as it contains a multitude of taxa that were not assigned to an order or family when assessed taxonomically. We use the division here to illustrate the status of taxon completeness contained therein and the impact of such incompleteness on taxonomic issues.

Spatial correlations and Lagerstätten. To investigate if acanthodian fossil record quality varies on a global scale, completeness scores were grouped by the hemispheres and geographical regions in which they were collected. The geographical localities are based on modern-day regions. Acanthodians have been recovered from all modern-day continents, including taxa from Africa (2), Asia (68), Australia and Oceania (17), Antarctica (5), North America (68), South America (9) and Europe (164). Previous studies have taken the influence of Lagerstätten, sites of exceptional fossil preservation, into account when calculating completeness scores (Brocklehurst *et al.* 2012; Dean *et al.* 2016; Brown *et al.* 2019; Cashmore & Butler 2019; Cashmore *et al.* 2020) as they can bias the overall trend of completeness through time. However, we follow completeness studies on other marine vertebrates (Cleary *et al.* 2015, Tutin & Butler 2017) and do not separate taxa derived from concentration or conservation Lagerstätten for statistical comparisons as there are rarely any clearly defined Lagerstätten for acanthodians.

Environment. To assess whether levels of completeness correlate with their depositional environment, we classified the information on the depositional settings of each specimen into benthic assemblage zones (BA). Benthic assemblage zones are categorized into fresh water (BA0); intertidal above typical wave base (BA1); shallow subtidal

and/or lagoon (BA2); deeper subtidal and/or reefs (BA3); middle to outer shelf (BA4 and BA5); and shelf margin toward the bathyal region (BA6) (Boucot & Janis 1983; Boucot & Lawson 1999; Sallan *et al.* 2018). While there is some inconsistency about the exact distinction between BA4 and BA5, we here consider BA4 as right at the limit of subtidal influence before getting into the deepest extremities of the shelf in BA5. Completeness scores were categorized into the benthic assemblage zones the specimens were deposited in. Additionally, completeness scores were divided into those from species obtained from marine or freshwater settings. The subdivided completeness scores were then compared to understand the impact of environmental taphonomic and preservational influences on the fossil record of acanthodians. Changes in average sea level through time were used as a sampling proxy for the environmental effect on acanthodian completeness. High sea levels have been previously proposed to lead to the expansion of marine environments and thus potentially increasing diversity and accumulation of fossiliferous sediments as well as habitat preservation (Sepkoski 1976; Peters 2005; Wall *et al.* 2009; Hannisdal & Peters 2011). Average sea level data was derived from Hannisdal & Peters (2011) who provided a composite Phanerozoic sea level reconstruction based on previous studies. For stages which were not represented in the reconstructions due to time bin resolution, we chose to use NA rather than an average of the sea level of the previous and next stage as sea level could potentially fluctuate quite drastically between time bins. After calculating initial sea level and completeness correlations, we subsequently excluded the two fragmentary specimens from the Kungurian and the two fragmentary OTUs from the Guadalupian for additional analyses as they could represent outliers. The lack of occurrence data together with substantial sea level changes as well as missing sea level data for most of the Permian may introduce a significant bias for the regression analyses and we argue that it is acceptable to exclude the four specimens for comparison.

2.2.4 Statistical analyses

The statistical analyses were performed in R v. 4.1.2 (R Core Team 2018). We largely follow the protocol of the most recent completeness studies in terms of statistical analyses (e.g., Brown *et al.* 2019; Cashmore & Butler 2019). Trends of completeness through time series were tested using linear regressions. Generalized least-squares regressions (GLS) with a first order autoregressive model (corARMA) were chosen as they reduce the chance of overestimating the statistical significance of the regression lines due to temporal autocorrelation. GLS were calculated using the function gls() in the R package nlme (Pinheiro *et al.* 2018). The time series and completeness scores were log-transformed prior to analysis, ensuring normality and homoskedasticity of residuals. For time bins with completeness values or taxonomic richness of 0 rather than NA, a value of 1 was added to allow the data series to be logged for subsequent analyses. Given that log(1) = 0 and the focus of these analyses lies on relative changes rather than absolute time bin values, we consider this approach appropriate for these analyses. Likelihood-ratio-based pseudo-R^2 values were calculated to determine the amount of variance explained by our GLS models using the function r.squaredLR() of the R package MuMIn (Barton 2018). GLS autoregressive models were used to make time series comparisons between completeness metrics through time as well as compare temporal changes in completeness to different combinations of potential explanatory variables (species richness, time bin length as well as stage midpoints and sea level). Similarly, we tested whether species richness through time correlates with any combinations of completeness scores, time bin length and stage midpoints and sea level. Stage midpoints were used to test for a general trend through time and time bin lengths were used to examine any effects of the variable time durations of the different stages. To measure how well the data fits the models while also taking the model's complexity into account, Akaike's information criterion (AICc) and consequently Akaike weights were calculated using the functions AICc() of the R package qpcR (Spiess 2018) and aic.w() of the R package phytools (Revell 2012).

Non-temporal pairwise comparisons of completeness values were calculated using non-parametric Mann-Whitney-Wilcoxon tests which assess the differences in standard deviations and medians of datasets. A variety of comparisons of median and standard deviation of SCM2 values were made between subsets of the original dataset, including the three subsets excluding isolated material, as well as subsets of the major acanthodian subgroups, comparisons with previously published vertebrate SCM2 values and geographical and environmental comparisons. For comparisons of more than two datasets/subsets, Kruskal-Wallis tests were performed which determine dominances of specific variables. The acanthodian completeness values were also compared to the published SCM2 data of other vertebrate groups, including sauropodomorphs (Mannion & Upchurch 2010; updated dataset by Cashmore *et al.* 2020), pelycosaurs (Brocklehurst & Fröbisch 2014), ichthyosaurs (Cleary *et al.* 2015), parareptiles (Verrière *et al.* 2016), plesiosaurs (Tutin & Butler 2017), bats (Brown *et al.* 2019) and theropods (Cashmore & Butler 2019).Time series plots were generated using the package ggplot2 (Wickham 2016) and completeness distribution plots (non-temporal) were generated using the package vioplot (Adler & Kelly 2020).

2.3 Results

2.3.1 Changes in acanthodian completeness through time

Mean skeletal (SCM2) and soft tissue (STCM2) completeness of acanthodians show highly consistent patterns to one another through time, with the STCM2 values (range between 0 and 92.6%) being slightly higher than the SCM2 (range between 3.8% and 60.6%) (Figure 2.2A, B). Mean completeness is lowest throughout the Silurian, rises throughout the Devonian and Carboniferous before reaching its maximum peak in the Asselian. There are no values in the Sakmarian and Artinskian but low mean SCM2 values are again recovered in the Kungurian up to the Capitanian where the last occurrences occur. Notable peaks include the Lochkovian (15.6% SCM2, 21% STCM2) and Givetian (19.6% SCM2, 27.2% STCM2) in the Devonian, the Bashkirian-

Moscovian (26.9-19.4% SCM2, 48.2-40.1% STCM2) in the Carboniferous and Asselian (60.6% SCM2, 92.6% STCM2) in the Permian. When taxa based on isolated scales are removed, overall mean SCM2 and STCM2 show slightly higher values throughout the Silurian and Devonian time bins but this difference diminishes in the Famennian. Mean values for the Carboniferous and Permian do not change considerably upon exclusion of isolated scale-based taxa. Excluding acanthodian taxa consisting of only isolated fin spines results in higher mean SCM2 and STCM2 values throughout almost all of the Palaeozoic time bins. The highest differences between original SCM2 and the subset excluding isolated fin spines can be observed in the Mississippian, specifically the

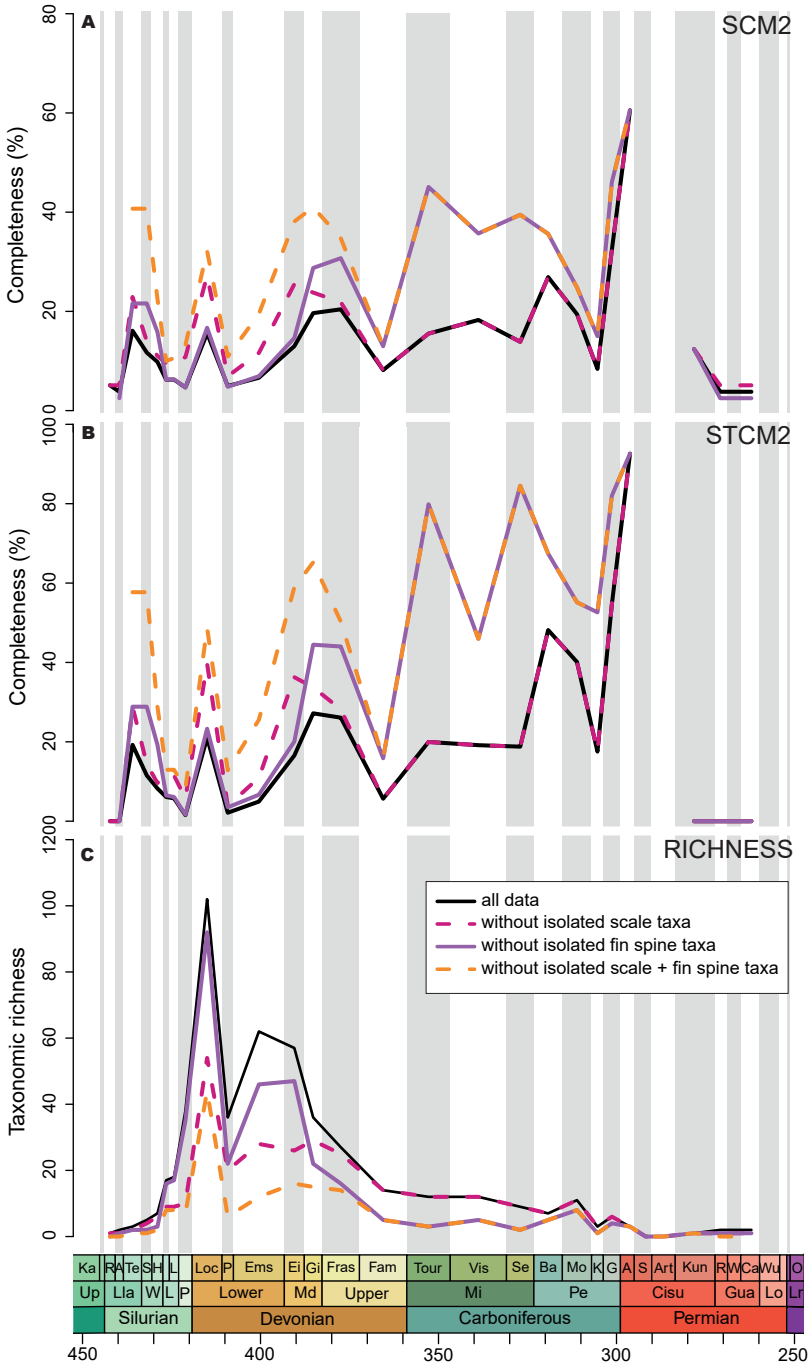


Figure 2.2: Changes in acanthodian completeness and raw taxonomic richness through time. A, mean skeletal completeness. B, mean soft tissue completeness. C, raw taxonomic richness.

Tournaisian and Visean, with over 20%. STCM2 values show notable peaks in the Telychian-Sheinwoodian (28.9%), Givetian (44.6%), Tournaisian (79.9%), Serpukhovian (84.5%) and Gzhelian-Asselian (82-92.6%). The highest difference between the original dataset and the STCM2 subset without fin spine taxa is in the Tournaisian with

about 60% higher values in the subset. Removal of isolated fin spine and isolated scale-based taxa yields the overall highest mean acanthodian skeletal completeness throughout the Palaeozoic, ranging between around 10 and 60.6%. STCM2 without isolated fin spine and isolated scale-based taxa has the highest values in the Silurian and Devonian, with highest overall peaks in the Telychian-Sheinwoodian (57.7%), Lochkovian (48.7%) and Givetian (65.2%). However, this subset then further shows the same pattern during the Carboniferous and early Permian compared to only excluding isolated fin spines.

When median acanthodian skeletal and soft tissue completeness values are calculated through time, they show similarly consistent patterns but are very different from the mean completeness curves (Figure A.2). Both median SCM2 and STCM2 stay at low levels throughout the Silurian, Devonian and Mississippian of the Carboniferous, with SCM2 values (range between 2.5% and 62.2%) offset to slightly higher values than STCM2 (range between 0 and 91.9%). Median completeness rises in the Bashkirian (20.7% SCM2, 79.7% STCM2) with a peak in the Moscovian (12% SCM2, 32.3% STCM2) before falling again in the Kasimovian and ultimately increasing to highest values in the Gzhelian-Asselian (28.8-62.2% SCM2, 70.9-91.9% STCM2) before dropping to low levels in the middle Permian. STCM2 values are higher than SCM2 values in these time bins. Excluding isolated scale-based taxa does not change the pattern of median SCM2 and STCM2 completeness for acanthodians except for some higher values in the later stages of the Silurian and Lower to Middle Devonian (maximum change from 0 to 26.9% STCM2 in the Lochkovian). When isolated fin spine-based taxa are removed from the dataset, both median SCM2 and STCM2 patterns change drastically. Median SCM2 rises and plateaus early on in the Silurian and then falls back to low levels throughout the Lower Devonian before rising again in the Givetian (33.7%). It dips again in the Famennian (4.8%) but increases throughout the Mississippian stages with values around 40% and the highest peak in the Asselian (62.2%, same as the other median SCM2 datasets). Median STCM2 shows notable peaks in

both the Telychian (28.9%) and Sheinwoodian (28.9%), Givetian (64.3%), Tournaisian (82.4%), Bashkirian (80.4%) and Asselian (91.9%), with a maximum change of values of about 82% within a stage compared to the original dataset. Removal of both isolated scale and fin spine-based taxa shows little variation in this scenario in both SCM2 and STCM2 for the later stages of the Palaeozoic. However, both median SCM2 and STCM2 values are higher in both the Silurian and Devonian with notable peaks in the Telychian-Sheinwoodian (40.7% SCM2, 57.7% STCM2), Lochkovian (34.4% SCM2, 51.4% STCM2) and the Eifelian-Givetian-Frasnian (41.6-43-42% SCM2, 71.6-75.2-68.7% STCM2) when both scale and fin spine-based acanthodian taxa are excluded. Mann-Whitney-Wilcoxon tests show significant differences between both the distributions of original SCM2 and STCM2 values and the different corresponding SCM2 and STCM2 subsets except for total SCM2/STCM2 and SCM2/STCM2 subset 2 excluding isolated fin spine taxa which is non-significant (Table A.1). There is a significant correlation of full acanthodian SCM2 with time bin length but the strength of the model is low ($p = 0.0352$; $R^2 = 0.22$) (Table A.2). A wider time bin results in higher levels of SCM2. Total STCM2 of acanthodians significantly correlates with taxonomic richness through time ($p = 0.017$; $R^2 = 0.39$) but also shows a low model fit, however, the richness coefficient is recovered as significant in all of the models within which it is included (Table A.3). Higher soft tissue completeness is recovered in time bins with lower taxonomic richness. SCM2 time series are best explained by the GLS models including sea level, time bin length + sea level and stage midpoints + sea level with high model fits but none of the coefficients are significant in any model. Similarly, STCM2 time series are best explained by the GLS models including sea level, richness + sea level and time bin length + sea level with high model fits but only the taxonomic richness coefficient is significant in the second model.

2.3.2 Correlations with taxonomic richness

Raw taxonomic richness of acanthodian species is initially low in the first stages of the Silurian and steeply rises from the Pridoli into the Lower Devonian with a maximum peak in the Lochkovian (121 species) (Figure 2.2C). Richness then falls in the Pragian but rises to a relative peak again in the Emsian before gradually sinking throughout the Middle and Upper Devonian, staying at a consistently low level throughout most of the Carboniferous, and then slightly decreasing again towards and into the Permian. Removing either isolated scale, isolated fin or both isolated scale and fin spine-based taxa does not substantially change the general pattern of acanthodian richness through the Palaeozoic. Species counts are reduced to lower values, especially when isolated scale-based taxa are excluded but peaks still occur in the Lochkovian and Emsian. There is a significant trend towards lower values through time in raw taxonomic richness throughout the Palaeozoic when STCM2 is used as the explanatory variable ($p = 0.008$; $R^2 = 0.90$). None of the other explanatory variables have a significant relationship with raw richness (Table A.4). The models that best explain the acanthodian taxonomic diversity time series include STCM2 ($R^2 = 0.90$; AIC weight = 0.18), sea level + STCM2 ($R^2 = 0.97$; AIC weight = 0.36) and SCM2 + STCM2 ($R^2 = 0.90$; AIC weight = 0.06) as explanatory variables with only the STCM2 coefficient being significant in all three models.

2.3.3 Differences between skeletal and soft tissue completeness metrics

The SCM values show a slight offset towards higher median values compared to the STCM while STCM has higher individual percentages of completeness than SCM2 (Figure A.3). A time series comparison of both metrics using GLS analyses shows a significant positive correlation ($p < 0.0001$, $R^2 = 0.96$). Non-temporal Mann-Whitney-Wilcoxon tests show that there is a significant difference between the observed acanthodian SCM2 and STCM2 values ($W = 71753$, $p = 5.8 \times 10^{-29}$) as well as

SCM1 and STCM1 values (W = 71633, p = 1.1 x 10^{-28}) (Table A.5). When comparing both variants of the completeness metrics, neither SCM1/SCM2 nor STCM1/STCM2 are significantly different from each other when Mann-Whitney-Wilcoxon tests are used, confirming results from previous studies. We additionally calculated the relative percentages of each of the acanthodian body region divisions to quantify how well they are represented in our dataset. Scales and fin spines together make up about 60% of the skeletal regions in the whole dataset while the neurocranium (3.1%), hyoid and gill arch (3.2%), teeth (2.9%) and vertebrae (0.1%) are the least likely to be recovered in the acanthodians investigated (Figure 2.3A). If both isolated scales and fin spines are removed, the relative percentages of each skeletal region approximately triple in quantity, with the scapula (38.9%) and Meckel's cartilage (25.5%) predominantly represented. For the soft tissue regions, the main body is preserved in 33.2% of taxa while the intermediate fin or fins and the pectoral fins are only present in about 0.3% and 1.3% respectively (Figure 2.3B).

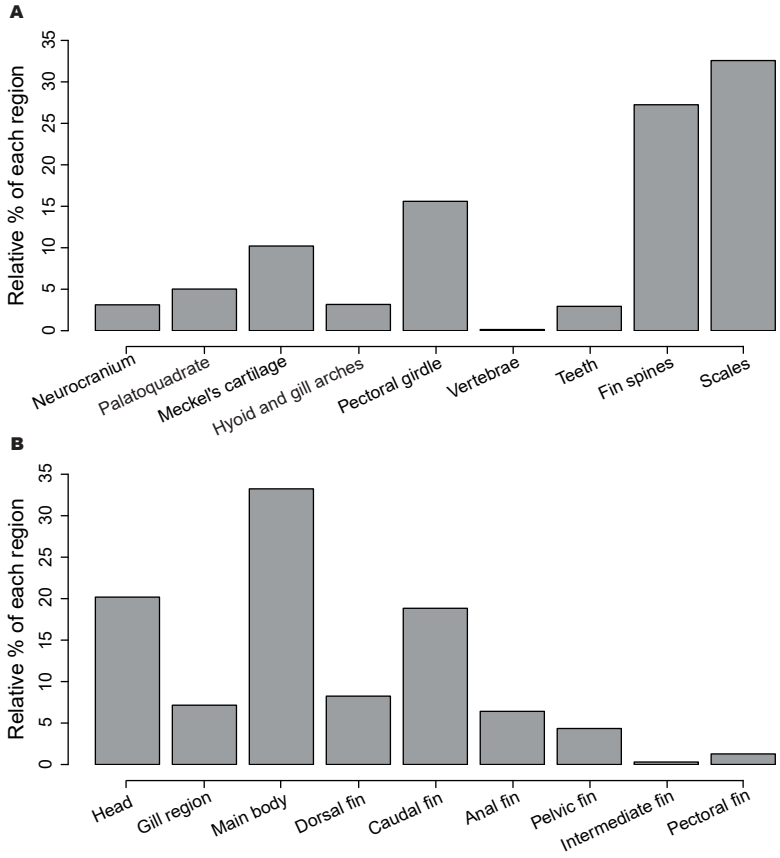


Figure 2.3: Relative percentage distributions of the different body regions used in the dataset. A, skeletal regions. B, soft tissue regions.

2.3.4 Acanthodian subgroups

Acanthodiformes have the widest distribution of SCM2 values with the highest median (42.5%) and interquartile range compared to any of the other subgroups (Figure 2.4A). Incerti sedis have the next highest SCM2 distribution with 5.1%. The remaining subgroups all have similar SCM2 distribution patterns and similar medians and interquartile ranges ($<$5%). Both Kruskal-Wallis and Mann-Whitney-Wilcoxon tests show that there is a significant difference between the subgroups (H = 47.477, p = 4.54E-09), with the latter demonstrating that there is a significant difference between SCM2 value distribution of Acanthodiformes and the other subgroups as well as between Diplacanthiformes and Climatiidae and Incerti sedis and Climatiidae (Table A.6). Removal of isolated fin spine taxa does not change the distribution of SCM2 values much (Figure A.4C, Table A.7). When isolated scales and isolated fin spines are ex-

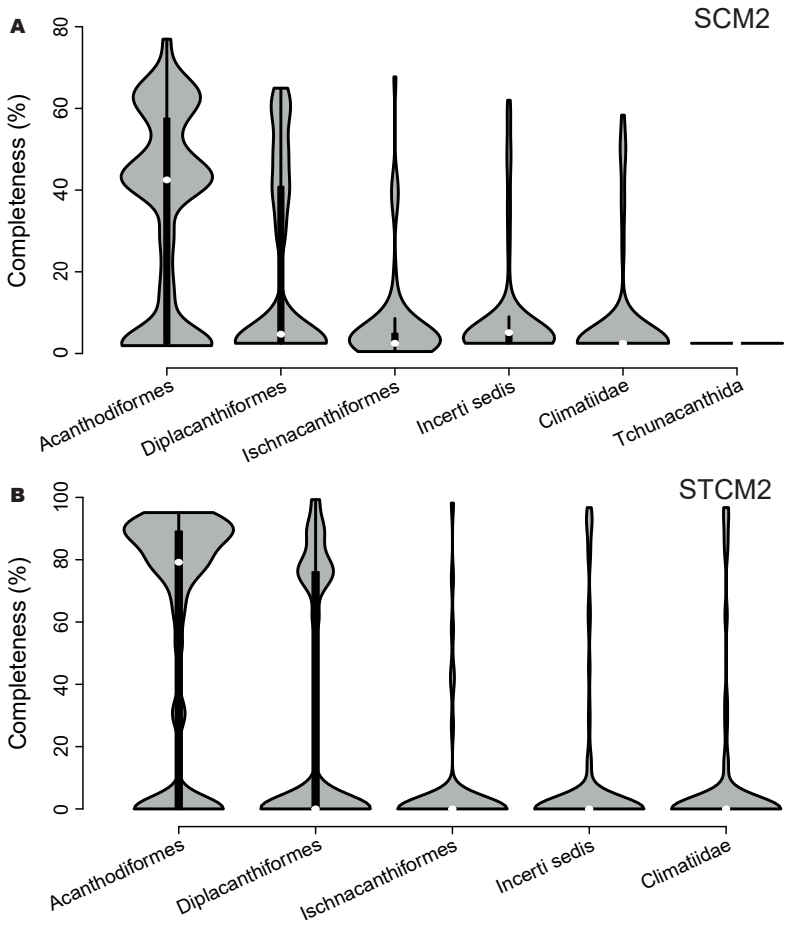


Figure 2.4: Distribution of completeness between different acanthodian subgroups. A, skeletal completeness. B, soft tissue completeness.

cluded, median SCM2 of diplacanthiform (39.8%), Incerti sedis (27.5%) and climatiid (29.7%) subgroups are considerably higher than the original dataset (Figure A.4E). While a Kruskal-Wallis test still confirms a significant difference between the distribution of SCM2 values (H = 38.251, p = 9.95E-08), Mann-Whitney-Wilcoxon tests do not recover a significant difference in SCM2 values between acanthodiforms and diplacanthiforms when taxa based on isolated scales and fin spines are excluded (Table A.8). Exclusion of only isolated scale-based taxa shows a similar pattern except for the Incerti sedis subgroup which is considerably lower (5.1%) and identical to the original dataset values Figure A.4A, Table A.9).

STCM2 distributions of acanthodian subgroups show a similar completeness pattern to the SCM2 (Figure 2.4B). Acanthodiforms have the highest median STCM2

(79.2%) and interquartile range, whereas all other subgroups have similar low ranges (median of 0%). A Kruskal-Wallis test suggests a significant difference between the subgroups (H = 90.024, $p < 2.2E\text{-}16$). Pairwise Mann-Whitney-Wilcoxon tests of the distribution of STCM2 values show a significant difference between acanthodiforms and the other subgroups just as with SCM2 (Table A.10). Diplacanthiform STCM2 is significantly different from Ischnacanthiformes, Incerti sedis and climatiids. Tchunacanthida do not show any soft tissue completeness in their fossil record. Upon removal of isolated fin spine and scale-based taxa, distribution of STCM2 values changes considerably for diplacanthiform (75.9%), Incerti sedis (45%) and climatiid (31%) subgroups while ischnacanthiforms (0%) are not affected (Figure A.4F). While Kruskal-Wallis tests are still significant (H = 44.09, p = 6.15E-09), Mann-Whitney-Wilcoxon tests no longer detect a significant difference between acanthodiform and diplacanthiform STCM2 (Table A.11). Acanthodiforms are still significantly different from ischnacanthiforms, Incerti sedis and climatiids as well as diplacanthiforms are from ischnacanthiforms. Ischnacanthiform STCM2 values are also significantly differentiable from Incerti sedis and climatiid subgroups. When only isolated scale-based taxa are removed, a similar pattern to the dataset without fin spines and scales is recovered (Figure A.4B, Table A.12). As with SCM2, exclusion of isolated fin spine-based taxa does not considerably change the distribution of STCM2 values (Figure A.4D, Table A.13).

2.3.5 Comparison to other vertebrate groups

Distribution of acanthodian median SCM2 scores in comparison to other vertebrate groups is considerably lower, with the exception of bats (Figure 2.5). Both SCM2 values for acanthodians and bats are concentrated at around 0-20% with more extreme distributions than any other vertebrate groups examined. A comparison using Mann-Whitney-Wilcoxon tests however still show a highly significant difference between acanthodian and bat SCM2 values (Table A.14). Even though total STCM2 values of acanthodians are considerably higher than their SCM2 values, STCM2 val-

ues are still significantly lower than the other vertebrate groups including bats (Figure A.5A, Table A.15).

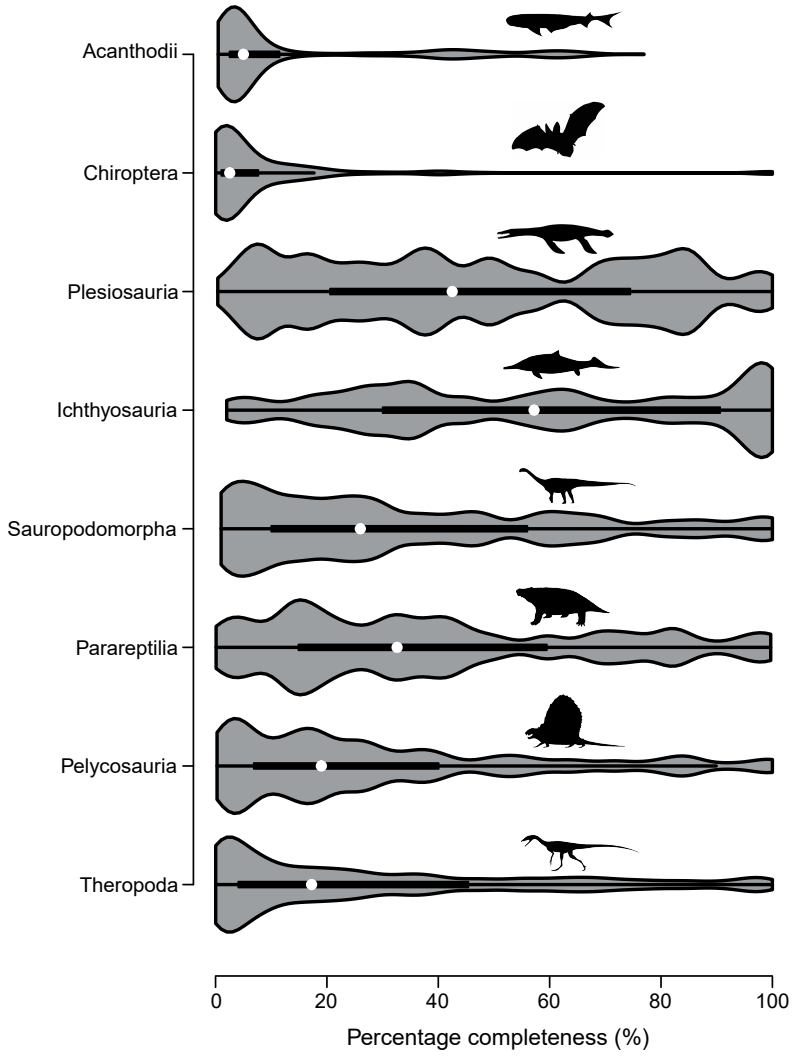


Figure 2.5: Distribution of acanthodian SCM2 values compared to other vertebrate groups. Comparative values from bats (Brown *et al.* 2019), plesiosaurs (Tutin & Butler 2017), ichthyosaurs (Cleary *et al.* 2015), sauropodomorphs (Mannion & Upchurch 2010; Cashmore *et al.* 2020), parareptiles (Verrière *et al.* 2016), pelycosaurs (Brocklehurst & Fröbisch 2014) and theropods (Cashmore & Butler 2019). Silhouettes were taken from http://phylopic.org/ and include work by N. Tamura (acanthodian), G. Monger (ichthyosaur), S. Hartman (plesiosaur), all CC BY 3.0, Smokeybjb (sauropodomorph), Karkemish (vectorized by T. M. Keesey) (parareptile) and D. Bogdanov (pelycosaur), all CC BY-SA 3.0, and S. Hartman (theropod) and Y. Wong (chiropteran), all CC0 1.0.

Violin plots show that median scores for acanthodian SCM2 (5%) are much lower than the scores for plesiosaurs (42.5%), ichthyosaurs (57.2%), sauropodomorphs (21.5%), theropods (17.2%), parareptiles (32.6%) and pelycosaurs (19%) but show a

similar score distribution to bats (2.5%). The interquartile range of acanthodians is also narrower than in these groups and comparable to bat SCM2. If isolated scales and fin spines are excluded from the dataset, acanthodian SCM2 scores are more evenly distributed throughout and median values as well as interquartile range are comparable to sauropodomorph, parareptiles and pelycosaurs (Figure A.5D, Table A.16).

2.3.6 Geographic comparisons

Taxon distribution is highly uneven between the different continents, with highest numbers in Europe (164), North America (68) and Asia (68), intermediate to low in Australia and Oceania (17) and South America (9), and lowest in both Antarctica (5) and Africa (2). For geographical completeness, acanthodian species from northern hemisphere localities were compared to southern hemisphere localities, with non-significant Mann-Whitney-Wilcoxon results for both SCM2 (W = 4170, p = 0.12) and STCM2 (W = 4958, p = 0.95) and very similar distribution patterns (Figure 2.6).

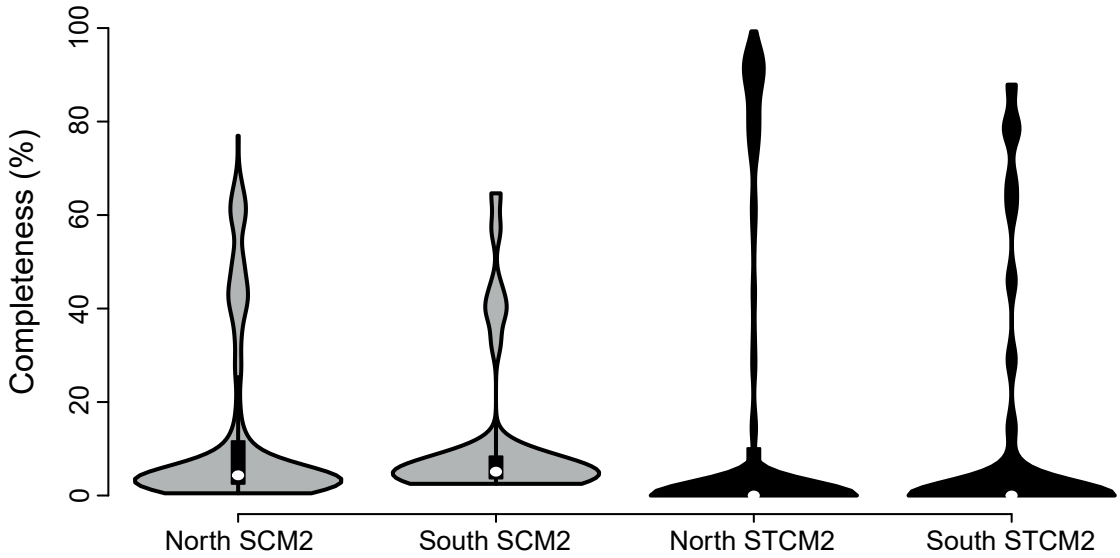


Figure 2.6: Distribution of acanthodian SCM2 (grey) and STCM2 (black) scores between the northern and southern hemispheres.

When SCM2 and STCM2 are categorized into continents, the range of values

do not vary substantially between most of the continents. Kruskal-Wallis tests however indicate a strong domination of variance of completeness distribution by at least one of the continents for both SCM2 (H = 29.3, p = 5.34E-05) and STCM2 (H = 18.495, p = 0.005). Europe and North America have the highest SCM2 (max. values of 77% vs. 68.3%) and STCM2 (max. values of 98.2% vs. 99.3%) ranges whereas Africa has the highest overall median SCM2 (24.6%) and Antarctica the highest overall median STCM2 (5.4%) (Figure 2.7). Taxa from South America have the least complete record with the lowest range for both SCM2 and STCM2 but the median values are similar to the other continents (5.1% SCM2, 0 STCM2). SCM2 values vary significantly between Europe and North America, North America and Asia and weakly (no adjusted p-values) between South America and Africa, South America and Asia, and Africa and Asia (Table A.17). STCM2 values show a somewhat different pattern, with strongly significant differences between North America and Asia only and weakly significant values (no adjusted p-values) between Europe - North America, North America and South America, South America and Antarctica, and Asia and Antarctica (Table A.18).

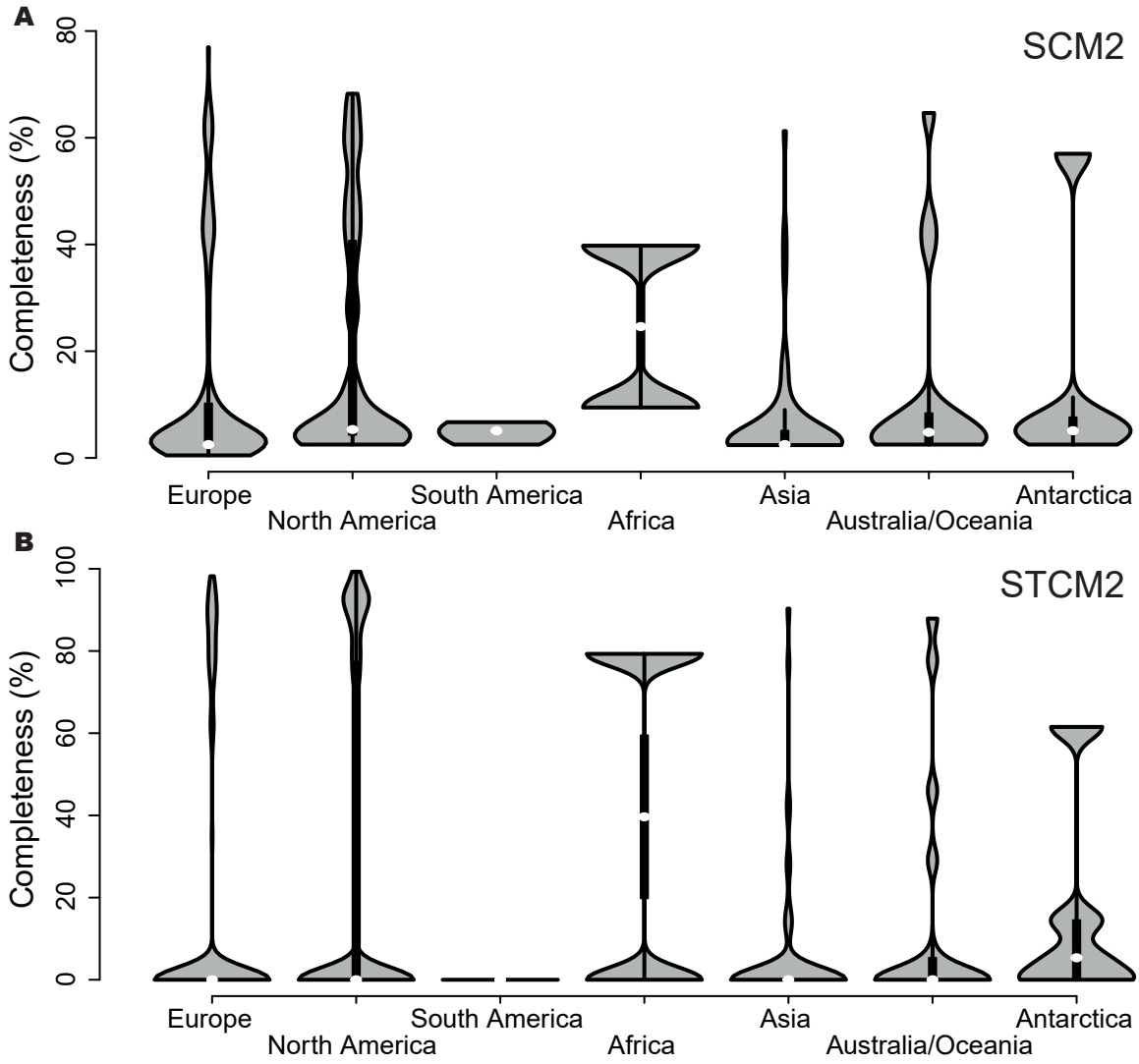


Figure 2.7: Distribution of acanthodian completeness between different continents. A, skeletal completeness. B, soft tissue completeness.

2.3.7 Depositional and environmental comparisons

SCM2 and STCM2 values are statistically different between acanthodian taxa from either freshwater or marine environmental settings (Table A.19). There is no difference between marine SCM2 and STCM2; however, there is a significant difference between freshwater SCM2 and STCM2. Specimens from freshwater deposits both have a higher median SCM2 as well as interquartile range than marine deposits while freshwater STCM2 values only show a higher interquartile range (Figure A.6). Mean

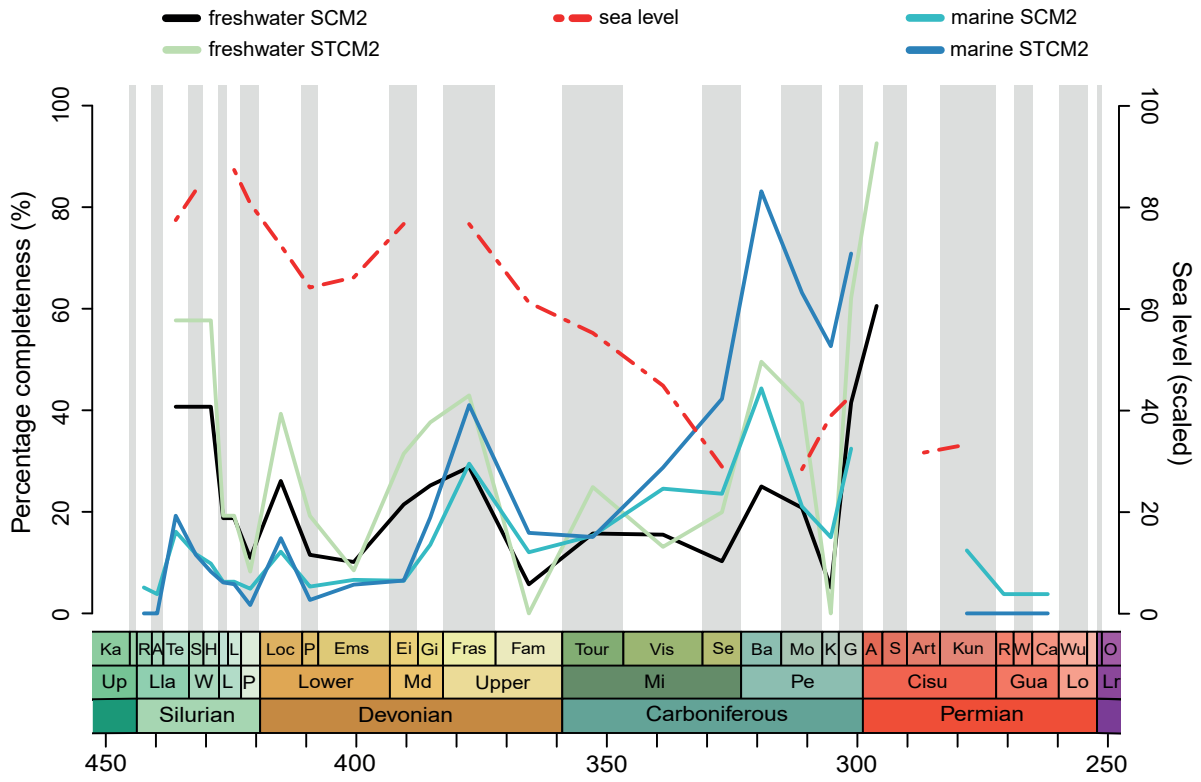


Figure 2.8: Changes in acanthodian completeness through time based on freshwater versus marine occurrences together with sea level changes. Sea level values represent arbitrary values taken from Hannisdal & Peters (2011).

temporal SCM2 and STCM2 based on taxa from freshwater deposits is initially higher throughout the Silurian and Lower to Middle Devonian compared to taxa from marine deposits (Figure 2.8). This pattern is then reversed in the Givetian-Frasnian and persists throughout most of the Carboniferous, with higher SCM2 and STCM2 values from marine sediments. It then reverts back to higher freshwater completeness in the Gzhelian and Asselian while the last occurrences in the late Cisuralian and Guadalupian come from marine deposits but only have very low completeness percentages.

For individual Benthic Assemblage zones (BA), Mann-Whitney Wilcoxon tests indicate a significant difference for SCM2 of taxa from BA0 compared to any of the other BA1-6 but only a weak signal between BA0 and BA2 (Table A.20). BA1 SCM2 is also significantly different from all of BA3, BA4 and BA6 and weakly BA5. The signal

for STCM2 is similar but not as clear as there are no significant differences between BA0 and BA1 and only a weak signal between BA0 and BA6 (Table A.21). There is, however, a significant difference between BA2 and BA4 and weakly BA2 and BA3 as well as BA2 and BA5. Subsequent Kruskal-Wallis tests further suggest that there are significant differences in SCM2 (H = 29.167, p = 5.66E-05) and STCM2 (H = 28.046, p = 9.21E-05) completeness distributions between the different BAs, with one or more dominating. GLS pairwise comparisons further show significant relationships between each BA0-4 SCM2 and total SCM2 as well as each BA0-BA4 STCM2 and total STCM2 through time (Tables 2.1, 2.2). Range of skeletal completeness of acanthodians is lowest in BA6 and range of soft tissue completeness is lowest in both BA5 and BA6 environments (Figure A.7). Violin plots of both SCM2 and STCM2 show similar distribution patterns for all BAs, with only a slightly wider top distribution in BA0.

Table 2.1: Results of pairwise comparisons between BA and total acanthodian SCM2 using GLS. Statistically significant results indicated in bold.

Comparison	Slope	t-value	p-value	R^2
BA0 SCM2 ~total SCM2	1.1	9.4	$<$**0.0001**	0.86
BA1 SCM2 ~total SCM2	0.65	4.5	**0.0002**	0.72
BA2 SCM2 ~total SCM2	1.1	5.2	**0.0001**	0.76
BA3 SCM2 ~total SCM2	0.94	4.2	**0.0005**	0.65
BA4 SCM2 ~total SCM2	0.87	3.0	**0.0083**	0.55
BA5 SCM2 ~total SCM2	0.19	0.71	0.50	0.12
BA6 SCM2 ~total SCM2	-0.18	-1.8	0.13	0.61

Table 2.2: Results of pairwise comparisons between BA and total acanthodian STCM2 using GLS. Statistically significant results indicated in bold.

Comparison	Slope	t-value	p-value	R^2
BA0 STCM2 ~total STCM2	0.64	2.6	**0.016**	0.24
BA1 STCM2 ~total STCM2	0.87	7.6	$<$**0.0001**	0.80
BA2 STCM2 ~total STCM2	1.1	5.8	$<$**0.0001**	0.72
BA3 STCM2 ~total STCM2	0.88	4.7	**0.0001**	0.65
BA4 STCM2 ~total STCM2	0.72	2.9	**0.0097**	0.52
BA5 STCM2 ~total STCM2	0.19	0.57	0.58	0.18
BA6 STCM2 ~total STCM2	-0.55	-1.0	0.36	0.41

Mean SCM2 and STCM2 by BA through time shows the low completeness of BA6 being restricted to the upper Silurian and Devonian (Figure 2.9). Interestingly, there is a peak of 46% in STCM2 of acanthodians from BA 6 in the Gorstian-Ludfordian. A similar low pattern to BA6 is observed for BA5. Acanthodian completeness in BA3 and BA4 zones is initially low throughout the Silurian and Devonian but heavily increases at the Devonian-Carboniferous boundary and plateauing at ~60% SCM2 and ~90% STCM2 throughout the Mississippian and into the early Pennsylvanian. Time series of mean SCM2 and STCM2 of taxa deposited in BA1 closely resemble the patterns observed in BA2 throughout the Palaeozoic. The biggest difference (maximum of 20%) between BA1 and BA2 are found in the Serpukhovian-Bashkirian for SCM2 and STCM2. A low record for BA1 is recovered again from the lower Permian Kungurian stage alone and for BA3-4 from the Roadian to the Capitanian.

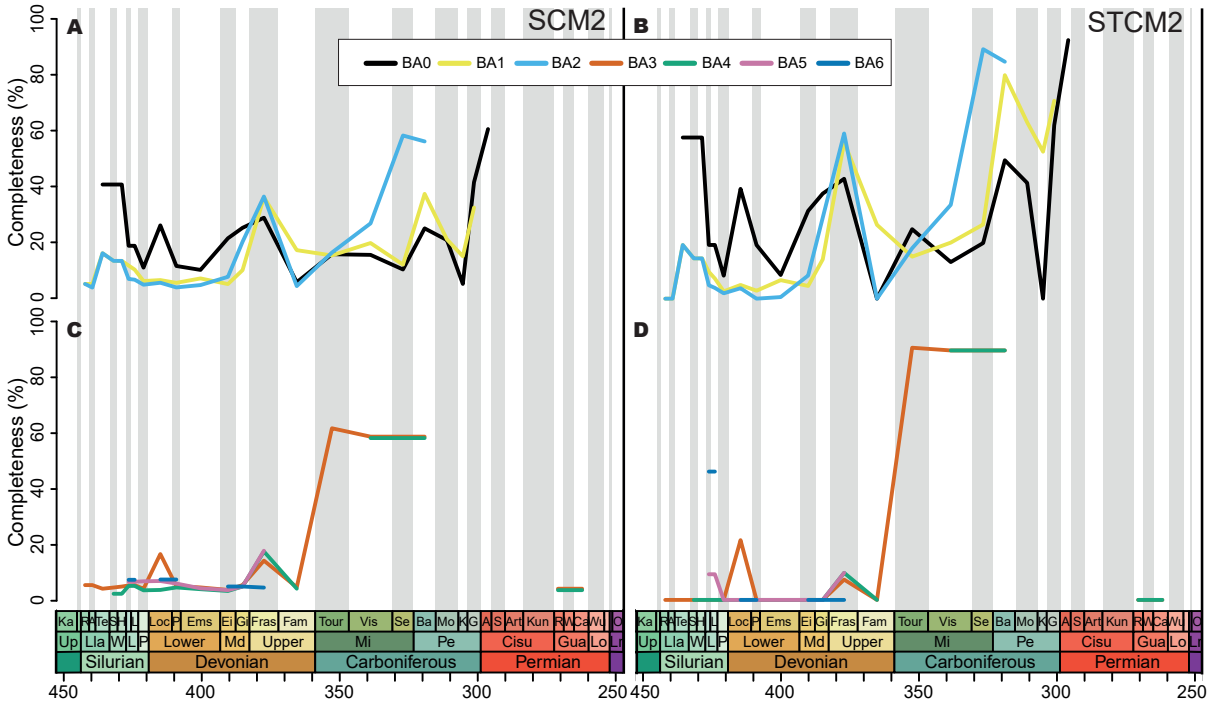


Figure 2.9: Changes in acanthodian completeness through time based on Benthic Assemblage (BA) zones. A, skeletal (SCM2) and B, soft tissue (STCM2) completeness of BA0 to BA2. C, skeletal (SCM2) and D, soft tissue (STCM2) completeness of BA3 to BA6.

2.3.8 Sea level correlations

Average sea level throughout the Palaeozoic does not significantly correlate with any of the completeness metrics or raw taxonomic richness, even when the completeness scores from marine and freshwater deposits are separated (Table A.22, Figure 2.8). However, on removal of the two fragmentary specimens from the Kungurian and the two OTUs from the Guadalupian, average sea level significantly correlates with total SCM2 and STCM2, as well as raw taxonomic richness (Table 2.3). When the data is divided into marine and freshwater completeness, marine SCM2 and STCM2 both recover significant relationships with sea level through time whereas freshwater SCM2 and STCM2 show non-significant correlations. All significant correlations between acanthodian completeness and sea level are negative, showing that acanthodian total SCM2 and STCM2, marine SCM2 and marine STCM2 are higher during

lower sea level through time and decrease when sea level rises.

Table 2.3: Results of pairwise comparisons for sea level trends in different time series using GLS excluding the Permian outliers. Statistically significant results indicated in bold.

Comparison	Slope	t-value	p-value	R^2
total SCM2 ∼sea level	-0.65	-2.3	**0.034**	0.80
total STCM2 ∼sea level	-0.39	-3.8	**0.0083**	0.83
marine SCM2 ∼sea level	-1.1	-3.1	**0.0075**	0.75
marine STCM2 ∼sea level	-0.86	-3.6	**0.0015**	0.82
freshwater SCM2 ∼sea level	0.52	1.7	0.12	0.62
freshwater STCM2 ∼sea level	0.16	0.74	0.47	0.96

2.4 Discussion

The earliest unambiguous acanthodians are recovered from sediments of early Silurian in age (Lower to Middle Llandovery) but consist of exclusively isolated scales and fin spines (Karatajūtė-Talimaa & Smith 2003; Valiukevičius & Burrow 2005; Burrow 2011). Throughout the Silurian, the acanthodian fossil record remains fragmentary with the exception of partially articulated individuals of one ischnacanthiform species, *Nerepisacanthus denisoni* (Burrow 2011). From the Lower Devonian Lochkovian onwards, the record expands significantly with several articulated acanthodian species found from localities in North America, Europe and Asia, next to the abundance of taxa known from isolated remains. This pattern continues throughout the Devonian and most of the Carboniferous. Towards the end of the Carboniferous and early Permian, several of the last known species in the acanthodian record are preserved as partly articulated and exceptionally complete skeletons; all are referred to the genus *Acanthodes*. The overall record of acanthodians, however, is reflected in their overall low completeness distribution here, with the bulk of taxa ranging between 2.5 and 10% skeletal completeness and 0 and 5% soft tissue completeness (Figure

A.3).

2.4.1 Completeness metrics comparisons

The quality of the acanthodian fossil record can be assessed differently depending on whether the skeletal or soft tissue completeness metrics is used. There is a significant difference between the distributions of skeletal completeness metric values and soft tissue completeness metric values for acanthodians. The STCM2 values have an increased interquartile range and distribution of acanthodian completeness scores compared to the SCM2 values, indicating that there is more variation of completeness in the soft tissue regions than the skeletal regions (Figure A.3). SCM2 has a higher overall median value compared to STCM2. In the time series, mean and median soft tissue completeness is slightly higher than skeletal completeness. The observed differences between the two metrics might be explained by a wide lack of preservation of specific skeletal regions in acanthodians, namely the vertebrae, neurocranium and branchial arches (Figure 2.3). As expected, soft tissue imprints of the head, main body and caudal fin were more commonly found in both partially articulated and articulated acanthodian specimens while imprints of the pectoral, pelvic and intermediate fins were regularly absent. However, the skeletal and soft tissue completeness metrics also positively correlate with each other through time, indicating that either one of these two could be used to accurately score completeness patterns of acanthodians. Thus, incorporating soft tissue completeness instead of or complimentary to skeletal completeness may broaden the applicability of the completeness methods to the fossil record of other groups, both vertebrate and invertebrate. Nevertheless, preservation of soft tissue components are unevenly spaced in the fossil record (Allison & Briggs 1993) and soft tissue completeness might be restricted to specific groups with a wide range of soft tissue preservation to allow quantitative analyses through time.

In comparison to total SCM2 and STCM2, the three subsets excluding isolated skeletal material (scales and/or fin spines) yield an overall higher mean completeness

through time while the general patterns and peaks are retained (Figure 2.2). While the overall spikes and drops in completeness are recovered in all of the subsets, mean completeness is considerably lowered by the inclusion of the isolated parts. STCM2 seems to be more heavily affected by limited material than SCM2, with subsets without isolated fin spines and scales leading to differences of up to 60% in mean completeness in specific stages through time, specifically the Tournaisian and Serpukhovian. This is not surprising as these isolated remains of skeletal origin result in a scoring of 0 in terms of soft tissue completeness and therefore may strongly decrease mean completeness through time. Identical curves of total SCM2 and the subset without isolated scale-based taxa as well as the subset without isolated fin spine-based taxa and the subset without both isolated scale and fin spine-based taxa in the Carboniferous can be explained by a lack of isolated scale-based taxa and a high number of isolated fin spine-based taxa during that time period.

Our results show how isolated remains such as scales and fin spines influence our interpretation of the acanthodian fossil record and potentially bias the completeness patterns we observe. While it has been argued that the inclusion of isolated elements could still contain important information on the taphonomic drivers of preservation (Driscoll *et al.* 2018), there are other potential drivers that have to be taken into account. Acanthodian species are predominantly named and assigned to higher level taxa on the basis of isolated scales and fin spines, potentially resulting in taxonomic 'over-splitting' at species and genus levels (42.81% isolated scale-based, 18.73% isolated fin spine-based species in our dataset) while a consistent application of a genus and species-level concept is yet to be established. One prominent example is the histological type genus *Nostolepis*, which was characterised based on histological structure rather than morphology of the scales (Gross 1947), and is known from isolated scales recovered from localities worldwide. Specimens of that genus were frequently erected into new species throughout the 20th century and subsequently transferred into different genera by Valiukevičius & Burrow (2005). The number of species, however,

was not significantly reduced and their validity is pending future investigations. Similarly, the genus *Gyracanthus* was originally erected based on ornamented isolated fin spines (Agassiz 1837). These spines range from the Lower Devonian to Upper Carboniferous and contain a multitude of species, some of which may well be synonymous (Denison 1979; Snyder *et al.* 2017). The Palaeozoic shark genus *Ctenacanthus* is also described based on isolated fin spines, specifically their ornament patterns along the fin spine ridge, and is subjected to synonymy and doubtful validity of the genus as is (Maisey 1981; Maisey 1984; Ginter *et al.* 2010). This synonymy reduces the utility of a clade record, as has been recognised for pelycosaurs (Brocklehurst & Fröbisch 2014), among many other instances. As our subset comparisons show, datasets excluding such skeletally limited material strongly increase estimates of acanthodian fossil record quality. The causes for this likely result from a combination of biases rather than a single factor but 'over-splitting' likely plays an important role in the observed trend.

2.4.2 Taxonomic group comparisons

We found significant differences between the skeletal and soft tissue completeness distributions of Acanthodiformes and all other subgroups (Figure 2.4). We excluded the Tchunacanthida for the statistical analyses between the subgroups as the limited distribution of only isolated scales within two single species resulted in analysis errors. Acanthodiformes have a significantly higher median skeletal and soft tissue completeness value as well interquartile range and show a visually different distribution to all other subgroups. All other subgroups exhibit a bottom heavy skeletal and soft tissue completeness distribution with few highly complete taxa. Interestingly, the Incerti sedis subgroup shows a similar total SCM2 and STCM2 distribution to the well-defined acanthodian subgroups such as Ischnacanthiformes or Diplacanthiformes. This suggests that levels of completeness cannot be solely argued to be a limiting factor for resolving the taxonomic issues of the taxa within this group as other acanthodian groups

show similar distributions of completeness while being taxonomically well resolved.

Acanthodiformes have been prominently featured in previous anatomical and phylogenetic assessments of skeletal characters, some of which are rarely found in other acanthodian subgroups (e.g., detailed neurocranial structures, remains of vertebrae and unusually complete hyoid arch and gill skeletons) as well as having more extensively perichondrally ossified endoskeletons compared to other acanthodian groups (Miles 1970; Miles 1973a; Beznosov 2009). Thus, their high levels of completeness are not surprising. Some of the most complete acanthodiform taxa, notably the completely articulated skeletons of *Acanthodes confusus*, *A. gracilis*, and *A. bronni* (Heidtke 2011), have been found in the late Carboniferous and early Permian shortly before the group's extinction, indicating a potential sampling bias where younger sediments have had less time to be destroyed by geological processes (see e.g. Raup 1972; Jablonski *et al.* 2003, Sahney & Benton 2017).

Removal of isolated scale-based taxa does significantly increase the overall completeness of diplacanthiform acanthodians with a high number of taxa in the 40-60% skeletal completeness as well as 60-95% soft tissue completeness ranges. This highlights a potential discrepancy in the fossil record of this subgroup with species being erected on the basis of either very limited material or almost complete skeletons. The lack of a well-sampled fossil record and an abundance of highly complete skeletons for any of the other subgroups has implications for understanding the evolutionary development of acanthodians as a clade in general and their morphology and ecology in particular.

2.4.3 Vertebrate group comparisons

Comparisons of completeness between acanthodians and other marine vertebrate groups such as Mesozoic plesiosaurs and ichthyosaurs illustrate a large discrepancy between clades living in similar environments. Plesiosaur and ichthyosaur skeletal completeness records exhibit the highest overall and median skeletal completeness

scores of all tetrapods published to date. These results are probably a consequence of similarities in preservation and coexistence in respective habitats (Cleary *et al.* 2015, Tutin & Butler 2017). Acanthodians, however, while also living in aquatic environments, show very low overall and median scores but are also considerably older than any of the other published vertebrate groups. This study represents the first thorough account of quantitative completeness analyses in Palaeozoic vertebrates. As there is currently no published data on the distribution of skeletal completeness of any other fish group, Palaeozoic or otherwise, it is difficult to compare groups from truly similar ecological niches and assess whether the low completeness scores are reflected in those groups as well. Fish groups like Palaeozoic actinopterygians might provide a worthwhile, but rather large and challenging, data set for comparison.

Acanthodians show a significantly lower skeletal completeness distribution than most of the tetrapod groups previously studied, but show a similar distribution shape relative to bats (Figure 2.5). Comparisons between acanthodians and bats reveal a significant difference between the two groups, with bats showing a slightly lower median completeness than acanthodians when total SCM2 is used. This is reversed when the subset without isolated scales and fin spines is used (Figure A.5D). Both groups show an abundance of isolated skeletal remains compared to partially articulated or articulated specimens which contributes to their poor skeletal completeness records (Brown *et al.* 2019).

2.4.4 Geographical impacts

Acanthodian fossils are recovered from all continents (Figure 2.7). We did not recognise significant differences or strong spatial biases between acanthodian completeness from the northern and southern hemisphere and the different continents (Figure 2.6). Surprisingly, Africa has the highest median SCM2 record and Antarctica the highest median STCM2 record even though the number of recovered taxa is low for both continents (Figure 2.7). This means that the relatively small number of

taxa obtained from those continents yield comparatively high skeletal or soft tissue information. The Waterloo Farm locality in the Witpoort Formation (South Africa) most notably yields fossils with exceptional preservation of soft tissue outlines in fine-grained anoxic sediments (Gess & Whitfield 2020), which can explain the high STCM2 scores. However, given the small sample sizes, this may be the result of sampling bias rather than an environmental or ecological bias and is difficult to establish for now.

There is a considerable difference in the number of taxa distributed between the different continents, with ten times more taxa from the northern compared to the southern hemisphere, which is most likely related to a higher historical collection effort and interest. While collection effort has yielded a considerably higher number of taxa from the northern hemisphere, the completeness records of both hemispheres are very similar, meaning that a comparatively smaller number of taxa from the southern hemisphere contain similar levels of completeness to the taxonomically richer records from the northern hemisphere. Thus, the presence of localities with rich acanthodian records such as MOTH (Canada) (Hanke & Wilson 2004), the 'Old Red Sandstone' (United Kingdom) (Miles 1973a; Brazeau 2009) or the Meisenheim Formation (Germany) (Heidtke 2011) in the northern hemisphere do not result in considerably higher SCM2 or STCM2 distribution as might have been expected. However, given the low number of taxa discovered from the southern compared to the northern hemisphere, it is likely that there is a considerable amount of undiscovered information on the acanthodian fossil record that could play an important role in widening our understanding on both acanthodian completeness and macroevolution.

The significant difference in SCM2 values between Europe and North America (Figure 2.7) is interesting given the heightened historical collection effort and interest within and between both continents that has been documented from other taxonomic groups (see e.g., Bernard *et al.* 2010; Brocklehurst *et al.* 2012; Cleary *et al.* 2015; Brown *et al.* 2019; Cashmore & Butler 2019, Cashmore *et al.* 2020). While there has been a high number of isolated scale-based taxa published from European localities

and especially the Baltics (e.g., Gross 1973; Valiukevičius & Karatajūtė-Talimaa 1986; Valiukevičius 2003, Pinakhina & Märss 2018) which might partially explain the lower median values for Europe, the causes for this are unknown. South America has the lowest acanthodian record of any of the continents which is in accordance with previous investigations highlighting the scarcity and discontinuity of the continent's Devonian vertebrate record (Gagnier *et al.* 1988; Maisey *et al.* 2002; Janvier & Maisey 2010). South America also currently provides very limited fossil evidence in terms of acanthodian diversity and skeletons beyond disarticulated spines and scales which provides something of a conundrum given that much of South America's fauna was suggested to be dominated by chondrichthyans and acanthodians during Devonian times (Janvier & Maisey 2010).

2.4.5 Environmental and ecological biases

Skeletal and soft tissue completeness of acanthodian species was highest in freshwater deposits (Figure A.6, Table A.19), suggesting that the best-preserved fossils are found in these types of environments. Some of the high completeness scores for freshwater acanthodian taxa most likely derive from lake deposits such as the Old Red Sandstone of Scotland where the anoxic conditions within the deeper, stratified parts of Lake Orcadie protected material from scavenging, weathering and decay (e.g. Donovan 1975; Burrow 1996; Dineley & Metcalf 1999). These lacustrine environments are generally characterized by low energy conditions (Rust 1982) where a lack of transport and physical disturbance may prevent disarticulation of skeletons. Conversely, fluvial depositional settings are generally associated with higher energy levels of transportation before burial (Behrensmeyer 1988; Evans 2016) which can impact the completeness of specimens preserved in these sediments. Our results, however, also suggest a high completeness of acanthodians from fluvio-lacustrine settings, specifically towards the end of the Carboniferous and early Permian. These are predominantly associated with deposits from the intermontane Saar-Nahe Basin in Germany where volcanic ash

fallout deposition together with fluvio-lacustrine dominated settings (Königer & Stollhofen 2001) may have led to a higher preservation potential of acanthodian skeletons.

Median acanthodian skeletal completeness is significantly lower for specimens from marine sediments compared to freshwater environments (Figure A.6, Table A.19). One possible explanation for the observed lower completeness in marine deposits may be the strong influence of physical processes acanthodian skeletons are subjected to in these environments, resulting in taphonomic modification through mechanical damage as well as a preservational bias against small and fragile elements (Boessenecker *et al.* 2014). Additionally, marine shelf environments may be less likely to develop dysoxic or anoxic conditions than restricted basins and lake environments which may lead to increased occurrences of scavenging and disturbance. However, while there have been attempts to determine if taphonomic processes are equivalent in different aquatic environments, including freshwater versus marine (Kidwell 1986; Cummins 1994), currently much of these comparisons remain uncertain.

Environmental and lithological information was used to assign acanthodian fossils to benthic assemblage zones to infer how specific environments impact the acanthodian fossil record rather than only looking at completeness of acanthodians from freshwater and marine sediments. Earlier in the present work, it was shown that acanthodians from non-marine deposits exhibit the highest level of overall completeness (Figure A.7). Within the marine realm, BA1 and BA2 exhibited the most consistent patterns throughout the Palaeozoic, ranging through all stratigraphic stages and closely track each other (Figure 2.9). This is perhaps not surprising as these juxtaposed intertidal and shallow subtidal environments are often coupled in interpretations of lithostratigraphic units and our results may derive from limitations in resolution between the two environments. Skeletal and soft tissue completeness of acanthodians throughout the Palaeozoic is comparatively higher in BA1 and BA2 environments than BA3-6 (Figure 2.9) suggesting that tidal flats, strandlines and subtidal lagoons yield higher levels of preservation and articulation than the deeper marine environments.

Notably, highest completeness was found in acanthodians from the Glencartholm Volcanic Member and the Mazon Creek locality where conditions of quick burial, low oxygen and low pH in nearshore, shallow bay type environments, in part representing death assemblages, allowed the fish bodies to remain intact after death (Baird 1979; Schram 1983; Dineley & Metcalf 1999; Clements *et al.* 2019). Fossils of the Glencartholm and Mazon Creek biotas have indeed been previously compared to show similar modes and details of preservation (Schram 1983; Briggs & Gall 1990). In shallow lagoon settings such as shelf lagoons, barriers commonly provide protection from the open sea (Fürsich *et al.* 2016) and can potentially prevent disarticulation by wave action or currents. Furthermore, environmental stress arising from elevated or fluctuating salinity values and decreased oxygen concentrations (Fürsich *et al.* 2016) could play a role in protecting carcasses from scavenging, weathering and decay. However, tidal flats can also be disrupted by physical constraints such as cyclic deposition of alternating sand and mud or the extremes of intertidal zones translating into poor preservation (Gao 2009; Davis 2012). However, the high levels of acanthodian completeness from BA1 and BA2 throughout the Palaeozoic suggest that these physical constraints may have only played a minor role during deposition.

Acanthodians from BA3 and BA4 (middle to outer shelf, reef settings as well as subtidal dynamic environments) zones show generally low completeness scores throughout the Silurian and Devonian but increase heavily in the Mississippian and early Pennsylvanian (Figure 2.9). This spike is surprising but can possibly be explained by a combination of environmental deposition and sampling bias. Only two species of acanthodians are present in the Carboniferous BA3 and BA4 and both belong to the genus *Acanthodes* which is known to be one of the most complete acanthodian taxa to date (Nelson 1969; Miles 1973b; Heidtke 2011; Davis *et al.* 2012). Additionally, the records for the Mississippian and lower Pennsylvanian BA3 and BA4 derive from two lithostratigraphic intervals, the Russian Lower Os'kin Subformation and the North American Heath Formation Lagerstätte, where individuals were rapidly buried in wide

shallow-water elevated salinity environments as such warm water settings would have otherwise led to rapid decay and disarticulation (Lund *et al.* 1993; Hagadorn 2002; Beznosov 2009).

The correlations between benthic assemblage zones BA0-4 and BA1 through BA4 SCM2/ STCM2 and total SCM2/ STCM2 suggest that they all play a significant role in the completeness of acanthodians and consequently our understanding of their fossil record (Tables 2.1, 2.2). Zones BA5 and BA6 do not significantly contribute to total SCM2 and STCM2 and completeness of specimens from these environments is very low. This is congruent with a general lack of acanthodians from deeper water settings shown in our dataset. Acanthodian occurrence in the deeper water BA5-6 settings is restricted to the late Silurian up until the Upper Devonian and is characterised by low specimen numbers and completeness values. Whether this absence from deeper water environments represents a true ecological signal, a preservational bias or a sampling bias due to limited rock outcrop availability remains unresolved for now.

Marine acanthodian completeness negatively correlates with average sea level, with higher completeness percentages at intervals when sea level is lower (Figure 2.8, Table 2.3). This negative slope is recovered when using the entire dataset but p-values are not significant for any of the correlations. Upon removing the four fragmentary specimens of the late lower and middle Permian, all of the relationships between total SCM2/STCM2 as well as marine SCM2/STCM2 and sea level are quantified as significant with the negative correlation remaining as observed before. We argue that these late occurrences thus represent outliers in the dataset and together with the absence of other occurrences in the majority of the Permian heavily skew the correlations and were thus removed for a subsequent analysis on the overall influence of sea level on acanthodian completeness. Furthermore, two of the four fragmentary specimens could not be taxonomically assigned beyond Acanthodii (Mutter & Richter 2007) but had to be included as separate taxa as we cannot ascertain if they represent distinct taxa

and may be of great value to the acanthodian fossil record similar to operational taxonomic units (OTUs) in some nonavian theropod analyses (Cashmore & Butler 2019). This inclusion, however, may have also introduced a bias with regards to the sea level comparisons.

A negative relationship with sea level has also been reported for ichthyosaurs (Cleary *et al.* 2015), plesiosaurs (Tutin & Butler 2017) and even sauropodomorphs (Mannion & Upchurch 2010; Cashmore *et al.* 2020) but was absent in mosasaurs (Driscoll *et al.* 2018). Ostracoderms, osteostracans and non-psammosteid heterostracans have also been found to show an inverse proportional relationship between recovery potential of fossils and sea level (Sansom *et al.* 2015). This might be unexpected as deeper water environments are thought to favour better conditions for preservation than shallow waters due to less high-energy deposition, different physical constraints and less potential for scavenging and weathering (Allison *et al.* 1991; Driscoll *et al.* 2018). Additionally, sea level rise can lead to bottom waters and basins in deep shelf areas being placed below physical barriers leading to anoxic conditions (Leggett 1980; Sarmiento *et al.* 1988) that usually favour completeness of skeletons. However, this is not the case for acanthodians as completeness is significantly inversely proportional to sea level. The causes for this inverse relationship are difficult to ascertain and previous hypotheses on this relationship in ichthyosaurs are limited to likely habitat preferences and death locations (Cleary *et al.* 2015).

As for acanthodians, a combination of habitat availability (potential ecological biases) and lack of available rock volume (sampling biases) might explain at least some of the observed relationships. Information on acanthodian ecology and habitat preference is scarce and limited to the general environment of the deposits they were recovered from such as freshwater, marine, deltas, tidal flats, estuaries and lagoons (Denison 1979; Blais 2017). However, as our results indicate, a significant proportion of more complete acanthodian specimens are obtained from benthic assemblage zones in shallow waters which suggests, tentatively, a habit preference. In times of high

sea level, the availability of these shallow water environments could be minimised as deeper water facies shift onto the inner shelf during transgression (Smith *et al.* 2002; Armstrong & Harper 2014). During this shift, the rise of the chemocline onto the shelf may reduce habitable space (Brenchley *et al.* 2001). The spread of deeper water facies may lead to a reduction in prospective niche space for acanthodians which are rarely found in deeper water environments. However, there is a bias against available outcrop for marine deep-water sediments compared to the continental shelf (Gregor 1970; Smith *et al.* 2002), which may result in fewer acanthodian skeletons being sampled from deep water environments compared to shallow waters. This in turn may influence the observed negative correlation patterns between acanthodian completeness and average sea level. We could not find a significant relationship between freshwater acanthodian completeness and average sea level in any of the time series analyses, indicating that acanthodian skeletal preservation in freshwater environments is decoupled from sea level fluctuations.

2.4.6 Impact on phylogenetic assessments

Subsequent to Brazeau (2009) and Davis *et al.* (2012), who initially found large acanthodian subgroups branching from the chondrichthyan stem, most phylogenetic analyses of early gnathostomes over the past 10 years have placed all acanthodians on the chondrichthyan stem, therefore seemingly resolving the debate surrounding their overall taxonomic position (Zhu *et al.* 2013; King *et al.* 2016; Coates *et al.* 2018; Dearden *et al.* 2019; Frey *et al.* 2020; King & Rücklin 2020). However, relationships within the acanthodians are far from settled. Diplacanthiformes, Ischnacanthiformes and Acanthodiformes have been repeatedly recovered as well-resolved monophyletic orders, but this likely reflects output from related (serially modified) morphological datasets; meanwhile, resolution of the climatiids is persistently poor at best (see e.g. Burrow *et al.* 2016; Coates *et al.* 2018; Dearden *et al.* 2019). Such instability is even more evident in the multitude of species that were not referable to a taxonomic

rank beyond genus or family and were grouped into the Incerti sedis subgroup in our analysis, comprising a disturbingly large proportion (one-third of the species) in the dataset.

The craniocentric character sets employed for phylogenetic analyses contribute significantly to this lack of phylogenetic resolution (Davis *et al.* 2012, Zhu *et al.* 2013; Dupret *et al.* 2014; Brazeau & de Winter 2015; Giles *et al.* 2015; Long *et al.* 2015; King *et al.* 2016; Qiao *et al.* 2016; Zhu *et al.* 2016; Coates *et al.* 2018; Dearden *et al.* 2019). At least 65% of characters used in the data matrices are restricted to cranial features (including the jaws) whereas the postcranial skeleton comprises only 25% of characters, with the rest of the character list comprising histological properties that could be assigned to either cranial or postcranial skeleton. This is clearly problematic given our results on the relative percentages of the different skeletal regions in acanthodians, but difficult to avoid because of the data-rich skeletal and dental systems in vertebrate heads. In our entire dataset, the neurocranium represents less than 4% of recovered skeletal regions (Figure 2.3). The palatoquadrate takes up 5% and the Meckel's cartilage 10%. In marked contrast, the 'character-poor' postcranial skeleton is recovered in over 80% of preserved skeletal regions in acanthodians. Our results emphasize how the currently used craniocentric character lists for phylogenetic analyses of acanthodians, chondrichthyans and early gnathostomes in general might be neglecting crucial information to better resolve the interrelationships of these taxa. However, postcranial data are limited and elusive, as exemplified by the still entirely unknown acanthodian pelvic skeleton.

Missing data are bound to diminish the quality of evolutionary hypotheses, ultimately resulting in loss of phylogenetic signal. Tests on a variety of datasets have shown that deletions of character information tend to result in stem-ward slippage (Sansom & Wills 2013). Thus, incomplete taxa are more prone to erroneously primitive placement in evolutionary trees. We do not propose that the set of least complete acanthodians harbours misidentified crown chondrichthyans. Nevertheless, the

present quantified assessment provides both a basis and a prompt for further investigation of errors likely besetting current macroevolutionary hypotheses of early chondrichthyan evolution.

2.5 Conclusions

1. The acanthodian fossil record is mainly derived from isolated remains, including isolated scales and fin spines. Complete skeletons are rare.

2. Acanthodian skeletal and soft tissue completeness fluctuates throughout the Palaeozoic, with notable peaks in the Lochkovian, Givetian, Bashkirian-Moscovian and Asselian. The Silurian record captures the lowest mean completeness scores.

3. Soft tissue completeness of acanthodians is higher than skeletal completeness but both metrics reveal similar completeness patterns through time. This indicates that either metric can be used to accurately quantify the fluctuating quality of the acanthodian fossil record.

4. Acanthodian skeletal completeness correlates, albeit weakly, with time bin length: higher levels of completeness are associated with wider time bins. Soft tissue completeness correlates significantly with raw richness through time.

5. Among all vertebrate groups investigated thus far, acanthodians have one of the poorest skeletal completeness records. With bats (that have a significantly poorer record) they share a similarly shaped distribution of SCM2 values that are mostly concentrated at around 0-20%.

6. Acanthodiformes exhibit significantly higher skeletal and soft tissue completeness compared to other major acanthodian subgroups.

7. There is no significant difference between acanthodian record metrics from the northern hemisphere compared to the southern hemisphere. However, taxon distribution is very uneven with higher numbers in the northern hemisphere which likely results from sampling and/or geological biases.

8. Acanthodian skeletal and soft tissue completeness from freshwater sediments is initially higher in the Silurian and the Lower to Middle Devonian. Between the Givetian and Frasnian, a transition to more complete fossils from marine sediments occurs which lasts throughout most of the Carboniferous before reverting back to higher freshwater completeness in the Gzhelian and Asselian shortly before their extinction.

9. Acanthodian skeletons deposited in freshwater environments are significantly more complete than in marine environments. This probably results from preservation under anoxic conditions (e.g. stratified lakes) and low turbulence. Soft tissue completeness, however, does not recover this trend. 10. Average sea level correlates significantly with skeletal and soft tissue completeness derived from marine but not freshwater deposits. The relationship is negative, with higher completeness recovered during times of low sea level. This pattern is consistent with previous reports on ichthyosaurs, plesiosaurs and sauropodomorphs and may be subject to both ecological and sampling biases.

CHAPTER 3

THE COMPLETENESS OF THE PALAEOZOIC CHONDRICHTHYAN FOSSIL RECORD

My contribution to this work involved conducting all parts of the research, including data collection, data analysis, interpretation of results and manuscript writing. The methodology was co-designed by my colleagues and myself. I. Sansom shared environmental data for Benthic Assemblage zone (BA) assignments. My colleagues provided feedback on the interpretations of the results and earlier versions of the manuscript. As in Chapter 2, the editorial "we" is used here to reflect these contributions.

3.1 Introduction

Chondrichthyans (elasmobranchs and chimaeroids) are a highly successful class of predominantly predatory fishes. They originated and first diversified in the Palaeozoic and persist until the present day (Janvier 1996; Stein *et al.* 2018). Extinct and extant chondrichthyans show adaptations to different habitats in both freshwater and marine environments, occupying various ecological niches (e.g., Zangerl 1981; Compagno 1990; Ebert & Winton 2010). Chondrichthyan remains have been collected

from all continents, highlighting their varied temporal and spatial distribution. Most notably, chondrichthyans possess an endoskeleton consisting mainly of cartilage rather than bone (Dean & Summers 2006; Dean *et al.* 2009; Maisey *et al.* 2020) which has traditionally been considered to represent the ancestral condition for jawed vertebrates while endochondral bone is an osteichthyan apomorphy (Donoghue *et al.* 2006; Friedman & Brazeau 2010; Brazeau & Friedman 2014). New fossil discoveries and revisions of gnathostome phylogenetic hypotheses (e.g., Zhu *et al.* 2013; Zhu 2014; Giles *et al.* 2015; Brazeau *et al.* 2020) have led to a reappraisal of a number of features of chondrichthyan skeletonization as ancestral to other jawed vertebrates. Notably, these include the presence of endochondral and perichondral bone in 'placoderm'-like fishes from Mongolia (Brazeau *et al.* 2020), further supporting a secondary loss of bone tissue in chondrichthyans (Miles 1973; Maisey 1986; Zhu *et al.* 2013; Giles *et al.* 2015).

The early history of chondrichthyans has undergone major revision in recent years but is strongly influenced by the poor quality of their fossil record due to the fragility of their predominantly cartilaginous skeletons (e.g., Maisey & Anderson 2001; Miller *et al.* 2003; Janvier & Maisey 2010; Maisey *et al.* 2017; Coates *et al.* 2018; Frey *et al.* 2020). Evidence of chondrichthyans potentially dates back to the Middle to Upper Ordovician, consisting of isolated scales of putative chondrichthyan origin (Young 1997; Sansom *et al.* 2001; Sansom *et al.* 2012; Andreev *et al.* 2015; Andreev *et al.* 2016). However, both isolated teeth and articulated specimens of undoubtedly chondrichthyan origin are found only from the Early Devonian onwards (e.g., Mader 1986; Maisey & Anderson 2001; Ginter *et al.* 2010; Maisey *et al.* 2019), with a major diversification event occurring in the Carboniferous (Sallan & Coates 2010). The recognition of the acanthodians, a group of Palaeozoic spiny fusiform fishes, as a grade of the chondrichthyan stem-group, has partially filled the stratigraphic gap in the Silurian (e.g., Brazeau 2009; Davis *et al.* 2012; Coates *et al.* 2018; Dearden *et al.* 2019). However, uncertainty remains as how the quality of these fossil remains might impact on patterns of diversity and phylogenetic relationships. Adding to this, the nature and

quality of the chondrichthyan fossil record has not been quantified to date.

While the fossil records of all groups are the fundamental sources of data for palaeontology, they are subject to inconsistent preservation on a variety of spatial, temporal, taxonomic and environmental scales (e.g., Newell 1959; Raup 1972; Foote & Raup 1996; Foote & Sepkoski 1999; Kidwell & Holland 2002). Biases resulting from geological, anthropogenic and taphonomic processes are commonly recognized to significantly influence observed patterns of diversity and fossil record quality (e.g., Raup 1976; Alroy *et al.* 2001; Peters and Foote 2001; Smith 2007a; Alroy *et al.* 2008). The influence of sampling and collector biases on our understanding of macroevolutionary changes and patterns of diversity through time has been highlighted in recent years (e.g., Barnosky *et al.* 2005; Hunter & Donovan 2005; Tarver *et al.* 2007; Vilhena & Smith 2013; Wagner & Marcot 2013; Benson *et al.* 2016; Close *et al.* 2017). A common approach to addressing fossil record quality involves estimating fossil specimen quality by assessing levels of fossil specimen completeness. Initially, this was implemented using relatively simple methods, that were subsequently expanded and refined (Benton *et al.* 2004; Fountaine *et al.* 2005; Smith 2007b; Benton 2008a, b; Beardmore *et al.* 2012a, b). The most comprehensive approach was developed by Mannion & Upchurch (2010) and consists of two completeness metrics that precisely quantify the completeness of individual specimens and species. These metrics measure either the absolute proportions of the preserved skeletons (relative to an estimated whole) or the phylogenetically informative characters of a species to assess the quality of their fossil record. Initially applied to sauropodomorph dinosaurs, subsequent studies have used these metrics to quantify fossil record completeness for several terrestrial (Brocklehurst *et al.* 2012; Walther & Fröbisch 2013; Brocklehurst & Fröbisch 2014; Dean *et al.* 2016; Gardner *et al.* 2016; Verrière *et al.* 2016; Davies *et al.* 2017; Brown *et al.* 2019; Cashmore & Butler 2019; Mannion *et al.* 2019; Cashmore *et al.* 2020) and marine vertebrate groups (Cleary *et al.* 2015; Tutin & Butler 2017; Driscoll *et al.* 2018), including acanthodian stem-chondrichthyans (Chapter 2, Schnetz *et al.* 2022 in press).

Here, we use modified versions of the previously published skeletal completeness metric (Mannion & Upchurch 2010; Beardmore *et al.* 2012a, b) to quantitatively examine the quality of the chondrichthyan fossil record for the first time. This work follows on from the preliminary assessment of the stem-chondrichthyan acanthodian completeness in Chapter 2, which we expand to the non-acanthodian, and consequently total-group, chondrichthyans from the Palaeozoic. Therefore, we exclude the acanthodian grade sensu Dearden *et al.* (2019) and Frey *et al.* (2020) for the initial analyses of chondrichthyan completeness and include the stem-group chondrichthyan taxa that more closely related to the chondrichthyan crown (e.g., *Pucapampella*, *Doliodus* and *Gladbachus*) to compare and contrast patterns with the previously published acanthodian grade. We arbitrarily define chondrichthyans as *Gladbachus* and all closer relatives of living chondrichthyans (the conventional chondrichthyans sensu Frey *et al.* 2020). We also include the Ordovician shark-like scale taxa *Solinalepis*, *Tantalepis*, *Canyonlepis* and *Tezakia* and the Silurian scale- and fin spine-based mongolepids, elegestolepids and sinacanthids, which may fall out with the acanthodians but are currently largely ignored in phylogenetic analyses of the total-group chondrichthyans (Sansom & Andreev 2017). The further aims of the current chapter are to correlate variations in completeness through geological time with potential palaeobiological and palaeoecological variables, including taxonomic richness, changes in sea level and depositional environment. We identify potential biases and highlight gaps that might affect the chondrichthyan fossil record by statistically comparing completeness values between different taxonomic groups, geographical regions, and depositional environments. These results are likely to guide future endeavours in resolving fossil record quality biased by missing data and add to our knowledge of factors likely to be shaping our perspectives on early chondrichthyan evolution.

3.2 Methods

3.2.1 Completeness metrics

The two most commonly used metrics for estimating the completeness of a fossil vertebrate skeleton are the character completeness metric (CCM) and the skeletal completeness metric (SCM) of Mannion & Upchurch (2010). CCM quantifies the number of phylogenetic characters attributed to each skeletal region in a given species and SCM measures the amount of the overall skeleton preserved in a given species. Both metrics were established with two variants: CCM1/SCM1, which establish the completeness of the most complete specimen for a given species or taxon, and CCM2/SCM2, which estimate completeness using all specimens of a given species or taxon (a composite of all investigated specimens). The latter variants have been preferred for both CCM and SCM in subsequent studies (see Brocklehurst *et al.* 2012; Dean *et al.* 2016; Verrière *et al.* 2016; Cashmore & Butler 2019; Cashmore *et al.* 2020, Chapter 2, Schnetz *et al.* 2022 in press), and these approaches are also used in this study.

Previous studies have shown a significant positive correlation between CCM and SCM in different vertebrate groups, suggesting that the metrics detect similar signals in fossil record quality (Mannion & Upchurch 2010; Tutin & Butler 2017). CCM is generally scored using the assumption that if one skeletal element is complete, all phylogenetic characters of that element can be assessed. As pointed out in Chapter 2, this correlation may hold true for the three-dimensionally preserved bones of the various previously studied tetrapod groups but is potentially problematic for groups with predominantly cartilaginous skeletons such as chondrichthyans as they are fragile and prone to fragmentation and erosion. It can result in a potential loss of informative characters on the skeletal element while the skeletal element by itself may still be mostly complete. Furthermore, chondrichthyans are often embedded in matrix, which can hide potentially informative characters from view, and the composition of this matrix

may preclude them from preparation methods (e.g., acid digestion) and limit the resolution gained by CT scanning. Considering these points, we follow Cashmore & Butler (2019) and Chapter 2 (Schnetz *et al.* in press (2022)) in assessing the quality of the chondrichthyan fossil record using SCM rather than CCM.

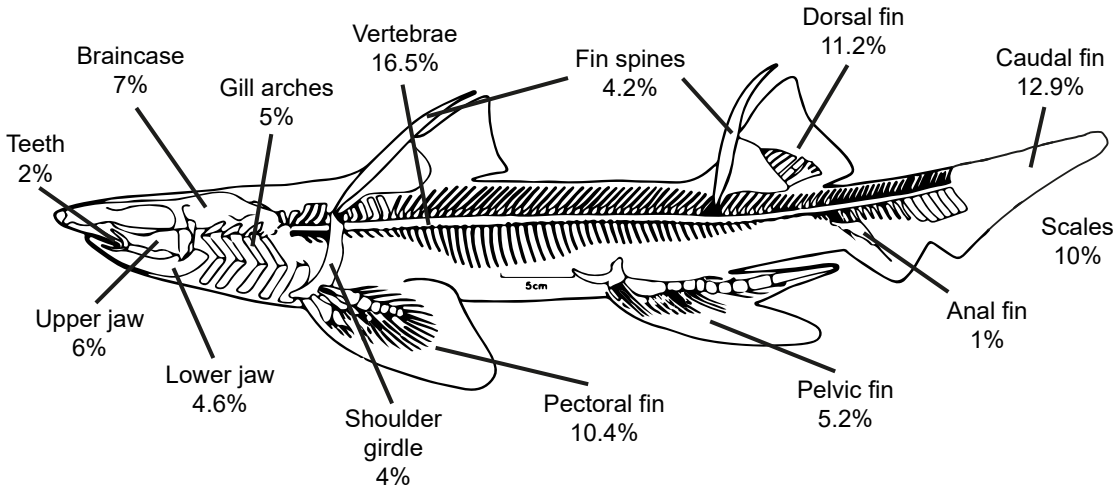


Figure 3.1: Skeletal reconstruction of *Tristychius arcuatus* Agassiz, 1837 (modified from Dick 1978), illustrating the mean skeletal proportions of chondrichthyan body exemplar 1.

We used a combination of the Mannion and Upchurch (2010) and Beardmore *et al.* (2012a, b) completeness metrics to calculate Palaeozoic chondrichthyan completeness, following the approach from Chapter 2 on the stem-chondrichthyan acanthodian grade. The completeness metric by Beardmore *et al.* (2012a,b) divides the body into equally weighted skeletal regions and uses an index of 0-4 to score the levels of completeness in each region, rather than scoring total numbers of individual bones as per the skeletal completeness metric (SCM) from Mannion and Upchurch (2010). Contrary to the original application of the SCM, assessing the relative percentage of the total skeleton made up by any individual bone within fossil fish specimens is not feasible. Thus, the skeleton was divided into 14 different anatomical regions, for each of which overall values between 0 (absent) and 4 (more than 75% complete) were assigned following the Beardmore's Skeletal Completeness Metric (BSCM) (Figure 3.1). Using this method, an isolated scale would receive an initial score of 1, while a chon-

drichthyan with more than 75% of the body covered in scales is given a score of 4. These regions were then assigned and corrected with a relative percentage based on how much of the total skeleton that region encompasses, following the SCM method. Detailed information on the scoring system and descriptions for each individual skeletal region is accessible in the supplementary material.

We divided the chondrichthyan skeleton into neurocranium, upper jaw, lower jaw, gill arches (including hyoid arch), vertebrae, pectoral girdle, dorsal fin, pectoral fin, pelvic fin (including pelvic girdle), anal fin, caudal fin, teeth, fin spines and scales. For utility and ease of scoring, skeletal regions were assigned broadly and are evaluated based on overall completeness rather than completeness of each singular anatomical element (those details would be captured more thoroughly by a CCM if the characters are used in current phylogenies). A degree of arbitrariness is especially present when coding up chondrichthyan dental system scores 2 and 3 compared to isolated teeth (1) and full dentitions (4) but should not considerably skew overall completeness patterns (see supplementary data for overall percentage scores of the different regions).

Chondrichthyans are known to exhibit a variety of body shapes, including the presence or absence of specific fins, a variable number or complete loss of fin spines and a dermis that is either predominantly naked or covered in scales which may result in a bias in relative proportions. To account for this, we estimated the relative proportions for eight chondrichthyan body exemplars that were assigned to the different taxa in the dataset depending on morphological fit (for more details on the definition of the different body exemplars, see supplementary information). The relative proportions of the different regions were determined by calculating their relative surface areas from published 2D reconstructions in Zangerl (1981) using the vector graphics software Inkscape (`https://inkscape.org/`). We calculated the skeletal proportions for representatives of eight chondrichthyan taxa from the literature: *Promexyele peyeri* Zangerl & Case, 1973, *Triodus sessilis* Jordan, 1849, *Cobelodus aculeatus* Cope, 1894, *Cladoselache fyleri* Newberry, 1889, *Stethacanthus altonensis* St. John & Worthen, 1875,

Tristychius arcuatus Agassiz, 1837, Ctenacanthidae Dean, 1909 and Hybodontoidea Zangerl, 1981 (see supplementary information and Zangerl 1981 for the reconstructions). The obtained proportions were then used to correct the initial 0 to 4 scores for each individual skeletal region before calculating the final SCM scores (ranging between 0 and 100%). The majority of chondrichthyan specimens are preserved in two-dimensional lateral compression. To account for this, we report completeness based on the side visible (assuming a similar preservation of the other side), following previous completeness studies (Cleary *et al.* 2015; Brown *et al.* 2019; Cashmore & Butler 2019; Chapter 2, Schnetz *et al.* 2022 in press).

3.2.2 Chondrichthyan completeness data

Dataset. In this study, we are following on from the work conducted in Chapter 2 (see also Schnetz *et al.* in press (2022)) on the completeness of the acanthodian grade and assess the completeness of the non-acanthodian stem-chondrichthyans and crown group chondrichthyans throughout the Palaeozoic. We compiled a dataset of 3021 specimens of Palaeozoic chondrichthyans, which is up to date as of August 2021 (see supplementary information for a full list of included genera and species). The final dataset contains 804 species and 287 genera of Palaeozoic chondrichthyans. Primary information was gathered from first hand observation of specimens during museum visits and augmented with information form the literature (both illustrations and text). Information on the lithostratigraphy (e.g., geological formation), geographical locality and chronostratigraphic age were recorded for each specimen together with their completeness scores. Additionally, palaeoenvironmental information was gathered from published sources where detailed lithostratigraphic descriptions for specimen occurrences were available. Taxonomic information from museum catalogues was checked for validity and corrected to the latest accepted taxonomic name and systematic position if applicable. Taxa were included based on the most recent taxonomic literature and reviews (e.g., Zangerl 1981, Stahl 1999, Ginter *et al.* 2010). We chose to re-

tain tooth-based taxa where taxonomic status is debated but has not been officially revised or considered a nomen dubium. As an example, the number of valid isolated tooth whorl species to represent distinctive species within several holocephalan genera, such as e.g., *Psephodus*, *Psammodus* or *Cochliodus*, has been debated but has yet to be formally revised and thus these remain as distinctive species in this dataset. We excluded species that could not be narrowed down to stage-level bin ages, as their inclusion in multiple time bins as a result of stratigraphic uncertainty would smoothen out the completeness distributions through time. The initial data was subdivided into two subsets, one excluding isolated tooth-based taxa and one excluding isolated tooth, scale and fin spine-based taxa and ran some of the analyses multiple times using each subset. Lastly, we added the acanthodian data from Chapter 2 to our non-acanthodian stem-chondrichthyans and crown group chondrichthyan data for some analyses to compare and contrast total-group chondrichthyan completeness patterns throughout the Palaeozoic with either dataset.

Time series. Temporal analyses and time series were conducted using stage-level time bins, starting from the Darriwilian (Middle Ordovician) up until the Changhsingian (Lopingian, upper Permian). Chronological ages, time bin lengths and stage midpoints were established in accordance with the latest information from the International Commission on Stratigraphy (IUGS) stratigraphic charts (v2020/03; Cohen *et al.* 2013). The resolution for the Pridoli (upper Silurian) had to be limited to an epoch-level time bin as there are currently no officially recognized stages within this epoch. We follow previous analyses in providing a stage-level resolution for completeness (e.g., Cashmore & Butler 2019; Cashmore *et al.* 2020; Chapter 2, Schnetz *et al.* 2022 in press), which is also the norm for most macroevolutionary and macroecological studies of the fossil record through deep time. Mean and median SCM2 completeness scores for each time bin were calculated using all taxa occurring within that time bin. Sampled-in-bin occurrences of specimens were used to determine the temporal range of individual taxa.

Taxonomic groups. To compare if completeness scores differ significantly within Palaeozoic Chondrichthyes, they were grouped into the following orders to assess differing levels of completeness on a finer scale: Altholepidiformes, Antarctilamniformes, Bransonelliformes, Chimaeriformes, Chondrenchelyiformes, Cochliodontiformes, Copodontiformes, Coronodontida, Ctenacanthiformes, Elegestolepidida, Eugeneodontiformes, Helodontiformes, Hybodontiformes, Iniopterygia, Menaspiformes, Mongolepidida, Omalodontiformes, Orodontiformes, Petalodontiformes, Phoebodontiformes, Polymerolepidiformes, Psammodontiformes, Sinacanthida, Symmoriiformes, Synechodontiformes, Xenacanthiformes and an informal Incerti ordinis subgroup. See supplemental information for details on which taxa were assigned to which order and supporting references were applicable. The Incerti ordinis subgroup is most likely a polyphyletic group as it contains a multitude of taxa that were not assigned to an order or family when assessed taxonomically. We use the Incerti ordinis subgroup here to illustrate the status of completeness of taxa within this group and measure the impact completeness may or may not have to resolve taxonomic issues.

Spatial correlations and Lagerstätten. Completeness scores were grouped by the present-day hemispheres and geographical regions in which they were collected, to assess if the chondrichthyan fossil record quality varies on a global scale. Palaeozoic chondrichthyans have been recovered from all modern-day continental regions, including taxa from Africa (18), Asia (78), Australia and Oceania (6), Antarctica (5), North America (456), South America (14) and Europe (297). The influence of Lagerstätten (sites of exceptional fossil preservation) can lead to biases in the overall trend of completeness of any given group through time (see previous completeness studies: Brocklehurst *et al.* 2012; Dean *et al.* 2016; Brown *et al.* 2019; Cashmore & Butler 2019; Cashmore *et al.* 2020). However, clearly defined Lagerstätten containing Palaeozoic chondrichthyans are limited to a few localities (e.g., the Bear Gulch and Mazon Creek biotas) and are unlikely to significantly bias the overall completeness patterns. We therefore follow the previously published completeness studies on other marine ver-

tebrates (Cleary *et al.* 2015, Tutin & Butler 2017; Driscoll *et al.* 2018; Chapter 2, Schnetz *et al.* 2022 in press) and do not separate taxa derived from concentration or conservation Lagerstätten for statistical comparisons.

Environment. We classified information on the depositional settings of each specimen into benthic assemblage zones (BA) to understand whether levels of completeness are influenced by the taphonomic, preservational and environmental processes they were deposited in. Benthic assemblage zones are categorized into fresh water (BA0); intertidal above typical wave base (BA1); shallow subtidal and/or lagoon (BA2); deeper subtidal and/or reefs (BA3); middle to outer shelf (BA4 and BA5); and shelf margin toward the bathyal region (BA6) (Boucot & Janis 1983; Boucot & Lawson 1999; Sallan *et al.* 2018). While there is some inconsistency about the exact distinction between BA4 and BA5, we here consider BA4 to be the limit of subtidal influence before getting into the deepest extremities of the shelf in BA5. Completeness scores for each taxon were subdivided between all benthic assemblage zones they were deposited in. Additionally, completeness of taxa was classified as originating from either freshwater or marine settings. Changes in average sea level through time were furthermore used as a sampling proxy for the environmental effect on chondrichthyan completeness. Average sea level data was derived from Hannisdal & Peters (2011) who provided a composite Phanerozoic sea level reconstruction based on previous studies. We excluded the value for the upper Wuchiapingian in the environmental analyses, which also represents the last sea level value for Palaeozoic data. We argue that this point represents an outlier which skews the correlations and distorts the patterns between sea level and completeness. There are very limited values for the middle and upper Permian stages (a total of two) in the reconstructions and there is a considerable drop in sea level between the two values. Data for the preceding and subsequent stages is missing and thus, this one value represents an extreme point compared to the rest of the Palaeozoic data.

3.2.3 Statistical analyses

All statistical analyses were performed in R v. 4.2.0 (R Core Team 2018). We largely follow the statistical protocols used in the most recent completeness studies (see e.g., Brown *et al.* 2019; Cashmore & Butler 2019; Cashmore *et al.* 2020; Chapter 2, Schnetz *et al.* in press 2022). Time series plots were generated using the package ggplot2 (Wickham 2016) and non-temporal completeness distribution plots were generated using the package vioplot (Adler & Kelly 2020). Linear regressions were used to test series of completeness trends through time. Generalized least-squares regressions (GLS) with a first order autoregressive model (corARMA) were performed as they reduce the chance of overestimating the statistical significance of the regression lines due to temporal autocorrelation. GLS were calculated using the function gls() in the R package nlme (Pinheiro *et al.* 2018). Time series were log-transformed prior to analysis, ensuring normality and homoskedasticity of residuals. Likelihood-ratio-based pseudo-R^2 values were calculated to determine the amount of variance explained by the GLS models using the function r.squaredLR() in the R package MuMIn (Barton 2018).

GLS autoregressive models were used to make time series comparisons between completeness metrics through time as well as compare temporal changes in completeness to multiple combinations of potential explanatory variables (species richness, time bin length, stage midpoints and sea level). Similarly, species richness through time was correlated to different combinations of potential explanatory variables (completeness scores, time bin length, stage midpoints and sea level). Stage midpoints were used to test for a general trend through time and time bin lengths were used to examine any effects of variable time durations of the different stages. We used NA for stages that were not represented in the sea level reconstructions by Hannisdal and Peters (2011) in order to calculate our regression analyses. To measure model fit of the data together with model complexity, Akaike's information criterion (AICc) and Akaike weights were calculated using the functions AICc() of the R package qpcR

(Spiess 2018) and aic.w() of the R package phytools (Revell 2012).

Non-parametric Mann-Whitney-Wilcoxon tests were used to perform non-temporal pairwise comparisons of completeness values by assessing differences in standard deviations and medians of datasets. For comparisons of more than two datasets/subsets, Kruskal-Wallis tests were calculated to determine any dominances of variables in the dataset. The chondrichthyan completeness values were additionally compared to the published SCM2 data of other vertebrate groups, including sauropodomorphs (Mannion & Upchurch 2010; updated dataset by Cashmore *et al.* 2020), pelycosaurs (Brocklehurst & Fröbisch 2014), ichthyosaurs (Cleary *et al.* 2015), parareptiles (Verrière *et al.* 2016), plesiosaurs (Tutin & Butler 2017), bats (Brown *et al.* 2019), theropods (Cashmore & Butler 2019) and acanthodians (Chapter 2, Schnetz *et al.* 2022 in press).

3.3 Results

3.3.1 Chondrichthyan completeness through time

Mean completeness is initially low within the Middle–Upper Ordovician and Silurian (2.1–3.5%), followed by slight increases through the Devonian ($\sim$ 3.2–7.8%) (Figure 3.2A). Completeness dips initially in the early Carboniferous but peaks in the Serpukhovian (16.2%), Moscovian (17.9%) and again in the Gzhelian–Asselian (19.2–20.2%) at the Carboniferous–Permian boundary. The remainder of the Permian exhibits lower levels of completeness except for a peak in the Wordian (18.5%) and a slight increase in completeness towards the end of the Permian. Excluding isolated tooth-based chondrichthyan taxa results in higher mean SCM2 values throughout most of the Palaeozoic time bins. SCM2 values do not change considerably in the Ordovician, Silurian and Lower–Middle Devonian but are overall 7–26% higher than the original dataset from the Upper Devonian onwards. The general patterns and peaks are retained except for a pronounced peak in the Gzhelian (40.2%), rather than in both the

Gzhelian and Asselian as in the original dataset. Removal of isolated tooth-, isolated scale- and isolated fin spine-based taxa yields the overall highest mean chondrichthyan skeletal completeness values of any subset throughout the Palaeozoic, ranging between 10 and 48%. In this subset there are no values for the Ordovician and Silurian, except for the Sheinwoodian.

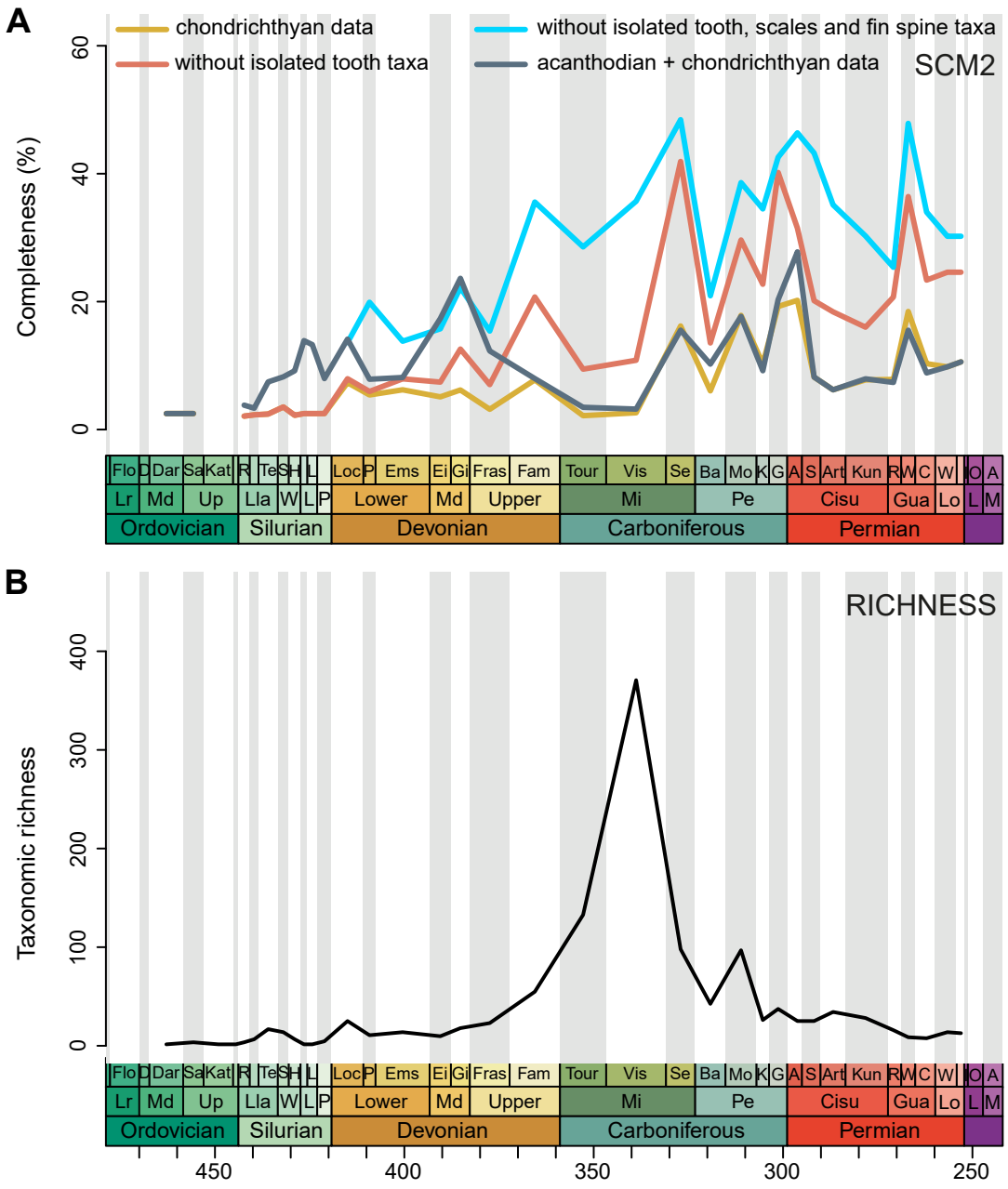


Figure 3.2: Changes in Palaeozoic chondrichthyan completeness and raw taxonomic richness through time. A, mean skeletal completeness. B, raw taxonomic richness (species level).

Median chondrichthyan SCM2 initially depicts similarly low values to mean SCM2 that range between 0.5% and 2.5% throughout the stages of the Palaeozoic (Figure B.1). No peaks or lows can be recovered. Excluding isolated tooth-based taxa from the chondrichthyan dataset alone greatly changes the median SCM2 completeness pattern for chondrichthyans through the Palaeozoic (Figure B.1). While completeness stays low throughout most stratigraphic stages, notable peaks are recovered in the Givetian (9.2%), Serpukhovian (32.7%), Moscovian (13.4%), Gzhelian (39.1%), Wordian (34%) and Capitanian (30.6%). Values remain higher in the uppermost stages of the Permian compared to the previous periods. Removal of isolated tooth-, isolated scale- and isolated fin spine-based taxa yields the overall highest median skeletal completeness values (Figure B.1). As observed in the mean completeness patterns, there is no data for the Ordovician and Silurian with the exception of the Sheinwoodian. Similar, albeit somewhat higher, peaks to the isolated tooth-based subset are recovered, with the addition of a pronounced peak in the Pragian (19.9%) and Asselian (44.9%).

The distributions of the total SCM2 values are significantly different from the two subsets (excluding isolated tooth-based taxa as well as excluding all isolated tooth, scale, and fin spine-based taxa) (Table B.1, Figure 3.3). Time series comparisons also show significant positive relationships between the original SCM2 values and SCM2 of all subsets (Table B.2). Additional GLS comparisons through time reveal a significant negative correlation between original chondrichthyan SCM2 and sea level ($p = 0.0086$, $R^2 = 0.80$) (Table B.3). Higher skeletal completeness is found in time bins with lower sea level. SCM2 time series are best explained by the three GLS models including sea level, including stage midpoints + sea level and including stage midpoints + richness + sea level (Table B.3). All three models have high strength (R^2), with the sea level coefficient in model 4 being significant and the stage midpoint coefficient in model 9 ($p = 0.0255$) and 10 ($p = 0.0475$) being significant.

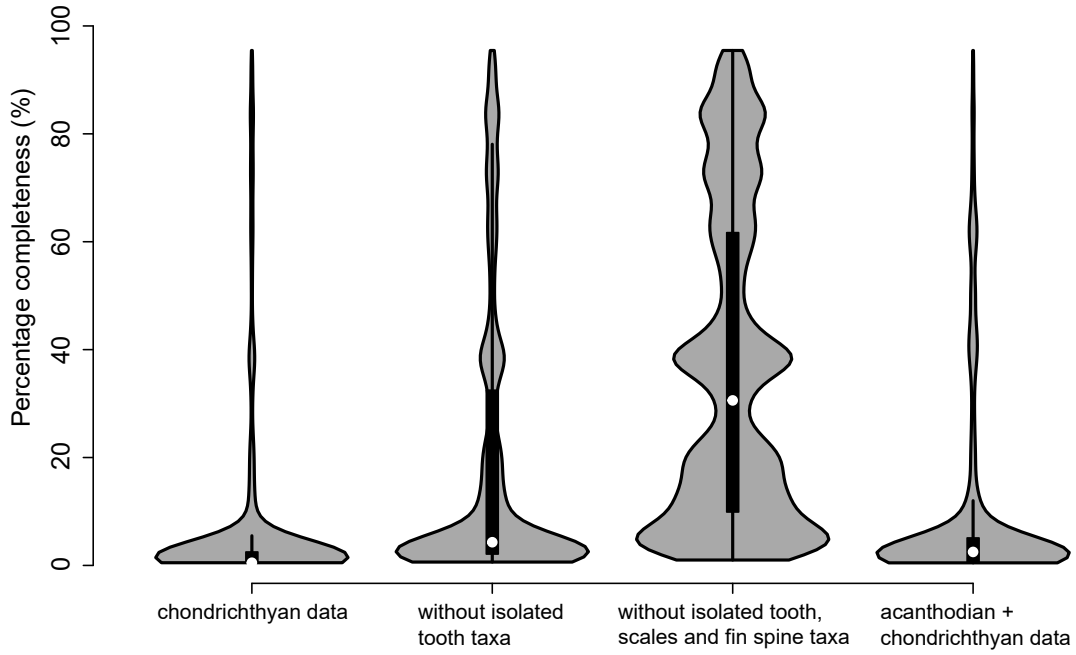


Figure 3.3: Distribution of original chondrichthyan SCM2 values compared to the subsets.

3.3.2 Correlations with taxonomic richness

Chondrichthyan raw taxonomic richness (species level) is low in the Ordovician and Silurian apart from a small peak in the Telychian (species count = 16) (Figure 3.2B). Richness peaks again in the Lower Devonian Lochkovian (species count = 24) but remains stable and at low levels until the Upper Devonian. It then rises steeply from the Famennian on before reaching a climax in the Visean stage of the Carboniferous (species count = 361). Raw taxonomic richness subsequently falls rapidly in the Serpukhovian and Bashkirian before increasing once more with a peak in the Moscovian (species count = 94). From the end-Carboniferous on, richness remains at lower levels and slightly decreases throughout the Guadalupian but remains fairly stable in the Lopingian towards the Permian–Triassic boundary. Generalised least squares regression models show that a combination of time bin length, SCM2 and sea level provides the best explanation for raw chondrichthyan taxonomic richness (Table B.4). The relationship between taxonomic richness and time bin length is significant and positive

(p = 0.012; R^2 = 0.75) but none of the other explanatory variables have a significant relationship with richness. The models that best explain taxonomic richness, ranked by AIC weight values, include time bin length + sea level, time bin length + SCM2 + sea level, and stage midpoints + SCM2 + time bin length + sea level, but only the time bin length coefficient is significant in the three models.

3.3.3 Taxonomic groups

Iniopterygia have the highest median SCM2 value (68.3%) of any subgroup and have a markedly different distribution to any of the other taxonomic groups (Figure B.2). Following this group, Antarctilamniformes (14.3%) have the next highest median SCM2 distribution. The remaining subgroups all have median SCM2 values of less than 10% and most of the SCM2 scores are concentrated at around 0-10%. A Kruskal-Wallis test suggests that the variance of completeness distributions is dominated by one or more subgroups (H = 383.09, p $<$ 2.2E-16). Mann-Whitney-Wilcoxon tests between each subgroup can be accessed in the supplementary information (Table B.5). Iniopterygians are found to have significantly different SCM2 scores to most subgroups.

3.3.4 Comparisons with the completeness of other vertebrate groups

Chondrichthyan completeness values were plotted against SCM2 values of other published vertebrate groups to facilitate comparisons (Figure 3.4). The distribution of chondrichthyan median SCM2 scores, visualised by violin plots, is significantly lower than any tetrapod group investigated, including the bat fossil record (Table B.6). Similar to bats and acanthodians, completeness of Palaeozoic chondrichthyans exhibits a distribution of most SCM2 values at low percentages with low numbers of highly complete taxa. A subset excluding isolated tooth-based taxa yields higher median completeness values than found in bats but is still considerably lower than other tetrapod groups (Figure B.3, Table B.7). Once isolated teeth, fin spine and scale-based

taxa are removed from the chondrichthyan dataset, SCM2 distribution and median value change drastically. There is no statistically significant difference between chondrichthyan SCM2 and that of either parareptiles or pelycosaurs (Table B.8). Median chondrichthyan SCM2 values are significantly higher than that of both sauropodomorph and theropod dinosaurs upon removal of these isolated remains from the dataset. Plesiosaur and ichthyosaur completeness both remain considerably higher than chondrichthyan completeness.

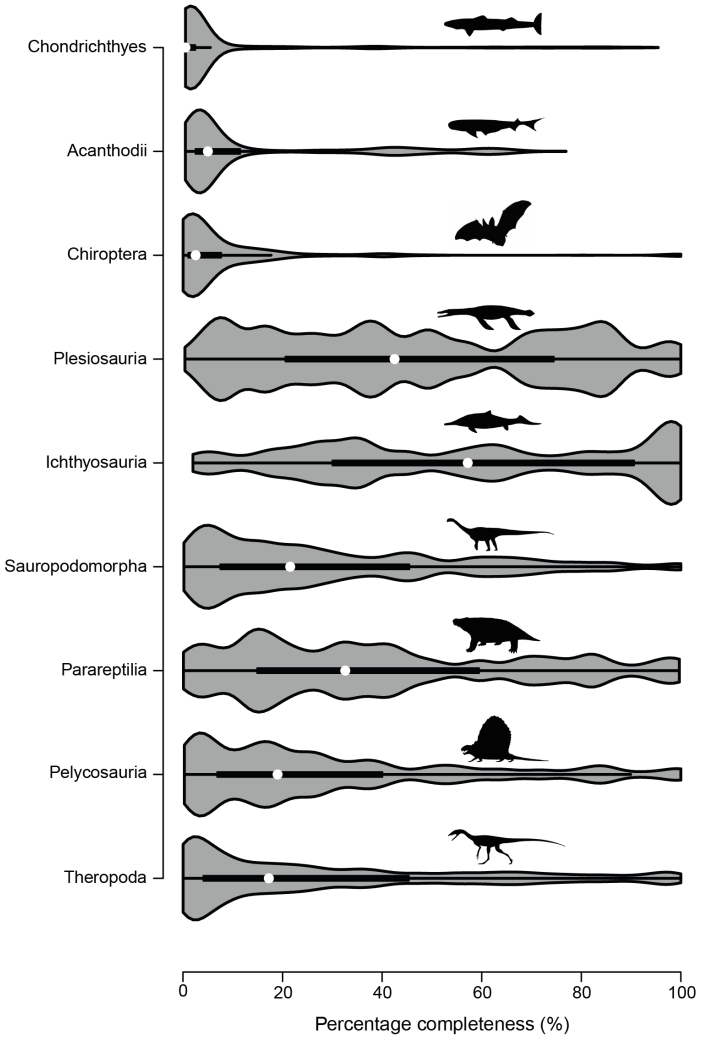


Figure 3.4: Range of chondrichthyan SCM2 values compared to other vertebrate groups. Comparative values from bats (Brown *et al.* 2019), plesiosaurs (Tutin & Butler 2017), ichthyosaurs (Cleary *et al.* 2015), sauropodomorphs (Mannion & Upchurch 2010; Cashmore *et al.* 2020), parareptiles (Verrière *et al.* 2016), pelycosaurs (Brocklehurst & Fröbisch 2014), theropods (Cashmore & Butler 2019) and acanthodians (Chapter 2, Schnetz *et al.* 2022 in press). Silhouettes taken from `http://phylopic.org/` and include work by N. Tamura, G. Monger, S. Hartman, D. Bogdanov, Karkemish and Smokeybjb.

3.3.5 Acanthodian versus non-acanthodian chondrichthyan completeness

Comparing non-acanthodian chondrichthyans to the previously investigated acanthodian group (Chapter 2, Schnetz *et al.* 2022 in press), SCM2 of both groups are significantly different and acanthodians have a slightly higher median distribution while chondrichthyans have a greater range of completeness percentage values. When both groups are combined to represent the chondrichthyan total-group, the distribution of SCM2 scores is flattened but the median is slightly increased relative to the original chondrichthyan dataset (Figure B.3B). As a result, total-group chondrichthyan completeness is no longer significantly different from the completeness of bats but still significantly lower than any of the other tetrapod groups (Table B.9). Total-group chondrichthyan SCM2 distribution values are statistically significantly different from the non-acanthodian chondrichthyan SCM2 values (Table B.1, Figure 3.4).

Addition of the acanthodian data to the chondrichthyan dataset for time series comparisons leads to an increase in mean SCM2 values by 5-10% through most of the Silurian with a notable peak in the Gorstian–Ludfordian (13.9-13.3%) compared to the non-acanthodian chondrichthyan data alone (Figure 3.2). SCM2 is higher throughout most of the Devonian (until the Famennian) as well. The peaks in the Lochkovian (14.1%) and Givetian (23.6%) especially show higher levels of completeness. Completeness does not change significantly post-Devonian apart from an increased peak in the Asselian (27.8%). Median SCM2 values of the total-group chondrichthyans, however, do not significantly increase throughout the Palaeozoic compared to the non-acanthodian chondrichthyan data (Figure B.1). Completeness does peak slightly in the Gorstian–Ludfordian (both 8.4%) and plateaus on moderately higher values from the Pragian through to the Frasnian (around 4.3 and 5.1%), with two more peaks later on in the Moscovian (4.7%) and Asselian (8.1%).

3.3.6 Geographical completeness

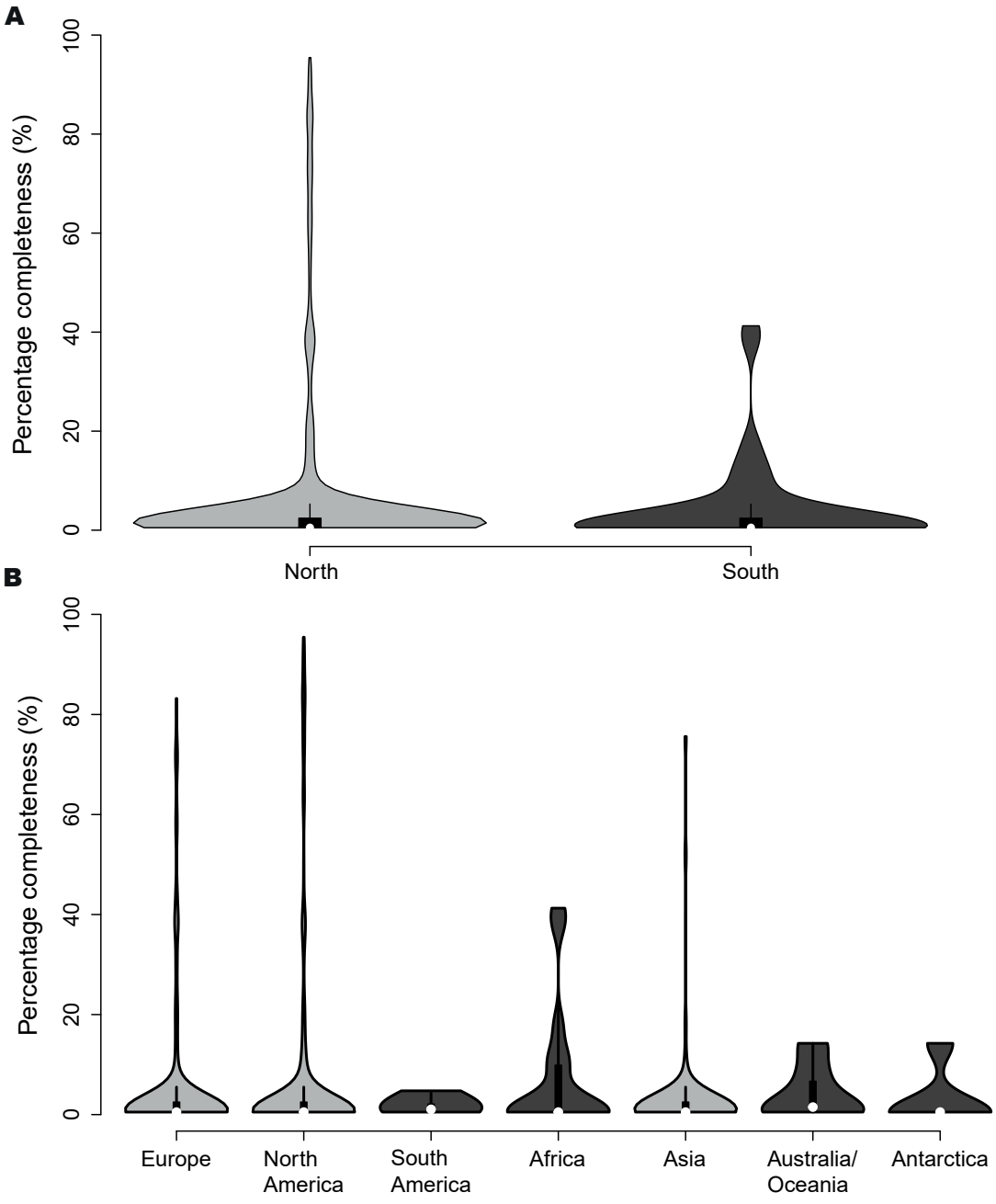


Figure 3.5: Distribution of chondrichthyan SCM2 scores between the modern northern and southern hemispheres (A) and between the different continents (B).

Chondrichthyan species from northern hemisphere localities are not significantly more complete than those from the southern hemisphere when compared using Mann-Whitney-Wilcoxon tests (W = 15491, p = 0.28) and have similar distribution pat-

terns with most SCM2 scores concentrated at low percentages (Figure 3.5A). However, the range of SCM2 values is greater in taxa from the northern hemisphere (0.5-95.5%) whereas the southern hemisphere does not yield completeness values above 41.3%. When divided into continental regions, Europe, North America and Asia all share similar distributions of the majority of completeness values but their range of percentage scores reaches to well above 70-80% (Figure 3.5B). South America exhibits the smallest range of SCM2 distribution with a minimum of 0.5% and a maximum of 4.8%. The SCM2 distributions of Australia and Oceania and Antarctica are very similar in shape and median values. Africa has a moderately high range of completeness values, reaching maximum values of 41.3% but only 0.5% median completeness. The chondrichthyan SCM2 distributions recovered from each continent are all statistically similar to one another (Table B.10). Additionally, Kruskal-Wallis tests do not indicate a strong dominance of any of the continents ($H = 3.2664$, $p = 0.77$).

3.3.7 Sea level correlations

There is a significant negative correlation between chondrichthyan completeness and changes in average sea level through time: chondrichthyan SCM2 values are higher during times of lower sea level and lower when sea level rises (Figure 3.6, Table 3.1). When chondrichthyan SCM2 values are grouped into marine and freshwater completeness, there is a significant negative relationship between marine SCM2 and sea level whereas freshwater SCM2 does not significantly correlate with sea level. Upon removal of the isolated tooth-based taxa from the dataset, average sea level is still significantly correlated with marine and total SCM2 values (Table B.11). When the acanthodian SCM2 values from previous investigation are added to the chondrichthyan dataset, a slightly positive and significant correlation between freshwater and sea level is recovered which stands in contrast with the other analyses (Table B.12).

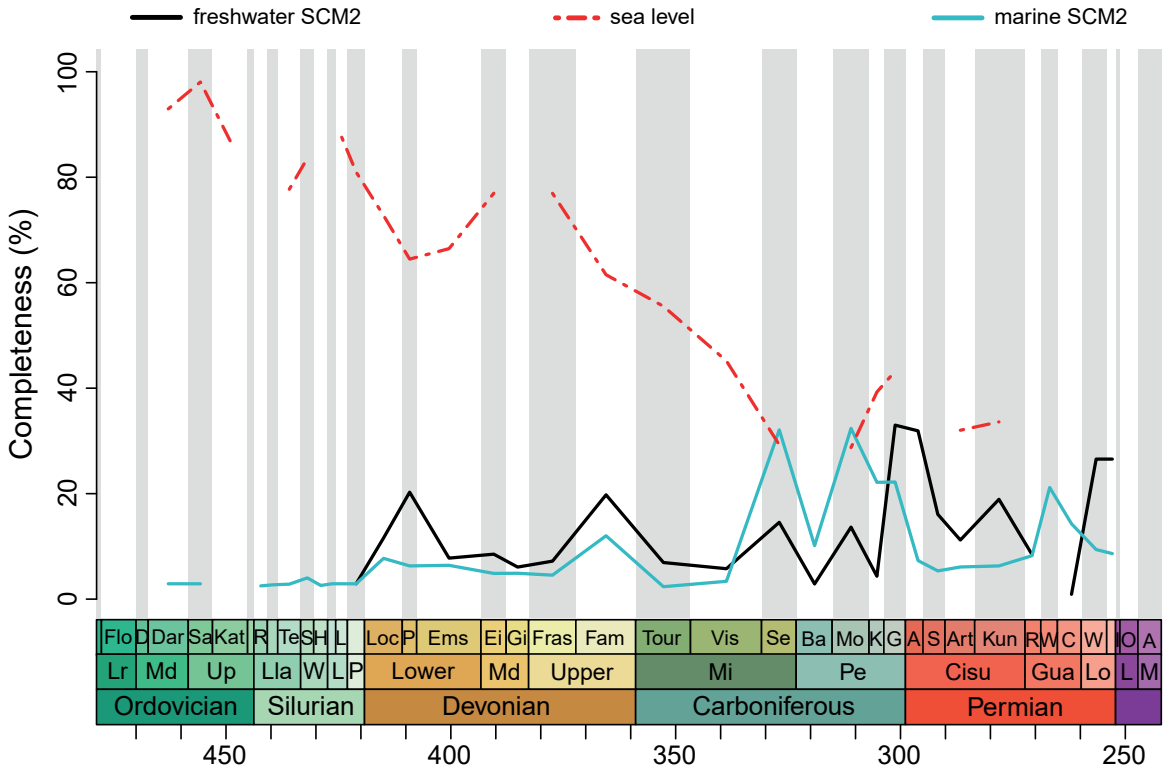


Figure 3.6: Chondrichthyan completeness through time based on freshwater versus marine occurrences plotted against sea level changes. Sea level values represent arbitrary values taken from Hannisdal & Peters (2011).

Table 3.1: Results of pairwise comparisons for sea level trends with chondrichthyan completeness using GLS. Statistically significant results indicated in bold.

Comparison	Slope	t-value	p-value	R^2
total SCM2 ~ sea level	-1.3	-5.1	**0.0001**	0.87
marine SCM2 ~ sea level	-1.6	-4.4	**0.0003**	0.85
freshwater SCM2 ~ sea level	-0.24	-0.75	0.47	0.92

3.3.8 Depositional and environmental variation

SCM2 values recovered from chondrichthyans deposited in freshwater environments are significantly different to those in marine settings (W = 509.5, p = 0.03), but median SCM2 values are both low (0.5%) and neither setting demonstrates higher

overall SCM2 completeness. Freshwater SCM2 values have a slightly higher upper interquartile range than marine SCM2 values which in turn have the highest maximum percentages (Figure B.4). Plotting the values through time, freshwater SCM2 values are higher throughout the Devonian and the Tournaisian-Visean in the Carboniferous as well as most of the Permian (Figure 3.6). Marine SCM2 peaks in the Serpukhovian and throughout most of the Pennsylvanian in the Carboniferous. The first chondrichthyan occurrences in the Ordovician and Silurian are from strictly marine deposits but marine SCM2 then remains lower than freshwater SCM2 until the late Mississippian.

Table 3.2: Results of pairwise comparisons between BA and total chondrichthyan SCM2 using GLS. Statistically significant results indicated in bold.

Comparison	Slope	t-value	p-value	^{2}
BA0 SCM2 ~ total SCM2	0.62	2.0	0.058	0.18
BA1 SCM2 ~ total SCM2	0.75	6.4	$<$ **0.0001**	0.89
BA2 SCM2 ~ total SCM2	0.53	3.1	**0.0041**	0.26
BA3 SCM2 ~ total SCM2	0.53	2.2	**0.038**	0.34
BA4 SCM2 ~ total SCM2	0.45	1.5	0.14	0.31
BA5 SCM2 ~ total SCM2	1.0	4.6	**0.0002**	0.63
BA6 SCM2 ~ total SCM2	1.3	3.9	**0.0009**	0.48

When the environmental information is categorized into individual Benthic Assemblage zones (BA) for more detail, a Kruskal-Wallis test suggests that the variance of SCM2 distributions between the different BA zones is strongly dominated by one or more of them (H = 36.451, p = 2.252E-06). Mann-Whitney Wilcoxon tests further indicate a significant difference for SCM2 from BA0 compared to BA2, BA3 and BA4 and BA1 compared to BA4. Median SCM2 values recovered from BAs 2, 3 and 4 are all significantly different to BAs 5 and 6 but not to each other (Table 3.2). Further GLS

pairwise analyses reveal significant relationships between each BA1, BA2, BA3, BA5 and BA6 and total SCM2 through time (Table 3.3). BA0 and BA4 do not show significant relationships with total SCM2 through time. Violin plots show similar distributions of SCM2 scores for all BAs (Figure B.5).

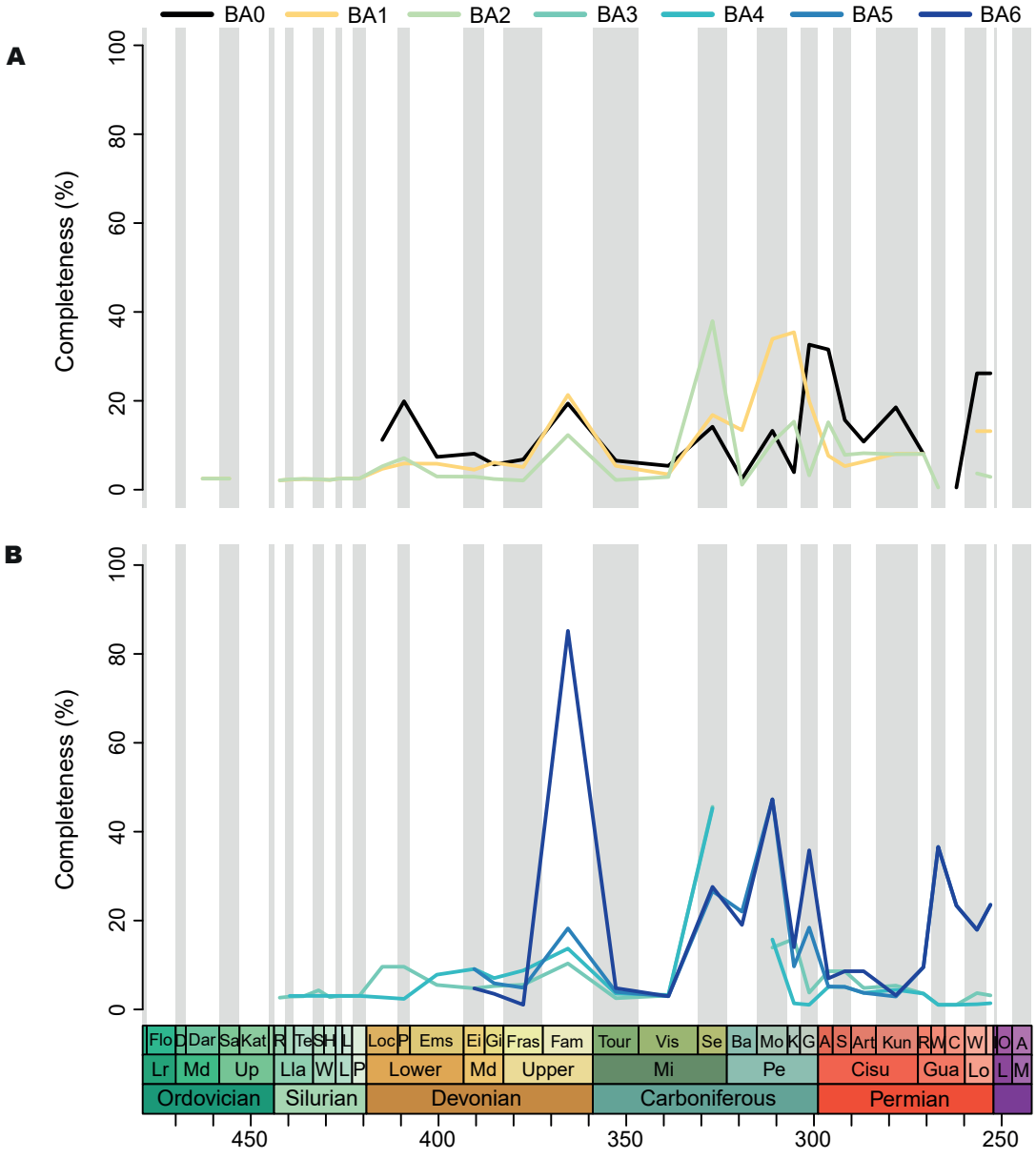


Figure 3.7: Changes in chondrichthyan completeness through time based on Benthic Assemblage (BA) zones. A, BA0 to BA2. B, BA3 to BA6.

Mean SCM2 through time sorted by individual BAs shows that completeness is initially restricted to low levels in BA1 and 2 in the Ordovician before extending to

BA1-4 in the Silurian (Figure 3.7). Time series of mean SCM2 patterns of taxa deposited in BA 1 and B2 closely resemble each other throughout most of the Palaeozoic. Similarly, completeness values for zones BA3 and BA4 follow a resembling pattern of mostly low levels throughout the Palaeozoic, and prominently, have no values for the Bashkirian in the Carboniferous. Mean SCM2 values of chondrichthyan taxa deposited in BA0 are restricted to the Devonian and upwards, with highest numbers in the Gzhelian-Asselian, Kungurian and Wuchiapingian-Changhsingian. Chondrichthyan SCM2 values from the deeper water BA5 and BA6 zones are limited to the Middle Devonian and upwards, with low scores initially in the Eifelian to Frasnian before heavily increasing in the Famennian (84.7% BA6). BA5 and BA6 completeness show similarly high patterns throughout most of the Carboniferous except for a low in the Tournaisian-Visean (2-4% SCM2) of the Mississippian. The patterns diverge slightly in the early Permian with higher completeness values reported for BA6 occurrences but merge again in the Guadalupian and Lopingian to show uniformly high scores.

Table 3.3: Mann-Whitney-Wilcoxon test results of comparisons of the distribution and median SCM2 values of chondrichthyans from different environments (measured as Benthic Assemblage zones). Statistically significant results indicated in bold.

Dataset 1	Dataset 2	Test statistic (W)	p-value	Adjusted p-value
BA 0	BA 1	479	**0.0327**	0.0572
BA 0	BA 2	568	**0.000638**	**0.00280**
BA 0	BA 3	530	**0.000896**	**0.00297**
BA 0	BA 4	533	**0.000239**	**0.00280**
BA 0	BA 5	233	0.951	0.951
BA 0	BA 6	211	0.661	0.731
BA 1	BA 2	624	0.0790	0.119
BA 1	BA 3	567	0.141	0.197
BA 1	BA 4	604	**0.0217**	**0.0457**
BA 1	BA 5	213	0.0625	0.101
BA 1	BA 6	197	**0.0299**	0.0570
BA 2	BA 3	436	0.544	0.644
BA 2	BA 4	505	0.552	0.644
BA 2	BA 5	138	**0.000637**	**0.00280**
BA 2	BA 6	144	**0.000990**	**0.00297**
BA 3	BA 4	517	0.215	0.283
BA 3	BA 5	146	**0.00236**	**0.00621**
BA 3	BA 6	151	**0.00337**	**0.00785**
BA 4	BA 5	111	**0.000276**	**0.00280**
BA 4	BA 6	122	**0.000666**	**0.002799**
BA 5	BA 6	190	0.808	0.848

3.4 Discussion

The chondrichthyan fossil record through time is dominated by sampling of isolated skeletal remains, namely teeth, scales, and fin spines, which mask most of the patterns and trends in their early fossil record (Figure 3.2). This is the poorest completeness range of any of the previously assessed vertebrate groups. Throughout the evolutionary history of chondrichthyans, isolated teeth, and to a lesser extent isolated scales and fin spines, make up most of the available material to classify them at ordinal and lower taxonomic levels (for an extensive summary, see Cappetta 1987 and Ginter *et al.* 2010). While this practice has been widely accepted for isolated tooth material, a consistent application of a taxonomic standard for naming and assigning chondrichthyan taxa on the basis of isolated scales and fin spines has yet to be established. In the absence of such a concept, there is great potential for taxonomic 'over-splitting' or 'over-lumping' at species and genus levels. Indeed, such a tendency of taxonomic 'over-splitting' of poor-quality material has been reported and linked to the inability to recognise characters that link specimens (Brocklehurst & Fröbisch 2014). More recent analyses based on fossil squamate data, however, suggest that the bias imposed by incomplete fossil record data does not necessarily prevent preservation of reliable phylogenetic signal (Woolley *et al.* 2022). Whether this is also the case for chondrichthyans will have to be established in future investigations.

The predominantly cartilaginous composition of the chondrichthyan skeleton leaves us with very little fossil material to work with as cartilage fossilizes poorly and only under favourable depositional conditions. While we are extracting more information from previously inaccessible fossils (e.g., from concretions) following technological advances such as CT scanning, a preservational bias is still largely at play (e.g., Pradel *et al.* 2014; Bronson *et al.* 2018; Coates & Tietjen 2018; Dearden *et al.* 2019; Frey *et al.* 2020). In contrast, isolated teeth consist of layers of dentine and enameloid which are some of the hardest biological tissues and can endure even the toughest

processes of preservation, often resulting in the only remains left of a decayed and fragmented cartilaginous fish. Thus, it is not surprising that in comparison to total SCM2, the two subsets excluding taxa based on isolated skeletal material (teeth only and all teeth, scales and fin spines) yield overall significantly higher mean completeness values through time (Figure 3.3. This shows how intensely specific isolated remains influence the observed completeness patterns of Palaeozoic chondrichthyans and, as a consequence, our accounts of the chondrichthyan fossil record. However, a strict exclusion of these isolated elements may not be a simple solution as they can still contain important information on the taphonomic drivers of preservation (Driscoll *et al.* 2018). Additionally, the overall patterns of peaks and drops in completeness are mostly retained between the original data and the subsets which indicates that the same trends in completeness over time are recovered from all datasets although absolute values of completeness change considerably (Figure 3.2).

Without the acanthodian fossils, completeness scores throughout the Silurian are limited to putative chondrichthyan taxa such as *Kannathalepis*, *Frigorilepis* and *Wellingtonella* (Märss & Gagnier 2001; Märss *et al.* 2002; Märss *et al.* 2006) as well as isolated scale-based taxa from elegestolepidid and mongolepidid chondrichthyans and isolated fin spine-based taxa from the order Sinacanthida (Karatajutè-Talimaa *et al.* 1990; Sansom *et al.* 2000; Andreev *et al.* 2017; Andreev *et al.* 2020). The addition of the acanthodian completeness scores to the chondrichthyan dataset significantly increases absolute values of completeness for the Silurian and Lower to Middle Devonian, while not majorly impacting on completeness scores post-Devonian (Figure 3.2). These findings reflect recent phylogenetic analyses that recognise an increasing proportion of acanthodians as the bulk of the chondrichthyan stem-group (Brazeau 2009; Davis *et al.* 2012; Zhu *et al.* 2013; Long *et al.* 2015; Brazeau & de Winter 2015; King *et al.* 2016; Qiao *et al.* 2016; Zhu *et al.* 2016; Coates *et al.* 2018; Dearden *et al.* 2019; Frey *et al.* 2020; King & Rücklin 2020), bridging an approx. 30-million-year gap in their fossil record.

3.4.1 Comparisons with other vertebrate groups

Initial chondrichthyan completeness is considerably lower than completeness of other marine vertebrate groups such as Mesozoic plesiosaurs and ichthyosaurs, which exhibit the highest overall and median skeletal completeness records of all published tetrapod groups (Cleary *et al.* 2015, Tutin & Butler 2017) (Figure 3.4). However, upon removal of isolated skeletal remains such as isolated teeth, scales, and fin spines, chondrichthyan completeness increases substantially. This illustrates how isolated skeletal remains have the potential to bias the completeness patterns we observe, a finding that has been outlined in detail in Chapter 2. Indeed, our results on chondrichthyan completeness comparisons with other vertebrate groups are for the most part similar to the results in Chapter 2: once isolated teeth, scales and fin spine-based taxa are removed from the data, median completeness of chondrichthyans is higher than most terrestrial tetrapod groups, including sauropodomorphs, theropods and pelycosaurs, a pattern also shown in acanthodians. While both groups' median SCM2 values are still somewhat lower than the completeness values of plesiosaurs and ichthyosaurs, it adds strength to the previously published idea that different taphonomic processes are at play in the vertebrate records between marine and terrestrial environments (Behrensmeyer *et al.* 2000; Tutin & Butler 2017). Early chondrichthyans, including acanthodian chondrichthyans, are considerably geologically older than any of the tetrapod groups of which completeness patterns have been published and might therefore face additional difficulties in terms of the preservation of their fossil record.

The acanthodian data in Chapter 2 represents the only other available Palaeozoic and fish group data, and both groups show very similar patterns. This somewhat expected given their phylogenetic relations in the total-group Chondrichthyes. Acanthodians and chondrichthyans coexisted throughout the Palaeozoic era, are found in the same formations and localities, and even show evidence of direct interactions (Kriwet *et al.* 2008). Similarities in preservation are therefore not surprising and additionally suggest common controls on preservation of their predominantly cartilaginous skele-

tons in the same environments. Comparison of completeness with other taxonomic groups such as Palaeozoic actinopterygians are warranted to provide a worthwhile, albeit large and challenging, data set to compare groups from similar ecological niches.

3.4.2 Completeness variation between chondrichthyan orders

The majority of Palaeozoic chondrichthyan orders have a high number of species recovered from fragmented and isolated remains, with the occasional discovery of a highly complete species(Figure B.2). In some of the investigated groups, the completeness distributions are extreme and consist of identical SCM2 values for each taxon included in the group, thus showing no further distribution than the median. This means that these groups are known entirely from specific isolated material, predominantly isolated teeth, isolated scales or isolated fin spines, e.g., Bransonelliformes, Mongolepidida and Sinacanthida.

The chimaera-like Iniopterygia have the highest median completeness of any group and show noticeably different distribution patterns. The significantly higher completeness of iniopterygians is most likely the result of a combination of contributing factors: they are limited to ten species and two taxa indeterminate at genus and species level and are almost entirely known from partial and complete skeletons, with findings of isolated skeletal remains being the exception. Additionally, iniopterygians have been exclusively recovered from shale settings that strikingly differ in terms of environment, belonging to either the very shallow near-shore waters in the Mecca Quarry Shale and Bear Gulch Limestone (Coveney & Glascock 1989; Rexroad *et al.* 2001; Hagadorn 2002) or the deep offshore deposits of the Stark and Wea Shales (Coveney & Glascock 1989; Heckel 2008), indicating potential environmental influences on preservation.

The Antarctilamniformes comprise a small group of Devonian chondrichthyans whose fossil discoveries, including braincase, fin spine, and tooth elements, have added important insights into the record of earliest chondrichthyans (Young 1982; Gagnier *et al.* 1988; Gess & Coates 2015; Potvin-Leduc 2017) which is also reflected in

their higher median and interquartile SCM2 distribution pattern compared to the majority of chondrichthyan orders.

Lastly, the Symmoriiformes show a range of both low and high completeness value distributions which suggests that taxa from this group are sampled at both low and high completeness levels. This is not surprising given the prominent members of this group such as *Symmorium* (Williams 1985), *Stethacanthus* (Williams 1985), *Cobelodus* (Zangerl & Case 1976) or *Falcatus* (Lund 1985) which are all known from at least partially articulated skeletons while the low completeness levels stem from species described from isolated remains alone such as *Kungurodus* (Ivanov 2016) or *Denaea williamsi* (Ginter & Hansen 2010).

3.4.3 Geographical controls on chondrichthyan completeness

Chondrichthyan fossils are recovered from all continents but vary greatly in terms of abundance. While there are no recovered significant differences between chondrichthyan completeness from the modern northern and southern hemisphere localities, total species numbers differ considerably. Chondrichthyan richness is dominated by species from North America and Europe. While this could be indicative of a higher diversity of chondrichthyans within these regions, it is more likely to represent a bias of greater collection effort, historical trend of increased sampling and outcrop availability within these areas. Sampling of any given fossil record varies geographically and across stratigraphic units introducing spatial biases resulting from underlying geological and anthropogenic factors (Brocklehurst *et al.* 2012). Additionally, geological biases may include a limited exposure of consistent availability of specific horizons that yield fossiliferous material due to climate, vegetation cover and subsequent erosion in certain modern-day localities (Cashmore & Butler 2019). Our findings highlight the potential of a wealth of undiscovered information on the chondrichthyan fossil record in the southern regions that could be crucial in terms of expanding our knowledge on chondrichthyan diversity and evolution.

There is no significant geographical variation in chondrichthyan SCM2 values, meaning that a considerably smaller number of taxa from the southern hemisphere and continents (including Africa, South America, Australia and Oceania and Antarctica) contain similar mean completeness levels to the taxonomically richer records from the northern hemisphere continents (North America, Europe and Asia) (Figure 3.5). North America, Europe and Asia do however show the highest range of completeness values compared to the southern continents, signifying that the individually most complete chondrichthyan taxa are found there even though this is not reflected in the mean levels of completeness. A limiting factor to this observation is likely related to the abundance of isolated tooth-based taxa found from each continent which similarly affects overall mean completeness values for each region. This would theoretically mask the occurrences of even the highest individually complete chondrichthyan taxa from the northern hemisphere localities. The chondrichthyan fossil record of South America exhibits the overall lowest SCM2 distribution and variability in the Palaeozoic which coincides with previous suggestions regarding its scarce and discontinuous nature of the Devonian vertebrate record (Gagnier *et al.* 1988; Maisey *et al.* 2002; Janvier & Maisey 2010). In accordance with this, South American acanthodians show a similarly limited fossil evidence of both skeleton completeness as well as taxonomic abundance (Chapter 2, Schnetz *et al.* 2022 in press). South America's fauna is suggested to be dominated by chondrichthyans and acanthodians during Devonian times, and these observations are based on assemblages of mostly fragmented material, including fin spines, endoskeletal elements, and scales (Janvier & Maisey 2010). This fragmentary pattern is reflected in the low SCM2 distributions we obtained for South American chondrichthyan occurrences and is not only limited to the Devonian but seemingly spans throughout the Palaeozoic.

3.4.4 Palaeoenvironmental and Palaeoecological biases

Changes in sea level throughout the Palaeozoic negatively correlate with chondrichthyan completeness but are mainly influenced by the marine occurrences (Figure 3.6, Table 3.1). This is similar to the sea level relationships reported in the stem-chondrichthyan acanthodians where sea level significantly negatively correlates with skeletal completeness recovered from marine environments but not freshwater (Chapter 2, Schnetz *et al.* 2022 in press). These inverse relationships in either group are challenging to explain but have been outlined previously (see Chapter 2, Schnetz *et al.* in press 2022). Besides chondrichthyans and acanthodians, inverse sea level relationships with completeness have also been shown in the marine ichthyosaurs (Cleary *et al.* 2015), plesiosaurs (Tutin & Butler 2017) and the terrestrial sauropodomorphs (Mannion & Upchurch 2010; Cashmore *et al.* 2020) while they were absent in the marine mosasaurs (Driscoll *et al.* 2018). More similar in terms of ecology and habitat are the ostracoderms, osteostracans and non-psammosteid heterostracans which have also been found to show an inverse proportional relationship between recovery potential of fossils and sea level (Sansom *et al.* 2015). While this may be surprising as a rise in sea level can lead to bottom waters and basins in deep shelf areas being placed below physical barriers resulting in anoxic conditions (Leggett 1980; Sarmiento *et al.* 1988) which are known to keep skeletons intact, it is not the case for either of these fish groups or for chondrichthyans.

Chondrichthyan skeletal completeness does not show a strong trend towards higher values from either freshwater or marine environments, which is markedly different from the higher freshwater completeness scores in acanthodians in the Palaeozoic. One main explanation for this difference may be the high completeness values recovered from deep water marine environments (BAs 5 and 6) in the Upper Devonian, throughout most of the Carboniferous and the later Permian stages (see Figure 3.7). Acanthodian fossils, however, are generally absent from these deep water settings (Chapter 2, Schnetz *et al.* 2022 in press). Deeper water marine environments are con-

sidered to provide better conditions for preservation than shallow waters due to a lower high-energy deposition, different physical constraints (e.g., anoxia) and less scavenging and weathering (Allison *et al.* 1991; Driscoll *et al.* 2018). The correlations between the deep water benthic assemblage zones (BA5 and BA6) with total SCM2 further illustrate the significant role they play in chondrichthyan completeness (Table 3.2). Benthic assemblage zone BA0, which accounts for freshwater settings, conversely, does not significantly correlate with total completeness and may provide less of an explanation for the freshwater versus marine trends in chondrichthyan completeness.

Nevertheless, time series of mean completeness do show higher freshwater SCM2 values compared to marine SCM2 specifically throughout the Devonian and the early Permian. These scores mainly derive from both lacustrine and fluvio-lacustrine deposits such as the middle Devonian Bunga Beds of New South Wales in Australia (Fergusson *et al.* 1979) and the Permo-Carboniferous Meisenheim Formation from the intermontane Saar-Nahe Basin in Germany (Königer & Stollhofen 2001). The low energy conditions together with a lack of transport and physical disturbance that characterise lacustrine environments (Rust 1982), such as the deep freshwater lake deposits of the Bunga Beds, may prevent disarticulation of skeletons and thus favouring higher completeness.

The absence of a strong trend towards higher completeness in either freshwater or marine settings may be further amplified by the high amount of chondrichthyan fossils found from both BA0 and BA1/BA1-2 environments. BA0, BA1 and BA2 zones exhibit similar patterns of completeness throughout the Palaeozoic. This may relate to a considerable number of anadromous taxa inhabiting the aquatic environments in the Palaeozoic, which migrate between freshwater and marine environments. Additionally, BA0 and BA1 SCM2 values are not significantly different from each other which further suggests the dominance of anadromous chondrichthyans in the dataset. The close relationship between the marine BA1 and B2 zones is not surprising as intertidal and shallow subtidal environments are often coupled in interpretations of lithostrati-

graphic units (see supplementary dataset) and there may be a limitation in resolution when it comes to differentiating between the two very similar environments (Chapter 2, Schnetz *et al.* 2022 in press).

Chondrichthyan fossils are found in BA3 and BA4 zones (middle to outer shelf, reef settings and subtidal dynamic environments) from the earliest Silurian through to the end of the Permian but show a generally low completeness except for spikes in the late Mississippian and late Pennsylvanian (Figure 3.7). A similar pattern has been recovered in acanthodians and attributed to a combination of environmental deposition and sampling bias (Chapter 2, Schnetz *et al.* 2022 in press). Indeed, the vast majority of chondrichthyan records from this interval and environment are derived from one stratigraphic unit, the North American Heath Formation Lagerstätte, where individuals were rapidly buried in wide shallow freshwater-influenced lagoon, preventing the warm water setting to rapidly decay and disarticulate the fish bodies (Lund *et al.* 1993; Hagadorn 2002).Thus, the spike found in BA3 and BA4 zones from the late Mississippian most likely account for a sampling bias rather than a genuine signal for high completeness in these BAs.

Chondrichthyans skeletal completeness sorted by benthic assemblage zones further reveals higher values in specific BAs at different points throughout the Palaeozoic which indicates potential ecological (habitat preferences) or preservational (depositional environment) biases. Chondrichthyan SCM2 is initially restricted to intertidal and shallow subtidal marine environments (BA1-BA2) in the Ordovician and Silurian and freshwater SCM2 is only found from the Devonian on. Extension of SCM2 values into truly deeper water settings (BA5 and BA6) only occur from the Middle Devonian on and high numbers are first seen in the Famennian towards the end of the Devonian and further in the Carboniferous. This may well coincide with an expansion into more diverse habitats and an availability of niches following the Hangenberg extinction at the Devonian-Carboniferous boundary as has been suggested before (Sallan & Coates 2010). Interestingly, in the latest stages of the Permian prior to the end-Permian mass

extinction, SCM2 is high in both BA0 and BA5-6 even though few specimens are recovered and shows that chondrichthyans may still occupy a high variety of habitats towards the end of the Palaeozoic.

3.5 Conclusions

The Palaeozoic chondrichthyan fossil record is subjected to spatial, temporal, and environmental biases, and is dominated by isolated teeth, scales, and fin spines, which obscure much of the patterns and trends of completeness through the Palaeozoic. Modern northern hemisphere localities do not yield significantly more complete chondrichthyans than the southern counterpart, albeit having a significantly higher total number of species, indicating a potential wealth of undiscovered information in the global south. Higher completeness is reported in specific environmental zones at different points throughout the Palaeozoic and corelates negatively with sea level, indicating potential ecological and preservational biases. Chondrichthyans exhibit the poorest completeness range of any of the previously investigated vertebrate groups but increase to levels similar to previously published pelycosaurs and parareptiles when taxa based on isolated remains are excluded from the analyses. A lack of consistent application of a taxonomic concept for naming and assigning chondrichthyan taxa based on isolated scales and fin spines and the resulting potential for taxonomic 'oversplitting' likely explain at least some of the observed low completeness trends. The influences of these biases illustrate some of the challenges of drawing conclusions on chondrichthyan macroevolutionary patterns based on a spatially, temporally, and taxonomically incomplete fossil record.

CHAPTER 4

PATTERNS OF CHONDRICHTHYAN DIVERSITY DURING THE PALAEOZOIC

My contribution to this work involved designing the basis of the chapter, conducting all aspects of the research, including data collection, data analysis, interpretation of results and manuscript writing. E. Dunne shared and troubleshooted R code for diversity data analyses and provided feedback on the methodology. My colleagues provided feedback on the interpretations of the results and earlier versions of the manuscript. As in the previous chapters, the editorial "we" is used here to reflect these contributions.

4.1 Introduction

The early fossil record of chondrichthyans (cartilaginous fishes) is limited but potentially dates back to the Late Ordovician, based on the discoveries of isolated shark-like scales or denticles (Young 1997; Sansom *et al.* 2001; Sansom *et al.* 2012; Andreev *et al.* 2015; Andreev *et al.* 2016). However, undoubted chondrichthyans first appear in the Silurian and rapidly diversified during the Devonian and early Carboniferous, alongside other major jawed vertebrate groups such as the Actinopterygii, Sarcopterygii and placoderms (Janvier 1996; Sepkoski 2002; Turner 2004; Brazeau 2009; Ginter *et al.* 2010; Sallan & Coates 2010). The recognition of the acanthodi-

ans, a group of Palaeozoic spiny fusiform fishes, as a grade within the chondrichthyan stem-group has added considerable data to the earliest chondrichthyan fossil record (e.g., Brazeau 2009; Davis *et al.* 2012; Coates *et al.* 2018; Dearden *et al.* 2019) and identified a crucial step in early chondrichthyan evolution. While this likely influences patterns of Palaeozoic chondrichthyan diversification, it has not been quantified to date.

The Palaeozoic era was a period of major geological, environmental and biotic changes. Breakup and assembly of continents resulted in the opening and closure of oceans and seas together with substantial changes in sea level, while terrestrial settings were shaped through collisions and uplifts as a result of shifting continental positions (Haq & Schutter 2008; Murphy 2009; Munnecke *et al.* 2010; Hannisdal & Peters 2011). Climate fluctuated greatly and included multiple periods of glaciation, intervals of substantial increase in global temperatures, the formation of tropical swamps in the Carboniferous, and increasingly dry conditions towards the end of the Palaeozoic (e.g., Veevers & Powell 1987; Munnecke *et al.* 2010; Davydov *et al.* 2012; Rosa & Isbell 2021). The Palaeozoic fossil record encompasses one of the most important events in the evolution of life on Earth, the rise and diversification of all major vertebrate lineages (Janvier 1996; Nelson 2006; Wen-Jin & Min 2007). By contrast, at the end of the Palaeozoic, the largest mass extinction recorded in Earth's history occurred at the boundary between the Permian and the Triassic, resulting in the loss of between 80 and 96% of all marine species (Raup & Sepkoski Jr. 1982; Hallam & Wignall 1997; Sahney & Benton 2008).

Despite the Palaeozoic being a crucial time interval for the initial early chondrichthyan radiation and diversification on both global and regional scales, diversity analyses of chondrichthyans within this interval are either constrained to shorter periods such as the Devonian-Carboniferous boundary and the Carboniferous (Sallan & Coates 2010; Feichtinger *et al.* 2021; Ginter 2021) or based on direct comparisons between and within selected faunal associations and geographic regions (e.g., Wen-Jin & Min 2007; Grogan *et al.* 2012). The Hangenberg extinction event during the transition

from the Devonian to the Carboniferous was recovered as representing a crucial bottleneck in the evolutionary history of vertebrates with subsequent large diversification events of major groups in the early Carboniferous, including chondrichthyans (Sallan & Coates 2010). Conversely, the prominent Kellwasser event (one of the 'Big Five' mass extinctions) at the Frasnian-Famennian stage boundary, previously reported to have caused a loss of 50-60% of marine genera (Raup & Sepkoski 1982; McGhee 1996), was shown in a subsequent study to be of minor significance in vertebrate groups, including chondrichthyans, and more likely to be biased by insufficient sampling (Sallan & Coates 2010). Furthermore, changes in elasmobranch diversity and the environment during the Carboniferous, including the on-going closure of the Rheic-Tethys Gateway and an unstable period of multiple glaciation phases and high sea-level fluctuations, were closely linked in a previous study (Feichtinger *et al.* 2021).

Aside from abiotic influences, it has long been established that our ability to estimate true diversity is complicated by uneven sampling of the fossil record (Raup 1972; Sepkoski *et al.* 1981; Alroy *et al.* 2001; Peters & Foote 2001). Several studies have investigated the influence of a variety of biases on observed diversity in different fossil groups, including terrestrial and marine vertebrates, marine invertebrates, insects and plants (Alroy *et al.* 2008; Barrett *et al.* 2009; Butler *et al.* 2011; Cascales-Miñana *et al.* 2013; Vilhena & Smith 2013; Clapham *et al.* 2016; Dunne *et al.* 2018; Close *et al.* 2020). To estimate diversity with the incompleteness of the fossil record in mind, statistical methods have been introduced to standardise samples to equal levels of completeness thus mitigating these biases (Alroy 2010; Chao & Jost 2012; Close *et al.* 2018).

Here, we present a compiled genus- and species-level dataset of Palaeozoic chondrichthyans from the Ordovician to the end-Permian to explore global diversity patterns with sampling standardization. We aim to address the following questions: how does the diversity of chondrichthyans change during the Palaeozoic? How does chondrichthyan diversity respond to the Kellwasser and Hangenberg extinction events,

specifically in terms of large-scale diversification? How do the environmental changes during the Palaeozoic (e.g., expansion of shallow carbonate platforms, glaciation, rapid warming) affect the diversification and extinction patterns of chondrichthyan groups?

4.2 Methods

4.2.1 Dataset

We newly compiled a dataset of 1318 occurrences, representing 443 genera of Palaeozoic total-group chondrichthyans, from the Late Ordovician (Darriwilian) to the end of the Permian (Changhsingian). Fossil occurrences were initially gathered from museum visits and augmented with peer-reviewed literature. Taxonomic information from museum catalogues was checked for validity and corrected to the latest accepted taxonomic name and systematic position if applicable. Taxa were included based on the most recent taxonomic literature and reviews (e.g., Denison 1979; Zangerl 1981, Stahl 1999, Ginter *et al.* 2010; Burrow 2021). The total-group chondrichthyan dataset includes the acanthodian grade as part of the chondrichthyan stem-group as well as putative stem chondrichthyan taxa such as *Kathemacanthus* or *Seretolepis* (e.g., Brazeau 2009; Davis *et al.* 2012; Coates *et al.* 2018; Dearden *et al.* 2019: Frey *et al.* 2020) and the Ordovician scale-based taxa *Tezakia*, *Canyonlepis*, *Tantalepis* and *Solinalepis* (Sansom *et al.* 2001; Sansom *et al.* 2012; Andreev *et al.* 2015; Andreev *et al.* 2016) (see supplementary information for a full list of included genera and species). In this study, we follow the phylogenetic analysis of Dearden *et al.* (2019), subsequently supported by Frey *et al.* (2020), which places the acanthodians as a grade of stem-group chondrichthyans.

Tooth-based taxa whose taxonomic status is debated but has not been officially revised or formally considered as *nomina dubia* were retained in the dataset. Most of the taxonomic uncertainty for fossils identified beyond family level in chondrichthyans occurs at species level (e.g., in several holocephalan lineages) and will not

substanially affect genus-based diversity analyses. Two iniopterygian specimens described as members of the Sibyrhynchidae by Pradel (2010) were included as separate operational taxonomic units (OTUs) because they probably represent distinct but currently unnamed taxa (following the approach of Cashmore & Butler (2019) in dealing with OTUs in theropods) and likely increase the diversity of the group in the Late Carboniferous. Additionally, two very incomplete acanthodian specimens were included in the analyses as separate OTUs because they extend the acanthodian occurrence range into the middle Permian (Mutter & Richter 2007). Information on lithostratigraphy (e.g., geological formation), geographical locality and chronostratigraphic age were recorded for each occurrence. Palaeoenvironmental information was gathered from published sources where detailed lithostratigraphic descriptions for the occurrences were available.

4.2.2 Subsets and explanation of phylogenetic concepts used

The dataset was subsampled using multiple parameters to compare and contrast the diversity patterns of different subsets. Total-group chondrichthyans examined in this study were subsampled to assess relative diversity patterns of major chondrichthyan groups. First, the data was arbitrarily divided into acanthodian chondrichthyans and non-acanthodian chondrichthyans following the divisions used in Chapters 1 and 2 of this thesis. Non-acanthodian chondrichthyans here include the non-acanthodian stem-chondrichthyans (*Gladbachus*, *Gydoselache*, *Pucapampella* and *Doliodus*) and the crown-group chondrichthyans throughout the Palaeozoic. Ordovician shark-like scale taxa *Solinalepis*, *Tantalepis*, *Canyonlepis* and *Tezakia* and the Silurian scale- and fin spine-based mongolepids, elegestolepids and sinacanthids are also included here. While they may fall out with the acanthodians, they are currently largely ignored in phylogenetic analyses of the total-group chondrichthyans and will be grouped with the ‘conventional’ chondrichthyans for now (Sansom & Andreev 2017).

Subsequently, the chondrichthyan crown was subsampled into total-group

Holocephali and total-group Elasmobranchii following the same phylogenetic analyses mentioned above. Clades that were not included within these analyses but are standardly included within either of the groups based on extensive catalogues (see Stahl *et al.* 1999 and Ginter *et al.* 2010) were also added. Additionally, we grouped together into what we suggest falls on the chondrichthyan stem (such as acanthodians, sinacanthids, mongolepids, elegestolepids, omalodontiforms, antarctilamniforms, etc.) to contrast their diversity trajectories with the patterns of the crown-group. This is an inclusive approach that has not been adopted before and we acknowledge that some may sit in *incertae sedis* or as a poorly defined group within the chondrichthyans. Further information is available in the supplementary data files. The total-group Holocephali was further subdivided into those possessing tooth plates, a distinctive characteristic of holocephalans, to assess whether the emergence of this type of dentition coincides with major patterns of diversification. This includes no prior assumption that tooth-plated forms constitute a monophyletic group.

The approach of using recent phylogenetic results was contrasted using the systematics and branching scheme of chondrichthyans into Elasmobranchii and Euchondrocephali of Ginter *et al.* (2010) (and in part Stahl *et al.* 1999) based primarily on tooth and dentition morphology not a character-based phylogeny. This was done to test how robust subgroup chondrichthyan diversity inferences are through time under conflicting sequences of interrelationships.

Following the subdivisions, we subsampled the data for chondrichthyans iteratively excluding Holocephali/Euchondrocephali to infer if they dominated specific time intervals. Lastly, possible environmental influences were tested by sub-setting the dataset into occurrences from freshwater or marine deposits. Depositional settings of each occurrence were then further divided into benthic assemblage zones (BA) in subsequent analyses (see Chapters 1 and 2 for explanations of the BAs).

4.2.3 Sampling and Diversity

All data manipulation, statistical analyses and data plotting were conducted in R v. 4.2.0 (R Core Team 2018). Fossil occurrences were binned into single geological stages and used to estimate raw global sampled-in-bin richness curves for chondrichthyans. We also counted the total number of formations and collections for each geological stage to check for sampling biases. Local richness, or alpha diversity, was estimated by counting genera per collection (equivalent to fossil locality) and genera by formation. The fossil record of any given group will have spatial and temporal variations in sampling which must be accounted for when reconstructing diversity patterns through time (e.g., Raup 1972; Benson & Upchurch 2013; Close *et al.* 2018; Alroy 2020). We largely follow the protocols used in recent fossil diversity studies (e.g., Dunne *et al.* 2018; Allen *et al.* 2020; Dean *et al.* 2020) and use Shareholder Quorum Subsampling or SQS as our method of coverage-based sampling standardization to correct for uneven sampling when estimating changes in global diversity through time (Alroy 2010). Diversity and subsampling analyses were generated using the R packages DivDyn (Kocsis *et al.* 2019) and iNEXT (Hsieh *et al.* 2016). DivDyn incorporates the inexact algorithm of SQS (see Close *et al.* 2018). iNEXT implements coverage-based rarefaction using the equations of Chao & Jost (2012) and is analogous to SQS. We did not conduct the optional three-collections-per-reference protocol proposed by Alroy (2010) for either analysis because Palaeozoic chondrichthyans are not subject to over-reporting of common taxa (Figure C.1). also be an option, but such methodsare biased downward when distributions are highly unevenand samples are very small (Close et al., 2018). Squares ismore robust to these biases

Subsampled richness estimates were additionally calculated using the squares estimation implemented by Alroy (2018). Squares is a simple extrapolator that was developed to minimise underestimation when abundance distributions are uneven (see Figure C.1 for the data used in this study) and is based on the proportion of singletons in a given sample (Alroy 2018). Contrary to coverage-based subsampling,

squares is more robust when distributions are highly uneven and samples are small (Alroy 2020). Squares richness estimates were calculated based on the protocol by Allen *et al.* (2020) which uses Alroy's squares equation (Alroy 2018). In addition to curves of diversity through time, we also conducted coverage-based rarefaction curves for each geological stage to illustrate how sampling coverage of genus richness estimates varies between time intervals. We analysed evolutionary dynamics of speciation and extinction for Palaeozoic chondrichthyans based on speciation and extinction rates using the package DivDyn. We calculated uncorrected rates as well as the second-for-third extinction rates implemented by Alroy (2015).

4.3 Results

Raw genus richness estimates of Palaeozoic chondrichthyans on a global scale peak in the early Devonian and early Carboniferous before dropping steeply over the Carboniferous-Permian boundary with no significant recovery throughout the Permian (Figure 4.1). The initial rise in the Devonian follows low diversity in the Middle-Upper Ordovician and the Silurian and numbers decrease slightly throughout the Devonian but remain high in comparison to previous stages. Most of the Permian diversity remains at a stable low level and similar in numbers to Middle Devonian richness. Diversity then falls in the Wordian (middle Permian) and continues at similarly low levels throughout the rest of the upper Permian. The greatest rises in raw richness occur during the Late Silurian to early Devonian (Ludfordian-Lochkovian) and the Late Devonian to Early Carboniferous (Frasnian-Visean). Local richness (alpha diversity) is highest during the Mississippian of the Carboniferous, with two exceptionally well-sampled sites in the Visean ($>$50 genera) (Figure 4.1). However, most collections (=localities) throughout the Palaeozoic contain fewer than 10 genera (Figure C.2). Raw genus richness closely tracks patterns of sampling, especially number of collections, which is equivalent to number of fossil localities (p = 3.3E-15, R^2 = 0.86). This relationship between raw richness and sampling is also strong for total number of formations (p =

7.7E-14, R^2 = 0.83).

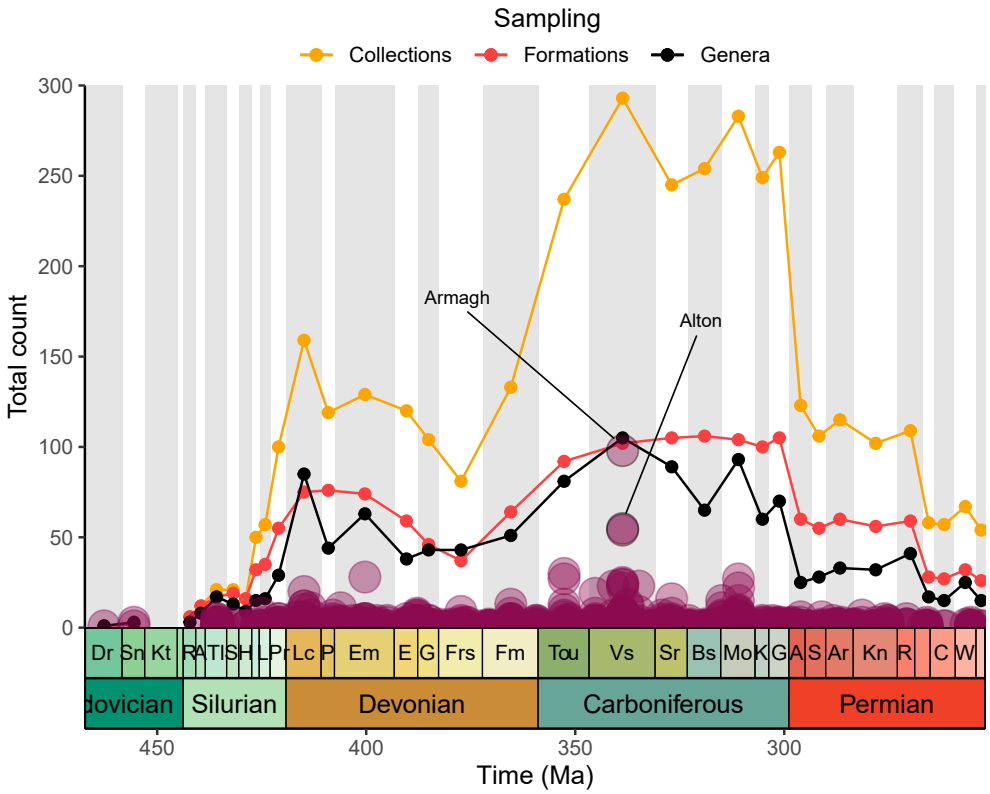


Figure 4.1: Chondrichthyan raw genus richness, local richness (alpha diversity) and sampling proxies in the Palaeozoic. Sampling proxies include counts of total collections and fossiliferous formations containing Palaeozoic chondrichthyans for each interval. Alpha diversity here is the number of genera per collection (=locality) and depicted as purple density circles.

Coverage-standardised richness estimates produce similar diversity-through-time curves to raw diversity (Figure 4.2A, Table 4.1). The timing and pattern of increases and drops in chondrichthyan diversity are generally the same as in raw genus richness. The most notable differences can be seen in the Middle and Upper Devonian: standardised diversity for chondrichthyans drops in the Eifelian and decreases from the Frasnian to Famennian which is the reverse of the pattern in the raw richness curve. The relative changes in diversity, specifically the prominent spikes in the Devonian, Carboniferous, and early Permian, are less pronounced at lower quorum levels (0.3 and 0.4) but are still recovered. The investigated intervals of the Palaeozoic have varying degrees of completeness as shown by the coverage estimates but most

are higher than 75% (Figure 4.3). The slopes of the rarefaction curves indicate that sampling is more complete in most stages of the Devonian and Carboniferous and limited in the Silurian. In the Permian, we find both stages with more complete sampling (e.g., Roadian, Wordian and Capitanian) and limited sampling (e.g., Changhsingian, Sakmarian and Asselian).

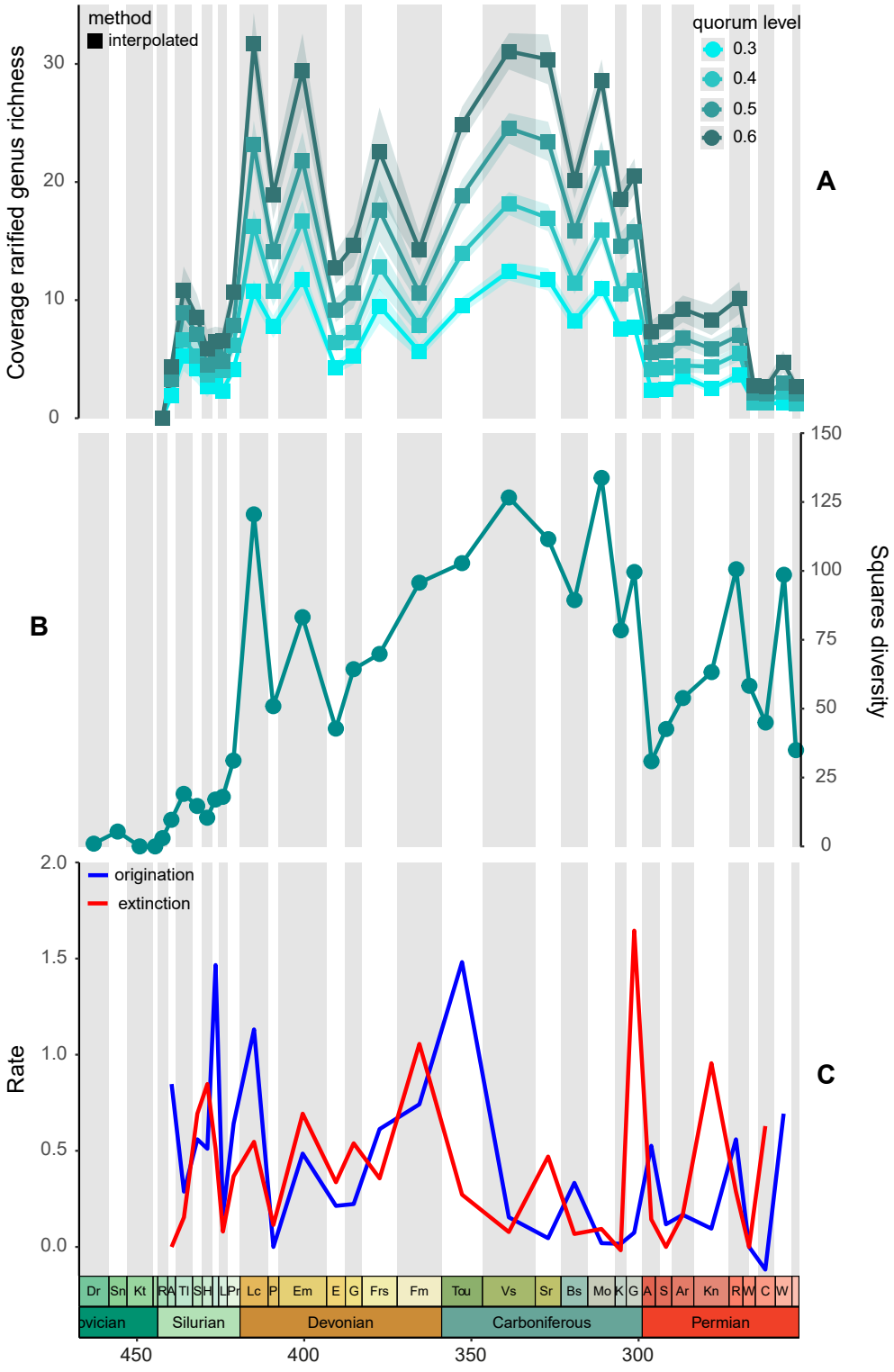


Figure 4.2: Chondrichthyan subsampled genus diversity and origination/extinction rates in the Palaeozoic. A, coverage-standardised diversity at different quorum levels. Quorum levels represent the target sampling (coverage) level. B, squares diversity. C, Second-for-third origination/extinction rates.

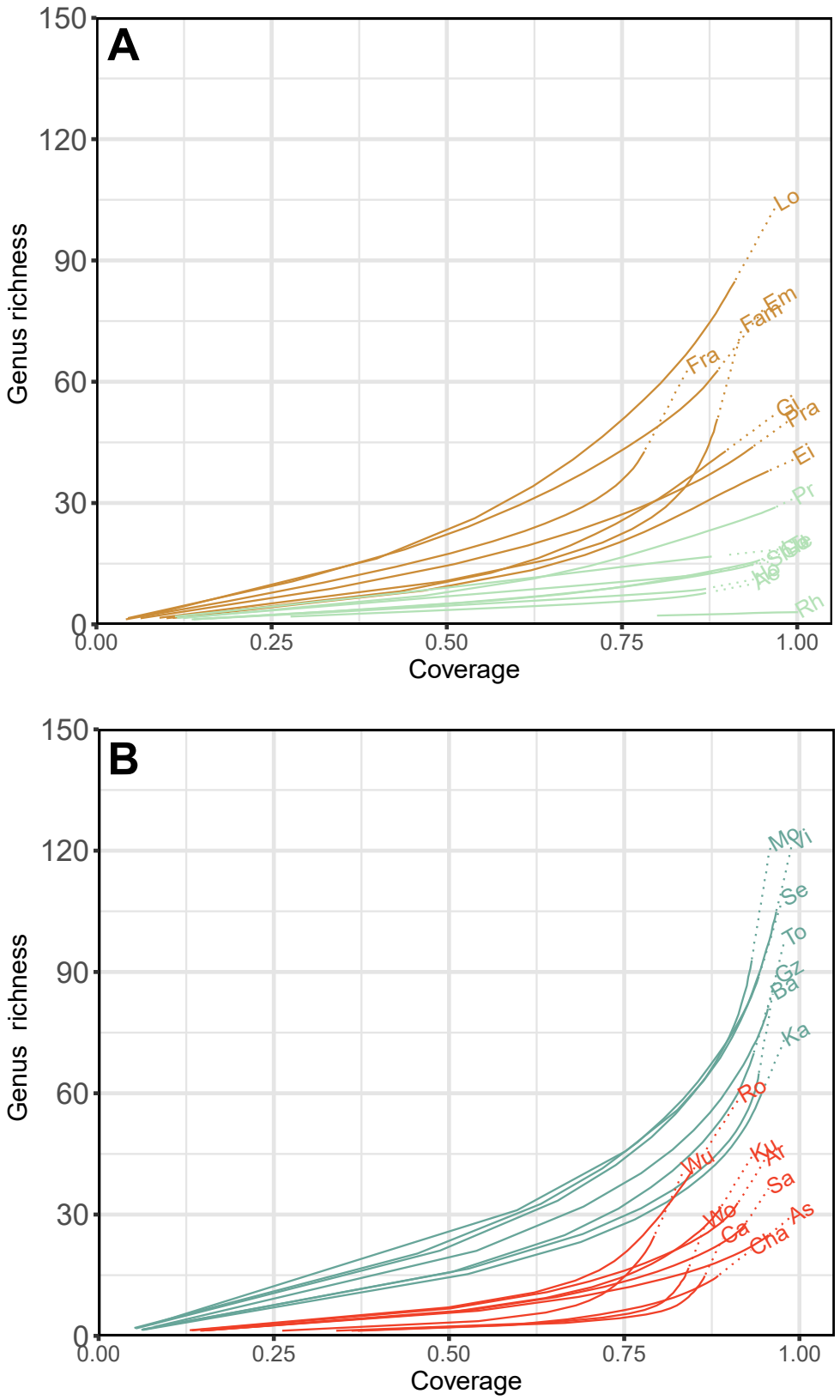


Figure 4.3: *Caption on next page.*

Figure 4.3: Coverage-based rarefaction curves (solid line) and extrapolation (dotted line) for all investigated intervals of the Palaeozoic, comparing sampling coverage in each time interval. A, Silurian (light-green) and Devonian (yellow). B, Carboniferous (blue) and Permian (red). Extrapolated lines (dotted) represent the Chao1 extrapolator (see Hsieh *et al.* 2016). Ae, Aeronian; Ar, Artinskian; As, Asselian; Ba, Bashkirian; Ca, Capitanian; Cha, Changhsingian; Ei, Eifelian; Em, Emsian; Fam, Fammenian; Fra, Frasnian; Gi, Givetian; Gz, Gzhelian; Ho, Homerian; Ka, Kasimovian; Ku, Kungurian; Lo, Lochkovian; Mo, Moscovian; Pr, Pridoli; Pra, Pragian; Rh, Rhuddanian; Ro, Roadian; Sa, Sakmarian; Se, Serpukhovian; Sh, Sheinwoodian; Te, Telychian; To, Tournaisian; Vi, Visean Wu, Wuchiapingian.

Squares diversity estimates produce a similar curve through time to raw and coverage-standardised richness (Figure 4.2B, Table 4.1). The main differences in the squares diversity curve when compared to the latter are the higher values in the Permian after an initial drop across the Carboniferous-Permian boundary. Squares produces more pronounced peak diversity estimates in the Roadian and Wuchiapingian than seen in either of the two other curves. Second-for-third (=corrected) origination and extinction rates show major origination peaks in the Gorstian, Lochkovian and Tournaisian, while rates of extinction are highest in the Homerian, Famennian, Gzhelian and Kungurian (Figure 4.2C, Table C.1). Squares diversity is dominated by acanthodian chondrichthyans in the late Silurian and the Devonian but this group decreases in diversity throughout the Upper Devonian (Figure 4.4A). Diversity of acanthodians plummets across the Devonian-Carboniferous boundary and steadily decreases throughout the Carboniferous and Permian. By contrast, non-acanthodian chondrichthyan richness rises substantially from the Middle Devonian through to the early Carboniferous (Eifelian-Visean) and remains at high levels during the remaining stages of the Carboniferous before decreasing substantially across the Carboniferous-Permian boundary (Figure 4.4B). The Permian is dominated by non-acanthodian chondrichthyans but diversity remains at generally lower levels than in the Carboniferous, except for the two diversity peaks in the Roadian and Wuchiapingian.

Table 4.1: Results of pairwise comparisons of different diversity estimates using GLS. Statistically significant results indicated in bold.

Comparison	Slope	t-value	p-value	R^2
Raw richness ~ squares diversity	0.543	11.7	> **0.00001**	0.915
Raw richness ~ SQS diversity (0.3)	6.34	9.64	> **0.00001**	0.867
Raw richness ~ SQS diversity (0.4)	4.49	11.2	> **0.00001**	0.898
Raw richness ~ SQS diversity (0.5)	12.0	3.32	> **0.00001**	0.909
Raw richness ~ SQS diversity (0.6)	12.6	2.53	> **0.00001**	0.918
Squares diversity ~ SQS diversity (0.3)	8.03	5.53	> **0.0001**	0.650
Squares diversity ~ SQS diversity (0.4)	5.92	6.23	> **0.00001**	0.694
Squares diversity ~ SQS diversity (0.5)	4.35	6.39	> **0.00001**	0.703
Squares diversity ~ SQS diversity (0.6)	3.44	6.93	> **0.00001**	0.730

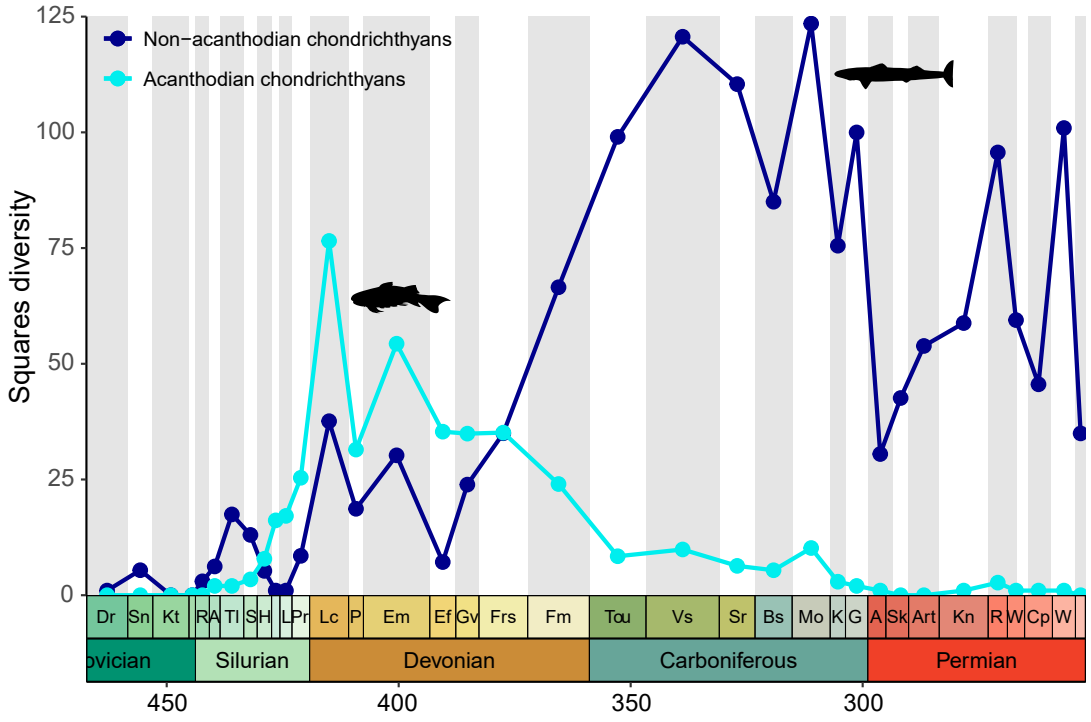


Figure 4.4: Squares diversity for acanthodian and non-acanthodian chondrichthyans through the Palaeozoic.

Total-group Elasmobranchii and Holocephali first appear in the early Devonian, albeit holocephalans emerge slighlty later in time (Figure 4.5). Holocephali dominate the rise in chondrichthyan diversity throughout the Carboniferous. Upon removal of holocephalans from the dataset, coverage-standardised richness estimates and squares diversity are considerably lower throughout the Carboniferous (Figure C.3).

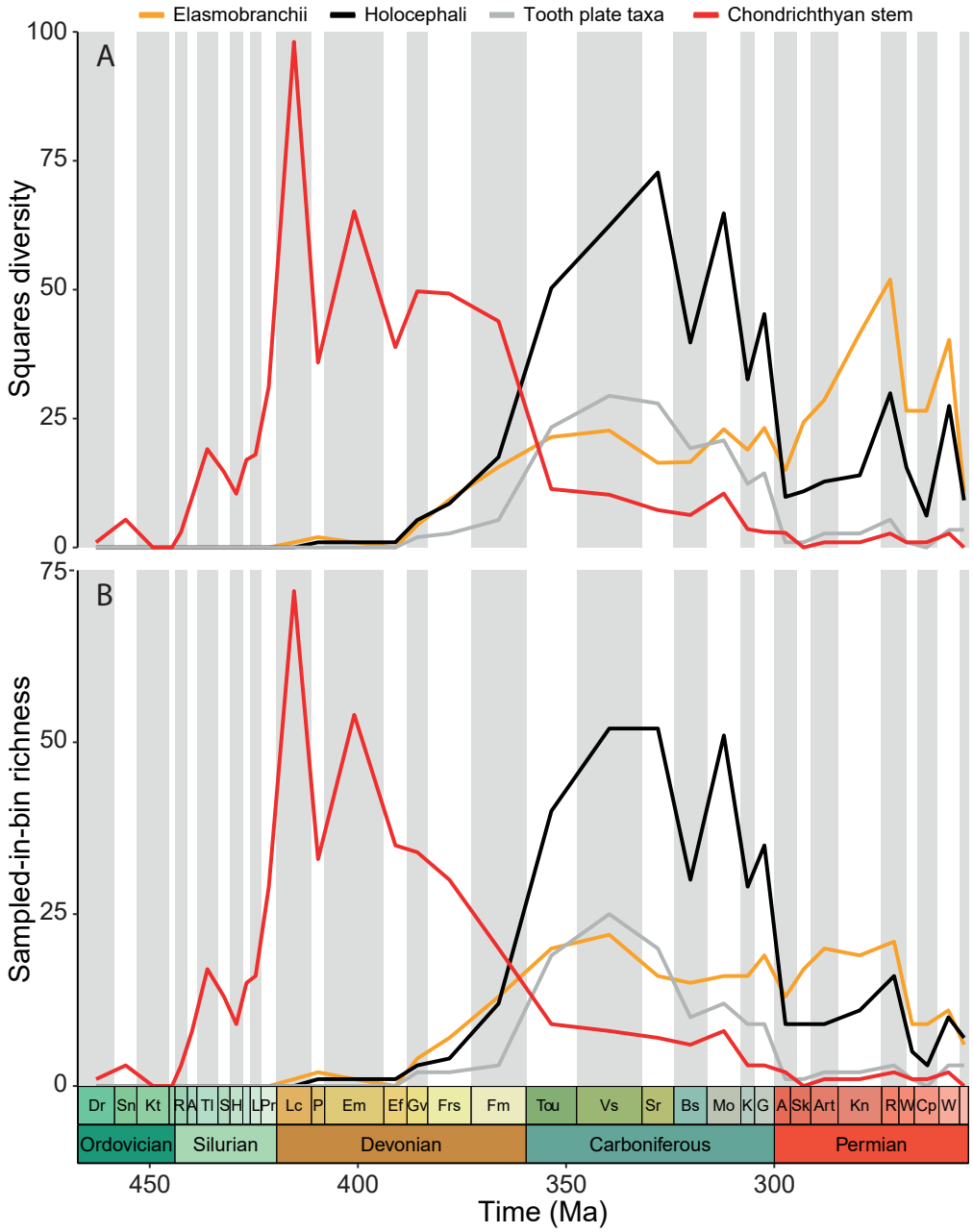


Figure 4.5: Subsampled and raw richness estimates of chondrichthyan subgroups. Subgroupings are based on the recent phylogenies from Coates *et al.* 2018, Dearden *et al.* 2019 and Frey *et al.* 2020. A, squares diversity. B, raw sampled-in-bin richness.

When the chondrichthyan stem is grouped together, the pattern of early Devonian diversification and Late Devonian fall, as already seen in the acanthodian chondrichthyans, is reinforced and further amplified (Figure 4.5). Stem chondrichthyans appear to persist throughout the remainder of the Palaeozoic but in low numbers.

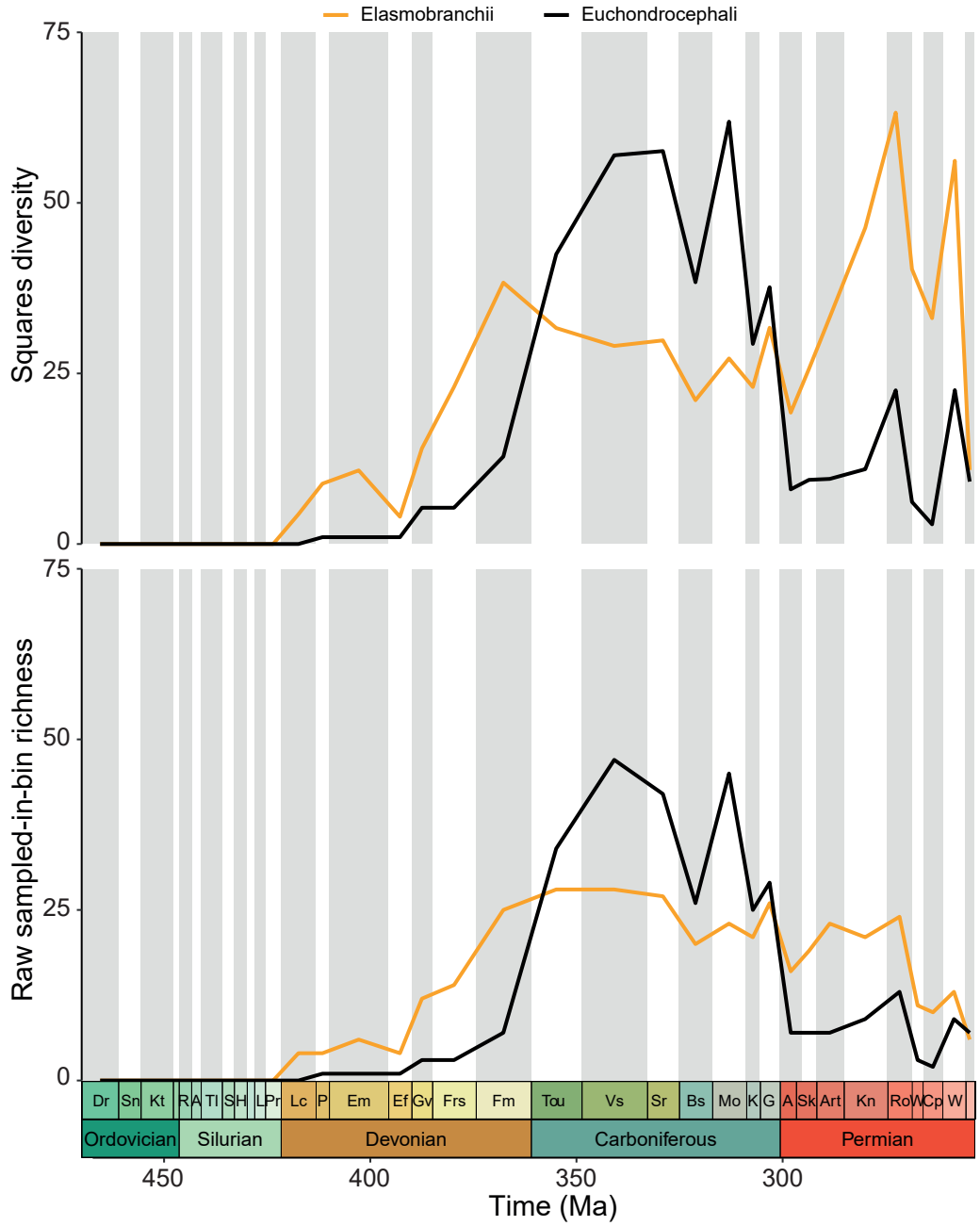


Figure 4.6: Subsampled and raw richness estimates of Chondrichthyan subclasses, based on the systematics from Ginter *et al.* 2010. A, squares diversity. B, raw sampled-in-bin richness.

Tooth-plated holocephalans emerge in the Middle Devonian and diversify con-

siderably post-Devonian before decreasing heavily at the Carboniferous-Permian boundary, together with all other subgroups (Figure 4.5). Raw and subsampled richness estimates recover similar patterns of diversity for total-group elasmobranchs and holocephalans, except for a slight temporal shift in holocephalan peak diversity from the Visean towards the Serpukhovian in the subsampled curve (Figure 4.5A, B). Comparisons with patterns of subclasses as implemented by Ginter *et al.* 2010 reveal highly similar diversity trajectories through time (Figure 4.6).

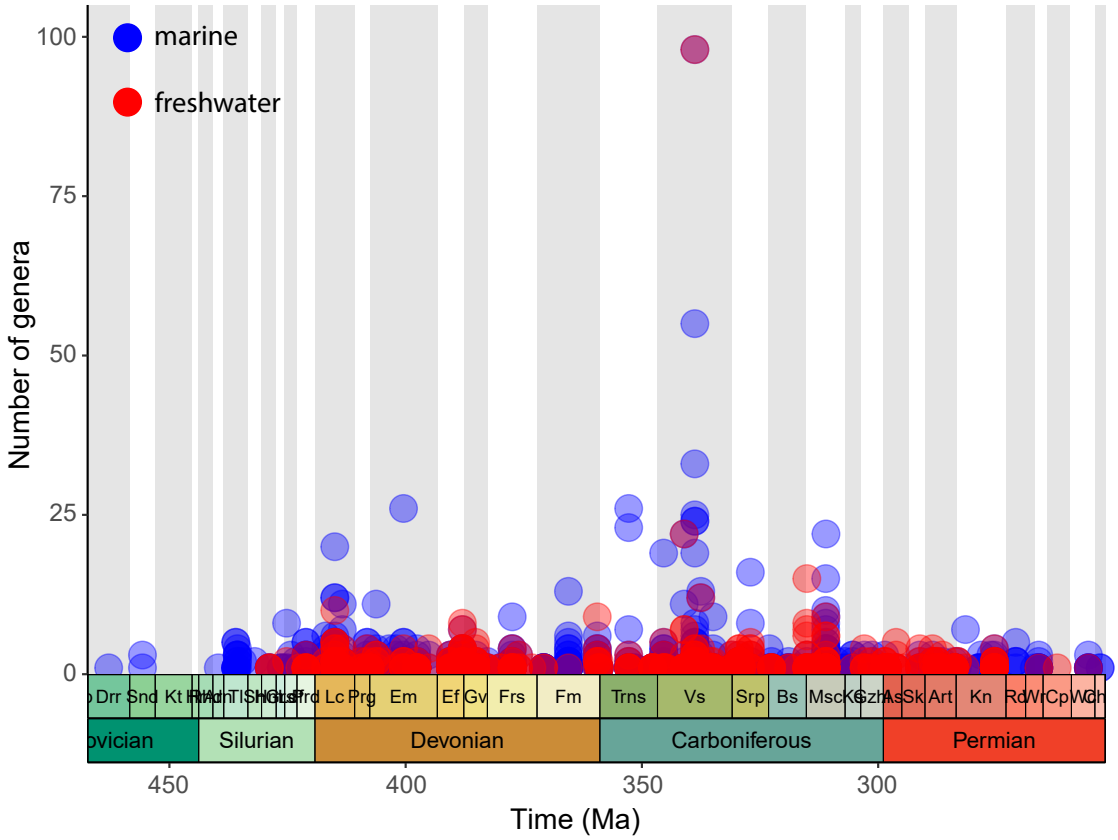


Figure 4.7: Local richness (alpha diversity) from the Ordovician to the Permian divided into freshwater and marine occurrences. Local richness is the number of genera per collection/ fossil locality.

Chondrichthyans do not appear in freshwater environments until the middle Silurian but are recovered solely from marine localities in the Ordovician and lower Silurian (Figure 4.7). The Carboniferous shows an increase in marine alpha diversity in the Mississippian, with exceptionally diverse localities in the Visean. Further division into benthic assemblage zones reveal that the initial origination of marine

chondrichthyans is restricted to the shallow marine BA1 and BA2 zones (Figure 4.8A). Chondrichthyan diversity expands into the deep water BA5 and BA6 zones in the upper Silurian, but local richness only increases in the Carboniferous (Figure 4.8B). Diverse deep-water localities are recovered in the Visean specifically.

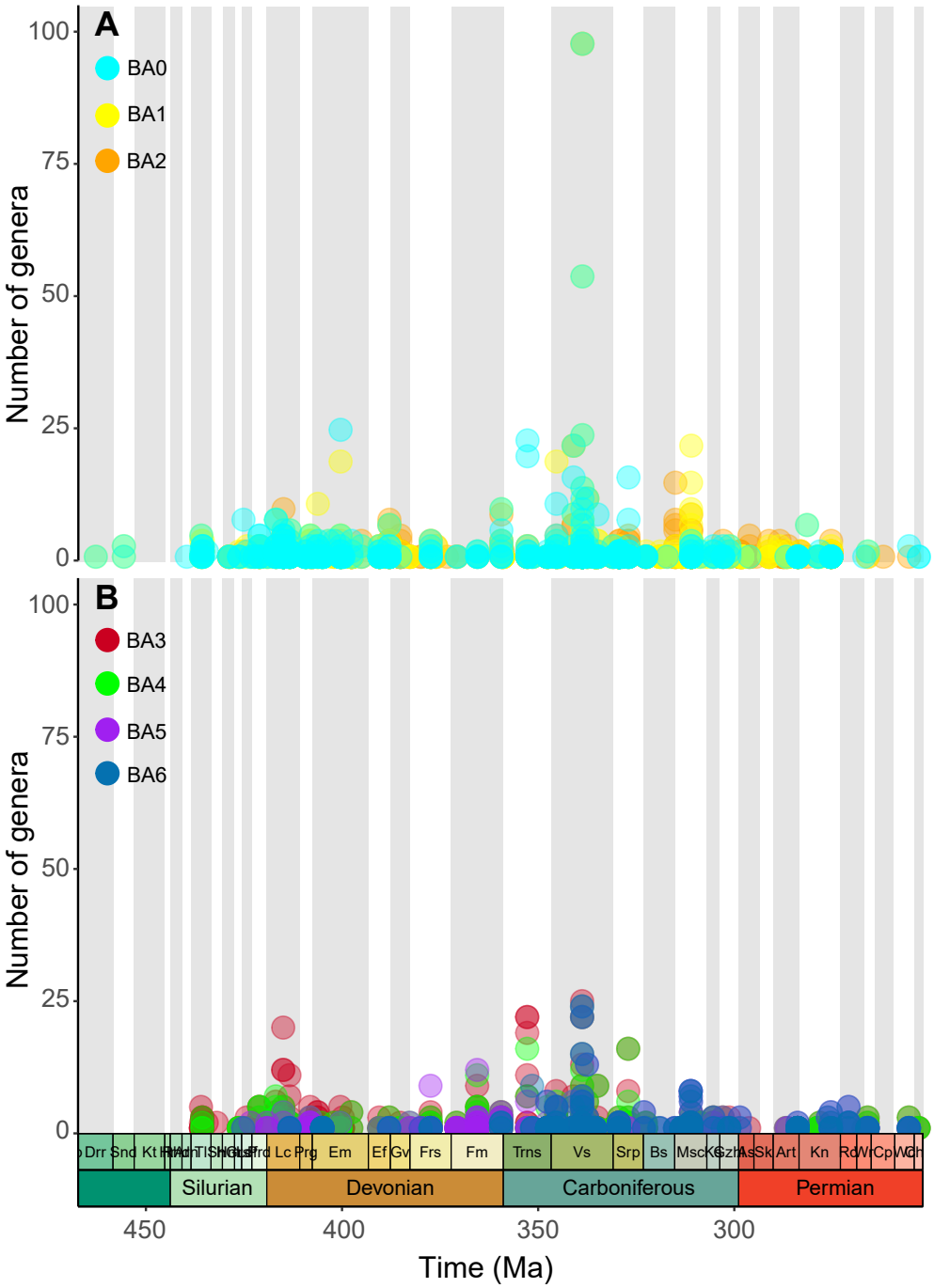


Figure 4.8: Local richness (alpha diversity) divided into benthic assemblage zones (BA) from the Ordovician to the Permian. Local richness is the number of genera per collection/ fossil locality.

4.4 Discussion

4.4.1 Patterns of Palaeozoic chondrichthyan diversity

We provide the first in-depth estimates of global chondrichthyan richness for the whole Palaeozoic. Direct comparisons of our estimates to previous studies are mostly limited to the Late Devonian, Carboniferous, and Permian (Sallan & Coates 2010; Koot 2013; Feichtinger *et al.* 2021), specifically the Frasnian-Famennian Kellwasser crisis, the end-Devonian Hangenberg extinction event that marks the transition from the Devonian to the Carboniferous, and the end-Permian mass extinction (Raup & Sepkoski 1982; McGhee 1996; Caplan & Bustin 1999). Sallan & Coates (2010) reported no major diversity losses for most jawed vertebrates, including chondrichthyans, through the Kellwasser event. Although we find some support for this using raw richness and squares estimates in our analyses, coverage-standardised richness is consistent with a decrease in diversity from the Frasnian to Famennian, albeit less pronounced than the drops in the Lochkovian-Pragian and Emsian-Eifelian (Figure 4.2A). Raw richness and squares diversity instead show steep increases in diversity during the Kellwasser event (Figures 4.1, 4.2B). When total-group chondrichthyans are separated into acanthodian and non-acanthodian chondrichthyans, squares diversity shows a significant loss for acanthodians while non-acanthodian chondrichthyans steeply increase in diversity across the Frasnian-Famennian (Figure 4.4). Sallan & Coates (2010) illustrated a similar pattern, albeit with a less severe decrease in acanthodians. As suggested previously, the Kellwasser event might be overreported in severity by insufficient sampling of Famennian localities relative to the Frasnian ones (Sallan & Coates 2010; Friedman & Sallan 2012). Our coverage-based rarefaction curves, however, do not show considerable differences between the two stages (Figure 4.3A).

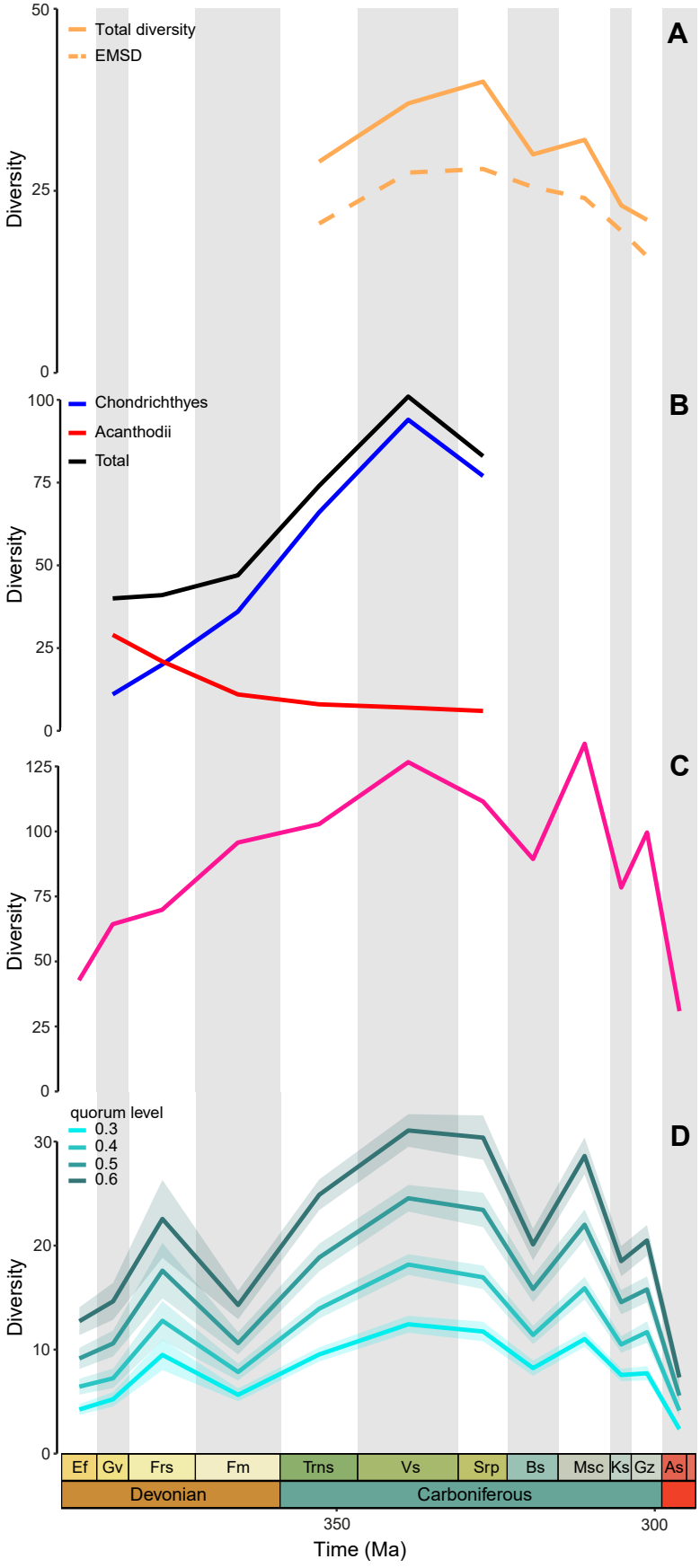


Figure 4.9: *Caption on next page.*

Figure 4.9: Comparisons of chondrichthyan diversity curves in the Devonian and Carboniferous. A, Total diversity and Estimated Mean Standing Diversity (EMSD) of Carboniferous elasmobranch genera by Feichtinger *et al.* (2021). B, raw chondrichthyan and acanthodian diversity by Sallan & Coates (2010). C, squares diversity of chondrichthyans investigated in this study. D, chondrichthyan coverage-standardised richness estimates calculated in this study.

In contrast, the increase in chondrichthyan diversity after the Hangenberg extinction reported here is comparable to that seen in the diversity curve of Sallan & Coates (2010) but differs from the diversity curve from Feichtinger *et al.* (2021), which was based solely on elasmobranchs (Figure 4.9). Chondrichthyan diversity steadily increased from the Givetian to the Visean and dropped in the Serpukhovian, as reported by Sallan & Coates (2010). This pattern is mostly congruent with our estimates of richness, except for a peak in the Frasnian in our coverage-standardised richness estimates that is not shown in Sallan & Coates (2010) (Figures 4.2A, 4.9).

Feichtinger *et al.* (2021) reported an increase in diversity through the Mississippian with highest numbers in the Serpukhovian rather than the Visean. However, they only analysed non-euchondrocephalian chondrichthyans and are therefore likely to differ to some degree from our analyses of total-chondrichthyan diversity. Chondrichthyan diversity follows a similar trend in both our analysis and those of Feichinger *et al.* (2021) in the early and middle Pennsylvanian, with an initial fall in the Bashkirian, a subsequent peak in the Moscovian and a decrease again in the Kasimovian. The curves differ in the Gzhelian in that diversity continues to drop in the analysis of Feichtinger *et al.* (2021) but slightly rises in our study. Our estimates of Permian chondrichthyan diversity also differ from those previously reported by Koot (2013) in an unpublished PhD thesis. Our sampled curves drop from the Roadian to the Wordian instead of increasing over that time interval (Figure 4.2A, B), and remain at low levels for the rest of the Permian (except for a squares diversity spike in the Changhsingian). Koot (2013) showed a gradual decline in richness throughout the middle-upper Permian, contrasting with our analyses. This difference in observed patterns may be related to a difference in methodology, as we used subsampling approaches to account

for an incomplete fossil record while Koot (2013) used counts of taxa and estimated mean standing diversity (EMSD), calculating both without standardisation.

Our squares diversity curves reveal opposing patterns between acanthodian and non-acanthodian chondrichthyans (Figure 4.4). Acanthodians thrived in the Lower and Middle Devonian but declined from the Upper Devonian onwards. The diversity of non-acanthodian chondrichthyans, conversely, is limited during the Lower-Middle Devonian but significantly increases from the latest Devonian on. Acanthodians survived the Hangenberg extinction but did not seem able to diversify substantially post-Devonian and appear to have been an outcompeted and niche-restricted "Dead Clade Walking" (Jablonski 2002; Sallan & Coates 2010). The earliest acanthodians inhabited the shallow seas of the lower Silurian but quickly expanded into freshwater habitats during the Late Silurian and Early Devonian (Figure 4.7), a pattern consistent with previously published hypothesis of early vertebrate diversification (Sallan *et al.* 2018). This transition may have allowed them to mitigate competition and predation pressure, particularly from the dominant Silurian macropredatory eurypterids (Lamsdell & Braddy 2010). By the end of the Devonian, diverse assemblages of jawed vertebrates, including chondrichthyans, osteichthyans, placoderms and tetrapods, are found in the increasingly productive and complex estuarine and freshwater ecosystems, linked to the expansion of terrestrial vascular plants during the Middle and Upper Devonian (Beerbower 1985; Davies & Gibling 2010). However, acanthodians started to decline during this time, possibly outcompeted by the other jawed vertebrate clades. Thus, post-Devonian, acanthodians primarily consist of only two specialised genera, *Gyracanthus* and *Acanthodes*.

While acanthodians struggled, non-acanthodian chondrichthyan diversity increased from the Lower Devonian on and peaked throughout the Carboniferous. Chondrichthyan alpha diversity showed an increase in deeper water localities in the Mississippian and again in the middle Pennsylvanian (see Figure 4.7). This indicates that Carboniferous chondrichthyans may have refilled the deep-water environments that

became available after the Hangenberg extinction. However, this apparent pattern may also be skewed by sampling biases against available outcrop for marine deep-water sediments compared to the continental shelf in other periods of the Palaeozoic (Gregor 1970; Smith *et al.* 2002). The great post-Hangenberg diversification of chondrichthyans is predominantly driven by the rise of the Holocephali or Euchondrocephali sensu Lund & Grogan (1997; 2004), a subclass of crown-group chondrichthyans of which the chimaeras still exist in today's deeper-water environments (Lund & Grogan 1997; Grogan & Lund 2000; Lund & Grogan 2004). They first appeared in the Lower Devonian, but their fossil record is scarce and fragmentary at best (see supplementary information).

Following the Hangenberg extinction, holocephalans greatly diversified and drove total chondrichthyan diversity throughout the Carboniferous before losing diversity across the Carboniferous-Permian boundary. This diversification follows major changes in the jawed vertebrate biota over the Late Devonian and Early Carboniferous, most notably the demise of placoderms and severe decreases in diversity of early sarcopterygians (Sallan & Coates 2010). It is possible that this faunal transformation is the subject of gradual and/or competitive displacement as well as the refilling of niche space following a large-scale mass extinction (Jablonski 2005; Janvier & Clement 2005; Zhao & Zhu 2007; Sallan *et al.* 2011). Holocephalans may have experienced a lowered predation pressure and competition for available niches, allowing them to thrive and establish themselves in the post-extinction conditions of the early Carboniferous (Janvier 1996; Blieck 2011). This is further supported by the response of invertebrate crinoid diversity to predator-prey interactions before, during and after the Hangenberg event, with reduced predation pressure after the extinction event due to removal of major vertebrate predators and increased predation pressure from 'new' durophagous fishes (such as most holocephalans) in the later Mississippian (Sallan *et al.* 2011). Tooth-plated forms greatly diversify only after the Hangenberg extinction event (Figure 4.5). Interestingly, Carboniferous holocephalans predominantly dispersed into both shallow

and deeper waters, a pattern similar to the mid-Palaeozoic diversification of micromeric stem-group gnathostomes such as the thelodonts (Sallan *et al.* 2018).

4.4.2 Environmental influences and the impact of biases on Palaeozoic chondrichthyan diversity

Raw global chondrichthyan richness estimates are subject to temporal and spatial sampling biases (Figure 4.1). This correlation is more evident for the number of collections where the peaks in collection counts are almost identical to raw richness. Surprisingly, coverage-standardised richness estimates of diversity and squares diversity both capture generally similar patterns to raw richness estimates. This suggests that temporal and spatial sampling biases, while undoubtedly present, may not considerably mask true patterns of global chondrichthyan diversity in the Palaeozoic. Sampling is limited in the Silurian and in most of the Permian stages, thus distinguishing between true low diversity and poor sampling is difficult and must be done with caution (Figure 4.3). Conversely, most of the Devonian (except for the Givetian, Pragian and Eifelian) and the Carboniferous stages are rather well sampled, suggesting that a more accurate and biologically meaningful signal of chondrichthyan diversity is obtainable during this time. Further sampling and new discoveries from the Ordovician, Silurian and Permian stages are needed to better resolve the observed distributions of diversity in the earliest chondrichthyans and during the Permian, specially in the context of the lead up to the end-Permian mass-extinction.

Some of the most prominent changes in chondrichthyan diversity are found across the transition from one time system to the next, i.e., Silurian-Devonian, Devonian-Carboniferous and Carboniferous-Permian. Silurian-Devonian and Devonian-Carboniferous boundaries mark steep increases in diversity while the Carboniferous-Permian boundary leads to a major drop in diversity. The pattern is not surprising for the Devonian-Carboniferous boundary given that this coincides with the Hangenberg extinction but is more difficult to explain for the Silurian-Devonian and Carboniferous-

Permian. Silurian diversity of chondrichthyans is critically undersampled, as shown by the rarefaction curves, while the stages of the Lower Devonian are fairly well-sampled. Together, these observations may explain the marked increase over the boundary (see Figure 4.3). The Late Carboniferous to Early Permian is marked by irregularly increasing climatic aridity, glaciation and de-glaciation sequences, and faunas are mostly represented by lacustrine assemblages (Isbell *et al.* 2003; Opluštil *et al.* 2013; Rosa & Isbell 2021). Additionally, tropical rainforests were replaced by dryland vegetation in large parts of the terrestrial settings during the Late Carboniferous through to the early Permian (the Carboniferous 'rainforest collapse' or CRC) and were shown to at least impact on terrestrial faunas (Cleal *et al.* 2009; Cleal *et al.* 2012; Dunne *et al.* 2018). These environmental and climatic conditions may have had a negative influence on chondrichthyan diversity, resulting in increased extinction rates, but sampling biases may also be present.

Our analyses suggest two initial radiations in Palaeozoic chondrichthyan diversity in the earliest Devonian and earliest Carboniferous (Figure 4.2). Another origination peak appears in the middle Silurian but is biased by very limited sampling throughout most of the Silurian. Conversely, extinction of chondrichthyan genera is heightened in the Famennian stage of the Late Devonian and the Kungurian stage of the Permian and is only surpassed by the peak in extinction in the Gzhelian just before the Carboniferous-Permian boundary. The extinction peak in the Kungurian is biased by lower sampling coverage but may be at least partially influenced by the complex climate dynamics during the large-scale icehouse-greenhouse transition in the late Palaeozoic (Nakazawa *et al.* 2015; Liu *et al.* 2017a). Widespread ocean stagnation and oxygen-deficient conditions (Liu *et al.* 2017b) may have contributed to a heightened extinction of chondrichthyan genera in the interval.

4.4.3 Comparisons with invertebrate diversity trends

Comparisons with global Palaeozoic diversity trends in marine invertebrate lineages may reveal further patterns regarding the initial diversification of chondrichthyans. The radiation of marine diversity in the early Devonian, both in invertebrates and chondrichthyans, coincides with the 'Devonian Nekton Revolution' where macroecological changes may have led to an expansion in benthic and demersal zones, culminating in a trophic level shift towards nektonic groups (Klug *et al.* 2010; Servais *et al.* 2016). This would suggest an initially high diversity of life accumulating in benthic habitats that became saturated in the Devonian and subsequently promoted dispersal of organisms from the benthos into the water column. Whether the rise in chondrichthyan diversity over the Silurian-Devonian can be attributed to this ecological key event or is masked by undersampling remains uncertain for now.

Genus-level diversity of global marine invertebrates shows a similar pattern to our chondrichthyan analysis throughout the Devonian, with higher initial diversity in the early stages and a subsequent fall in the Middle-Upper Devonian (Sepkoski 1996; Alroy *et al.* 2008). Major metazoan reef builders, including corals and stromatoporoids, also increased in diversity in the early Devonian before declining in the Frasnian and subsequently collapsing in the Famennian (McGhee 1996; Copper 2002). This general decline in diversity indicates severe changes in conditions that affected multiple trophic levels and may not be solely explained by the Frasnian-Famennian Kellwasser extinction event. The evolutionary role of reefs in harbouring and proliferating marine diversity, at least in part through generation of habitat complexity, was highlighted by Kiessling *et al.* (2010). Specifically, coral and fish diversity share a close relationship and may even depend on each other in some circumstances.

Moreover, comparative analyses of habitat-mediated diversification in modern sharks have indicated a strong influence of coral reef-associated habitats on the diversification of carcharhinid sharks (Sorenson *et al.* 2014). Carcharhinid sharks are

predominantly known to be reef-associated species and belong to the Carcharhiniformes, which, together with the Squaliformes, comprise the two most diverse lineages of extant sharks (Sorenson *et al.* 2014). Thus, reef-associated habitats seemingly have an accelerating effect on lineage diversification in modern sharks, a pattern which may have also been present in their Palaeozoic predecessors. A similar pattern is also found in the rapid synchronous diversification of both teleost and coral lineages in the Oligocene-Miocene, concurrent with increasing reef area and habitat complexity (Bellwood *et al.* 2015; Bellwood *et al.* 2017).

By contrast, the middle Palaeozoic origins and earliest diversification of all major non-tetrapod vertebrate clades were found in inter- and subtidal zones rather than reef habitats (Sallan *et al.* 2018). This highlights the need for further investigations into the role of invertebrate diversity and turnover, specifically reef builders, on chondrichthyan diversity, which is beyond the scope of this thesis. Identification of the causes for the Middle-Upper Devonian decline in particular are warranted to understand the large ecological changes in Devonian ecosystems.

4.5 Conclusions

Using a newly compiled genus-level dataset and a range of quantitative approaches to estimate diversity, our results show that Palaeozoic chondrichthyans first diversified in the early Devonian and peaked in the early Carboniferous, before heavily decreasing across the Carboniferous-Permian boundary and remaining at low levels throughout the Permian. The Palaeozoic era was a highly complex time period with major geological, environmental and biotic changes that shaped chondrichthyan diversity (Figure 4.10). The early diversification in the Devonian was led by acanthodian chondrichthyans, which subsequently decreased in diversity towards the end-Devonian.

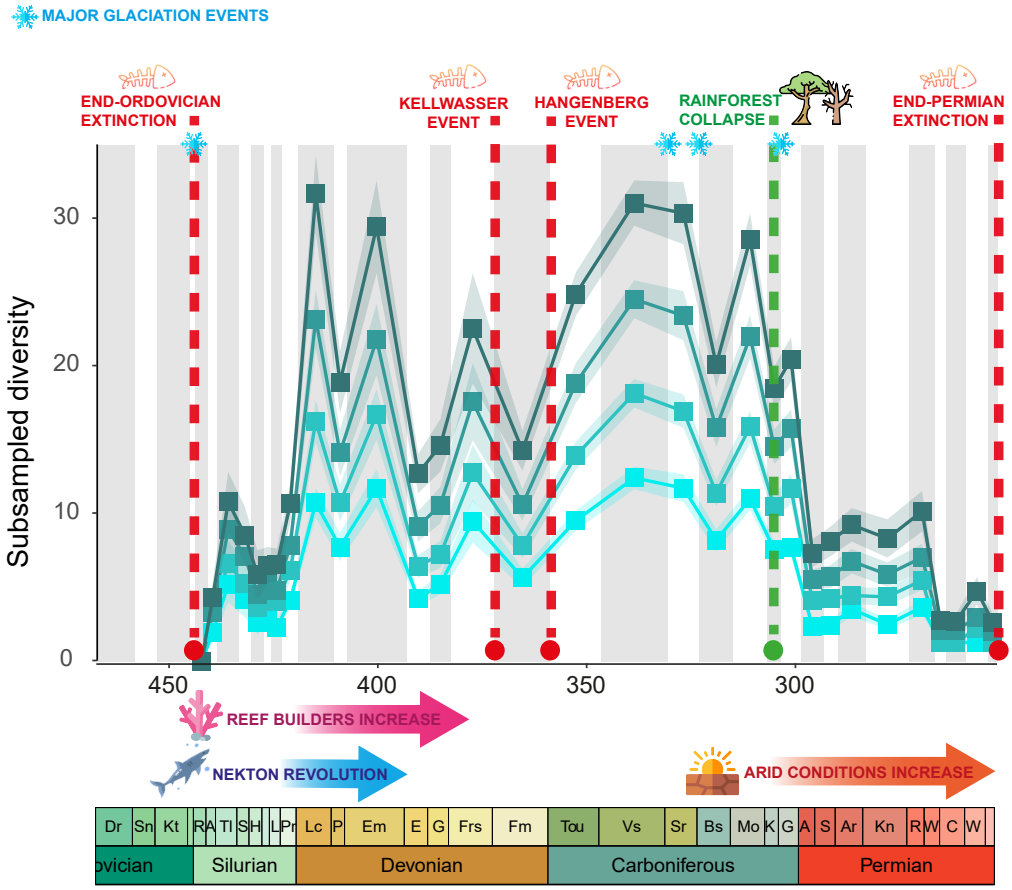


Figure 4.10: Simplified timeline of major events shaping chondrichthyan diversity.

The peak in diversity in the Carboniferous was likely driven by a faunal turnover following the Hangenberg extinction and major environmental changes. The increase in diversity was led by non-acanthodian chondrichthyans and dominated by the diversification of the holocephalans in both shallow and deep waters. The plummet in chondrichthyan diversity in the early Permian might be a response to the unstable conditions during that time, most prominently the rise in temperatures and reduction in marine habitats following the reconfiguration of landmasses. However, sampling in the Permian is also subject to considerable temporal and spatial biases which may mask a true biological signal. Increased sampling intensity and further re-examinations of museum collections may help to further advance our understanding of the drivers of diversity in this time interval, particularly environmental changes and unstable conditions.

CHAPTER 5

SUMMARY AND PERSPECTIVES

Extensive quantitative methods were employed in this thesis to assess the patterns and drivers of stem- and crown-group chondrichthyan completeness and diversity during their initial origination and diversification throughout the Palaeozoic. An array of natural and human-driven biases was identified and provides important insights into our understanding of chondrichthyan evolution and early history.

Chapters 2 and 3 investigated levels of completeness in acanthodian and non-acanthodian chondrichthyans from the Ordovician to the Permian, and how they impact fossil record quality. The results show that chondrichthyan completeness is not fundamentally connected to changes in diversity, i.e., time intervals with higher counts of diversity do not necessarily result in higher counts of completeness. This may be somewhat surprising but highlights the influence of other controls and biases on Palaeozoic chondrichthyan completeness and diversity trends. Implementation of a novel Soft Tissue Completeness Metric (STCM) when assessing completeness of the poorly preserved acanthodian chondrichthyans revealed similar patterns of completeness to estimates using the previously published skeletal metric, indicating that either one of the two could be used to accurately quantify completeness of the grade. In comparison to the previously assessed completeness patterns of several vertebrate groups, chondrichthyans initially have the lowest completeness scores, even when

compared to the poor and fragmentary fossil record of Cenozoic bats. Removal of taxa based solely on isolated material such as fin spines, scales, and teeth greatly increase completeness of the total group (as well as acanthodian and non-acanthodian chondrichthyans separately), highlighting the dominance of isolated remains on current interpretations on their early history. Environmental conditions play a vital role in shaping patterns of chondrichthyan completeness and potentially reflect shifts in habitat availability throughout their geological record. However, when discussing macroevolutionary patterns in the fossil record, one must also account for a potential array of biases that may influence the observed patterns. While neither acanthodian nor non-acanthodian chondrichthyan completeness is seemingly affected by spatial biases in our analyses, there are indications of temporal and environmental biases which may skew true signals.

Chapter 4 used the dataset initially compiled for Chapters 2 and 3 and extended it to investigate patterns of chondrichthyan diversity, origination, and extension throughout the Palaeozoic. Total group diversity using sampling standardisation showed that richness was initially low in the Silurian, increased substantially in the early Devonian and reached its maximum in the lower and middle Carboniferous before dropping across the Carboniferous-Permian boundary and throughout the Permian. When focussing on biotic interactions within the total group, our analyses suggest that acanthodian chondrichthyans drove the initial early diversification in the Devonian, while euchondrocephalans dominated the post-Hangenberg extinction diversification throughout the Carboniferous. Changes in chondrichthyan diversity appear to be affected by changes in climatic and palaeogeographical conditions throughout the Palaeozoic, including instability, glaciation events, temperature changes and reconfiguration of landmasses. Contrary to previous work on chondrichthyan diversity dynamics in the Palaeozoic (Sallan & Coates 2010; Koot 2013; Feichtinger *et al.* 2021), this chapter aims to analyse and address potential spatial and temporal sampling biases. Silurian and Permian intervals, specifically, are subjected to low sampling which masks

most of the observed patterns. However, the overall patterns of diversity for the total group chondrichthyans remain robust throughout the various analyses, specifically for the Devonian and Carboniferous, and demonstrate a promising array of tools to expand on for further macroevolutionary studies.

5.1 Future work and directions

Patterns of completeness, whilst extensively studied in some Mesozoic vertebrate groups, to date are comparatively constrained temporally and taxonomically. In order to accurately compare global macroevolutionary patterns, extensive completeness estimates for a wide range of temporal intervals as well as different vertebrate and invertebrate clades are required. In this thesis, I have provided the first accounts of completeness for a fish group and body plan and have expanded into a geological period other than the Mesozoic. Chapters 2 and 3 thoroughly investigated the completeness patterns of the total group chondrichthyan fossil record in the Palaeozoic but lacked comparisons with other contemporary and competing groups (e.g., actinopterygians, placoderms and jawless fishes) as has been achieved for Mesozoic tetrapods. Future research should continue to focus on completeness of specifically Palaeozoic as well as Cenozoic groups and continue to extend to cover a more diverse array of vertebrate and invertebrate groups and body plans. This will allow for a better comparison and contrast of global trends and a more thorough identification of the biases that are influencing fossil record quality.

Chapter 4 aimed to assess estimates of early chondrichthyan diversity using the most comprehensive and elaborate subsampling techniques to accurately capture the origination and early diversification of this group (given their current fossil record status) while also accounting for sampling bias influences. However, as technology and computational skills are advancing, future directions should continue to explore integrative and advanced analyses and modelling techniques to further overcome the biases and constraints of an incomplete fossil record. One such endeavour that has been de-

veloped in recent years is the program PyRate, a Bayesian framework-based program to estimate and model speciation, extinction, and preservation rates using a variety of tools (Silvestro *et al.* 2014; Silvestro *et al.* 2019), which may provide a potential pathway for future investigations on diversity through time next to traditional statistical methods. While this thesis focussed on quantifying early chondrichthyan diversity, both total and between different higher groups, and made some conclusions about potential environmental and biotic factors, future investigations should dive deeper into the abiotic and biotic drivers of their diversity patterns. Correlations of the diversity patterns established in this work with palaeobiogeography and palaeoclimate reconstructions using modelling approaches may especially provide a promising future direction into the influences of climate and geographical constraints on past diversity but also inform current scenarios of climate driven diversity changes in living chondrichthyans.

REFERENCES

ADLER, D. and KELLY, S. T. 2020. vioplot: violin plot. R package v. 0.3.5. https://github.com/TomKellyGenetics/vioplot.

AGASSIZ, L. 1833–1844. *Recherches sur les poissions fossiles*. V vols. Neuchâtel: Imprimerie de Petitpierre et Prince.

AGASSIZ, L. 1844–1845. *Monographie des poissons fossiles du Vieux Grès Rouge ou système Dévonien (Old Red Sandstone) des Iles britanniques et de Russie*. Neuchâtel, XXXVI + 171 pp.

AHLBERG, P. E., TRINAJSTIC, K., JOHANSON, Z. and LONG, J. A. 2009. Pelvic claspers confirm chondrichthyan-like internal fertilization in arthrodires. *Nature*, **460**, 888–889.

ALLEN, B. J., WIGNALL, P. B., HILL, D. J., SAUPE, E. E. and DUNHILL, A. M. 2020. The latitudinal diversity gradient of tetrapods across the Permo-Triassic mass extinction and recovery interval. *Proceedings of the Royal Society B*, **287**, 20201125.

ALLISON, P. A. and BRIGGS, D. E. G. 1993. Exceptional fossil record: distribution of soft-tissue preservation through the Phanerozoic. *Geology*, **21**, 527–530.

ALLISON, P. A., SMITH, C. R., KUKERT, H., DENNING, J. W. and BENNETT, B. A. 1991. Deep-water taphonomy of vertebrate carcasses: a whale skeleton in the bathyal Santa Catalina. *Paleobiology*, **17**, 78–89.

ALROY, J. 2010. Fair sampling of taxonomic richness and unbiased estimation of origination and extinction rates. *The Paleontological Society Papers*, **16**, 55–80.

ALROY, J. 2015. A more precise speciation and extinction rate estimator. *Paleobiology*,

41, 633–639.

ALROY, J. 2018. Limits to species richness in terrestrial communities. *Ecological Letters*, **21**, 1781–1789.

ALROY, J. 2020. On four measures of taxonomic richness. *Paleobiology*, **46**, 158–175.

ALROY, J., MARSHALL, C. R., BAMBACH, R. K., BEZUSKO, K., FOOTE, M., F€U RSICH, F. T., HANSEN, T. A., HOLLAND, S. M., IVANY, L. C., JABLONSKI, D., JACOBS, D. K., JONES, D. C., KOSNIK, M. A., LIDGARD, S., LOW, S., MILLER, A. I., NOVACKGOTTSHALL, P. M., OLSZEWSKI, T. D., PATZKOWSKY, M. E., RAUP, D. M., ROY, K., SEPKOSKI, J. J. Jr, SOMMERS, M. G., WAGNER, P. J. and WEBBER, A. 2001. Effects of sampling standardization on estimates of Phanerozoic marine diversification. *Proceedings of the National Academy of Sciences of the USA*, **98**, 6261–6266.

ALROY, J., ABERHAN, M., BOTTJER, D. J., FOOTE, M., FÜRSICH, F. T., HARRIES, P. J., HENDY, A. J., HOLLAND, S. M., IVANY, L. C., KIESSLING, W., KOSNIK, M. A., MARSHALL, C. R., MCGOWAN, A. J., MILLER, A. I., OLSZEWSKI, T. D., PATZKOWSKY, M. E., PETERS, S. E., VILLIER, L., WAGNER, P. J., BONUSO, M., BORKOW, P. S, BRENNEIS, B., CLAPHAM, M. E., FALL, L. M., FERGUSON, C. A., HANSON, V. L., KRUG, A. Z., LAYOU, K. M., LECKEY, E. H., NÜRNBERG, S., POWERS, C. M., SESSA, J. A., SIMPSON, C., TOMAŠOVYCH, A. and VISAGGI, C. C. 2008. Phanerozoic trends in the global diversity of marine invertebrates. *Science*, **321**, 97–100.

ANDREEV, P. S., COATES, M. I., SHELTON, R. M., COOPER, P. R., SMITH, M. P., and SANSOM, I. J. 2015. Upper Ordovician chondrichthyan-like scales from North America. *Palaeontology*, **58**, 691–704.

ANDREEV, P. S., COATES, M. I., KARATAJŪTĖ-TALIMAA, V., SHELTON, R. M., COOPER, P. R., WANG, N.-Z., and SANSOM, I. J. 2016. The systematics of the Mongolepidida

(Chondrichthyes) and the Ordovician origins of the clade. *PeerJ*, **4**, e1850.

ANDREEV, P. S., COATES, M. I., KARATAJŪTĖ-TALIMAA, V., SHELTON, R. M., COOPER, P. R. and SANSOM, I. J. 2017. *Elegestolepis* and its kin, the earliest monodontode chondrichthyans. *Journal of Vertebrate Paleontology*, **37**, e1245664.

ANDREEV, P. S., ZHAO, W., WANG, N.-Z., SMITH, M. M., LI, Q., CUI, X., ZHU, M. and SANSOM, I. J. 2020. Early Silurian chondrichthyans from the Tarim Basin (Xinjiang, China). *PLOS ONE*, **15**, e0228589.

ARMSTRONG, H. A. and HARPER, D. A. T. 2014. An earth system approach to understanding the end-Ordovician (Hirnantian) mass extinction. *In* KELLER, G. and KERR, A. (eds). *Volcanism, impacts, and mass extinctions: causes and effects*. The Geological Society of America Special Papers, **505**, 287–300.

ARSENAULT, M., DESBIENS, S., JANVIER, P. and KERR, J. 2004. New data on the soft tissues and external morphology of the antiarch *Bothriolepis canadensis* (Whiteaves, 1880), from the Upper Devonian of Miguasha, Quebec. *In* ARRATIA, G., WILSON, M. V. H. and CLOUTIER, R. (eds). *Recent advances in the origin and early radiation of vertebrates*. Verlag Dr. Friedrich Pfeil, 703 pp.

BAIRD, G. 1979. Lithology and fossil distribution, Francis Creek Shale in northeastern Illinois. *In* NITECKI, M. H. (ed.). *Mazon Creek Fossils*. Academic Press, 600 pp.

BARNOSKY, A. D., CARRASCO, M. A. and DAVIS, E. B. 2005. The impact of the species-area relationship on estimates of paleodiversity. *PLoS Biology*, **3**, e266.

BARRETT, P. M., MCGOWAN, A. J. and PAGE, V. 2009 Dinosaur diversity and the rock record. *Proceedings of the Royal Society B*, **276**, 2667–2674.

BARTON, K. 2018. MuMIn: multi-model inference. R package v. 1.43.17. https://CRAN.R-

project.org/package=MuMIn

BEARDMORE, S. R., ORR, P. J., MANZOCCHI, T. and FURRER, H. 2012a. Float or sink: modelling the taphonomic pathway of marine crocodiles (Mesoeucrocodylia, Thalattosuchia) during the death-burial interval. *Palaeobiodiversity and Palaeoenvironments*, **92**, 83–98.

BEARDMORE, S. R., ORR, P. J., MANZOCCHI, T., FURRER, H. and JOHNSON, C. 2012b. Death, decay and disarticulation: modelling the skeletal taphonomy of marine reptiles demonstrated using *Serpianosaurus* (Reptilia; Sauropterygia). *Palaeogeography, Palaeoclimatology, Palaeoecology*, **337**, 1–13.

BEERBOWER, J. R. 1985. Early development of continental ecosystems. *In* TIFFNEY, B. H. (ed.). *Geological factors and the evolution of plants*. Yale University Press, 476 pp.

BEHRENSMEYER, A. 1988. Vertebrate preservation in fluvial channels. *Palaeogeography, Palaeoclimatology, Palaeoecology*, **63**, 183–199.

BEHRENSMEYER, A., KIDWELL, S. M. and GASTALDO, R. A. 2000. Taphonomy and paleobiology. *Paleobiology*, **26**, 103–147.

BELLWOOD, D. R., GOATLEY, C. H. R., COWMAN, P. F. and BELLWOOD, O. 2015. The evolution of fishes on coral reefs: fossils, phylogenies, and functions. *In* MORA, C. (ed.). *Ecology of fishes on coral reefs*. Cambridge University Press, 374 pp.

BELLWOOD, D. R., GOATLEY, C. H. R. and BELLWOOD, O. 2017. The evolution of fishes and corals on reefs: form, function and interdependence. *Biological Reviews*, **92**, 878–901.

BENSON, R. B. J. and BUTLER, R. J. 2011. Uncovering the diversification history of

marine tetrapods: ecology influences the effect of geological sampling biases. *Geological Society, London, Special Publications*, **358**, 191–208.

BENSON, R. B. J. and UPCHURCH, P. 2013. Diversity trends in the establishment of terrestrial vertebrate ecosystems: interactions between spatial and temporal sampling biases. *Geology*, **41**, 43–46.

BENSON, R. B. J., BUTLER, R. J., ALROY, J., MANNION, P. D., CARRANO, M. T. and LLOYD, G. T. 2016. Near-stasis in the long-term diversification of Mesozoic tetrapods. *PLoS Biology*, **14**, e1002359.

BENSON, R. B. J., BUTLER, R. J., CLOSE, R. A., SAUPE, E. and RABOSKY, D. L. 2021. Biodiversity across space and time in the fossil record. *Current Biology*, **31**, R1225–R1236.

BENTON, M. J. 2008a. How to find a dinosaur, and the role of synonymy in biodiversity studies. *Paleobiology*, **34**, 516–533.

BENTON, M. J. 2008b. Fossil quality and naming dinosaurs. *Biology Letters*, **4**, 729–732.

BENTON, M. J. and EMERSON, B. C. 2007. How did life become so diverse? The dynamics of diversification according to the fossil record and molecular phylogenetics. *Palaeontology*, **50**, 23–40.

BENTON, M. J. and STORRS, G. W. 1994. Testing the quality of the fossil record: paleontological knowledge is improving. *Geology*, **22**, 111–114.

BENTON, M. J., TVERDOKHLEBOV, V. P. and SURKOV, M. V. 2004. Ecosystem remodelling among vertebrates at the Permian-Triassic boundary in Russia. *Nature*, **432**, 97–100.

BERG, L. S. 1940. Classification of fishes, both recent and fossil. *Trudy Instituta Zoologicheskikh Akademiia Nauk*, **5**, 85–517.

BERNARD, E. L., RUTA, M., TARVER, J. E. and BENTON, M. J. 2010. The fossil record of early tetrapods: worker effort and the end-Permian mass extinction. *Acta Palaeontologica Polonica*, **55**, 229–239.

BEZNOSOV, P. 2009. A redescription of the early Carboniferous acanthodian *Acanthodes lopatini* Rohon, 1889. *Acta Zoologica (Stockholm)*, **90** (Suppl. 1), 183–193.

BLAIS, S. A. 2017. Precise occlusion and trophic niche differentiation indicate specialized feeding in early Devonian jawed vertebrates. *FACETS*, **2**, 513–530.

BLIECK, A. 2011. From adaptive radiations to biotic crises in Palaeozoic vertebrates: a geobiological approach. *Geologica Belgica*, **14**, 203–227.

BOESSENECKER, R. W., PERRY, F. A. and SCHMITT, J. G. 2014. Comparative taphonomy, taphofacies, and bonebeds of the Mio-Pliocene Purisima Formation, central California: strong physical control on marine vertebrate preservation in shallow marine settings. *Plos One*, **9**, e91419.

BOTELLA, H., DONOGHUE, P. C. J. and MARTINEZ-PÉREZ, C. 2009. Enameloid microstructure in the oldest known chondrichthyan teeth. *Acta Zoologica (Stockholm)*, **90** (Suppl. 1), 103–108.

BOUCOT, A. J. and JANIS, C. 1983. Environment of the early Paleozoic vertebrates. *Palaeogeography, Palaeoclimatology, Palaeoecology*, **41**, 251–287.

BOUCOT, A. J. and LAWSON, J. 1999. *Paleocommunities: a case study from the Silurian and Lower Devonian*. Cambridge University Press, 912 pp.

BRAZEAU, M. D. 2009. The braincase and jaws of a Devonian 'acanthodian' and modern gnathostome origins. *Nature*, **457**, 305–308.

BRAZEAU, M. D. and DE WINTER, V. 2015. The hyoid arch and braincase anatomy of *Acanthodes* support chondrichthyan affinity of 'acanthodians'. *Proceedings of the Royal Society B*, **282**, 20152210.

BRAZEAU, M. D. and FRIEDMAN, M. 2014. The characters of Palaeozoic jawed vertebrates. *Zoological Journal of the Linnean Society*, **170**, 779–821.

BRAZEAU, M. D. and FRIEDMAN, M. 2015. The origin and early phylogenetic history of jawed vertebrates. *Nature*, **520**, 490–497.

BRAZEAU, M. D., GILES, S., DEARDEN, R. P., JERVE, A., ARIUNCHIMEG, YA., ZORIG, E., SANSOM, R., GUILLERME, T. and CASTIELLO, M. 2020. Endochondral bone in an early Devonian 'placoderm' from Mongolia. *Nature Ecology & Evolution*, **4**, 1477–1484.

BRENCHLEY, P. J., MARSHALL, J. D. and UNDERWOOD, C. J. 2001. Do all mass extnctions represent an ecological crisis? Evidence from the Late Ordovician. *Geological Journal*, **36**, 329–340.

BRIGGS, D. E. G. and GALL, J.–C. 1990. The continuum in soft-bodied biotas from transitional environments: a quantitative comparison of Triassic and Carboniferous Konservat-Lagerstatten. *Paleobiology*, **16**, 204–218.

BROCKLEHURST, N. and FRÖBISCH, J. 2014. Current and historical perspectives on the completeness of the fossil record of pelycosaurian-grade synapsids. *Palaeogeography, Palaeoclimatology, Palaeoecology*, **399**, 114–126.

BROCKLEHURST, N., UPCHURCH, P., MANNION, P. D. and O'CONNOR, J. 2012.

The completeness of the fossil record of Mesozoic birds: implications for early avian evolution. *PLoS One*, **7**, e39056.

BRONSON, A. W., MAPES, R. H. and MAISEY, J. G. 2018. Chondrocranial morphology of *Carcharopsis wortheni* (Chondrichthyes, Euselachii incertae sedis) based on new material from the Fayetteville Shale (upper Mississippian, middle Chesterian). *Papers in Palaeontology*, **4**, 349–362.

BROWN, E. E., CASHMORE, D. D., SIMMONS, N. B. and BUTLER, R. J. 2019. Quantifying the completeness of the bat fossil record. *Palaeontology*, **62**, 757–776.

BURROW, C. J. 1996. Taphonomy of acanthodians from the Devonian Bunga Beds (late Givetian/early Frasnian) of New South Wales. *Historical Biology*, **11**, 213–228.

BURROW, C. J. 2004. Acanthodian fishes with dentigerous jaw bones: the Ischnacanthiformes and Acanthodopsis. *Fossils and Strata*, **50**, 8–22.

BURROW, C. J. 2011. A partial articulated acanthodian from the Silurian of New Brunswick, Canada. *Canadian Journal of Earth Sciences*, **48**, 1329–1341.

BURROW, C. J. 2021. Acanthodii, Stem Chondrichthyes. *In* SCHULTZE, H.–P. (ed.). *Handbook of palaeoichthyology, volume 5*. Verlag Dr. Friedrich Pfeil, 135 pp.

BURROW, C. J. and RUDKIN, D. 2014. Oldest near-complete acanthodian: the first vertebrate from the Silurian Bertie Formation Konservat-Lagerstätte, Ontario. *PLOS ONE*, **9**, e104171.

BURROW, C. J. and TURNER, S. 2010. Reassessment of *"Protodus" scoticus* from the early Devonian of Scotland. *In* ELLIOTT, D. K., MAISEY, J. G., YU, X. and MIAO, D. (eds). *Morphology, phylogeny and paleobiogeography of fossil fishes*. Verlag Dr. Friedrich Pfeil, 472 pp.

BURROW, C. J., DEN BLAAUWEN, J., NEWMAN, M. and DAVIDSON, R. 2016. The diplacanthid fishes (Acanthodii, Diplacanthiformes, Diplacanthidae) from the Middle Devonian of Scotland. *Palaeontologia Electronica*, **19**, 1–83.

BUTLER, R. J., BENSON, R. B. J., CARRANO, M. T., MANNION, P. D. and UPCHURCH, P. 2011. Sea level, dinosaur diversity and sampling biases: investigating the 'common cause' hypothesis in the terrestrial realm. *Proceedings of the Royal Society B*, **278**, 1165–1170.

CAILLIET, G. M., MUSICK, J. A., SIMPFENDORFER, C. A. and STEVENS, J. D. 2005. Chapter 3, Ecology and life history characteristics of chondrichthyan fish. *In* FOWLER, S. L., CAVANAGH, R. D., CAMHI, M., BURGESS, G. H., CAILLIET, G., FORDHAM, S. V., SIMPFENDORFER, C. A. and MUSICK, J. A. (eds). *Sharks, rays and chimaeras: the status of the chondrichthyan fishes, status survey*. IUCN/Shark Specialist Group, X + 461 pp.

CAPLAN, M. L. and BUSTIN, R. M. 1999. Devonian-Carboniferous mass extinction event, widespread organic-rich mudrock and anoxia: causes and consequences. *Palaeogeography, Palaeoclimatology, Palaeoecology*, **148**, 187–207.

CAPPETTA, H. 1987. Chondrichthyes II. Mesozoic and Cenozoic Elasmobranchii. *In* SCHULTZE, H.-P. (ed.). *Handbook of palaeoichthyology, volume 3B*. Verlag Dr. Friedrich Pfeil, 193 pp.

CASCALES-MIÑANA, B., CLEAL, C. J., and DIEZ, J. B. 2013. What is the best way to measure extinction? A reflection from the palaeobotanical record. *Earth-Science Reviews*, **124**, 126–147.

CASHMORE, D. D. and BUTLER, R. J. 2019. Skeletal completeness of the non-avian theropod dinosaur fossil record. *Palaeontology*, **62**, 951–981.

CASHMORE, D. D., MANNION, P. D., UPCHURCH, P. and BUTLER, R. J. 2020. Ten more years of discovery: revisiting the quality of the sauropodomorph dinosaur fossil record. *Palaeontology*, **63**, 951–978.

CHAO, A. and JOST, L. 2012. Coverage-based rarefaction and extrapolation: standardizing samples by completeness rather than size. *Ecology Letters*, **93**, 2533–2547.

CHEVRINAIS, M., BALAN, E. and CLOUTIER, R. 2015. New insights in the ontogeny and taphonomy of the Devonian acanthodian *Triazeugacanthus affinis* from the Miguasha Fossil-Lagerstätte, eastern Canada. *Minerals*, **6**, 1.

CHOO, B., ZHU, M., QU, Q., YU, X., JIA, L. and ZHAO, W. 2017. A new osteichthyan from the late Silurian of Yunnan, China. *PLOS ONE*, **12**, e0170929.

CLAPHAM, M. E., KARR, J. A., NICHOLSON, D. B. , ROSS, A. J. and MAYHEW, P. J. 2016. Ancient origin of high taxonomic richness among insects. *Proceedings of the Royal Society B*, **283**, 20152476.

CLEAL C. J., OPLUŠTIL, S., THOMAS, B. A., TENCHOV, Y., ABBINK, O. A., BEK, J., DIMITROVA, T., DRÁBKOVÁ, J., HARTKOPF-FRÖDER, CH. and VAN HOOF, T. 2009. Late Moscovian terrestrial biotas and palaeoenvironments of Variscan Euramerica. *Netherlands Journal of Geosciences*, **88**, 181–278.

CLEAL C. J., UHL, D., CASCALES-MIÑANA B., THOMAS, B. A., BASHFORTH, A. R., KING, S. C. and ZODROW, E. I. 2012. Plant biodiversity changes in Carboniferous tropical wetlands. *Earth-Science Reviews*, **114**, 124–155.

CLEARY, T. J., MOON, B. C., DUNHILL, A. M. and BENTON, M. J. 2015. The fossil record of ichthyosaurs, completeness metrics and sampling biases. *Palaeontology*, **58**, 521–536.

CLEMENTS, T., PURNELL, M. and GABBOTT, S. 2019. The Mazon Creek lagerstätte: a diverse late Paleozoic ecosystem entombed within siderite concretions. *Journal of the Geological Society*, **176**, 1–11.

CLOSE, R. A., BENSON, R. B. J., UPCHURCH, P. and BUTLER, R. J. 2017. Controlling for the species-area effect supports constrained long-term Mesozoic terrestrial vertebrate diversification. *Nature Communications*, **8**, 15381.

CLOSE, R. A., EVERS, S. W., ALROY, J. and BUTLER, R. J. 2018. How should we estimate diversity in the fossil record? Testing richness estimators using sampling-standardised discovery curves. *Methods in Ecology & Evolution*, **9**, 1386–1400.

CLOSE, R. A., BENSON, R. J., ALROY, J., CARRANO, M. T., CLEARY, T. J., DUNNE, E. M., MANNION, P. D., UHEN, M. D. and BUTLER, R. 2020. The apparent exponential radiation of Phanerozoic land vertebrates is an artefact of spatial sampling biases. *Proceedings of the Royal Society B*, **287**, 1–10.

COATES, M. I., FINARELLI, J. A., SANSOM, I. J., ANDREEV, P. S., CRISWELL, K. E., TIETJEN, K., RIVERS, M. L. and LA RIVIERE, P. J. 2018. An early chondrichthyan and the evolutionary assembly of a shark body plan. *Proceedings of the Royal Society B*, **285**, 20172418.

COATES, M. I. and TIETJEN, K. 2018. The neurocranium of the Lower Carboniferous shark *Tristychius arcuatus* (Agassiz, 1837). *Earth and Environmental Science Transactions of The Royal Society of Edinburgh*, **108**, 19–35.

COHEN, K. M., FINNEY, S. C., GIBBARD, P. L. and FAN, J.-X. 2013. Updated. The ICS international chronostratigraphic chart. *Episodes*, **36**, 199–204.

COMPAGNO, L. J. V. 1990. Alternative life-history styles of cartilaginous fishes in time and space. *Environmental Biology of Fishes*, **28**, 33–75.

CONWAY MORRIS, S. and CARON, J.–B. 2012. *Pikaia gracilens* Walcott, a stem-group chordate from the Middle Cambrian of British Columbia. *Biological Reviews*, **87**, 480–512.

COPPER, P. 2002. Silurian and Devonian reefs: 80 million years of global greenhouse between two ice ages. *In* KIESSLING, W., FLÜGEL, E. and GOLONKA, J. (eds). *Phanerozoic reef patterns*. SEPM Special Publication 72, 735 pp.

COVENEY JR, R. M. and GLASCOCK, M. D. 1989. A review of the origins of metal-rich Pennsylvanian black shales, central U.S.A., with an inferred role for basinal brines. *Applied Geochemistry*, **4**, 347–367.

CUMMINS, R. H. 1994. Taphonomic processes in modern freshwater molluscan death assemblages: implications for the freshwater fossil record. *Palaeogeography, Palaeoclimatology, Palaeoecology*, **108**, 55–73.

DAVIES, N. S. and GIBLING, M. R. 2010. Cambrian to Devonian evolution of alluvial systems: the sedimentological impact of the earliest land plants. *Earth Science Reviews*, **98**, 171–200.

DAVIDSON, R. G. and TREWIN, N. H. 2005. Unusual preservation of the internal organs of acanthodian and actinopterygian fish in the Middle Devonian of Scotland. *Scottish Journal of Geology*, **41**, 129–134.

DAVIES, T. W., BELL, M. A., GOSWAMI, A. and HALLIDAY, T. J. 2017. Completeness of the eutherian mammal fossil record and implications for reconstructing mammal evolution through the Cretaceous/Paleogene mass extinction. *Paleobiology*, **43**, 521–536.

DAVIS, R. A. Jr. 2012. Tidal signatures and their preservation potential in stratigraphic sequences. *In* DAVIS, R. A. Jr and DALRYMPLE, R. W (eds). *Principles of tidal sedimentology*. Springer Netherlands, 621 pp.

DAVIS, S. P., FINARELLI, J. A. and COATES, M. I. 2012. *Acanthodes* and shark-like conditions in the last common ancestor of modern gnathostomes. *Nature*, **486**, 247–250.

DAVYDOV, V. I., KORN, D. and SCHMITZ, M. D. 2012. Chapter 23: The Carboniferous period. *In* GRADSTEIN, F. M., OGG, J. G., SCHMITZ, M. D. and OGG, G. M. (eds). *The geologic time scale*. Elsevier, 1390 pp.

DEAN, C. D., CHIARENZA, A. A. and MAIDMENT, S. C. R. 2020. Formation binning: a new method for increased temporal resolution in regional studies, applied to the late Cretaceous dinosaur fossil record of North America. *Palaeontology*, **63**, 881–901.

DEAN, C. D., MANNION, P. D. and BUTLER, R. J. 2016. Preservational bias controls the fossil record of pterosaurs. *Palaeontology*, **59**, 225–247.

DEAN, M. N. and SUMMERS, A. P. 2006. Mineralized cartilage in the skeleton of chondrichthyans fishes. *Zoology*, **109**, 164–168.

DEARDEN, R. P. 2018. The anatomy and evolution of “acanthodian” stem-chondrichthyans. Unpublished PhD thesis, Imperial College London, 354 pp.

DEARDEN, R. P., STOCKEY, C. and BRAZEAU, M. D. 2019. The pharynx of the stem-chondrichthyan *Ptomacanthus* and the early evolution of the gnathostome gill skeleton. *Nature Communications*, **10**, 1–7.

DEARDEN, R. P., DEN BLAAUWEN, J. L., SANSOM, I. J., BURROW, C. J., DAVIDSON, R. G., NEWMAN, M. J., KO, A. and BRAZEAU, M. D. 2021. A revision of *Vernicomacanthus* Miles with comments on the characters of stem-group chondrichthyans. *Papers in Palaeontology*, **7**, 1949–1976.

DENISON, R. 1978. Placodermi. *In* SCHULTZE, H.–P. (ed.). *Handbook of palaeoichthy-*

ology, volume 5. Verlag Dr. Friedrich Pfeil, 128 pp.

DENISON, R. 1979. Acanthodii. *In* SCHULTZE, H.–P. (ed.). *Handbook of palaeoichthyology, volume 5*. Verlag Dr. Friedrich Pfeil, 62 pp.

DICK, J. R. F. 1978. On the Carboniferous shark *Tristychius arcuatus* Agassiz from Scotland. *Transactions of the Royal Society of Edinburgh*, **70**, 63–109.

DINELEY, D. L. and METCALF, S. J. 1999. *Fossil fishes of Great Britain*. Joint Nature Conservation Committee, 675 pp.

DONOGHUE, P. C. J. 2002. Evolution of development of the vertebrate dermal and oral skeletons: unraveling concepts, regulatory theories, and homologies. *Paleobiology*, **284**, 474–507.

DONOGHUE, P. C. J., SANSOM, I. J. and DOWNS, J. P. 2006. Early evolution of vertebrate skeletal tissues and cellular interactions, and the canalization of skeletal development. *Journal of Experimental Zoology Part B: Molecular and Developmental Evolution*, **306**, 278–294.

DONOVAN, R. N. 1975. Devonian lacustrine limestones at the margin of the Orcadian basin, Scotland. *Journal of the Geological Society*, **131**, 489–510.

DRISCOLL, D. A., DUNHILL, A. M., STUBBS, T. L. and BENTON, M. J. 2018. The Mosasaur fossil record through the lens of fossil completeness. *Palaeontology*, **62**, 51–75.

DUFF, P. 1842. *Sketch of the geology of Moray*. Forsyth and Young, 72 pp.

DUNNE, E. M., CLOSA, R. A., BUTTON, D. J., BROCKLEHURST, N., CASHMORE, D. D., LLOYD, G. T. and BUTLER, R. J. 2018. Diversity change during the rise of

tetrapods and the impact of the 'Carboniferous rainforest collapse'. *Proceedings of the Royal Society B*, **285**, 20172730.

DUPRET, V., SANCHEZ, S., GOUJET, D., TAFFOREAU, P. and AHLBERG, P. E. 2014. A primitive placoderm sheds light on the origin of the jawed vertebrate face. *Nature*, **507**, 500–503.

EBERT, D. A. and WINTON, M. V. 2010. Chondrichthyans of high latitude seas. *In* CARRIER, J. C., MUSICK, J. A. and HEITHAUS, M. R. (eds). *Sharks and their relatives II – biodiversity, adaptive physiology, and conservation*. CRC Press, 746 pp.

EGERTON, P. 1861. British fossils. (Descriptions of *Tristichopterus, Acanthodes, Climatius, Diplacanthus, Cheiracanthus*). *Memoirs of the Geological Survey of the United Kingdom (British Organic Remains)*, **Dec. X.**, 51-75.

EVANS, J. 2016. Fluvial environments. *In* BOBROWSKY, P. T. and MARKER, B. (eds). *Encyclopedia of engineering geology*. Springer, Cham, 978 pp.

FEICHTINGER, I., IVANOV, A. O., WINKLER, V., DOJEN, C., KINDLIMANN, R., KRIWET, J., PFAFF, C., SCHRAUT, G. and STUMPF, S. 2021. Scarce ctenacanthiform sharks from the Mississippian of Austria with an analysis of Carboniferous elasmobranch diversity in response to climatic and environmental changes. *Journal of Vertebrate Paleontology*, **41**, e1925902.

FERGUSSON, C. L., CAS, R. A. F., COLLINS, W. J., CRAIG, G. Y., CROOK, K. A. W., POWELL, C. McA., SCOTT, P. A. and YOUNG, G. C. 1979. The Late Devonian Boyd volcanic complex, Eden, N.S.W. *Journal of the Geological Society of Australia*, **26**, 87–105.

FOOTE, M. and RAUP, D. M. 1996. Fossil preservation and the stratigraphic ranges of taxa. *Paleobiology*, textbf22, 121–140.

FOOTE, M. and SEPKOSKI, J. J. Jr. 1999. Absolute measures of the completeness of the fossil record. *Nature*, **398**, 415–417.

FOUNTAINE, T. M. R., BENTON, M. J., NUDDS, R. L. and DYKE, G. J. 2005. The quality of the fossil record of Mesozoic birds. *Proceedings of the Royal Society of London B*, **272**, 289–294.

FREY, L., COATES, M. I., GINTER, M., HAIRAPETIAN, V. RÜCKLIN, M., JERJEN, I. and KLUG, C. 2019. The early elasmobranch *Phoebodus*: phylogenetic relationships, ecomorphology and a new time-scale for shark evolution. *Proceedings of the Royal Society B*, **286**, 20191336.

FREY, L., COATES, M. I., TIETJEN, K., RÜCKLIN, M. and KLUG, C. 2020. A symmoriiform from the Late Devonian of Morocco demonstrates a derived jaw function in ancient chondrichthyans. *Communications Biology*, **3**, 681.

FRIEDMAN, M. and BRAZEAU, M. 2010. A reappraisal of the origin and basal radiation of the Osteichthyes. *Journal of Vertebrate Paleontology*, **30**, 36–56.

FRIEDMAN, M. and SALLAN, L. C. 2012. Five hundred million years of extinction and recovery: a phanerozoic survey of large-scale diversity patterns in fishes. *Palaeontology*, **55**, 707–742.

FRITSCH, A. 1895. TextitFauna der Gaskohle und der Kalksteine der Permformation Böhmens. Band III. Heft 2. Selachii Traquairia, Protacanthodes, Acanthodes). Actinopterygii (*Megalichthys, Trissolepis)*. Selbstverlag, 31 pp.

FÜRSICH, F. T., PAN, Y., WILMSEN, M. and MAJIDIFARD, M. R. 2016. Biofacies, taphonomy, and paleobiogeography of the Kamar-e-Mehdi Formation of east-central Iran, a Middle to Upper Jurassic shelf lagoon deposit. *Facies*, **62**, 1–23.

GAGNIER, P.-Y., HANKE, G. F. and WILSON, M. V. H. 1999. *Tetanopsyrus lindoei* gen. et sp. nov., an early Devonian acanthodian from the Northwest Territories, Canada. *Acta Geologica Polonica*, **49**, 81–96.

GAGNIER, P.–Y., TURNER, S., FRIMAN, L., SUÁREZ-RIGLOS, M. and JANVIER, P. 1988. The Devonian vertebrate and mollusc fauna from Seripona (Dept. of Chuquisaca, Bolivia). *Neues Jahrbuch für Geologie und Paläontologie – Abhandlungen*, **176**, 269–297.

GAO, S. 2009. Modeling the preservation potential of tidal flat sedimentary records, Jiangsu coast, eastern China. *Continental Shelf Research*, **29**, 1927–1936.

GARDNER, E. E., WALKER, S. E. and GARDNER, L. I. 2016. Palaeoclimate, environmental factors, and bird body size: a multivariable analysis of avian fossil preservation. *Earth-Science Reviews*, **162**, 177–197.

GESS, R. W. and COATES, M. I. 2015. High-latitude chondrichthyans from the late Devonian (Famennian) Witpoort Formation of South Africa. *Paläontologische Zeitschrift*, **89**, 147–169.

GESS, R. W. and WHITFIELD, A. K. 2020. Estuarine fish and tetrapod evolution: insights from a late Devonian (Famennian) Gondwanan estuarine lake and a southern African Holocene equivalent. *Biological Reviews*, **95**, 865–888.

GILES, S., FRIEDMAN, M., BRAZEAU, M. 2015. Osteichthyan-like cranial conditions in an early Devonian stem gnathostome. *Nature*, **520**, 82–85.

GINTER, M. 2021. The biostratigraphy of Carboniferous chondrichthyans. *Geological Society, London, Special Publications*, **512**, 769–790.

GINTER, M. and HANSEN, M. 2010. Teeth of the cladodont shark *Denaea* from the Carboniferous of central North America. *In* NOWAKOWSKI, D. (ed.). *Morphology and*

systematics of fossil vertebrates, 153 pp.

GINTER, M., HAMPE, O. and DUFFIN, C. 2010. Chondrichthyes. Paleozoic Elasmobranchii: Teeth. *In* SCHULTZE, H.-P. (ed.). *Handbook of palaeoichthyology, volume 3D.* Verlag Dr. Friedrich Pfeil, 168 pp.

GREGOR, C. B. 1970. Denudation of the continents. *Nature*, **228**, 273–275.

GROGAN, E. D. and LUND, R. 2000. *Debeerius ellefseni* (fam. nov., gen. nov., spec. nov.), an autodiastylic chondrichthyan From the Mississippian Bear Gulch Limestone of Montana (USA), the relationships of the Chondrichthyes, and comments on gnathostome evolution. *Journal of Morphology*, **243**, 219–245.

GROGAN, E. D. and LUND, R. 2004. The origin and relationships of early Chondrichthyes. *In* CARRIER, J. C., MUSICK, J. A. and HEITHAUS, M. R. (eds). *Biology of sharks and their relatives*. 1st edition. CRC Press, 616 pp.

GROGAN, E. D., LUND, R. and GREENFEST-ALLEN, E. 2012. The origin and relationships of early chondrichthyans. *In* CARRIER, J. C., MUSICK, J. A. and HEITHAUS, M. R. (eds). *Biology of sharks and their relatives*. 2nd edition. CRC Press, 666 pp.

GROSS, W. 1947. Die Agnathen und Acanthodier des obersilurischen Beyrichienkalks. *Palaeontographica A*, **96**, 91–161.

GROSS, W. 1968. Fragliche Actinopterygier-Schuppen aus dem Silur Gotlands. *Lethaia*, **1**, 184–218.

GROSS, W. 1973. Kleinschuppen, Flossenstacheln und Zähne von Fischen aus europäischen und nordamerikanischen Bonebeds des Devons. *Palaeontographica Abteilung A*, **142**, 51–155.

HAGADORN, J. W. 2002. Bear Gulch: an exceptional Upper Carboniferous Plattenkalk. *In* BOTTJER, D. J., ETTER, W., HAGADORN, J. W. and TANG, C. M. (eds). *Exceptional fossil preservation*. Columbia University Press, 424 pp.

HALLAM, A. and WIGNALL, P. B. 1997. *Mass extinctions and their aftermath*. Oxford University Press, 328 pp.

HANCOCK, A. and ATTHEY, T. 1868. Notes on the remains of some reptiles and fishes from the shales of the Northumberland coal field. *Annals and Magazine of Natural History*, **1**, 346–378.

HANKE, G. F. 2002. *Paucicanthus vanelsti* gen. et. sp. nov., an early Devonian (Lochkovian) acanthodian that lacks paired fin-spines. *Canadian Journal of Earth Sciences*, **39**, 1071–1083.

HANKE, G. F. and DAVIS, S. P. 2008. Redescription of the acanthodian *Gladiobranchus probaton* Bernacsek & Dineley, 1977, and comments on diplacanthid relationships. *Geodiversitas*, **30**, 303–330.

HANKE, G. F. and DAVIS, S. P. 2012. A re-examination of *Lupopsyrus pygmaeus* Bernacsek & Dineley, 1977 (Pisces, Acanthodii). *Geodiversitas*, **34**, 469–487.

HANKE, G. F. and WILSON, M. V. H. 2004. New teleostome fishes and acanthodian systematics. *In* ARRATIA, G., WILSON, M. V. H. and CLOUTIER, R. (eds). *Recent advances in the origin and early radiation of vertebrates*. Verlag Dr. Friedrich Pfeil, 703 pp.

HANKE, G. F. and WILSON, M. V. H. 2006. Anatomy of the early Devonian acanthodian *Brochoadmones milesi* based on nearly complete body fossils, with comments on the evolution and development of paired fins. *Journal of Vertebrate Paleontology*, **26**, 526–537.

HANKE, G. F. and WILSON, M. V. H. 2010. The putative stem-group chondrichthyans *Kathemacanthus* and *Seretolepis* from the Lower Devonian MOTH locality, Mackenzie Mountains, Canada. *In* ELLIOTT, D. K., MAISEY, J. G., YU, X. and MIAO, D (eds). *Morphology, phylogeny and paleobiogeography of fossil fishes*. Verlag Dr. Friedrich Pfeil, 472 pp.

HANKE, G. F., DAVIS, S. P. and WILSON, M. V. H. 2001. New species of the acanthodian genus *Tetanopsyrus* from northern Canada, and comments on related taxa. *Journal of Vertebrate Paleontology*, **21**, 740–753.

HANNISDAL, B. and PETERS, S. E. 2011. Phanerozoic earth system evolution and marine biodiversity. *Science*, **334**, 1121–1124.

HAQ, B. U. and SCHUTTER, S. R. 2008. A chronology of paleozoic sea-level changes. *Science*, **322**, 64–68.

HECKEL, P. H. 2008. Pennsylvanian cyclothems in midcontinent North America as far-field effects of waxing and waning of Gondwana ice sheets. *In* FIELDING, C. R., FRANK, T. D., and ISBELL, J. L. (eds). *Resolving the late Paleozoic ice age in time and space*. Geological Society of America Special Paper 441, 354 pp.

HEIDTKE, U. H. J. 2011. Neue Erkenntnisse über *Acanthodes bronni* Agassiz 1833. *Mitteilungen der Pollichia*, **95**, 1–14.

HSIEH, T. C., MA, K. H. and CHAO, A. 2016. iNEXT: an R package for rarefaction and extrapolation of species diversity (Hill numbers). *Methods in Ecology and Evolution*, **7**, 1451–1456.

HUNTER, A. W. and DONOVAN, S. K. 2005. Field sampling bias, museum collections and completeness of the fossil record. *Lethaia*, **38**, 305–314.

ISBELL, J. L., MILLER, M. F., WOLFE, K. L. And LENAKER, P. A. 2003. Timing of late Paleozoic glaciation in Gondwana: was glaciation responsible for the development of northern hemisphere cyclothems. *In* CHAN, M. A. and ARCHER, A. A. (eds). *Extreme depositional environments: mega end members in geologic time*. Geological Society of America, 281 pp.

IVANOV, A. O. 2016. Chondrichthyans from the lower Permian of Mechetlino, South Urals. *Bulletin of Geosciences*, **91**, 717–729.

JABLONSKI, D. 2002. Survival without recovery after mass extinctions. *Proceedings of the National Academy of Sciences of the USA*, **99**, 8139–8144.

JABLONSKI, D. 2005. Mass extinctions and macroevolution. *Paleobiology*, **31**, 192–210.

JABLONSKI, D., ROY, K., VALENTINE, J. W., PRICE, R. M. and ANDERSON, P. S. 2003. The impact of the pull of the recent on the history of marine diversity. *Science*, **300**, 1133–1135.

JANVIER, P. 1996. *Early vertebrates*. Clarendon Press, 393 pp.

JANVIER, P. and CLEMENT, G. 2005. A new groenlandaspid arthrodire (Vertebrata: Placodermi) from the Famennian of Belgium. *Geologica Belgica*, **8**, 51–67.

JANVIER, P. and MAISEY, J. G. 2010. The Devonian vertebrates of South America and their biogeographical relationships. *In* ELLIOTT, D. K., MAISEY, J. G., YU, X. and MIAO, D. (eds). *Morphology, phylogeny and paleobiogeography of fossil fishes*. Verlag Dr. Friedrich Pfeil, 472 pp.

JANVIER, P. and PRADEL, A. 2015. Elasmobranchs and their extinct relatives: diversity, relationships, and adaptations through time. *In* SHADWICK, R. E., FARRELL, A. P. and BRAUNER, C. J. (eds). *Physiology of elasmobranch fishes: structure and*

interaction with environment. Academic press, 422 pp.

JARVIK, E. 1977. The systematic position of acanthodian fishes. *In* ANDREWS, S. M., MILES, R. S. and WALKER, A. (eds). *Problems in vertebrate evolution: essays presented to Professor T. S. Westoll (Linnean Society symposium series ; no. 4)*. Academic Press, 411 pp.

KARATEJŪTĖ-TALIMAA, V. 1992. The early stages of the dermal skeleton formation in chondrichthyans. *In* MARK-KURIK, E. (ed.). *Fossil fishes as living animals*. Institute of Geology, 299 pp.

KARATEJŪTĖ-TALIMAA, V. 1995. The Mongolepidida: scale structure and systematic position. *Geobios*, **19**, 35–37.

KARATEJŪTĖ-TALIMAA, V. and SMITH, M. M. 2003. Early acanthodians from the Lower Silurian of Asia. *Transactions of the Royal Society of Edinburgh Earth Sciences*, **93**, 277–299.

KARATAJŪTĖ-TALIMAA, V., NOVISKAYA, L. I., ROZMAN, K. S. and SODOV, Z. 1990. *Mongolepis* - a new lower Silurian genus of elasmobranchs from Mongolia. *Paleontologicheskii zhurnal*, **1**, 76–86.

KIDWELL, S. M. 1986. Models for fossil concentrations: paleobiologic implications. *Paleobiology*, **12**, 6–24.

KIDWELL, S. M. and HOLLAND, S. M. 2002. The quality of the fossil record: implications for evolutionary analyses. *Annual Review of Ecology and Systematics*, **33**, 561–588.

KIESSLING, W., SIMPSON, C. and FOOTE, M. 2010. Reefs as cradles of evolution and sources of biodiversity in the Phanerozoic. *Science*, **327**, 196–198.

KING, B. and RÜCKLIN, M. 2020. A Bayesian approach to dynamic homology of morphological characters and the ancestral phenotype of jawed vertebrates.*eLife Sciences*, **9**.

KING, B., QIAO, T., LEE, M. S. Y., ZHU, M. and LONG, J. A. 2016. Bayesian morphological clock methods resurrect placoderm monophyly and reveal rapid early evolution in jawed vertebrates. *Systematic Biology*, **66**, 499–516.

KOCSIS, A. T., REDDIN, C. J., ALROY, J. and KIESSLING, W. 2019. The r package divDyn for quantifying diversity dynamics using fossil sampling data. *Methods in Ecology & Evolution*, **10**, 735–743.

KÖNIGER, S. and STOLLHOFEN, H. 2001. Environmental and tectonic controls on preservation potential of distal fallout ashes in fluvio-lacustrine settings: the Carboniferous–Permian Saar–Nahe Basin, south-west Germany. *Special Publications of the International Association of Sedimentologists*, **30**, 263–284.

KOOT, M. B. 2013. Effects of the late Permian mass extinction on chondrichthyan palaeobiodiversity and distribution patterns. Unpublished PhD thesis, University of Plymouth, Plymouth, 853 pp.

KRIWET, J., WITZMANN, F., KLUG, S. and HEIDTKE, U. H. 2008. First direct evidence of a vertebrate three-level trophic chain in the fossil record. *Proceedings of the Royal Society B: Biological Sciences*, **275**, 181–186.

LAMSDELL, J. C. and BRADDY, S. J. 2010. Cope's rule and Romer's theory: patterns of diversity and gigantism in eurypterids and Palaeozoic vertebrates. *Biological Letters*, **6**, 265–269.

LEGGETT, J. K. 1980. British Lower Palaeozoic black shales and their palaeo-oceanographic significance. *Journal of the Geological Society*, **137**, 139–156.

LIU, C., JAROCHOWSKA, E., DU, Y., VACHARD, D. and MUNNECKE, A., 2017a. Stratigraphical and δ13C records of Permo-Carboniferous platform carbonates, South China: responses to late Paleozoic icehouse climate and icehouse–greenhouse transition. *Palaeogeography, Palaeoclimatology, Palaeoecology*, **474**, 113–129.

LIU, C., JAROCHOWSKA, E., DU, Y., MUNNECKE, A. and DAI, X. 2017b. Prevailing anoxia in the Kungurian (Permian) of South China: possible response to divergent climate trends between the tropics and Gondwana. *Gondwana Research*, **49**, 81–93.

LONG, J. A. 1986. New ischnacanthid acanthodians from the Early Devonian of Australia, with comments on acanthodian interrelationships. *Zoological Journal of the Linnean Society*, **87**, 321–339.

LONG, J. A., MARK-KURIK, E., JOHANSON, Z., LEE, M. S. Y., YOUNG, G. C., MIN, Z., AHLBERG, P. E., NEWMAN, M., JONES, R., DEN BLAAUWEN, J., CHOO, B. and TRINAJSTIC, K. 2015. Copulation in antiarch placoderms and the origin of gnathostome internal fertilization. *Nature*, **517**, 196–199.

LÜBKE, A., ENAX, J., LOZA, K., PRYMAK, O., GAENGLER, P., FABRITIUS, H.-O., RAABE, D. and EPPLE, M. 2015. Dental lessons from past to present: ultrastructure and composition of teeth from plesiosaurs, dinosaurs, extinct and recent sharks. *RSC Advances*, **5**, 61612–61622.

LUND, R. 1985. The morphology of *Falcatus falcatus* (St. John and Worthen), a Mississippian stethacanthid chondrichthyan from the Bear Gulch Limestone of Montana. *Journal of Vertebrate Paleontology*, **5**, 1–19.

LUND, R. and GROGAN, E. D. 1997. Relationships of the Chimaeriformes and the basal radiation of the Chondrichthyes. *Reviews in Fish Biology and Fisheries*, **7**, 65–123.

LUND, R. and GROGAN, E. D. 2004. Five new euchondrocephalan Chondrichthyes from the Bear Gulch Limestone (Serpukhovian, Namurian E2b) of Montana, USA. *In* ARRATIA, G., WILSON, M. V. H. and CLOUTIER, R.(eds.). *Recent advances in the origin and early radiation of vertebrates*. Verlag Dr. Friedrich Pfeil, 703 pp.

LUND, R., FELDMAN, H., LUND, W. L. and MAPLES, C. G. 1993. The depositional environment of the Bear Gulch Limestone, Fergus County, Montana. *In* HUNTER, L. V. (ed.). *Energy and mineral resources of central Montana: 1993 Field Conference Guidebook*. Billings: Montana Geological Society, 292 pp.

MADER, H. 1986. Schuppen und Zähne von Acanthodiern und Elasmobranchiern aus dem Unterdevon Spaniens (Pisces). *Göttinger Arbeiten zur Geologie und Paläontologie*, **28**, 1–58.

MÄRSS, T. and GAGNIER, P.-Y. 2001. A new chondrichthyan from the Wenlock, Lower Silurian, of Baillie-Hamilton Island, the Canadian Arctic. *Journal of Vertebrate Paleontology*, **21**, 693–701.

MÄRSS, T., WILSON, M. V. H. and THORSTEINSSON, R. 2002. New thelodont (Agnatha) and possible chondrichthyan (Gnathostomata) taxa established in the Silurian and Lower Devonian of the Canadian Arctic Archipelago. *Proceedings of the Estonian Academy of Sciences*, **51**, 88–120.

MÄRSS, T., WILSON, M. V. H. and THORSTEINSSON, R. 2006. Silurian and Lower Devonian thelodonts and putative chondrichthyans from the Canadian Arctic Archipelago. *Special Papers in Palaeontology*, **75**, 1–140.

MAISEY, J. G. 1981. Studies on the Paleozoic selachian genus *Ctenacanthus* Agassiz No. 1. historical review and revised diagnosis of *Ctenacanthus*, with a list of referred taxa. *American Museum Novitates*, **2718**, 1–22.

MAISEY, J. G. 1984. Chondrichthyan phylogeny: a look at the evidence. *Journal of Vertebrate Paleontology*, **4**, 359–371.

MAISEY, J. G. 1986. Heads and tails: a chordate phylogeny. *Cladistics*, **2**, 201–256.

MAISEY, J. G. 2001. A primitive chondrichthyan braincase from the Middle Devonian of Bolivia. *In* AHLBERG, P (ed.). *Major Events in Early Vertebrate Evolution*. Taylor and Francis. 448 pp.

MAISEY, J. G. 2013. The diversity of tessellated calcification in modern and extinct chondrichthyans. *Revue de Paléobiologie*, **32**, 355–371.

MAISEY, J. G. and ANDERSON, M. E. 2001. A primitive chondrichthyan braincase from the early Devonian of South Africa. *Journal of Vertebrate Paleontology*, **21**, 702–713.

MAISEY, J. G., BORGHI, L. and DE CARVALHO, M. G. P. 2002. Lower Devonian fish remains from the Falkland Islands. *Journal of Vertebrate Paleontology*, **22**, 708–711.

MAISEY, J. G., MILLER, R. and TURNER, S. 2009. The braincase of the chondrichthyan *Doliodus* from the Lower Devonian Campbellton Formation of New Brunswick, Canada. *Acta Zoologica*, **90** (Suppl. 1), 109–122.

MAISEY, J. G., MILLER, R., PRADEL, A., DENTON, J. S. S., BRONSON, A. and JANVIER, P. 2017. Pectoral morphology in *Doliodus*: bridging the 'acanthodian'–chondrichthyan divide. *American Museum Novitates*, **3875**, 1–15.

MAISEY, J. G., JANVIER, P., PRADEL, A., DENTON, J. S. S., BRONSON, A., MILLER, R. F. and BURROW, C. J. 2019. *Doliodus* and pucapampellids: contrasting perspectives on stem chondrichthyan morphology. *In* JOHANSON, Z., UNDERWOOD, C. and RICHTER, M. (eds). *Evolution and development of fishes*. Cambridge Univer-

sity Press, 274 pp.

MAISEY, J. G., DENTON, J. S. S., BURROW, C. and PRADEL, A. 2021. Architectural and ultrastructural features of tessellated calcified cartilage in modern and extinct chondrichthyan fishes. *Journal of Fish Biology*, **98**, 919–941.

MANNION, P. D. and UPCHURCH, P. 2010. Completeness metrics and the quality of the sauropodomorph fossil record through geological and historical time. *Paleobiology*, **36**, 283–302.

MANNION, P. D., CHIARENZA, A. A., GODOY, P. L. and CHEAH, Y. N. 2019. Spatiotemporal sampling patterns in the 230 million year fossil record of terrestrial crocodylomorphs and their impact on diversity. *Palaeontology*, **62**, 615–637.

MCGHEE, G. R. 1996. *The late Devonian mass extinction: the Frasnian-Famennian crisis*. Columbia University Press, 303 pp.

MILES, R. S. 1970. Remarks on the vertebral column and caudal fin of acanthodian fishes. *Lethaia*, **3**, 343–362.

MILES, R. S. 1973a. Articulated acanthodian fishes from the Old Red Sandstone of England, with a review of the structure and evolution of the acanthodian shoulder girdle. *Bulletin of the British Museum (Natural History): Geology*, **24**, 113–213.

MILES, R. S. 1973b. Relationships of acanthodians. *In* GREENWOOD, P., MILES, R. S. and PATTERSON, C. (eds). *Interrelationships of fishes*. Academic Press, 536 pp.

MILLER, R. F., CLOUTIER, R. and TURNER, S. 2003. The oldest articulated chondrichthyan from the Early Devonian period. *Nature*, **425**, 501–504.

MOY-THOMAS, J. A. 1971. Subclass Acanthodii. *In* MOY-THOMAS, J. A. and MILES,

R. S. (eds). *Palaeozoic fishes*. Springer, 260 pp.

MUNNECKE, A., CALNER, M., HARPER, D. A. T. and SERVAIS, T. 2010. Ordovician and Silurian sea-water chemistry, sea level, and climate: a synopsis. *Palaeogeography, Palaeoclimatology, Palaeoecology*, **296**, 389–413.

MURPHY, J. B., NANCE, R. D. and CAWOOD, P. A. 2009. Contrasting modes of supercontinent formation and the conundrum of Pangea. *Gondwana Research*, **15**, 408–420.

MUTTER, R. J. and RICHTER, M. 2007. Acanthodian remains from the Middle-Late Permian of Brazil. *Geological Journal*, **42**, 213–224.

NAKAZAWA, T., UENO, K., NONOMURA, N. and FUJIKAWA, M. 2015. Microbial community from the lower Permian (Artinskian–Kungurian) paleoclimatic transition, mid-Panthalassan Akiyoshi atoll, Japan. *Palaeogeography, Palaeoclimatology, Palaeoecology*, **420**,116–127.

NELSON, G. J. 1969. Gill arches and the phylogeny of fishes, with notes on the classification of vertebrates. *Bulletin of the American Museum of Natural History*, **141**, 475–552.

NELSON, J. S. 2006. *Fishes of the world*. John Wiley & Sons, 601 pp.

NEWELL, N. D. 1959. The nature of the fossil record. *Proceedings of the American Philosophical Society*, **103**, 264–285.

NICOL, D. 1982. Some characteristics of extinct major groups of animals. *Florida Scientist*, **45**, 76–80.

OPLUŠTIL, S., ŠIMŮNEK, Z., ZAJÍC, J. and MENCL, V. 2013. Climatic and biotic

changes around the Carboniferous-Permian boundary recorded in the continental basins of the Czech Republic. *International Journal of Coal Geology*, **119**, 114–151.

ØRVIG, T. 1957. Notes on some Paleozoic lower vertebrates from Spitsbergen and North America. *Norsk Geologisk Tidsskrift*, **37**, 285–353. PETERS, S. E. 2005. Geologic constraints on the macroevolutionary history of marine animals. *Proceedings of the National Academy of Sciences of the United States of America*, **102**, 12326–12331.

PETERS and FOOTE, M. 2001. Biodiversity in the Phanerozoic: a reinterpretation. *Paleobiology*, **27**, 583–601.

PINAKHINA, D. V. and MÄRSS, T. 2018. The Middle Devonian acanthodian assemblage of the Karksi outcrop in Estonia. *Estonian Journal of Earth Sciences*, **67**, 96–111.

PINHEIRO, J., BATES, D., DEBROY, S. and SARKAR, D. and R CORE TEAM. 2018. nlme: linear and nonlinear mixed effects models. R package v. 3.1-137. https://cran.r-project.org/package=nlme

POTVIN-LEDUC, D. 2017. *Wellerodus priscus, un chondrichthyen avec aiguillons pairs du Devonien moyen (Givetien) de l'etat de New York, Etats-Unis*. Université du Québec à Rimouski, 139 pp.

PRADEL, A. 2010. Skull and brain anatomy of late Carboniferous Sibyrhynchidae (Chondrichthyes, Iniopterygia) from Kansas and Oklahoma (U.S.A.). *Geodiversitas*, **32**, 595–661.

PRADEL, A., MAISEY, J. G., TAFFOREAU, P., MAPES, R. H. and MALLATT, J. 2014. A Palaeozoic shark with osteichthyan-like branchial arches. *Nature*, **509**, 608–611.

PURNELL, M. A., DONOGHUE, P. J. C., GABBOTT, S. E., MCNAMARA, M. E., MURDOCK, D. J. E. and SANSOM, R. S. 2018. Experimental analysis of soft-tissue fos-

silization: opening the black box. *Palaeontology*, **61**, 317–323.

QIAO, T., KING, B., LONG, J. A., AHLBERG, P. E. and ZHU, M. 2016. Early gnathostome phylogeny revisited: multiple method consensus. *PLoS ONE*, **11**, e0163157.

QU, Q., SANCHEZ, S., BLOM, H., TAFFOREAU, P. and AHLBERG, P. E. (2013a). Scales and tooth whorls of ancient fishes challenge distinction between external and oral 'teeth'. *PLoS ONE*, **8**.

QU, Q., ZHU, M. and WANG, W. (2013b). Scales and dermal skeletal histology of an early bony fish *Psarolepis romeri* and their bearing on the evolution of rhombic scales and hard tissues. *PLoS ONE*, **8**.

R CORE TEAM 2019. R: a language and environment for statistical computing. v. 4.2.0. R Foundation for Statistical Computing. https://www.r-project.org

RAUP, D. M. 1972. Taxonomic diversity during the Phanerozoic. *Science*, **177**, 1065–1071.

RAUP, D. M. 1976. Species diversity in the Phanerozoic: an interpretation. *Paleobiology*, **2**, 289–297.

RAUP, D. M. and SEPKOSKI, J. J. Jr. 1982. Mass extinctions in the marine fossil record. *Science*, **215**, 1501–1503.

REVELL, L. J. 2012. phytools: an R package for phylogenetic comparative biology (and other things). *Methods in Ecology and Evolution*, **3**, 217–223.

REXROAD, C. B., WADE, J. A., MERRILL, G. K., BROWN, L. M. and PADGETT, P. 2001. Conodont biostratigraphy and depositional environments of the Mecca Quarry Shale Member and the Velpen Limestone Member of the Linton Formation (Pennsylvanian, Desmoinesian) in the eastern part of the Illinois Basin, USA. *Indiana Geological*

Survey, Special Report, **63**, 1–19.

ROMER, A. S. 1966. *Vertebrate paleontology*. University of Chicago Press, 468 pp.

ROSA, E. L. M., and ISBELL, J. L. 2021. Late Paleozoic glaciation. *In* ALDERTON, D. and ELIAS, S. A. (eds). *Encyclopedia of geology (second edition)*. Elsevier, 5622 pp.

RUST, B. R. 1982. Sedimentation in fluvial and lacustrine environments. *Hydrobiologia*, **91**, 59–70.

SAHNEY, S. and BENTON, M. J. 2008. Recovery from the most profound mass extinction of all time. *Proceedings of the Royal Society B: Biological Sciences*, **275**, 759–765.

SAHNEY, S. and BENTON, M. J. 2017. The impact of the pull of the recent on the fossil record of tetrapods. *Evolutionary Ecology Research*, **18**, 7–23.

SALLAN, L. C. and COATES, M. I. 2010. End-Devonian extinction and a bottleneck in the early evolution of modern jawed vertebrates. *Proceedings of the National Academy of Sciences*, **107**, 10131–10135.

SALLAN, L., FRIEDMAN, M., SANSOM, R. S., BIRD, C. M. and SANSOM, I. J. 2018. The nearshore cradle of early vertebrate diversification. *Science*, **26**, 460–464.

SALLAN, L. C., KAMMER, T. W., AUSICH, W. I. and COOK, L. A. 2011. Persistent predator–prey dynamics revealed by mass extinction. *Proceedings of the National Academy of Sciences of the United States of America*, **108**, 8335–8338.

SANSOM, I. and ANDREEV, P. 2017. The Ordovician enigma: fish, first appearances and phylogenetic controversies. *In* JOHANSON, Z., RICHTER, M. and UNDERWOOD, C. (eds). *Evolution and development of fishes*. Cambridge University Press, 280 pp.

SANSOM, I. J., AILDRIDGE, R. J. and SMITH, M. M. 2000. A microvertebrate fauna

from the Llandovery of South China. *Transactions of the Royal Society of Edinburgh: Earth Sciences*, **90**, 255–272.

SANSOM, I. J., SMITH, M. M. and SMITH, M. P. 2001. The Ordovician radiation of vertebrates. *In* AHLBERG, P. (ed.). *Major events in early vertebrate evolution: palaeontology, phylogeny, genetics and development*. Taylor Francis, 448 pp.

SANSOM, I. J., WANG, N.-Z. and SMITH, M. 2005. The histology and affinities of sinacanthid fishes: primitive gnathostomes from the Silurian of China. *Zoological Journal of the Linnean Society*, **144**, 379–386.

SANSOM, I. J., DAVIES, N. S., COATES, M. I., NICOLL, R. S., and RITCHIE, A. 2012. Chondrichthyan-like scales from the Middle Ordovician of Australia. *Palaeontology*, **55**, 243–247.

SANSOM, R. S. and WILLS, M. A. 2013. Fossilization causes organisms to appear erroneously primitive by distorting evolutionary trees. *Scientific Reports*, **3**, 2545.

SANSOM, R. S., GABBOTT, S. E. and PURNELL, M. A. 2011. Decay of vertebrate characters in hagfish and lamprey (Cyclostomata) and the implications for the vertebrate fossil record. *Proceedings of the Royal Society B,* **278**, 1150–1157.

SANSOM, R. S., RANDLE, E. and DONOGHUE, P. C. J. 2015. Discriminating signal from noise in the fossil record of early vertebrates reveals cryptic evolutionary history. *Proceedings of the Royal Society B*, **282**, 20142245.

SARMIENTO, J. L., HERBERT, T. D. and TOGGWEILER, J. R. 1988. Causes of anoxia in the world ocean. *Global Biogeochemical Cycles*, **2**, 115–128.

SCHRAM, F. R. 1983. Lower Carboniferous biota of Glencartholm, Eskdale, Dumfriesshire. *Scottish Journal of Geology*, **19**, 1–15.

SCHWEITZER, M. H. 2011. Soft tissue preservation in terrestrial Mesozoic vertebrates. *Annual Review of Earth and Planetary Sciences*, **39**, 187–216.

SEPKOSKI, J. 1996. Patterns of Phanerozoic extinction: a perspective from global data bases. *In* WALLISER, O. H. (ed.). *Global events and event stratigraphy in the Phanerozoic*. Springer-Verlag, 333 pp.

SEPKOSKI, J. J. 1976. Species diversity in the Phanerozoic: species-area effects. *Paleobiology*, **2**, 298–303.

SEPKOSKI, J. J. 2002. A compendium of fossil marine animal genera. *Bulletins of American Paleontology*, **363**, 1–560.

SEPKOSKI, J. J., BAMBACH, R. K., RAUP, D. M. and VALENTINE, J. W. 1981. Phanerozoic marine diversity and the fossil record. *Nature*, **293**, 435–443.

SERVAIS, T., PERRIER, V., DANELIAN, T., KLUG, C., MARTIN, R., MUNNECKE, A., NOWAK, H., NÜTZEL, A., VANDENBROUCKE, T. R. A., WILLIAMS, M. And RASMUSSEN, C. M. Ø. 2016. The onset of the 'Ordovician Plankton Revolution' in the late Cambrian. *Palaeogeography, Palaeoclimatology, Palaeoecology*, **458**, 12–28.

SILVESTRO, D., SCHNITZLER, J., LIOW, L. H., ANTONELLI, A. and SALAMIN, N. 2014. Bayesian estimation of speciation and extinction from incomplete fossil occurrence data. *Systematic Biology*, **63**, 349–367.

SILVESTRO, D., SALAMIN, N., ANTONELLI, A. and MEYER, X. 2019. Improved estimation of macroevolutionary rates from fossil data using a Bayesian framework. *Paleobiology*, **45**, 546–570.

SMITH, A. B. 2001. Large-scale heterogeneity of the fossil record: implications for Phanerozoic biodiversity studies. *Philosophical Transactions of the Royal Society B:*

Biological Sciences, **356**, 351–367.

SMITH, A. B. 2007a. Marine diversity through the Phanerozoic: problems and prospects. *Journal of the Geological Society*, **164**, 731–745.

SMITH, A. B. 2007b. Intrinsic versus extrinsic biases in the fossil record: contrasting the fossil record of echinoids in the Triassic and early Jurassic using sampling data, phylogenetic analysis, and molecular clocks. *Paleobiology*, **33**, 310–323.

SMITH, A. B. and MCGOWAN, A. J. 2007. The shape of the Phanerozoic marine palaeodiversity curve: how much can be predicted from the sedimentary rock record of Western Europe? *Palaeontology*, **50**, 765–774.

SMITH, A. B., LLOYD, G. T. and MCGOWAN, A. J. 2012. Phanerozoic marine diversity: rock record modelling provides an independent test of large-scale trends. *Proceedings of the Royal Society B: Biological Sciences*, **279**, 4489–4495.

SMITH, M. P., DONOGHUE, C. J. and SANSOM, I. J. 2002. The spatial and temporal diversification of early Palaeozoic vertebrates. *In* CRANE, J. A. and OWEN, A. W (eds). *Palaeobiogeography and biodiversity change: the Ordovician and Mesozoic-Cenozoic radiations*. The Geological Society, 216 pp.

SNYDER, D., TURNER, S., BURROW, C. J. and DAESCHLER, E. B. 2017. *"Gyracanthus" sherwoodi* (Gnathostomata, Gyracanthidae) from the late Devonian of North America. *Proceedings of the Academy of Natural Sciences of Philadelphia*, **165**, 195–220.

SORENSON, L., SANTINI, F. and ALFARO, E. 2014. The effect of habitat on modern shark diversification. *Journal of Evolutionary Biology*, **27**, 1536–1548.

SPIESS, A.-N. 2018. qpcR: modelling and analysis of real-time PCR data. R package v. 1.4-1. https://cran.r-project.org/web/ packages/qpcR

ST. JOHN, O. and WORTHEN, A. H. 1875. Description of fossil fishes. *Geological Survey of Illinois, Paleontology*, **6**, 245–488.

STAHL, B. J. 1999. Chondrichthyes III. Holocephali. *In* SCHULTZE, H.-P. (ed.). *Handbook of palaeoichthyology, volume 4*. Verlag Dr. Friedrich Pfeil, 164 pp.

STEIN, R. W., MULL, C. G., KUHN, T. S., ASCHLIMAN, N. C., DAVIDSON, L. N. K., JOY, J. B., SMITH, G. J., DULVY, N. K. and MOOERS, A. O. 2018. Global priorities for conserving the evolutionary history of sharks, rays and chimaeras. *Nature Ecology & Evolution*, **2**, 288–298.

TAPANILA, L., PRUITT, J., WILGA, C. D. and PRADEL, A. 2020. Saws, scissors, and sharks: late Paleozoic experimentation with symphyseal dentition. *The Anatomical Record*, **303**, 363–376.

TARVER, J. E., BRADDY, S. J. and BENTON, M. J. 2007. The effects of sampling bias on Palaeozoic faunas and implications for macroevolutionary studies. *Palaeontology*, **50**, 177–184.

TRINAJSTIC, K., MARSHALL, C., LONG, J. and BIFIELD, K. 2007. Exceptional preservation of nerve and muscle tissues in late Devonian placoderm fish and their evolutionary implications. *Biological Letters*, **3**, 197–200.

TURNER, S. 2004. Early vertebrates: analysis from microfossil evidence. *In* ARRATIA, G., WILSON, M. V. H. and CLOUTIER, R. (eds). *Recent advances in the origin and early radiation of vertebrates*. Verlag Dr. Friedrich Pfeil, 703 pp.

TUTIN, S. L. and BUTLER, R. J. 2017. The completeness of the fossil record of plesiosaurs, marine reptiles from the Mesozoic. *Acta Palaeontologica Polonica*, **62**, 563–573.

UNDERWOOD, C. J. 2006. Diversification of the Neoselachii (Chondrichthyes) during the Jurassic and Cretaceous. *Paleobiology*, **32**, 215–235.

VALIUKEVIČIUS, J. 2003. New Silurian nostolepids (Acanthodii, Pisces) of Lithuania. *Geologija*, **42**, 51–68.

VALIUKEVIČIUS, J. and BURROW, C. J. 2005. Diversity of tissues in acanthodians with *Nostolepis*-type histological structure. *Acta Palaeontologica Polonica*, **50**, 635–649.

VALIUKEVIČIUS, J. and KARATEJŪTĖ-TALIMAA, V. 1986. Acanthodian scale assemblage from the base of the Middle Devonian of the Baltic and Byelorussia. *In* BRANGULIS, A.P. (ed). *Biofacies and fauna of the Silurian and Devonian basins of the Baltic region*. Zinatne, 110–122. [in Russian]

VEEVERS, J. J. and POWELL, C. McA. 1987. Late Paleozoic glacial episodes in Gondwanaland reflected in transgressive-regressive depositional sequences in Euramerica. *Geological Society of America Bulletin*, **98**, 475–487.

VERRIÈRE, A., BROCKLEHURST, N. and FRÖBISCH, J. 2016. Assessing the completeness of the fossil record: comparison of different methods applied to parareptilian tetrapods (Vertebrata: Sauropsida). *Paleobiology*, **42**, 680–695.

VILHENA, D. A. and SMITH, A. B. 2013. Spatial bias in the marine fossil record. *PLoS ONE*, **8**, e74470.

WAGNER, P. J. and MARCOT, J. D. 2013. Modelling distributions of fossil sampling rates over time, space and taxa: assessment and implications for macroevolutionary studies. *Methods in Ecology & Evolution*, **4**, 703–713.

WALL, P. D., IVANY, L. C. and WILKINSON, B. H. 2009. Revisiting Raup: exploring

the influence of outcrop area on diversity in light of modern sample-standardisation techniques. *Paleobiology*, **35**, 146–167.

WALTHER, M. and FRÖBISCH, J. 2013. The quality of the fossil record of anomodonts (Synapsida, Therapsida). *Comptes Rendus Palevol*, **12**, 495–504.

WATSON, D. M. S. 1937. The acanthodian fishes. *Philosophical Transactions of the Royal Society of London B*, **228**, 49–146.

WEIGMANN, S. 2016. Annotated checklist of the living sharks, batoids and chimaeras (Chondrichthyes) of the world, with a focus on biogeographical diversity. *Journal of Fish biology*, **88**, 837–1037.

WEN-JIN, Z. and MIN, Z. 2007. Diversification and faunal shift of Siluro-Devonian vertebrates of China. *Geological Journal*, **42**, 351–369.

WICKHAM, H. 2016. *ggplot2: elegant graphics for data analysis*. Springer-Verlag New York, 260 pp.

WILLIAMS, M. E. 1985. The “cladodont level” sharks of the Pennsylvanian black shales of central North America. *Palaeontographica A,* **190**, 83–158.

WOOLLEY, C. H., THOMPSON, J. R., WU, Y.-H., BOTTJER, D. J. and SMITH, N. D. 2022. A biased fossil record can preserve reliable phylogenetic signal. *Paleobiology*, 1–16.

YOUNG, G. C. 1982. Devonian sharks from south eastern Australia and Antarctica. *Palaeontology*, **25**, 817–843.

YOUNG, G. C. 1997. Ordovician microvertebrate remains from the Amadeus Basin, Central Australia. *Journal of Vertebrate Paleontology*, **17**, 1–25.

ZANGERL, R. 1981. Chondrichthyes I. Paleozoic Elasmobranchii. *In* SCHULTZE, H.-P. (ed.). *Handbook of palaeoichthyology, volume 3A*. Verlag Dr. Friedrich Pfeil, 113 pp.

ZANGERL, R. and CASE, G. R. 1976. *Cobelodus aculeatus* (Cope), an anacanthous shark from Pennsylvanian black shales of North America. *Palaeontographica Abteilung A*, **154**, 107–157.

ZHU, M. 1998. Early Silurian sinacanths (Chondrichthyes) from China. *Palaeontology*, **41**, 157–171.

ZHU, M. 2014. Bone gain and loss: insights from genomes and fossils. *National Science Review*, **1**, 490–492.

ZHU, M., YU, X. and JANVIER, P. 1999. A primitive fossil fish sheds light on the origin of bony fishes. *Nature*, **397**, 607–610.

ZHU, M., ZHAO, W., JIA, L., LU, J., QIAO, T. And QU, Q. 2009. The oldest articulated osteichthyan reveals mosaic gnathostome characters. *Nature*, **458**, 469–474.

ZHU, M., YU, X., AHLBERG, P. E., CHOO, B., LU, J., QIAO, Q. L., ZHAO, J., BLOM, H. and ZHU, Y. 2013. A Silurian placoderm with osteichthyan-like marginal jaw bones. *Nature*, **502**, 188–193.

ZHU, M., AHLBERG, P., PAN, Z., ZHU, Y., QIAO, T., ZHAO, W., JIA, L. and LU, J. 2016. A Silurian maxillate placoderm illuminates jaw evolution. *Science*, **354**, 334–336.

APPENDICES

APPENDIX A

SKELETAL AND SOFT TISSUE COMPLETENESS OF THE ACANTHODIAN FOSSIL RECORD

A.1 Justification for the acanthodian body exemplars

We assigned the acanthodian taxa investigated in this study to different acanthodian body exemplars to account for the differences that both skeletal and soft tissue regions contribute to the overall body. We determined relative proportions of the different regions by calculating them from 2D reconstructions taken from the literature. Different members of acanthodians are known to encompass a varying number of fins, including an absence of specific fins, fin spines and presence/absence of teeth which may result in a bias in relative proportions. In order to account for this, we calculated both skeletal and soft tissue proportions for representatives of eight acanthodian taxa as well as an averaged exemplar calculated from all eight body exemplars. The averaged acanthodian body exemplar was used primarily for Incerti sedis taxa based on isolated remains. We primarily followed the extensive review by Denison (1979) as a guide

to the body descriptions. Additional references are noted throughout. Scales for the skeletal proportions were artificially set to 10%. Below are short justifications for each body exemplar:

Diplacanthid-exemplar. Primarily based on *Diplacanthus crassisimus* Duff, 1842. Deep and ventrally flattened body, with two prominent dorsal fins. Characterised by possessing all pectoral, pelvic and anal fins as well as intermediate fins and fin spines (typically two). Teeth are absent. Vertebrae proportions taken from Acanthodid-exemplar A as there are currently no reconstructions of the vertebral column for other acanthodian taxa.

Acanthodid-exemplar A. Primarily based on *Acanthodes* Agassiz, 1833. Long and slender body, with one rather posterior dorsal fin. Characterised by possessing all pectoral, pelvic and anal fins but no intermediate fins and fin spines. Teeth are absent.

Acanthodid-exemplar B. Primarily based on *Traquairichthys pygmaeus* Fritsch, 1875 and *Acanthodes* Agassiz, 1833. Long and slender body, with one rather posterior dorsal fin. Characterised by possessing only pectoral and anal fins but no pelvic or intermediate fins and fin spines. Teeth are absent. Body proportions taken from Acanthodid-exemplar A but calculated with regards to the absence of pelvic fins.

Acanthodopsis-exemplar. An informal exemplar. Primarily based on *Acanthodopsis* Hancock & Atthey, 1868 and *Acanthodes* Agassiz, 1833. Known from dentigerous jaw bones only. As positioned within the Acanthodidae (see Burrow 2004), the body proportions other than the teeth are taken from the Acanthodid-exemplar A, including possession of one dorsal fin, all pectoral, pelvic and anal fins but no intermediate fins and fin spines. Teeth are present.

Mesacanthid-exemplar. Primarily based on *Mesacanthus mitchelli* Egerton, 1861 and *Acanthodes* Agassiz, 1833. Small, slender and laterally compressed body, with one

rather posterior dorsal fin. Characterised by possessing all pectoral, pelvic and anal fins and one intermediate fin and fin spine. Teeth are absent. Body proportions taken from Acanthodid-exemplar A but calculated with regards to the intermediate fin spine and fin.

Ischnacanthid-exemplar. Primarily based on the Ischnacanthiformes Berg, 1940. Slender, laterally compressed body, with two dorsal fins. Characterised by possessing all pectoral, pelvic and anal fins as well as an intermediate fin spine. Teeth are present. Vertebrae proportions taken from Acanthodid-exemplar A as there are currently no reconstructions of the vertebral column for other acanthodian taxa.

Climatiid-exemplar. Primarily based on *Climatius reticulatus* Agassiz, 1845. Slender body, with two dorsal fins. Characterised by possessing all pectoral, pelvic and anal fins as well as intermediate fins and fin spines. Teeth are present. Vertebrae proportions taken from Acanthodid-exemplar A as there are currently no reconstructions of the vertebral column for other acanthodian taxa.

Tetanopsyrus-exemplar. An informal exemplar. Primarily based on *Tetanopsyrus lindoei* Gagnier, Hanke & Wilson, 1999. Small acanthodian, with two dorsal fins (see Gagnier *et al.* 1999). Characterised by possessing all pectoral, pelvic and anal fins but no intermediate fins and fin spines. Teeth are absent. Vertebrae proportions taken from Acanthodid-exemplar A as there are currently no reconstructions of the vertebral column for other acanthodian taxa.

A.2 Scoring acanthodian completeness

Skeletal Completeness Metric (modified from Beardmore et al. 2012 and Driscoll et al. 2018)

Score	0	1	2	3	4
Braincase (Neurocranium)	Braincase absent	Only single, scattered and disarticulated fragments present (1-25% complete)	Approximately 50% of the braincase present: moderate completeness	Braincase is clearly identifiable (50-75% complete), with only few elements missing	All major skull elements present; If all, only small fragments missing
Upper jaw (Palatoquadrate)	Upper jaw absent	Only single, scattered and disarticulated fragments present (1-25% complete)	Approximately 50% of the upper jaw present: moderate completeness	Upper jaw clearly identifiable (50-75% complete), with only few elements missing (50-75%)	Complete upper jaw (more than 75%)
Lower jaw (Meckel's cartilage)	Lower jaw absent	Only single, scattered and disarticulated fragments present (1-25% complete)	Approximately 50% of the lower jaw present: moderate completeness	Lower jaw clearly identifiable (50-75% complete), with only few elements missing	Complete lower jaw (more than 75%)
Hyoid and gill arches (branchial arches including hyomandibular)	Gill arches absent	Only single, scattered and disarticulated fragments present (1-25% complete)	Approximately 50% of the gill arches present: moderate completeness	Gill arches clearly identifiable (50-75% complete), with only few elements missing	Complete gill arches (more than 75%)
Shoulder girdle (pectoral girdle)	Shoulder girdle absent	Only single, scattered and disarticulated fragments present (1-25% complete)	Approximately 50% of the shoulder girdle present: moderate completeness	Shoulder girdle clearly identifiable (50-75% complete), with only few elements missing	All major shoulder girdle elements present; If all, only small fragments missing
Vertebrae	Vertebrae absent	1-25% of vertebrae present (measured along the axis of the main body)	25-50% of vertebrae present (measured along the axis of the main body)	50-75% of vertebrae present (measured along the axis of the main body)	Most vertebrae present (more than 75%)
Teeth	Teeth absent	1 to 3 teeth present at most; 1-25% of jaw bones toothed	50% of jaw bones toothed	50-75% of jaw bones toothed	Dentition nearly complete (more than 75% of jaw bones toothed)
Fin spines	Fin spines absent	One fin spine or fragments of it present, no association with one of the fins	2 or 3 fin spines present, may or may not be assigned to a specific fin	4 fin spines present, can be assigned to specific fin regions	All major fin spines (dorsal, pectoral, pelvic, anal, at least one intermediate) present
Scales	Scales absent	Single scales present, up to 25% of the body covered	25-50% of the body covered in scales	50-75% of the body covered in scales	Most of the body covered in scales (more than 75%)

Soft Tissue Completeness Metric

Score	0	1	2	3	4
Head	Head absent	1-25% of the head present, may be fragmented and scattered	25-50% of the head present, moderately complete	50-75% of the head present, highly complete	Complete head (more than 75% present)
Gill region	Gill region absent	1-25% of the gill region present, may be fragmented and scattered	25-50% of the gill region present, moderately complete	50-75% of the gill region present, highly complete	Most of the gill region present (more than 75%)
Main body	Main body absent	1-25% of the main body surface present (estimated from end of gill region to the caudal keel), may be fragmented and scattered	25-50% of the main body surface present (estimated from end of gill region to the caudal keel), moderately complete, “no edges”	50-75% of the main body surface present (estimated from end of gill region to the caudal keel), highly complete, contours of fish body are clearly visible	More than 75% of the main body surface present (estimated from end of gill region to the caudal keel)
Dorsal fin(s)	Dorsal fin(s) absent	Limited completeness; 1-25% of fin(s) present, only one fin present at most	Moderate completeness; 25-50% of fin(s) present	Extensive completeness; 50-75% of fin(s) present, all fins have to be present to some extent	Complete dorsal fin(s) (each more than 75% present)
Caudal fin	Caudal fin absent	Limited completeness; 1-25% of fin present, may be fragmented and scattered	Moderate completeness; 25-50% of fin present	Extensive completeness; 50-75% of fin present	Complete caudal fin (more than 75% present)
Anal fin	Anal fin absent	Limited completeness; 1-25% of fin present, may be fragmented and scattered	Moderate completeness; 25-50% of fin present	Extensive completeness; 50-75% of fin present	Complete anal fin (more than 75% present)
Pelvic fin	Pelvic fin absent	Limited completeness; 1-25% of fin present, may be fragmented and scattered	Moderate completeness; 25-50% of fin present	Extensive completeness; 50-75% of fin present	Complete pelvic fin (more than 75% present)
Intermediate fin(s)	Intermediate fin(s) absent	Limited completeness; 1-25% of fin(s) present, only one fin present at most	Moderate completeness; 25-50% of fin(s) present	Extensive completeness; 50-75% of fin(s) present, all fins have to be present to some extent	All intermediate fins present (each more than 75% complete)
Pectoral fin	Pectoral fin absent	Limited completeness; 1-25% of fin present, may be fragmented and scattered	Moderate completeness; 25-50% of fin present	Extensive completeness; 50-75% of fin present	Complete pectoral fin (more than 75% present)

A.3 Figures and tables

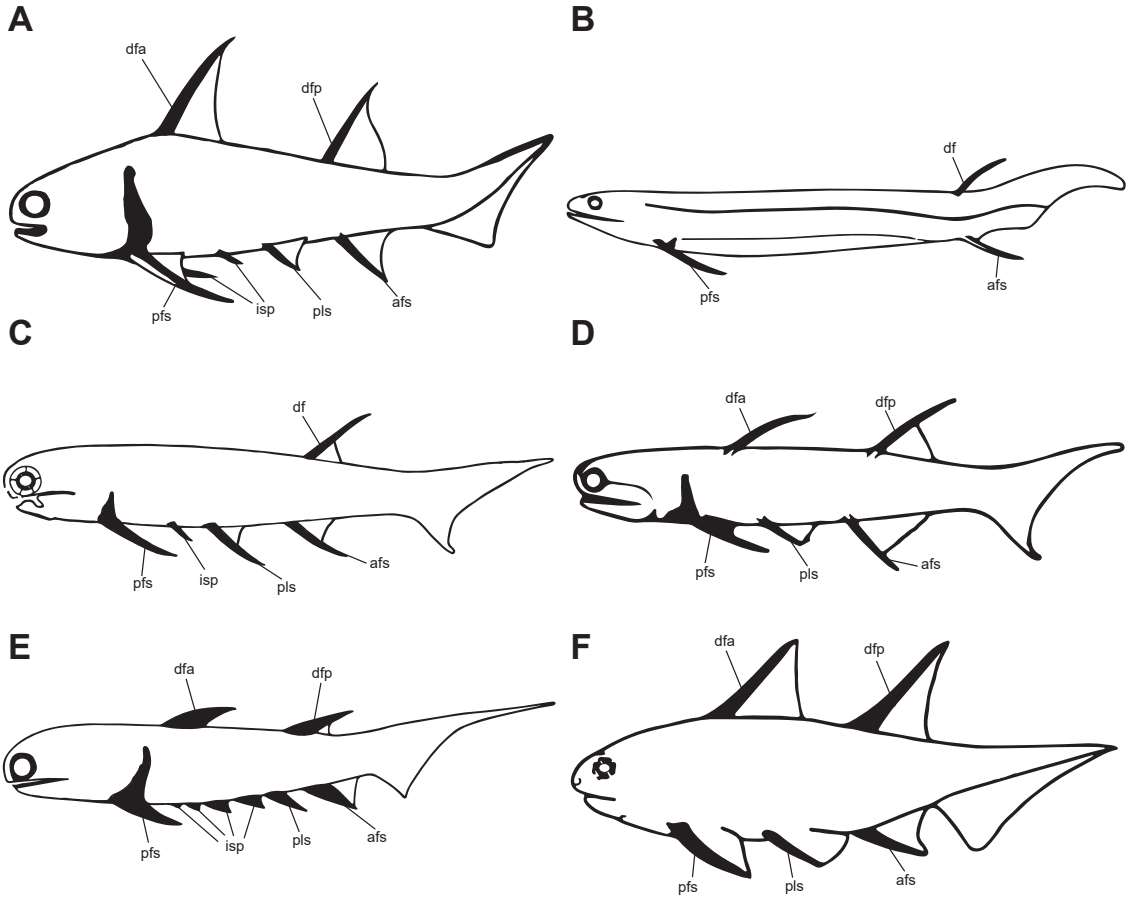


Figure A.1: Illustrations of acanthodian taxa used for the acanthodian body exemplars. A, Diplacanthid exemplar. B, Acanthodid-exemplar B. C, Mesacanthid-exemplar. D, Ischnacanthid-exemplar. E, Climatiid-exemplar. F, Tetanopsyrus-exemplar. A, C-E, illustrations modified from Watson (1937). B, illustration modified from Fritsch (1895). F, illustration modified from Gagnier, Hanke & Wilson (1999). afs, anal fin spine; df, dorsal fin; dfa, anterior dorsal fin; dfp, posterior dorsal fin; isp, intermediate fin spine; pfs, pectoral fin spine; pls, pelvic fin spine.

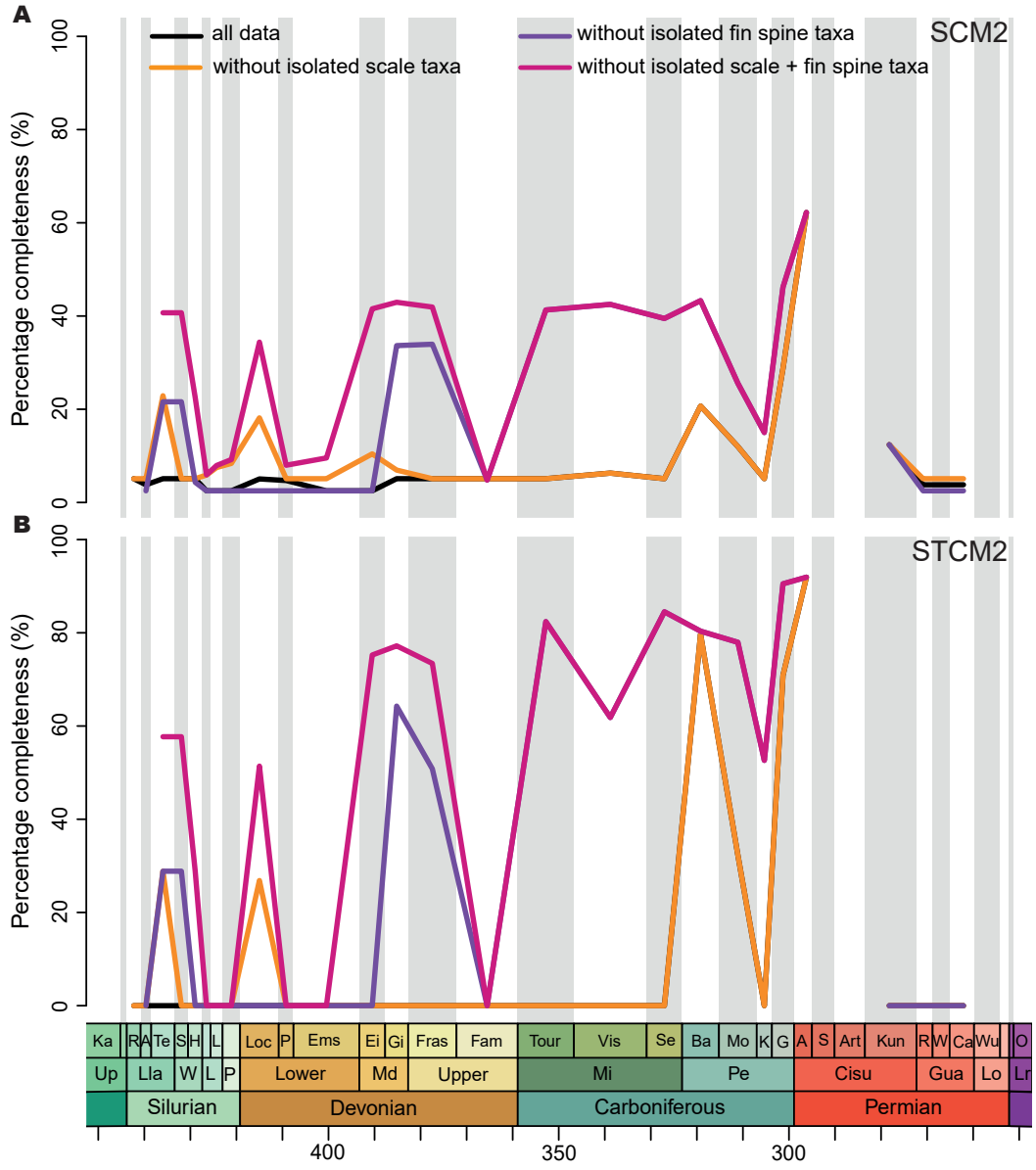


Figure A.2: Changes in median acanthodian completeness through time. A, skeletal completeness. B, soft tissue completeness.

Table A.1: Mann-Whitney-Wilcoxon test results of comparisons of the distribution and median of total SCM2/ STCM2 with SCM2/STCM2 of the three subsets sub1 (subset without isolated scale based taxa), sub2 (subset without fin spine based taxa) and sub3 (subset without isolated scale and fin spine based taxa). Statistically significant results indicated in bold.

Dataset 1	Dataset 2	Test statistic (W)	p-value	Adjusted p-value
SCM2	SCM2 sub1	16552	**3.10E-13**	**9.31E-13**
STCM2	STCM2 sub2	21805.5	**1.54E-05**	**2.63E-05**
SCM2	SCM2 sub2	40554	0.321242	0.321242
STCM2	STCM2 sub2	36430.5	0.123446	0.134668
SCM2	SCM2 sub3	9365.5	**2.30E-15**	**2.76E-14**
STCM2	STCM2 sub3	10495.5	**7.52E-15**	**4.51E-14**
SCM2 sub1	SCM2 sub2	30645.5	**3.68E-12**	**8.84E-12**
STCM2 sub1	STCM2 sub2	25125.5	**0.005544**	**0.006653**
SCM2 sub2	SCM2 sub3	8026	**2.78E-13**	**9.31E-13**
STCM2 sub2	STCM2 sub3	9422.5	**5.27E-10**	**1.05E-09**
SCM2 sub1	SCM2 sub3	8301.5	**0.003490**	**0.004653**
STCM2 sub1	STCM2 sub3	8035	**0.000568**	**0.000852**

Table A.2: Results of model-fitting analyses using GLS testing the best explanations of observed acanthodian SCM2. The models with the highest AIC weights are indicated in bold, with none of the coefficients being significant. The time bin length coefficient in model 1 is significant but has a low strength (R^2).

Model	Comparison	R^2	AIC weight
1	SCM2 ∼stage midpoints	0.220201	0.000020
2	SCM2 ∼richness	0.290388	0.000061
3	SCM2 ∼time bin length	0.368618	0.000228
4	SCM2 ∼sea level	0.785375	**0.342665**
5	SCM2 ∼richness + time bin length	0.398057	0.000085
6	SCM2 ∼richness + stage midpoints	0.303191	0.000016
7	SCM2 ∼richness + sea level	0.787144	0.055824
8	SCM2 ∼time bin length + sea level	0.836812	**0.420710**
9	SCM2 ∼stage midpoints + sea level	0.804648	**0.108427**
10	SCM2 ∼stage midpoints + richness + sea level	0.807335	0.013463
11	SCM2 ∼time bin length + richness + sea level	0.839266	0.052535
12	SCM2 ∼stage midpoints + time bin length + richness + sea level	0.848134	0.005966

Table A.3: Results of model-fitting analyses using GLS testing the best explanations of observed acanthodian STCM2. The three models with the highest AIC weights are indicated in bold, with the taxonomic richness coefficient in model 7 being significant. The taxonomic richness coefficient is also significant in all other models with varying strength (R^2).

Model	Comparison	R^2	AIC weight
1	STCM2 ∼stage mid points	0.227843	0.000001
2	STCM2 ∼richness	0.386176	0.000026
3	STCM2 ∼time bin length	0.273273	0.000003
4	STCM2 ∼sea level	0.826282	**0.337407**
5	STCM2 ∼richness + time bin length	0.398304	0.000007
6	STCM2 ∼richness + stage midpoints	0.392254	0.000006
7	STCM2 ∼richness + sea level	0.859590	**0.358860**
8	STCM2 ∼time bin length + sea level	0.842289	**0.124661**
9	STCM2 ∼stage midpoints + sea level	0.830064	0.063029
10	STCM2 ∼stage midpoints + richness + sea level	0.867000	0.065509
11	STCM2 ∼time bin length + richness + sea level	0.861448	0.045220
12	STCM2 ∼stage midpoints + time bin length + richness + sea level	0.868036	0.005270

Table A.4: Results of model-fitting analyses using GLS testing the best explanations of observed acanthodian taxonomic richness. The three models with the highest AIC weights are indicated in bold, with the SCM2 coefficient being significant in all three models.

Model	Comparison	R^2	AIC weight
1	richness ~stage midpoints	0.828522	0.001943
2	richness ~SCM2	0.8786035	0.028324
3	richness ~time bin length	0.849937	0.009655
4	richness ~sea level	0.930780	0.012324
5	richness ~STCM2	0.897625	**0.184252**
6	richness ~stage midpoints + SCM2	0.881110	0.007820
7	richness ~stage midpoints + time bin length	0.852392	0.002697
8	richness ~stage midpoints + sea level	0.930941	0.002061
9	richness ~stage midpoints + STCM2	0.899179	0.047558
10	richness ~time bin length + SCM2	0.879886	0.006977
11	richness ~time bin length + sea level	0.936516	0.004419
12	richness ~time bin length + STCM2	0.900604	0.055430
13	richness ~sea level + SCM2	0.955463	0.025940
14	richness ~sea level + STCM2	0.967486	**0.357975**
15	richness ~SCM2 + STCM2	0.901134	**0.058709**
16	richness ~stage midpoints + time bin length + SCM2	0.883043	0.001763
17	richness ~stage midpoints + SCM2 + sea level	0.957532	0.004334
18	richness ~stage midpoints + SCM2 + STCM2	0.902693	0.013085
19	richness ~stage midpoints + sea level + STCM2	0.968891	0.057304
20	richness ~time bin length + SCM2 + sea level	0.955469	0.002900
21	richness ~time bin length + SCM2 + STCM2	0.909984	0.029907
22	richness ~time bin length + stage midpoints + sea level	0.936869	0.000576
23	richness ~time bin length + stage midpoints + STCM2	0.902753	0.013172
24	richness ~sea level + SCM2 + STCM2	0.968486	0.051583
25	richness ~stage midpoints + SCM2 + time bin length + sea level	0.957533	0.000325
26	richness ~stage midpoints + SCM2 + time bin length + STCM2	0.912796	0.006576
27	richness ~stage midpoints + time bin length + sea level + STCM2	0.969451	0.004977
28	richness ~time bin length + SCM2 + sea level + STCM2	0.970710	0.006992
29	richness ~stage midpoints + SCM2 + time bin length + sea level + STCM2	0.971809	0.000424

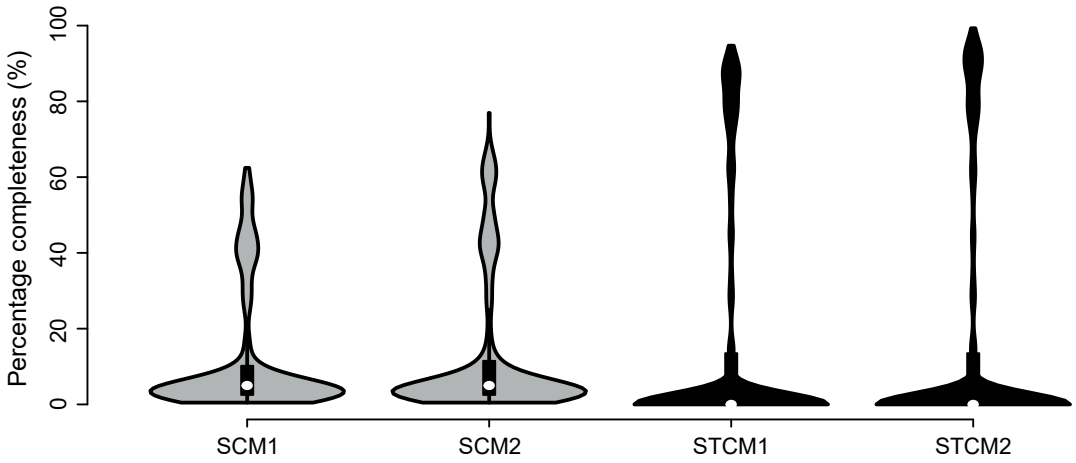


Figure A.3: Distribution of acanthodian SCM1/SCM2 values compared to STCM1/ STCM2 values.

Table A.5: Mann-Whitney-Wilcoxon test results of comparisons of the distribution and median of different acanthodian completeness metrics. Statistically significant results indicated in bold.

Dataset 1	Dataset 2	Test statistic (W)	p-value	Adjusted p-value
SCM2	STCM2	71753	**5.77E-29**	**2.12E-28**
SCM1	STCM1	71633	**1.06E-28**	**2.12E-28**
SCM1	SCM2	46795.5	0.655077	0.773513
STCM1	STCM2	47246	0.773513	0.773513

Table A.6: Mann-Whitney-Wilcoxon test results of comparisons of the distribution and median SCM2 values of different acanthodian subgroups. Statistically significant results indicated in bold.

Dataset 1	Dataset 2	Test statistic (W)	p-value	Adjusted p-value
Acanthodiformes	Diplacanthiformes	878	**0.024238**	0.060595
Acanthodiformes	Ischnacanthiformes	2090.5	**6.08E-07**	**3.04E-06**
Acanthodiformes	Incerti sedis	6178	**3.85E-08**	**5.78E-07**
Acanthodiformes	Climatiidae	2058	**1.55E-07**	**1.17E-06**
Diplacanthiformes	Ischnacanthiformes	971	0.059644	0.127809
Diplacanthiformes	Incerti sedis	2793	0.147965	0.221947
Diplacanthiformes	Climatiidae	1005	**0.006662**	**0.019986**
Ischnacanthiformes	Incerti sedis	4110.5	0.079848	0.149715
Ischnacanthiformes	Climatiidae	1707	0.259794	0.299762
Incerti sedis	Climatiidae	5824.5	**0.004559**	**0.017098**

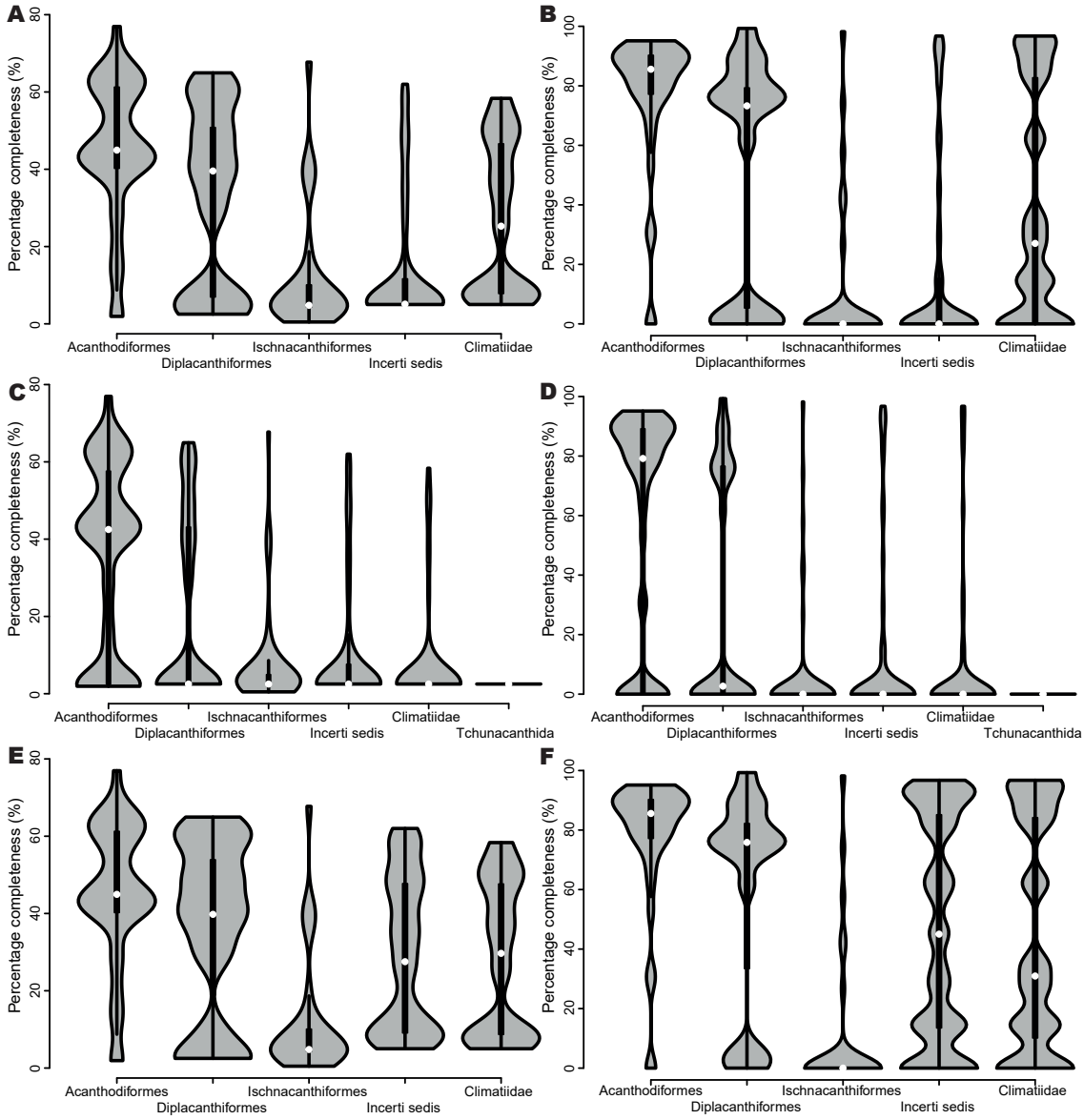


Figure A.4: Distribution of completeness between different acanthodian subgroups. A, SCM2 subset without isolated scale-based taxa. B, STCM2 subset without isolated scale-based taxa. C, SCM2 subset without isolated fin spine-based taxa. D, STCM2 subset without isolated fin spine-based taxa. E, SCM2 subset without isolated scale and fin spine-based taxa. F, STCM2 subset without isolated scale and fin spine-based taxa.

Table A.7: Mann-Whitney-Wilcoxon test results of comparisons of the distribution and median SCM2 values of a subset of different acanthodian subgroups without isolated fin spine-based taxa. Statistically significant results indicated in bold.

Dataset 1	Dataset 2	Test statistic (W)	p-value	Adjusted p-value
Acanthodiformes	Diplacanthiformes	808	**0.034094**	0.085236
Acanthodiformes	Ischnacanthiformes	2090.5	**6.08E-07**	**3.04E-06**
Acanthodiformes	Incerti sedis	4253	**1.07E-08**	**1.60E-07**
Acanthodiformes	Climatiidae	2023	**1.50E-07**	**1.12E-06**
Diplacanthiformes	Ischnacanthiformes	885	0.095303	0.195978
Diplacanthiformes	Incerti sedis	1864	**0.031832**	0.085236
Diplacanthiformes	Climatiidae	905	**0.010282**	**0.038559**
Ischnacanthiformes	Incerti sedis	3364	0.743029	0.743029
Ischnacanthiformes	Climatiidae	1694	0.211023	0.351705
Incerti sedis	Climatiidae	3410	0.289915	0.395338

Table A.8: Mann-Whitney-Wilcoxon test results of comparisons of the distribution and median SCM2 values of a subset of different acanthodian subgroups without isolated scale and fin spine-based taxa. Statistically significant results indicated in bold.

Dataset 1	Dataset 2	Test statistic (W)	p-value	Adjusted p-value
Acanthodiformes	Diplacanthiformes	346	0.169556	0.242222
Acanthodiformes	Ischnacanthiformes	988	**4.80E-08**	**4.80E-07**
Acanthodiformes	Incerti sedis	932	**0.001375**	**0.004582**
Acanthodiformes	Climatiidae	322	**0.020698**	**0.034497**
Diplacanthiformes	Ischnacanthiformes	341.5	**0.005074**	**0.010148**
Diplacanthiformes	Incerti sedis	306	0.362550	0.453187
Diplacanthiformes	Climatiidae	107	0.420468	0.467187
Ischnacanthiformes	Incerti sedis	207	**2.88E-05**	**0.000144**
Ischnacanthiformes	Climatiidae	77	**0.004178**	**0.010148**
Incerti sedis	Climatiidae	218	0.854721	0.854721

Table A.9: Mann-Whitney-Wilcoxon test results of comparisons of the distribution and median SCM2 values of a subset of different acanthodian subgroups without isolated scale-based taxa. Statistically significant results indicated in bold.

Dataset 1	Dataset 2	Test statistic (W)	p-value	Adjusted p-value
Acanthodiformes	Diplacanthiformes	416	0.059928	0.066587
Acanthodiformes	Ischnacanthiformes	988	**4.80E-08**	**2.40E-07**
Acanthodiformes	Incerti sedis	2857	**8.03E-11**	**8.03E-10**
Acanthodiformes	Climatiidae	357	**0.010296**	**0.014708**
Diplacanthiformes	Ischnacanthiformes	375.5	**0.007705**	**0.012842**
Diplacanthiformes	Incerti sedis	1071	**0.006341**	**0.012681**
Diplacanthiformes	Climatiidae	123	0.615315	0.615315
Ischnacanthiformes	Incerti sedis	953.5	**0.013095**	**0.016369**
Ischnacanthiformes	Climatiidae	90	**0.005555**	**0.012681**
Incerti sedis	Climatiidae	322.5	**0.006057**	**0.012681**

Table A.10: Mann-Whitney-Wilcoxon test results of comparisons of the distribution and median STCM2 values of different acanthodian subgroups. Statistically significant results indicated in bold.

Dataset 1	Dataset 2	Test statistic (W)	p-value	Adjusted p-value
Acanthodiformes	Diplacanthiformes	925.5	**0.005188**	**0.007412**
Acanthodiformes	Ischnacanthiformes	2237	**4.14E-11**	**2.07E-10**
Acanthodiformes	Incerti sedis	6642.5	**4.45E-16**	**4.45E-15**
Acanthodiformes	Climatiidae	2114	**5.84E-09**	**1.95E-08**
Diplacanthiformes	Ischnacanthiformes	1078	**0.000144**	**0.000307**
Diplacanthiformes	Incerti sedis	3159.5	**0.000154**	**0.000307**
Diplacanthiformes	Climatiidae	1006	**0.003492**	**0.005819**
Ischnacanthiformes	Incerti sedis	4572	0.353298	0.440095
Ischnacanthiformes	Climatiidae	1454	0.396086	0.440095
Incerti sedis	Climatiidae	4697.5	0.905508	0.905508

Table A.11: Mann-Whitney-Wilcoxon test results of comparisons of the distribution and median STCM2 values of a subset of different acanthodian subgroups without isolated scale and fin spine-based taxa. Statistically significant results indicated in bold.

Dataset 1	Dataset 2	Test statistic (W)	p-value	Adjusted p-value
Acanthodiformes	Diplacanthiformes	375	0.050031	0.071473
Acanthodiformes	Ischnacanthiformes	1026	**9.74E-10**	**9.74E-09**
Acanthodiformes	Incerti sedis	913	**0.002792**	**0.005584**
Acanthodiformes	Climatiidae	313	**0.035273**	0.058788
Diplacanthiformes	Ischnacanthiformes	389	**1.18E-05**	**5.89E-05**
Diplacanthiformes	Incerti sedis	299	0.444117	0.530916
Diplacanthiformes	Climatiidae	105	0.477824	0.530916
Ischnacanthiformes	Incerti sedis	221	**2.08E-05**	**6.95E-05**
Ischnacanthiformes	Climatiidae	82	**0.001538**	**0.003845**
Incerti sedis	Climatiidae	213.5	0.941248	0.941248

Table A.12: Mann-Whitney-Wilcoxon test results of comparisons of the distribution and median STCM2 values of a subset of different acanthodian subgroups without isolated scale-based taxa. Statistically significant results indicated in bold.

Dataset 1	Dataset 2	Test statistic (W)	p-value	Adjusted p-value
Acanthodiformes	Diplacanthiformes	447	**0.013887**	**0.019839**
Acanthodiformes	Ischnacanthiformes	1026	**9.74E-10**	**4.87E-09**
Acanthodiformes	Incerti sedis	2893	**2.58E-12**	**2.58E-11**
Acanthodiformes	Climatiidae	349	**0.016814**	**0.021018**
Diplacanthiformes	Ischnacanthiformes	413	**8.62E-05**	**0.000287**
Diplacanthiformes	Incerti sedis	1132	**0.000324**	**0.000809**
Diplacanthiformes	Climatiidae	123	0.612128	0.612128
Ischnacanthiformes	Incerti sedis	1211	0.285994	0.317771
Ischnacanthiformes	Climatiidae	100	**0.003317**	**0.006634**
Incerti sedis	Climatiidae	354.5	**0.007295**	**0.012159**

Table A.13: Mann-Whitney-Wilcoxon test results of comparisons of the distribution and median STCM2 values of a subset of different acanthodian subgroups without isolated fin spine-based taxa. Statistically significant results indicated in bold.

Dataset 1	Dataset 2	Test statistic (W)	p-value	Adjusted p-value
Acanthodiformes	Diplacanthiformes	842.5	**0.011614**	**0.016591**
Acanthodiformes	Ischnacanthiformes	2237	**4.14E-11**	**4.14E-10**
Acanthodiformes	Incerti sedis	4360	**1.57E-10**	**7.83E-10**
Acanthodiformes	Climatiidae	2072.5	**8.48E-09**	**2.83E-08**
Diplacanthiformes	Ischnacanthiformes	1028	**5.41E-05**	**0.000135**
Diplacanthiformes	Incerti sedis	1942	**0.005420**	**0.009033**
Diplacanthiformes	Climatiidae	940.5	**0.001887**	**0.003774**
Ischnacanthiformes	Incerti sedis	2867	0.053225	0.066531
Ischnacanthiformes	Climatiidae	1423	0.375059	0.375059
Incerti sedis	Climatiidae	3360.5	0.348659	0.375059

Table A.14: Mann-Whitney-Wilcoxon test results of the comparisons of acanthodian SCM2 value distribution and median in comparison to other vertebrate groups. Statistically significant results indicated in bold.

Dataset 1	Dataset 2	Test statistic (W)	p-value	Adjusted p-values
Acanthodians	Chiroptera	99761	**1.96E-14**	**2.75E-14**
Acanthodians	Plesiosauria	5140	**4.79E-30**	**1.68E-29**
Acanthodians	Ichthyosauria	3733.5	**4.12E-32**	**2.88E-31**
Acanthodians	Sauropodomorpha	25878.5	**9.66E-23**	**2.25E-22**
Acanthodians	Parareptilia	4831	**3.79E-16**	**6.62E-16**
Acanthodians	Pelycosauria	9113.5	**5.65E-09**	**5.65E-09**
Acanthodians	Theropoda	50819	**6.76E-11**	**7.89E-11**

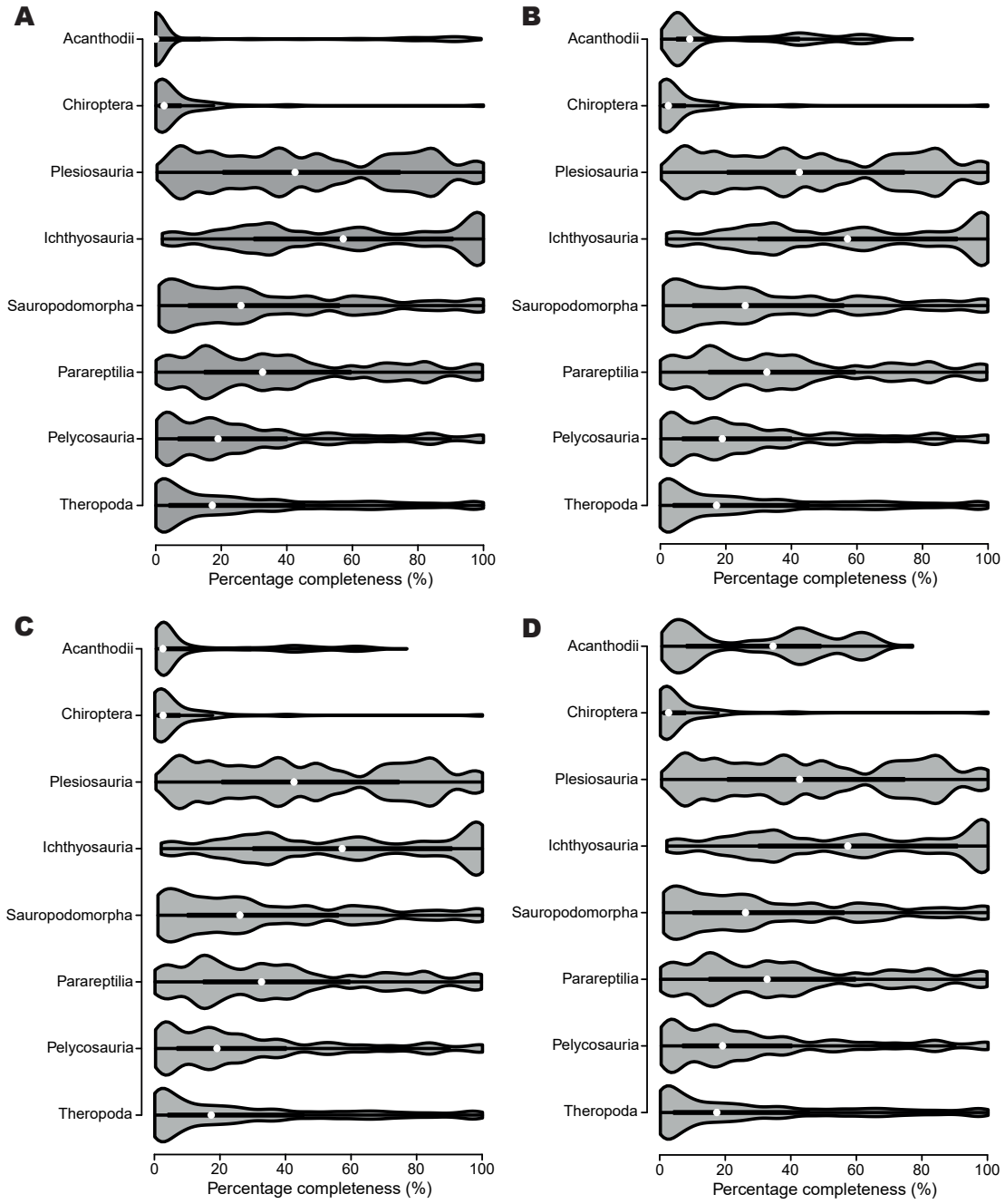


Figure A.5: Distribution of acanthodian completeness values compared to other vertebrate groups. A, STCM2 values. B, SCM2 subset without isolated scale-based taxa. C, SCM2 subset without isolated fin spine-based taxa. D, SCM2 subset without isolated scale and fin spine-based taxa. Comparative SCM2 scores from Chiroptera (Brown *et al.* 2019), plesiosaurs (Tutin & Butler 2017), ichthyosaurs (Cleary *et al.* 2015), sauropodomorphs (Mannion & Upchurch 2010, Cashmore *et al.* 2020), parareptiles (Verrière *et al.* 2016), pelycosaurs (Brocklehurst & Fröbisch 2014) and theropods (Cashmore & Butler 2019).

Table A.15: Mann-Whitney-Wilcoxon test results of the comparisons of acanthodian STCM2 value distribution and median in comparison to other vertebrate groups. Statistically significant results indicated in bold.

Dataset 1	Dataset 2	Test statistic (W)	p-value	Adjusted p-values
Acanthodians	Chiroptera	38046	**5.47E-33**	**1.91E-32**
Acanthodians	Plesiosauria	6656.5	**1.09E-26**	**1.53E-26**
Acanthodians	Ichthyosauria	4864	**1.31E-30**	**3.06E-30**
Acanthodians	Sauropodomorpha	21184	**3.19E-34**	**1.12E-33**
Acanthodians	Parareptilia	4758.5	**1.78E-19**	**1.78E-19**
Acanthodians	Pelycosauria	6525	**5.82E-20**	**6.79E-20**
Acanthodians	Theropoda	30992	**2.11E-40**	**1.48E-39**

Table A.16: Mann-Whitney-Wilcoxon test results of the comparisons of the distribution and median of SCM2 values of the acanthodian subset without isolated fin spine and scale-based taxa in comparison to other vertebrate groups. Statistically significant results indicated in bold.

Dataset 1	Dataset 2	Test statistic (W)	p-value	Adjusted p-values
Acanthodians	Chiroptera	48751	**2.63E-31**	**1.84E-30**
Acanthodians	Plesiosauria	4604.5	**3.32E-05**	**7.75E-05**
Acanthodians	Ichthyosauria	3288	**6.72E-09**	**2.35E-08**
Acanthodians	Sauropodomorpha	19262.5	0.310955	0.310955
Acanthodians	Parareptilia	3870	0.108017	0.151224
Acanthodians	Pelycosauria	6180.5	0.252035	0.294041
Acanthodians	Theropoda	30891	**0.011589**	**0.020281**

Table A.17: Mann-Whitney-Wilcoxon test results of comparisons of the distribution and median of acanthodian SCM2 values between continents. Statistically significant results indicated in bold.

Dataset 1	Dataset 2	Test statistic (W)	p-value	Adjusted p-values
Europe	North America	4073	**0.000175**	**0.001833**
Europe	South America	639.5	0.408010	0.534503
Europe	Africa	74	0.146895	0.280435
Europe	Asia	6488.5	0.074390	0.195273
Europe	Australia and Oceania	1281.5	0.458146	0.534503
Europe	Antarctica	312.5	0.298439	0.482094
North America	South America	396.5	0.175128	0.306474
North America	Africa	47	0.450577	0.534503
North America	Asia	3457.5	**6.23E-07**	**1.31E-05**
North America	Australia and Oceania	726.5	0.126254	0.265133
North America	Antarctica	185	0.793819	0.833510
South America	Africa	0	**0.028905**	0.151750
South America	Asia	421	**0.045260**	0.190091
South America	Australia and Oceania	80.5	0.847942	0.847942
South America	Antarctica	16.Mai	0.416094	0.534503
Africa	Asia	125.5	**0.023193**	0.151750
Africa	Australia and Oceania	29	0.120340	0.265133
Africa	Antarctica	8	0.328565	0.492847
Asia	Australia and Oceania	420	0.055938	0.195273
Asia	Antarctica	95.5	0.069791	0.195273
Australia and Oceania	Antarctica	34	0.523814	0.578952

Table A.18: Mann-Whitney-Wilcoxon test results of comparisons of the distribution and median of acanthodian STCM2 values between continents. Statistically significant results indicated in bold.

Dataset 1	Dataset 2	Test statistic (W)	p-value	Adjusted p-value
Europe	North America	4865.5	**0.012592**	0.092330
Europe	South America	922.5	0.118871	0.248734
Europe	Africa	125.5	0.405252	0.53189304
Europe	Asia	6274.5	0.089788	0.235693
Europe	Australia and Oceania	1378	0.748436	0.873176
Europe	Antarctica	314	0.195620	0.342335
North America	South America	427.5	**0.029862**	0.125420
North America	Africa	64.5	0.873481	0.902664
North America	Asia	2980	**0.000427**	**0.008967**
North America	Australia and Oceania	672	0.283457	0.425185
North America	Antarctica	167	0.902664	0.902664
South America	Africa	04.Mai	0.059346	0.207713
South America	Asia	261	0.227084	0.366828
South America	Australia and Oceania	54	0.084861	0.235693
South America	Antarctica	9	**0.015871**	0.092330
Africa	Asia	96	0.125887	0.248734
Africa	Australia and Oceania	22	0.468726	0.579015
Africa	Antarctica	6	0.840730	0.902664
Asia	Australia and Oceania	486	0.130289	0.248734
Asia	Antarctica	97	**0.017587**	0.092330
Australia and Oceania	Antarctica	32.5	0.387726	0.531893

Table A.19: Mann-Whitney-Wilcoxon test results of comparisons of the distribution and median SCM2 and STCM2 values of freshwater versus marine acanthodians. Statistically significant results indicated in bold.

Dataset 1	Dataset 2	Test statistic (W)	p-value	Adjusted p-value
Freshwater SCM2	Marine SCM2	397.5	**0.007941**	**0.015881**
Freshwater STCM2	Marine STCM2	381.5	**0.020491**	**0.027322**
Freshwater SCM2	Freshwater STCM2	170	**0.000878**	**0.003512**
Marine SCM2	Marine STCM2	351	0.818881	0.818881

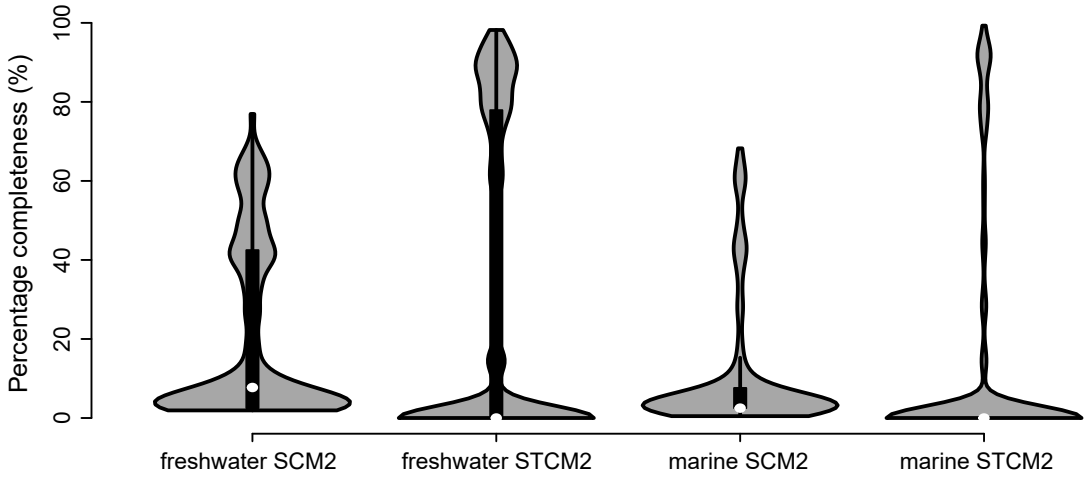


Figure A.6: Distribution of acanthodian SCM2 and STCM2 between freshwater and marine deposits.

Table A.20: Mann-Whitney-Wilcoxon test results of comparisons of the distribution and median SCM2 values of acanthodians from different environments (measured as Benthic Assemblage zones). Statistically significant results indicated in bold.

Dataset 1	Dataset 2	Test statistic (W)	p-value	Adjusted p-value
BA 0	BA 1	343	**0.017595**	**0.048356**
BA 0	BA 2	282.5	**0.025407**	0.053354
BA 0	BA 3	364.5	**0.001217**	**0.006387**
BA 0	BA 4	307.5	**0.000878**	**0.006146**
BA 0	BA 5	170.5	**0.000627**	**0.006146**
BA 0	BA 6	138	**0.000672**	**0.006146**
BA 1	BA 2	245.5	0.502808	0.502808
BA 1	BA 3	374	**0.006159**	**0.021556**
BA 1	BA 4	319	**0.003378**	**0.014188**
BA 1	BA 5	158	**0.023541**	0.053354
BA 1	BA 6	129	**0.018421**	**0.048356**
BA 2	BA 3	275.5	0.083864	0.146762
BA 2	BA 4	243	**0.029564**	0.056440
BA 2	BA 5	107	0.301325	0.372225
BA 2	BA 6	82	0.385313	0.449531
BA 3	BA 4	228.5	0.412445	0.455860
BA 3	BA 5	73.5	0.274901	0.360808
BA 3	BA 6	53	0.228970	0.320558
BA 4	BA 5	50	0.115701	0.182397
BA 4	BA 6	37	0.121598	0.182397
BA 5	BA 6	24	0.456391	0.479211

Table A.21: Mann-Whitney-Wilcoxon test results of comparisons of the distribution and median STCM2 values of acanthodians from different environments (measured as Benthic Assemblage zones). Statistically significant results indicated in bold.

Dataset 1	Dataset 2	Test statistic (W)	p-value	Adjusted p-value
BA 0	BA 1	316	0.081762	0.132078
BA 0	BA 2	280	**0.029916**	0.063764
BA 0	BA 3	355	**0.001821**	**0.012748**
BA 0	BA 4	300	**0.001249**	**0.012748**
BA 0	BA 5	171	**0.000512**	**0.010750**
BA 0	BA 6	112	**0.0420075**	0.080196
BA 1	BA 2	245.5	0.501904	0.702666
BA 1	BA 3	365	**0.008465**	**0.029627**
BA 1	BA 4	314	**0.003690**	**0.019371**
BA 1	BA 5	170	**0.005147**	**0.021616**
BA 1	BA 6	117.5	0.070745	0.123804
BA 2	BA 3	288.5	**0.027967**	0.063764
BA 2	BA 4	248.5	**0.012817**	**0.038451**
BA 2	BA 5	129	**0.030364**	0.063764
BA 2	BA 6	91	0.156411	0.234616
BA 3	BA 4	208.5	0.719963	0.944951
BA 3	BA 5	99	1	1
BA 3	BA 6	78	0.974172	1
BA 4	BA 5	77.5	0.841078	0.998504
BA 4	BA 6	61	0.903408	0.998504
BA 5	BA 6	30	0.897375	0.998504

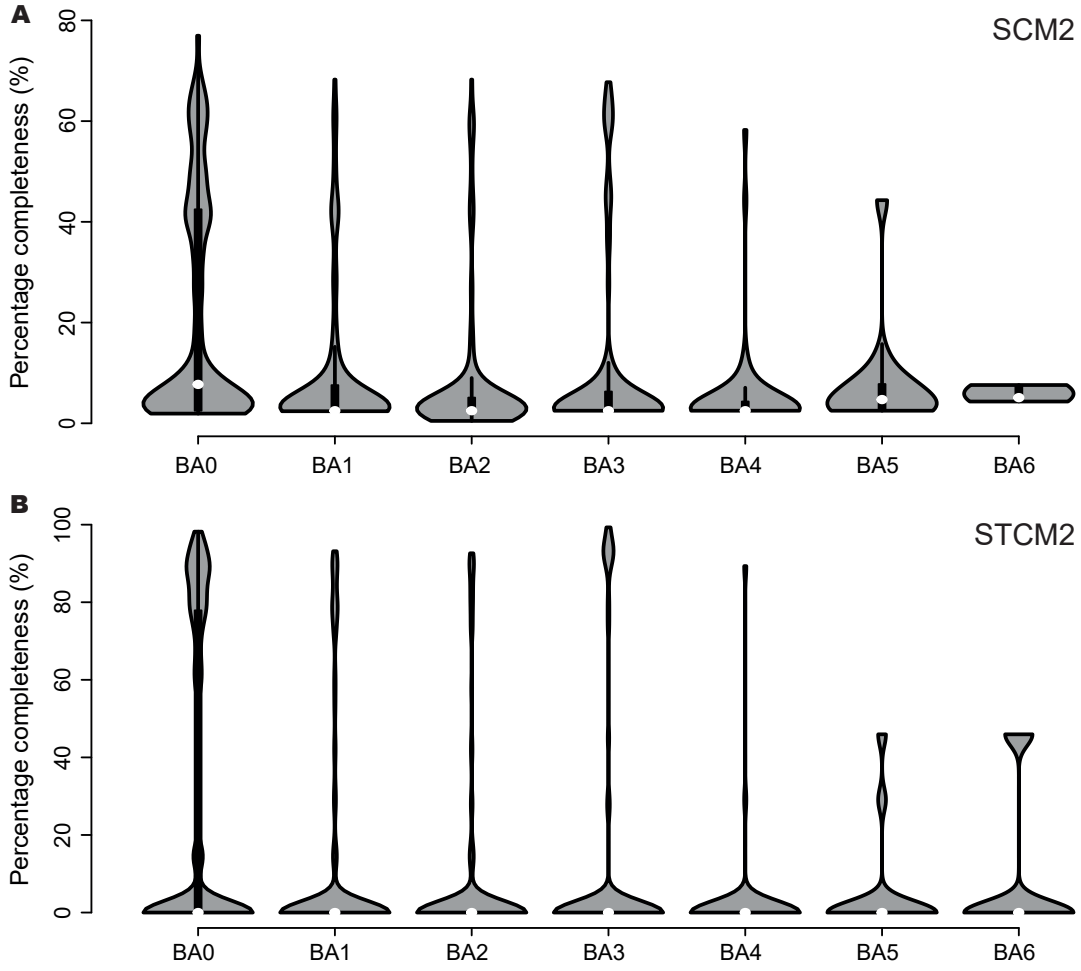


Figure A.7: Distribution of acanthodian completeness between the different Benthic Assemblage (BA) zones. A, skeletal completeness. B, soft tissue completeness.

Table A.22: Results of pairwise comparisons for sea level trends in different time series using GLS. Statistically significant results indicated in bold.

Comparison	Slope	t-value	p-value	R^2
total SCM2 ~ sea level	-0.235125	-0.7697051	0.4520	0.7853754
total STCM2 ~ sea level	-0.20595	-1.548912	0.8974	0.8262818
marine SCM2 ~ sea level	-0.1821522	-0.4020857	0.6926	0.7098517
marine STCM2 ~ sea level	-0.31705	-1.047047	0.8341	0.799784
freshwater SCM2 ~ sea level	0.5235253	1.6565592	0.1198	0.623399
freshwater STCM2 ~ sea level	0.160845	0.7386898	0.3577	0.6793172

APPENDIX B

THE COMPLETENESS OF THE PALAEOZOIC CHONDRICHTHYAN FOSSIL RECORD

B.1 Characteristics of the different chondrichthyan body exemplars

Chondrichthyan taxa examined in this study were assigned to different chondrichthyan body exemplars to account for the varying number of body proportions that make up the skeletal regions of different chondrichthyans. Members of the chondrichthyans to exhibit either a presence or absence of specific fins, a variable number or complete loss of fin spines and a dermis that is either predominantly naked or covered in scales. In order to account for this and minimise any biases, we calculated the skeletal proportions for representatives of eight chondrichthyan taxa from the literature and averaged each region. The iniopterygian body plan was calculated separately from that due to its very different nature and body proportions (see chondrichthyan body exemplar 6

for details). The chondrichthyan taxa included *Promexyele peyeri* Zangerl & Case, 1973, *Triodus sessilis* Jordan, 1849, *Cobelodus aculeatus* Cope, 1894, *Cladoselache fyleri* Newberry, 1889, *Stethacanthus altonensis* St. John & Worthen, 1875, *Tristychius arcuatus* Agassiz, 1837, morphotype Ctenacanthidae Dean, 1909 and morphotype Hybodontoidea Zangerl, 1981. Regions were then excluded and proportions recalculated to account for morphological variations in Palaeozoic chondrichthyan body plans. The body exemplars were assigned to the different taxa in the dataset depending on morphological fit. Scales for the skeletal proportions were artificially set to 10% and teeth to 2%. Below are the characteristics for each body exemplar:

Chondrichthyan body exemplar 1. Dorsal, pectoral, pelvic and anal fins all present. Fin spines present. Scales cover most if not all of the body.

Chondrichthyan body exemplar 2. Dorsal, pectoral and pelvic fins present, anal fin absent. Fin spines present. Scales cover most if not all of the body.

Chondrichthyan body exemplar 3. Dorsal, pectoral and pelvic fins present, anal fin absent. Fin spines absent. Scales cover most if not all of the body.

Chondrichthyan body exemplar 4. Pectoral and pelvic fins present, dorsal and anal fins absent. Fin spines absent. Scales cover most if not all of the body.

Chondrichthyan body exemplar 5. Dorsal and pectoral fins present, pelvic and anal fins absent. Fin spines absent. Scales cover most if not all of the body.

Chondrichthyan body exemplar 6. Chondrichthyans with a similar habitus to that of modern chimaeras. Dorsal, pectoral and pelvic fins present, anal fin absent. Fin spines absent. Scales only cover specific regions of the body, skin is generally naked.

Chondrichthyan body exemplar 7. Dorsal, pectoral and pelvic fins present, anal fin absent. Only one dorsal fin. Fin spines absent. Scales only cover specific regions of

the body, skin is generally naked.

Chondrichthyan body exemplar 8. Dorsal (usually two), pectoral and pelvic fins present, anal fin absent. One fin spine present. Scales only cover specific regions of the body, skin is generally naked.

B.2 Chondrichthyan completeness scores

Skeletal Completeness Metric (modified from Beardmore et al. 2012 and Driscoll et al. 2018)

Score	0	1	2	3	4
Braincase (Neurocranium)	Braincase absent	Only single, scattered and disarticulated fragments present (1-25% complete)	Approximately 50% of the braincase present: moderate completeness	Braincase is clearly identifiable (50-75% complete), with only few elements missing	All major skull elements present; If all, only small fragments missing
Upper jaw (Palatoquadrate)	Upper jaw absent	Only single, scattered and disarticulated fragments present (1-25% complete)	Approximately 50% of the upper jaw present: moderate completeness	Upper jaw clearly identifiable (50-75% complete), with only few elements missing	Complete upper jaw (more than 75%)
Lower jaw (Meckel's cartilage)	Lower jaw absent	Only single, scattered and disarticulated fragments present (1-25% complete)	Approximately 50% of the lower jaw present: moderate completeness	Lower jaw clearly identifiable (50-75% complete), with only few elements missing	Complete lower jaw (more than 75%)
Gill arches (branchial arches including hyomandibular)	Gill arches absent	Only single, scattered and disarticulated fragments present (1-25% complete)	Approximately 50% of the gill arches present: moderate completeness	Gill arches clearly identifiable (50-75% complete), with only few elements missing	Complete gill arches (more than 75%)
Vertebrae (Vertebral column)	Vertebrae absent	1-25% of vertebrae present (measured along the axis of the main body)	25-50% of vertebrae present (measured along the axis of the main body)	50-75% of vertebrae present (measured along the axis of the main body)	Most vertebrae present (more than 75%)
Dorsal fin(s)	Dorsal fin(s) skeletal elements absent	Limited completeness; 1-25% of fin elements present; if two dorsal fins, only elements of one may be present	Moderate completeness; 25-50% of fin elements present	Extensive completeness; 50-75% of fin elements present, all fins have to be present to some extent	Complete dorsal fin elements (each more than 75% present)
Shoulder girdle (pectoral girdle)	Shoulder girdle absent	Only single, scattered and disarticulated fragments present (1-25% complete)	Approximately 50% of the shoulder girdle present: moderate completeness	Shoulder girdle clearly identifiable (50-75% complete), with only few elements missing	All major shoulder girdle elements present; If all, only small fragments missing
Pectoral fins	Pectoral fin skeletal elements absent	Limited completeness; 1-25% of fin elements present, may be fragmented/ scattered	Moderate completeness; 25-50% of fin elements present	Extensive completeness; 50-75% of fin elements present	Complete pectoral fins (more than 75% elements of each fin present)
Pelvic fins (including pelvic girdle)	Pelvic fin skeletal elements absent	Limited completeness; 1-25% of fin elements present, either the fins or the pelvic girdle may be absent	Moderate completeness; 25-50% of fin elements (including pelvic girdle) present	Extensive completeness; 50-75% of fin elements present, pectoral girdle clearly identifiable (but may be fragmented)	Complete pelvic fin (more than 75% elements of each fin + pelvic girdle present)
Anal fin (If not known in a taxon, NA)	Anal fin skeletal elements absent	Limited completeness; 1-25% of fin elements present, may be	Moderate completeness; 25-50% of fin elements present	Extensive completeness; 50-75% of fin elements present	Complete anal fin (more than 75% of elements present)

Caudal fin	Caudal fin skeletal elements absent	Limited completeness; 1-25% of fin elements present, may be fragmented/ scattered	Moderate completeness; 25-50% of fin elements present	Extensive completeness; 50-75% of fin elements present	Complete caudal fin (more than 75% of elements present)
Teeth	Teeth absent	1 to 3 teeth present at most; 1-25% of jaw bones toothed	50% of jaw bones toothed	50-75% of jaw bones toothed	Dentition nearly complete (more than 75% of jaw toothed)
Fin spines (number and association with fin(s) depending on the taxon)	Fin spine(s) absent	One fin spin fragment present, may have no association with the fin	One or more fin spines may be present but overall fin spine completeness has to meet 25-50%	Fin spine(s) moderately complete (50-75%) and associated to the respective fin(s)	All fin spines are present and more than 75% complete
Scales	Scales absent	Single scales present, up to 25% of the body covered	25-50% of the body covered in scales	50-75% of the body covered in scales	Most of the body covered in scales (more than 75%)

B.3 Figures and tables

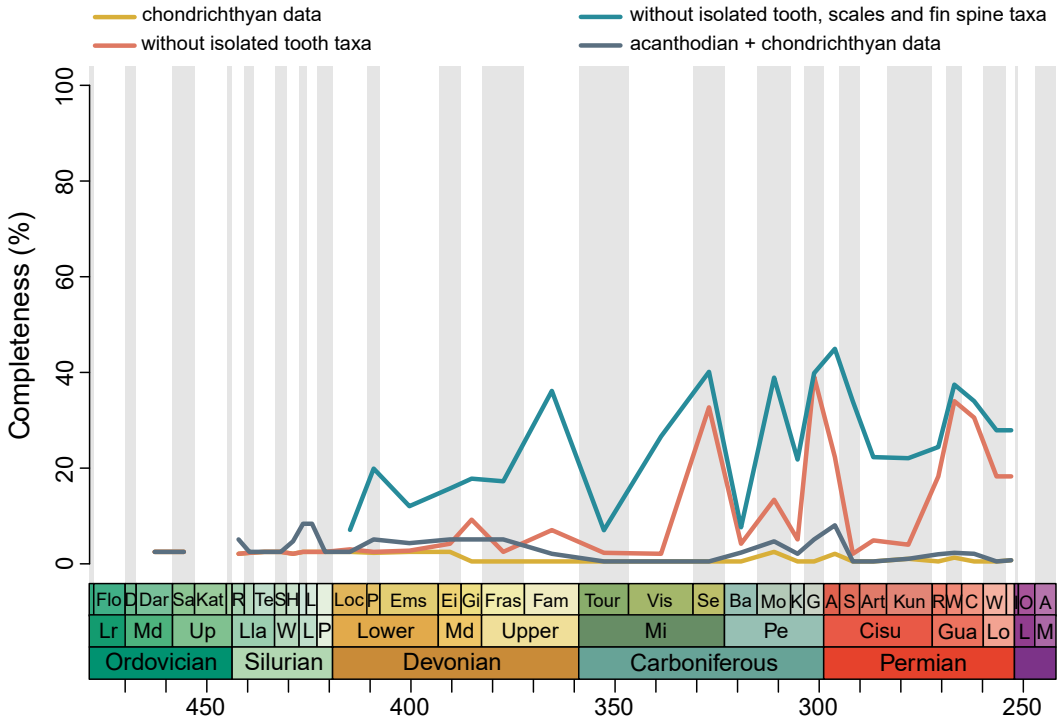


Figure B.1: Changes in median chondrichthyan skeletal completeness through time.

Table B.1: Mann-Whitney-Wilcoxon test results of comparisons of the distribution and median of original SCM2 with SCM2 of the two subsets sub1 (subset without isolated tooth-based taxa) and sub2 (subset without isolated scale, isolated fin spine and isolated tooth-based taxa) as well as a dataset combining acanthodian and chondrichthyan SCM2 values (SCM2 all). Statistically significant results indicated in bold.

Dataset 1	Dataset 2	Test statistic (W)	p-value	Adjusted p-value
SCM2	SCM2 sub1	43950.5	**1.85E-67**	**1.11E-66**
SCM2	SCM2 sub2	12489	**8.13E-66**	**2.44E-65**
SCM2	SCM2 all	427352.5	**1.98E-29**	**2.98E-29**
SCM2 sub1	SCM2 sub2	12408	**9.08E-15**	**9.08E-15**
SCM2 sub1	SCM2 all	280375	**7.92E-23**	**9.50E-23**
SCM2 sub2	SCM2 all	180923.5	**9.35E-48**	**1.87E-47**

Table B.2: Results of pairwise comparisons for completeness metric trends (original SCM2 and subsets) in different time series using GLS. sub1 (subset without isolated tooth-based taxa), sub2 (subset without isolated scale, isolated fin spine and isolated tooth-based taxa) and SCM2 all (dataset combining acanthodian and chondrichthyan SCM2 values). Statistically significant results indicated in bold.

Comparison	Slope	t-value	p-value	R^2
total SCM2 ~ SCM2 all	0.815541	6.105839	**0.0000**	0.803484
total SCM2 ~ SCM2 sub1	1.086923	15.442640	**0.0000**	0.917311
total SCM2 ~ SCM2 sub2	1.097887	4.286459	**0.0003**	0.889286
SCM2 all ~ SCM2 sub1	0.571020	4.208741	**0.0002**	0.628679
SCM2 all ~ SCM2 sub2	0.356395	1.268221	0.2180	0.742022
SCM2 sub2 ~ SCM2 sub1	0.576097	8.237676	**0**	0.805382

Table B.3: Results of model-fitting analyses using GLS testing the best explanations of observed chondrichthyan SCM2. The models with the highest AIC weights are indicated in bold. The sea level coefficient in model 4 is significant and the stage midpoint coefficient in model 9 and 10 are significant with high strength (R^2).

Model	Comparison	R^2	AIC weight
1	SCM2 ~ stage midpoints	0.6642261	0.03659177
2	SCM2 ~ richness	0.4669808	0.00009982
3	SCM2 ~ time bin length	0.4298999	0.00004028
4	SCM2 ~ sea level	0.8005004	**0.17808750**
5	SCM2 ~ richness + time bin length	0.4732881	0.00002896
6	SCM2 ~ richness + stage midpoints	0.6695526	0.01097714
7	SCM2 ~ richness + sea level	0.8097508	0.05324457
8	SCM2 ~ time bin length + sea level	0.8005029	0.03408292
9	SCM2 ~ stage midpoints + sea level	0.8534136	**0.57368121**
10	SCM2 ~ stage midpoints + richness + sea level	0.8534142	**0.08928361**
11	SCM2 ~ time bin length + richness + sea level	0.8146959	0.01059554
12	SCM2 ~ stage midpoints + time bin length + richness + sea level	0.8567458	0.01328666

Table B.4: Results of model-fitting analyses using GLS testing the best explanations of observed raw chondrichthyan taxonomic richness. The three models with the highest AIC weights are indicated in bold, with the time bin length coefficient being significant in all three models.

Model	Comparison	R^2	AIC weight
1	richness ~ stage midpoints	0.7045436	0.00005568
2	richness ~ SCM2	0.7661208	0.00070872
3	richness ~ time bin length	0.7469158	0.00064400
4	richness ~ sea level	0.9032088	0.05201797
5	richness ~ stage midpoints + SCM2	0.7765465	0.00034701
6	richness ~ stage midpoints + time bin length	0.7695139	0.00070661
7	richness ~ stage midpoints + sea level	0.9088806	0.02052612
8	richness ~ time bin length + SCM2	0.8230967	0.01091840
9	richness ~ time bin length + sea level	0.9210933	**0.10378214**
10	richness ~ sea level + SCM2	0.9264784	0.06775020
11	richness ~ stage midpoints + time bin length + SCM2	0.8383576	0.00897271
12	richness ~ stage midpoints + SCM2 + sea level	0.9303939	0.01907175
13	richness ~ time bin length + SCM2 + sea level	0.9490074	**0.53293171**
14	richness ~ time bin length + stage midpoints + sea level	0.9272779	0.04255886
15	richness ~ stage midpoints + SCM2 + time bin length + sea level	0.9525716	**0.13900813**

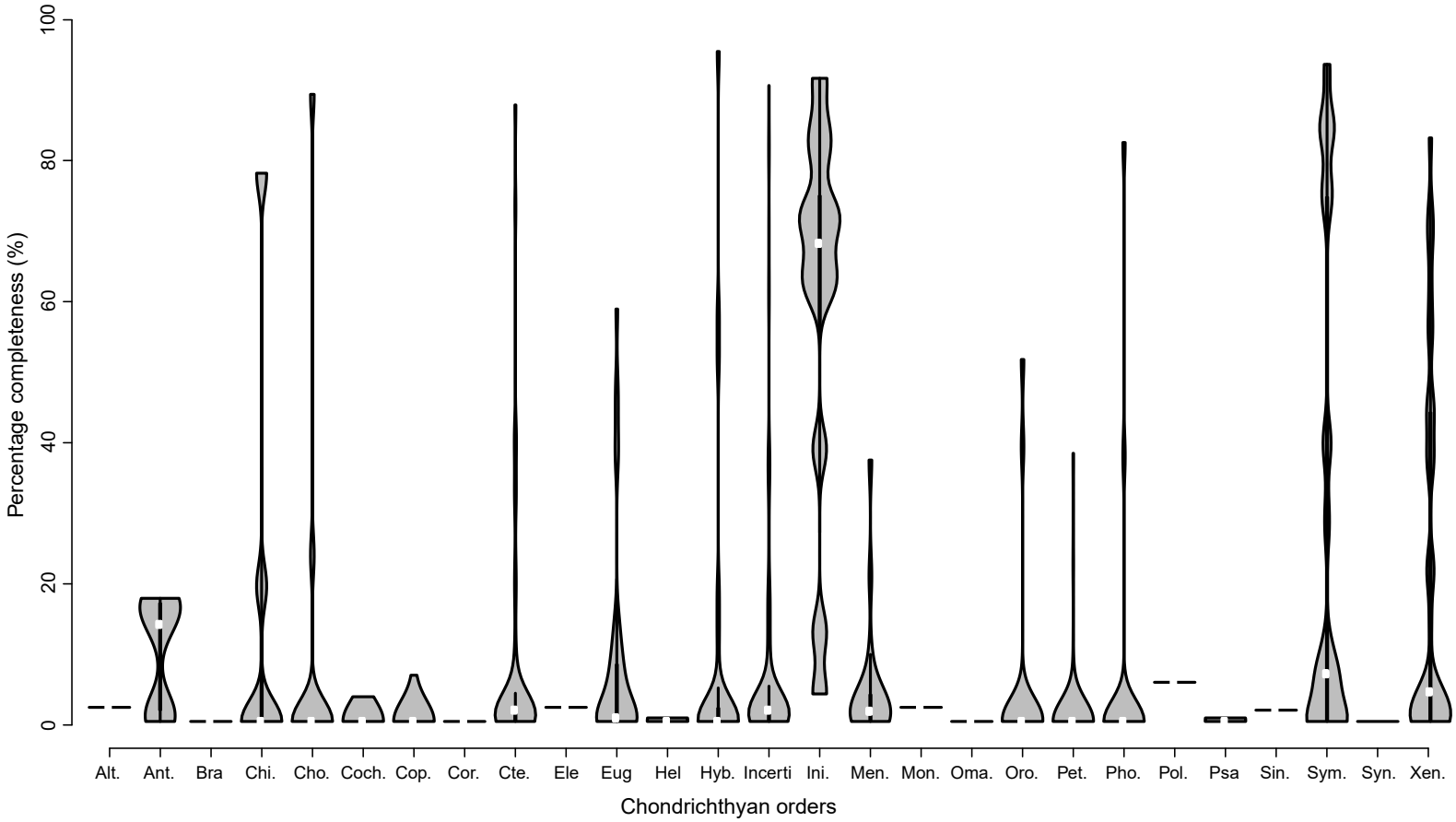


Figure B.2: Distribution of chondrichthyan SCM2 between the different subgroups. Alt, Altholepidiformes. Ant, Antarctilamniformes. Bra, Bransonelliformes. Chi, Chimaeriformes. Cho, Chondrenchelyiformes. Coch, Cochliodontiformes. Cop, Copodontiformes. Cor, Coronodontida. Cte, Ctenacanthiformes. Ele, Elegestolepidida. Eug, Eugeneodontiformes. Hel, Helodontiformes. Hyb, Hybodontiformes. Incerti, Incerti ordinis. Ini, Iniopterygia. Men, Menaspiformes. Mon, Mongolepidida. Oma, Omalodontiformes. Oro, Orodontiformes. Pet, Petalodontiformes. Pho, Phoebodontiformes. Pol, Polymerolepidiformes. Psa, Psammodontiformes. Sin, Sinacanthida. Sym, Symmoriiformes. Syn, Synechodontiformes. Xen, Xenacanthiformes.

Table B.5: Mann-Whitney-Wilcoxon test results of comparisons of the distribution and median SCM2 values of different chondrichthyan subgroups (order level). Statistically significant results indicated in bold.

Dataset 1	Dataset 2	Test statistic (W)	p-value	Adjusted p-value
Altholepidiformes	Antarctilamniformes	2	1	1
Altholepidiformes	Bransonelliformes	6	**0.041227**	0.094607
Altholepidiformes	Chimaeriformes	4	0.782672	0.872811
Altholepidiformes	Chondrenchelyiformes	11	0.167366	0.285968
Altholepidiformes	Cochliodontiformes	130	**2.27E-08**	**2.65E-07**
Altholepidiformes	Copodontiformes	17	**0.010214**	**0.028555**
Altholepidiformes	Coronodontida	1	1	1
Altholepidiformes	Ctenacanthiformes	40	0.362764	0.508895
Altholepidiformes	Elegestolepidida	2.5	NA	NA
Altholepidiformes	Eugeneodontiformes	22	0.857795	0.932999
Altholepidiformes	Helodontiformes	62	**3.35E-08**	**3.60E-07**
Altholepidiformes	Hybodontiformes	19.5	0.358535	0.504746
Altholepidiformes	Incerti sedis	99.5	0.530211	0.668234
Altholepidiformes	Iniopterygia	0	0.153846	0.267881
Altholepidiformes	Menaspiformes	11	0.930987	0.988241
Altholepidiformes	Mongolepidida	5.5	NA	NA
Altholepidiformes	Omalodontiformes	5	0.073638	0.147648
Altholepidiformes	Orodontiformes	14.5	0.238593	0.375878
Altholepidiformes	Petalodontiformes	125	**0.003166**	**0.011222**
Altholepidiformes	Phoebodontiformes	17	0.050849	0.111531
Altholepidiformes	Polymerolepidiformes	0	1	1
Altholepidiformes	Psammodontiformes	17	**0.004750**	**0.015331**
Altholepidiformes	Sinacanthida	4	0.133614	0.241113
Altholepidiformes	Symmoriiformes	13	0.623033	0.761058
Altholepidiformes	Synechodontiformes	1	1	1
Altholepidiformes	Xenacanthiformes	13	0.642985	0.778239
Antarctilamniformes	Bransonelliformes	27	**0.015024**	**0.040031**
Antarctilamniformes	Chimaeriformes	18	0.632142	0.767463
Antarctilamniformes	Chondrenchelyiformes	49.5	0.052711	0.114979
Antarctilamniformes	Cochliodontiformes	590.5	**5.22E-15**	**1.04E-13**
Antarctilamniformes	Copodontiformes	79.5	**0.000448**	**0.002092**
Antarctilamniformes	Coronodontida	4.5	0.372858	0.517569
Antarctilamniformes	Ctenacanthiformes	170	0.251213	0.392013
Antarctilamniformes	Elegestolepidida	15	0.655836	0.779542
Antarctilamniformes	Eugeneodontiformes	131	0.208526	0.342086
Antarctilamniformes	Helodontiformes	278.5	**1.20E-10**	**1.69E-09**
Antarctilamniformes	Hybodontiformes	93.5	0.086560	0.168452
Antarctilamniformes	Incerti sedis	476.5	0.237282	0.375878
Antarctilamniformes	Iniopterygia	6	**0.009373**	**0.026579**
Antarctilamniformes	Menaspiformes	68.5	0.204501	0.336874
Antarctilamniformes	Mongolepidida	33	0.491012	0.635095
Antarctilamniformes	Omalodontiformes	22.5	**0.025370**	0.064004
Antarctilamniformes	Orodontiformes	69	**0.039444**	0.093211
Antarctilamniformes	Petalodontiformes	577	**5.77E-07**	**5.21E-06**
Antarctilamniformes	Phoebodontiformes	76.5	**0.007744**	**0.022277**
Antarctilamniformes	Polymerolepidiformes	3	1	1
Antarctilamniformes	Psammodontiformes	76	**0.000430**	**0.002034**
Antarctilamniformes	Sinacanthida	14	0.347654	0.493328
Antarctilamniformes	Symmoriiformes	82.5	0.647588	0.778239
Antarctilamniformes	Synechodontiformes	4.5	0.372858	0.517569
Antarctilamniformes	Xenacanthiformes	81	0.664367	0.785008
Bransonelliformes	Chimaeriformes	12	0.175734	0.295621
Bransonelliformes	Chondrenchelyiformes	33	0.365551	0.510999
Bransonelliformes	Cochliodontiformes	387	0.725357	0.832274
Bransonelliformes	Copodontiformes	51	0.630428	0.767463
Bransonelliformes	Coronodontida	3	NA	NA
Bransonelliformes	Ctenacanthiformes	42	**0.002621**	**0.009635**
Bransonelliformes	Elegestolepidida	0	**0.002237**	**0.008704**
Bransonelliformes	Eugeneodontiformes	48	**0.014905**	**0.039981**
Bransonelliformes	Helodontiformes	183	0.795452	0.879650
Bransonelliformes	Hybodontiformes	54	0.135754	0.242767
Bransonelliformes	Incerti sedis	132	**0.002966**	**0.010703**
Bransonelliformes	Iniopterygia	0	**0.000708**	**0.003157**
Bransonelliformes	Menaspiformes	27	**0.027176**	0.067429
Bransonelliformes	Mongolepidida	0	**8.17E-05**	**0.000477**

Bransonelliformes	Omalodontiformes	15	NA	NA
Bransonelliformes	Orodontiformes	42	0.237781	0.375878
Bransonelliformes	Petalodontiformes	372	0.475331	0.621163
Bransonelliformes	Phoebodontiformes	51	0.457170	0.602447
Bransonelliformes	Polymerolepidiformes	0	**0.041227**	0.094607
Bransonelliformes	Psammodontiformes	48	0.620548	0.760363
Bransonelliformes	Sinacanthida	0	**0.004040**	**0.013709**
Bransonelliformes	Symmoriiformes	21	**0.001320**	**0.005574**
Bransonelliformes	Synechodontiformes	3	NA	NA
Bransonelliformes	Xenacanthiformes	36	**0.006659**	**0.020027**
Chimaeriformes	Chondrenchelyiformes	45	0.498860	0.643011
Chimaeriformes	Cochliodontiformes	522	**5.18E-05**	**0.000316**
Chimaeriformes	Copodontiformes	70	0.072237	0.147648
Chimaeriformes	Coronodontida	4	0.755189	0.851570
Chimaeriformes	Ctenacanthiformes	124	0.406461	0.544613
Chimaeriformes	Elegestolepidida	10	0.376659	0.518431
Chimaeriformes	Eugeneodontiformes	105	0.687554	0.802821
Chimaeriformes	Helodontiformes	246	**0.000300**	**0.001469**
Chimaeriformes	Hybodontiformes	84	0.746611	0.851570
Chimaeriformes	Incerti sedis	364	0.475651	0.621163
Chimaeriformes	Iniopterygia	11	**0.021079**	0.054340
Chimaeriformes	Menaspiformes	56	0.819233	0.902081
Chimaeriformes	Mongolepidida	22	0.213028	0.345192
Chimaeriformes	Omalodontiformes	20	0.222994	0.356970
Chimaeriformes	Orodontiformes	62	0.511006	0.652313
Chimaeriformes	Petalodontiformes	513	**0.028682**	0.069858
Chimaeriformes	Phoebodontiformes	69	0.251797	0.392013
Chimaeriformes	Polymerolepidiformes	2	0.782672	0.872811
Chimaeriformes	Psammodontiformes	66	0.082968	0.163872
Chimaeriformes	Sinacanthida	8	0.426030	0.565666
Chimaeriformes	Symmoriiformes	67	0.108244	0.202703
Chimaeriformes	Synechodontiformes	4	0.755189	0.851570
Chimaeriformes	Xenacanthiformes	81	0.288231	0.428569
Chondrenchelyiformes	Cochliodontiformes	973.5	**0.011810**	**0.032560**
Chondrenchelyiformes	Copodontiformes	129.5	0.349182	0.493328
Chondrenchelyiformes	Coronodontida	7.5	0.838729	0.914768
Chondrenchelyiformes	Ctenacanthiformes	175	**0.005481**	**0.017269**
Chondrenchelyiformes	Elegestolepidida	10	**0.012412**	**0.033982**
Chondrenchelyiformes	Eugeneodontiformes	161	**0.035998**	0.085576
Chondrenchelyiformes	Helodontiformes	459.5	**0.020971**	0.054340
Chondrenchelyiformes	Hybodontiformes	147	0.403965	0.544613
Chondrenchelyiformes	Incerti sedis	520	**0.005539**	**0.017316**
Chondrenchelyiformes	Iniopterygia	13	**0.000246**	**0.001266**
Chondrenchelyiformes	Menaspiformes	88.5	0.086054	0.168294
Chondrenchelyiformes	Mongolepidida	22	**0.001595**	**0.006527**
Chondrenchelyiformes	Omalodontiformes	37.5	0.416656	0.555075
Chondrenchelyiformes	Orodontiformes	111	0.749579	0.851570
Chondrenchelyiformes	Petalodontiformes	949	0.327267	0.472454
Chondrenchelyiformes	Phoebodontiformes	129.5	0.713467	0.821004
Chondrenchelyiformes	Polymerolepidiformes	2	0.167366	0.285968
Chondrenchelyiformes	Psammodontiformes	122	0.376677	0.518431
Chondrenchelyiformes	Sinacanthida	8	**0.019375**	0.051280
Chondrenchelyiformes	Symmoriiformes	96.5	**0.000900**	**0.003968**
Chondrenchelyiformes	Synechodontiformes	7.5	0.838729	0.914768
Chondrenchelyiformes	Xenacanthiformes	127	**0.008512**	**0.024312**
Cochliodontiformes	Copodontiformes	1147.5	0.407159	0.544613
Cochliodontiformes	Coronodontida	67.5	0.919339	0.981123
Cochliodontiformes	Ctenacanthiformes	997.5	**8.53E-25**	**6.77E-23**
Cochliodontiformes	Elegestolepidida	10	**1.79E-19**	**7.90E-18**
Cochliodontiformes	Eugeneodontiformes	1094	**2.82E-18**	**1.02E-16**
Cochliodontiformes	Helodontiformes	4120	0.759334	0.851570
Cochliodontiformes	Hybodontiformes	1219	**1.31E-07**	**1.27E-06**
Cochliodontiformes	Incerti sedis	3113	**3.81E-29**	**1.51E-26**
Cochliodontiformes	Iniopterygia	0	**3.80E-27**	**5.03E-25**
Cochliodontiformes	Menaspiformes	613.5	**1.70E-14**	**3.22E-13**
Cochliodontiformes	Mongolepidida	22	**4.44E-25**	**4.41E-23**
Cochliodontiformes	Omalodontiformes	337.5	0.751287	0.851570
Cochliodontiformes	Orodontiformes	949	**0.000161**	**0.000867**
Cochliodontiformes	Petalodontiformes	8373	**0.027688**	0.067852
Cochliodontiformes	Phoebodontiformes	1147.5	0.055039	0.118110

Cochliodontiformes	Polymerolepidiformes	0	**8.11E-09**	**9.76E-08**
Cochliodontiformes	Psammodontiformes	1082.5	0.405591	0.544613
Cochliodontiformes	Sinacanthida	8	**8.30E-18**	**2.75E-16**
Cochliodontiformes	Symmoriiformes	490.5	**3.43E-27**	**5.03E-25**
Cochliodontiformes	Synechodontiformes	67.5	0.919339	0.981123
Cochliodontiformes	Xenacanthiformes	814	**1.23E-21**	**6.95E-20**
Copodontiformes	Coronodontida	9.5	1	1
Copodontiformes	Ctenacanthiformes	162	**1.43E-05**	**9.81E-05**
Copodontiformes	Elegestolepidida	5	**0.000122**	**0.000680**
Copodontiformes	Eugeneodontiformes	162	**0.000312**	**0.001499**
Copodontiformes	Helodontiformes	580.5	0.348650	0.493328
Copodontiformes	Hybodontiformes	174	**0.043905**	0.099601
Copodontiformes	Incerti sedis	494	**8.19E-06**	**5.81E-05**
Copodontiformes	Iniopterygia	1	**6.25E-07**	**5.51E-06**
Copodontiformes	Menaspiformes	93.5	**0.002258**	**0.008704**
Copodontiformes	Mongolepidida	11	**5.19E-06**	**3.96E-05**
Copodontiformes	Omalodontiformes	47.5	0.673290	0.793164
Copodontiformes	Orodontiformes	135	0.163262	0.281804
Copodontiformes	Petalodontiformes	1183	0.701993	0.811271
Copodontiformes	Phoebodontiformes	161.5	0.563513	0.705724
Copodontiformes	Polymerolepidiformes	1	**0.010214**	**0.028555**
Copodontiformes	Psammodontiformes	153	1	1
Copodontiformes	Sinacanthida	4	**0.000242**	**0.001263**
Copodontiformes	Symmoriiformes	78.5	**1.49E-06**	**1.26E-05**
Copodontiformes	Synechodontiformes	9.5	1	1
Copodontiformes	Xenacanthiformes	122	**4.35E-05**	**0.000270**
Coronodontida	Ctenacanthiformes	7	0.211297	0.343791
Coronodontida	Elegestolepidida	0	0.073638	0.147648
Coronodontida	Eugeneodontiformes	8	0.321056	0.465179
Coronodontida	Helodontiformes	30.5	1	1
Coronodontida	Hybodontiformes	9	0.577870	0.719167
Coronodontida	Incerti sedis	22	0.222457	0.356970
Coronodontida	Iniopterygia	0	0.153846	0.267881
Coronodontida	Menaspiformes	4.5	0.378703	0.518431
Coronodontida	Mongolepidida	0	**0.002569**	**0.009531**
Coronodontida	Omalodontiformes	2.5	NA	NA
Coronodontida	Orodontiformes	7	0.701019	0.811271
Coronodontida	Petalodontiformes	62	0.787649	0.873454
Coronodontida	Phoebodontiformes	8.5	0.867814	0.934803
Coronodontida	Polymerolepidiformes	0	1	1
Coronodontida	Psammodontiformes	8	1	1
Coronodontida	Sinacanthida	0	0.133614	0.241113
Coronodontida	Symmoriiformes	3.5	0.179422	0.298795
Coronodontida	Synechodontiformes	0.5	NA	NA
Coronodontida	Xenacanthiformes	6	0.263820	0.402832
Ctenacanthiformes	Elegestolepidida	60	**0.044428**	0.100214
Ctenacanthiformes	Eugeneodontiformes	1052	0.758380	0.851570
Ctenacanthiformes	Helodontiformes	2782.5	**2.94E-15**	**6.15E-14**
Ctenacanthiformes	Hybodontiformes	872	**0.030364**	0.073059
Ctenacanthiformes	Incerti sedis	3506.5	0.403763	0.544613
Ctenacanthiformes	Iniopterygia	37	**1.56E-06**	**1.28E-05**
Ctenacanthiformes	Menaspiformes	534	0.861806	0.934800
Ctenacanthiformes	Mongolepidida	132	**0.004544**	**0.015034**
Ctenacanthiformes	Omalodontiformes	225	**0.005700**	**0.017548**
Ctenacanthiformes	Orodontiformes	660	**0.007240**	**0.021134**
Ctenacanthiformes	Petalodontiformes	5696.5	**1.46E-17**	**4.47E-16**
Ctenacanthiformes	Phoebodontiformes	770	**0.000162**	**0.000867**
Ctenacanthiformes	Polymerolepidiformes	10	0.296050	0.436921
Ctenacanthiformes	Psammodontiformes	757.5	**3.73E-06**	**2.90E-05**
Ctenacanthiformes	Sinacanthida	84	0.518218	0.655199
Ctenacanthiformes	Symmoriiformes	660	**0.006835**	**0.020402**
Ctenacanthiformes	Synechodontiformes	45	0.211297	0.343791
Ctenacanthiformes	Xenacanthiformes	696.5	**0.024707**	0.062877
Elegestolepidida	Eugeneodontiformes	110	0.648859	0.778239
Elegestolepidida	Helodontiformes	310	**9.47E-14**	**1.63E-12**
Elegestolepidida	Hybodontiformes	97.5	0.054298	0.117154
Elegestolepidida	Incerti sedis	497.5	0.159929	0.277256
Elegestolepidida	Iniopterygia	0	**0.001642**	**0.006583**
Elegestolepidida	Menaspiformes	55	0.752322	0.851570
Elegestolepidida	Mongolepidida	27.5	NA	NA

Elegestolepididae	Omalodontiformes	25	**0.003977**	**0.013610**
Elegestolepididae	Orodontiformes	72.5	**0.020798**	0.054320
Elegestolepididae	Petalodontiformes	625	**5.41E-09**	**6.93E-08**
Elegestolepididae	Phoebodontiformes	85	**0.000979**	**0.004224**
Elegestolepididae	Polymerolepidiformes	0	0.073638	0.147648
Elegestolepididae	Psammodontiformes	85	**2.32E-05**	**0.000151**
Elegestolepididae	Sinacanthida	20	**0.007210**	**0.021134**
Elegestolepididae	Symmoriiformes	65	0.261268	0.402759
Elegestolepididae	Synechodontiformes	5	0.073638	0.147648
Elegestolepididae	Xenacanthiformes	65	0.288078	0.428569
Eugeneodontiformes	Helodontiformes	1912	**5.14E-11**	**7.55E-10**
Eugeneodontiformes	Hybodontiformes	620	0.103615	0.194953
Eugeneodontiformes	Incerti sedis	2786	0.835004	0.914768
Eugeneodontiformes	Iniopterygia	28	**3.54E-06**	**2.81E-05**
Eugeneodontiformes	Menaspiformes	435	0.458284	0.602447
Eugeneodontiformes	Mongolepidida	187	0.517852	0.655199
Eugeneodontiformes	Omalodontiformes	155	**0.025507**	0.064004
Eugeneodontiformes	Orodontiformes	473	**0.023992**	0.061451
Eugeneodontiformes	Petalodontiformes	3960.5	**4.47E-12**	**6.83E-11**
Eugeneodontiformes	Phoebodontiformes	531	**0.003332**	**0.011604**
Eugeneodontiformes	Polymerolepidiformes	14	0.654187	0.779542
Eugeneodontiformes	Psammodontiformes	517	**0.000255**	**0.001284**
Eugeneodontiformes	Sinacanthida	68	0.683130	0.802374
Eugeneodontiformes	Symmoriiformes	481	**0.007337**	**0.021260**
Eugeneodontiformes	Synechodontiformes	31	0.321056	0.465179
Eugeneodontiformes	Xenacanthiformes	552	0.071517	0.147648
Helodontiformes	Hybodontiformes	567	**3.36E-05**	**0.000215**
Helodontiformes	Incerti sedis	1386	**1.82E-17**	**5.17E-16**
Helodontiformes	Iniopterygia	0	**2.14E-16**	**5.67E-15**
Helodontiformes	Menaspiformes	283.5	**3.56E-09**	**4.72E-08**
Helodontiformes	Mongolepidida	0	**3.13E-16**	**7.76E-15**
Helodontiformes	Omalodontiformes	157.5	0.820280	0.902081
Helodontiformes	Orodontiformes	441	**0.001378**	**0.005760**
Helodontiformes	Petalodontiformes	3906.5	0.071137	0.147648
Helodontiformes	Phoebodontiformes	535.5	0.071009	0.147648
Helodontiformes	Polymerolepidiformes	0	**3.35E-08**	**3.60E-07**
Helodontiformes	Psammodontiformes	504.5	0.334776	0.479806
Helodontiformes	Sinacanthida	0	**4.59E-13**	**7.58E-12**
Helodontiformes	Symmoriiformes	226.5	**3.40E-16**	**7.94E-15**
Helodontiformes	Synechodontiformes	31.5	1	1
Helodontiformes	Xenacanthiformes	378	**6.90E-13**	**1.10E-11**
Hybodontiformes	Incerti sedis	1368	**0.019543**	0.051382
Hybodontiformes	Iniopterygia	22	**9.25E-06**	**6.44E-05**
Hybodontiformes	Menaspiformes	215	0.269290	0.409610
Hybodontiformes	Mongolepidida	71.5	**0.010554**	**0.029302**
Hybodontiformes	Omalodontiformes	85	0.173431	0.292988
Hybodontiformes	Orodontiformes	256.5	0.503233	0.646457
Hybodontiformes	Petalodontiformes	2159	**0.000938**	**0.004093**
Hybodontiformes	Phoebodontiformes	293	0.150802	0.266082
Hybodontiformes	Polymerolepidiformes	5	0.251195	0.392013
Hybodontiformes	Psammodontiformes	280	0.041031	0.094607
Hybodontiformes	Sinacanthida	30	0.137486	0.244762
Hybodontiformes	Symmoriiformes	238	**0.000313**	**0.001499**
Hybodontiformes	Synechodontiformes	17	0.577870	0.719167
Hybodontiformes	Xenacanthiformes	293.5	**0.005702**	**0.017548**
Incerti sedis	Iniopterygia	80	**1.03E-07**	**1.02E-06**
Incerti sedis	Menaspiformes	1493	0.868873	0.934803
Incerti sedis	Mongolepidida	511.5	**0.040554**	0.094607
Incerti sedis	Omalodontiformes	620	**0.006550**	**0.019851**
Incerti sedis	Orodontiformes	1827	**0.005451**	**0.017269**
Incerti sedis	Petalodontiformes	15667	**5.05E-22**	**3.34E-20**
Incerti sedis	Phoebodontiformes	2118	**0.000115**	**0.000655**
Incerti sedis	Polymerolepidiformes	26	0.261742	0.402759
Incerti sedis	Psammodontiformes	0	1	1
Incerti sedis	Sinacanthida	306	0.871690	0.935300
Incerti sedis	Symmoriiformes	1765.5	**0.000462**	**0.002106**
Incerti sedis	Synechodontiformes	124	0.222457	0.356970
Incerti sedis	Xenacanthiformes	1899	**0.004487**	**0.014968**
Iniopterygia	Menaspiformes	235	**6.33E-06**	**4.65E-05**
Iniopterygia	Mongolepidida	132	**1.95E-05**	**0.000129**

Iniopterygia	Omalodontiformes	60	**0.001642**	**0.006583**
Iniopterygia	Orodontiformes	210	**5.83E-06**	**4.37E-05**
Iniopterygia	Petalodontiformes	1608	**4.53E-19**	**1.80E-17**
Iniopterygia	Phoebodontiformes	216	**6.69E-06**	**4.83E-05**
Iniopterygia	Polymerolepidiformes	11	0.307692	0.450752
Iniopterygia	Psammodontiformes	204	**8.40E-07**	**7.25E-06**
Iniopterygia	Sinacanthida	48	**0.004092**	**0.013767**
Iniopterygia	Symmoriiformes	324	**0.029604**	0.071663
Iniopterygia	Synechodontiformes	12	0.153846	0.267881
Iniopterygia	Xenacanthiformes	377	**0.000295**	**0.001465**
Menaspiformes	Mongolepidida	99	0.652604	0.779542
Menaspiformes	Omalodontiformes	77.5	**0.042462**	0.096881
Menaspiformes	Orodontiformes	235	0.070556	0.147648
Menaspiformes	Petalodontiformes	1966	**6.16E-08**	**6.43E-07**
Menaspiformes	Phoebodontiformes	263.5	**0.014357**	**0.038774**
Menaspiformes	Polymerolepidiformes	3	0.260236	0.402759
Menaspiformes	Psammodontiformes	259	**0.001161**	**0.004956**
Menaspiformes	Sinacanthida	40	1	1
Menaspiformes	Symmoriiformes	201.5	**0.003214**	**0.011291**
Menaspiformes	Synechodontiformes	15.5	0.378703	0.518431
Menaspiformes	Xenacanthiformes	244	**0.031241**	0.074714
Mongolepidida	Omalodontiformes	55	**0.000143**	**0.000790**
Mongolepidida	Orodontiformes	159.5	**0.002857**	**0.010407**
Mongolepidida	Petalodontiformes	1375	**4.96E-14**	**8.96E-13**
Mongolepidida	Phoebodontiformes	187	**5.75E-05**	**0.000341**
Mongolepidida	Polymerolepidiformes	0	**0.002569**	**0.009531**
Mongolepidida	Psammodontiformes	187	**4.68E-07**	**4.32E-06**
Mongolepidida	Sinacanthida	44	**0.000256**	**0.001284**
Mongolepidida	Symmoriiformes	143	0.113404	0.211367
Mongolepidida	Synechodontiformes	11	**0.002569**	**0.009531**
Mongolepidida	Xenacanthiformes	143	0.135477	0.242767
Omalodontiformes	Orodontiformes	35	0.283973	0.425424
Omalodontiformes	Petalodontiformes	310	0.515821	0.655199
Omalodontiformes	Phoebodontiformes	42.5	0.504790	0.646457
Omalodontiformes	Polymerolepidiformes	0	0.073638	0.147648
Omalodontiformes	Psammodontiformes	40	0.664389	0.785008
Omalodontiformes	Sinacanthida	0	**0.007210**	**0.021134**
Omalodontiformes	Symmoriiformes	17.5	**0.003116**	**0.011145**
Omalodontiformes	Synechodontiformes	2.5	NA	NA
Omalodontiformes	Xenacanthiformes	30	**0.012670**	**0.034453**
Orodontiformes	Petalodontiformes	1388	0.058337	0.124514
Orodontiformes	Phoebodontiformes	189	0.407431	0.544613
Orodontiformes	Polymerolepidiformes	2	0.125783	0.232259
Orodontiformes	Psammodontiformes	180	0.150714	0.266082
Orodontiformes	Sinacanthida	16	0.053236	0.115489
Orodontiformes	Symmoriiformes	127	**0.000109**	**0.000625**
Orodontiformes	Synechodontiformes	11	0.701019	0.811271
Orodontiformes	Xenacanthiformes	167.5	**0.001748**	**0.006938**
Petalodontiformes	Phoebodontiformes	1242	0.648550	0.778239
Petalodontiformes	Polymerolepidiformes	6	**0.001587**	**0.006527**
Petalodontiformes	Psammodontiformes	1178.5	0.702966	0.811271
Petalodontiformes	Sinacanthida	40	7.93e-08	8.07e-07
Petalodontiformes	Symmoriiformes	638	**5.94E-21**	**2.95E-19**
Petalodontiformes	Synechodontiformes	73	0.787649	0.873454
Petalodontiformes	Xenacanthiformes	964.5	**9.65E-16**	**2.13E-14**
Phoebodontiformes	Polymerolepidiformes	2	0.050849	0.111531
Phoebodontiformes	Psammodontiformes	170	0.596981	0.740629
Phoebodontiformes	Sinacanthida	8	**0.001870**	**0.007351**
Phoebodontiformes	Symmoriiformes	114.5	**1.47E-05**	**9.89E-05**
Phoebodontiformes	Synechodontiformes	10.5	0.867814	0.934803
Phoebodontiformes	Xenacanthiformes	163	**0.000454**	**0.002097**
Polymerolepidiformes	Psammodontiformes	17	**0.004750**	**0.015331**
Polymerolepidiformes	Sinacanthida	4	0.133614	0.241113
Polymerolepidiformes	Symmoriiformes	14	0.687549	0.802821
Polymerolepidiformes	Synechodontiformes	1	1	1
Polymerolepidiformes	Xenacanthiformes	20	0.926137	0.985728
Psammodontiformes	Sinacanthida	0	**5.38E-05**	**0.000324**
Psammodontiformes	Symmoriiformes	69	**1.58E-06**	**1.28E-05**
Psammodontiformes	Synechodontiformes	9	1	1
Psammodontiformes	Xenacanthiformes	108	**3.53E-05**	**0.000222**

Sinacanthida	Symmoriiformes	52	0.311502	0.454655
Sinacanthida	Synechodontiformes	4	0.133614	0.241113
Sinacanthida	Xenacanthiformes	50	0.295080	0.436921
Symmoriiformes	Synechodontiformes	34.5	0.179422	0.298795
Symmoriiformes	Xenacanthiformes	823	0.201462	0.333252
Synechodontiformes	Xenacanthiformes	6	0.263820	0.402832

Table B.6: Mann-Whitney-Wilcoxon test results of the comparisons of chondrichthyan SCM2 value distribution and median in comparison to other vertebrate groups. Statistically significant results indicated in bold.

Dataset 1	Dataset 2	Test statistic (W)	p-value	Adjusted p-values
Chondrichthyes	Acanthodii	44112.5	**8.20E-73**	**2.19E-72**
Chondrichthyes	Chiroptera	140186	**9.42E-23**	**9.42E-23**
Chondrichthyes	Plesiosauria	7440	**3.44E-58**	**5.51E-58**
Chondrichthyes	Ichthyosauria	4898	**1.70E-58**	**3.40E-58**
Chondrichthyes	Sauropodomorpha	31725	**6.96E-94**	**5.57E-93**
Chondrichthyes	Parareptilia	6697	**4.92E-37**	**5.62E-37**
Chondrichthyes	Pelycosauria	11248.5	**2.12E-37**	**2.83E-37**
Chondrichthyes	Theropoda	70186	**8.09E-84**	**3.24E-83**

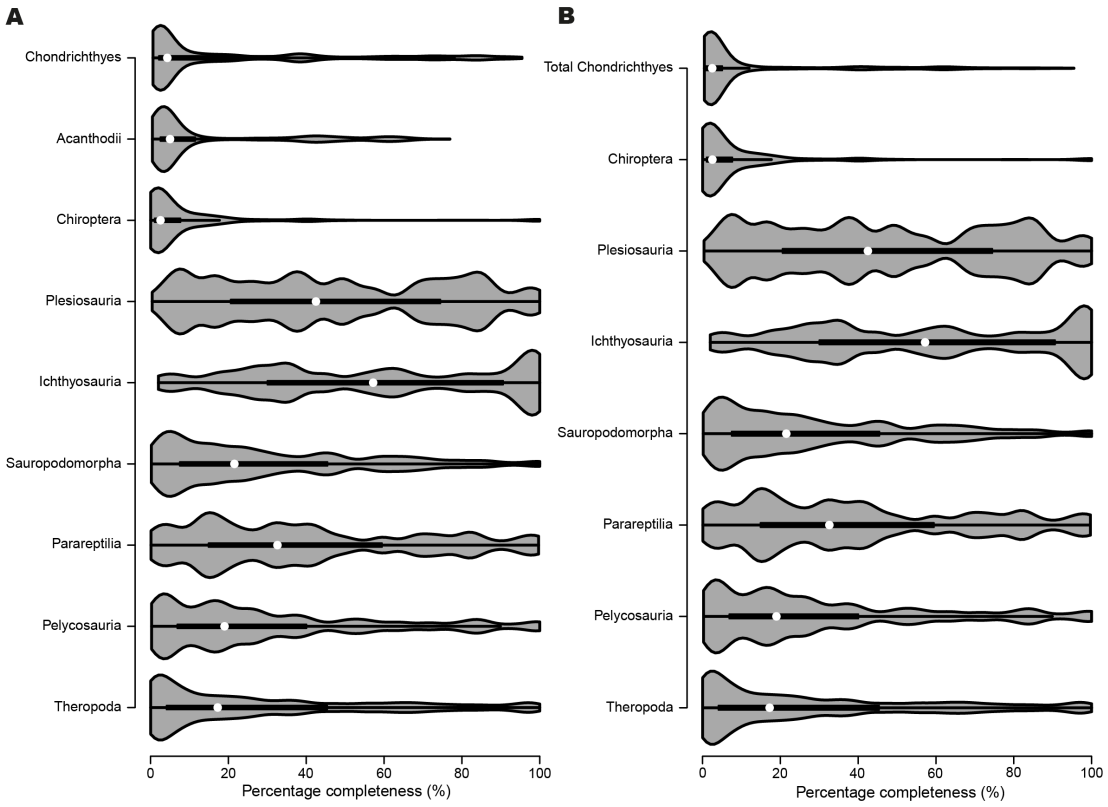


Figure B.3: Distribution of chondrichthyan SCM2 values compared to other vertebrate groups. A, subset without isolated tooth-based taxa. B, joint acanthodian and chondrichthyan dataset for a total chondrichthyan dataset. Comparative values from acanthodians (Schnetz *et al.* 2021), bats (Brown *et al.* 2019), plesiosaurs (Tutin & Butler 2017), ichthyosaurs (Cleary *et al.* 2015), sauropodomorphs (Mannion & Upchurch 2010; Cashmore *et al.* 2020), parareptiles (Verrière *et al.* 2016), pelycosaurs (Brocklehurst & Fröbisch 2014) and theropods (Cashmore & Butler 2019).

Table B.7: Mann-Whitney-Wilcoxon test results of the comparisons of the distribution and median of SCM2 values of the chondrichthyan subset without isolated tooth-based taxa in comparison to other vertebrate groups. Statistically significant results indicated in bold.

Dataset 1	Dataset 2	Test statistic (W)	p-value	Adjusted p-values
Chondrichthyes	Acanthodii	43147.5	0.250428	0.250428
Chondrichthyes	Chiroptera	94941	**1.10E-13**	**2.92E-13**
Chondrichthyes	Plesiosauria	6887	**1.65E-20**	**6.58E-20**
Chondrichthyes	Ichthyosauria	4887	**2.11E-24**	**1.69E-23**
Chondrichthyes	Sauropodomorpha	29888	**5.15E-13**	**1.03E-12**
Chondrichthyes	Parareptilia	5866	**1.27E-10**	**2.04E-10**
Chondrichthyes	Pelycosauria	9577.5	**1.78E-06**	**2.38E-06**
Chondrichthyes	Theropoda	53570	**2.95E-06**	**3.37E-06**

Table B.8: Mann-Whitney-Wilcoxon test results of the comparisons of the distribution and median of SCM2 values of the chondrichthyan subset without isolated tooth, fin spine and scale-based taxa in comparison to other vertebrate groups. Statistically significant results indicated in bold.

Dataset 1	Dataset 2	Test statistic (W)	p-value	Adjusted p-values
Chondrichthyes	Acanthodii	36570.5	**5.72E-23**	**2.29E-22**
Chondrichthyes	Chiroptera	63587	**4.50E-40**	**3.60E-39**
Chondrichthyes	Plesiosauria	6633.5	**0.001078**	**0.001725**
Chondrichthyes	Ichthyosauria	4687	**9.34E-08**	**2.49E-07**
Chondrichthyes	Sauropodomorpha	26164.5	**0.034218**	**0.045624**
Chondrichthyes	Parareptilia	5301	0.312202	0.312202
Chondrichthyes	Pelycosauria	8273.5	0.075806	0.086635
Chondrichthyes	Theropoda	41507	**0.000215**	**0.000431**

Table B.9: Mann-Whitney-Wilcoxon test results of the comparisons of the distribution and median of total chondrichthyan SCM2 values (combined with the acanthodian SCM2 values) in comparison to other vertebrate groups. Statistically significant results indicated in bold.

Dataset 1	Dataset 2	Test statistic (W)	p-value	Adjusted p-values
Total Chondrichthyes	Chiroptera	324950	0.086243	0.086243
Total Chondrichthyes	Plesiosauria	17197.5	**1.83E-46**	**3.20E-46**
Total Chondrichthyes	Ichthyosauria	11890	**2.53E-47**	**5.91E-47**
Total Chondrichthyes	Sauropodomorpha	80327.5	**9.63E-69**	**6.74E-68**
Total Chondrichthyes	Parareptilia	15716.5	**1.67E-26**	**2.34E-26**
Total Chondrichthyes	Pelycosauria	28185.5	**1.24E-22**	**1.45E-22**
Total Chondrichthyes	Theropoda	164827.5	**1.28E-55**	**4.49E-55**

Table B.10: Mann-Whitney-Wilcoxon test results of comparisons of the distribution and median of chondrichthyan SCM2 values between continents. Statistically significant results indicated in bold.

Dataset 1	Dataset 2	Test statistic (W)	p-value	Adjusted p-values
Europe	North America	70729	0.906516	0.940665
Europe	South America	1748	0.219755	0.784113
Europe	Africa	2527.5	0.583179	0.784113
Europe	Asia	12600	0.592644	0.784113
Europe	Australia and Oceania	768	0.472095	0.784113
Europe	Antarctica	862.5	0.518912	0.784113
North America	South America	2713.5	0.188338	0.784113
North America	Africa	4004	0.630965	0.784113
North America	Asia	19797.5	0.551117	0.784113
North America	Australia and Oceania	1225.5	0.511226	0.784113
North America	Antarctica	1349	0.521724	0.784113
South America	Africa	133	0.793865	0.877430
South America	Asia	665.5	0.249617	0.784113
South America	Australia and Oceania	37	0.701834	0.818806
South America	Antarctica	48	0.223862	0.784113
Africa	Asia	824	0.321923	0.784113
Africa	Australia and Oceania	52.5	0.940665	0.940665
Africa	Antarctica	53	0.510992	0.784113
Asia	Australia and Oceania	187.5	0.287983	0.784113
Asia	Antarctica	225	0.634758	0.784113
Australia and Oceania	Antarctica	18.5	0.524565	0.784113

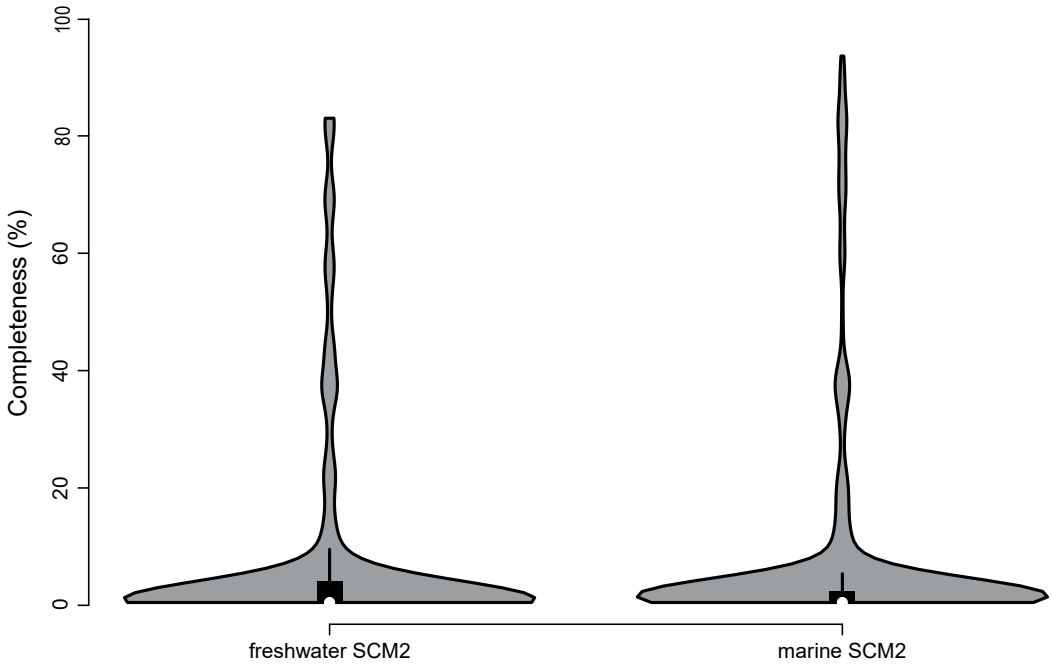


Figure B.4: Distribution of chondrichthyan SCM2 and STCM2 between freshwater and marine deposits.

Table B.11: Results of pairwise comparisons of chondrichthyan SCM2 values without tooth based taxa for sea level trends in different time series using GLS. Statistically significant results indicated in bold.

Comparison	Slope	t-value	p-value	R^2
total SCM2 ~ sea level	-1.926799	-6.159501	**0**	0.9527183
marine SCM2 ~ sea level	-2.073294	-5.985975	**0**	0.9468177
freshwater SCM2 ~ sea level	-0.527898	-2.100665	0.0575	0.790235

Table B.12: Results of pairwise comparisons of both acanthodian and chondrichthyan SCM2 values for sea level trends in different time series using GLS. Statistically significant results indicated in bold.

Comparison	Slope	t-value	p-value	R^2
total SCM2 ~ sea level	-0.597977	-1.516054	0.1452	0.711887
marine SCM2 ~ sea level	-0.903890	-2.044982	0.0542	0.7161166
freshwater SCM2 ~ sea level	0.8807290	2.7697905	0.0137	0.9288316

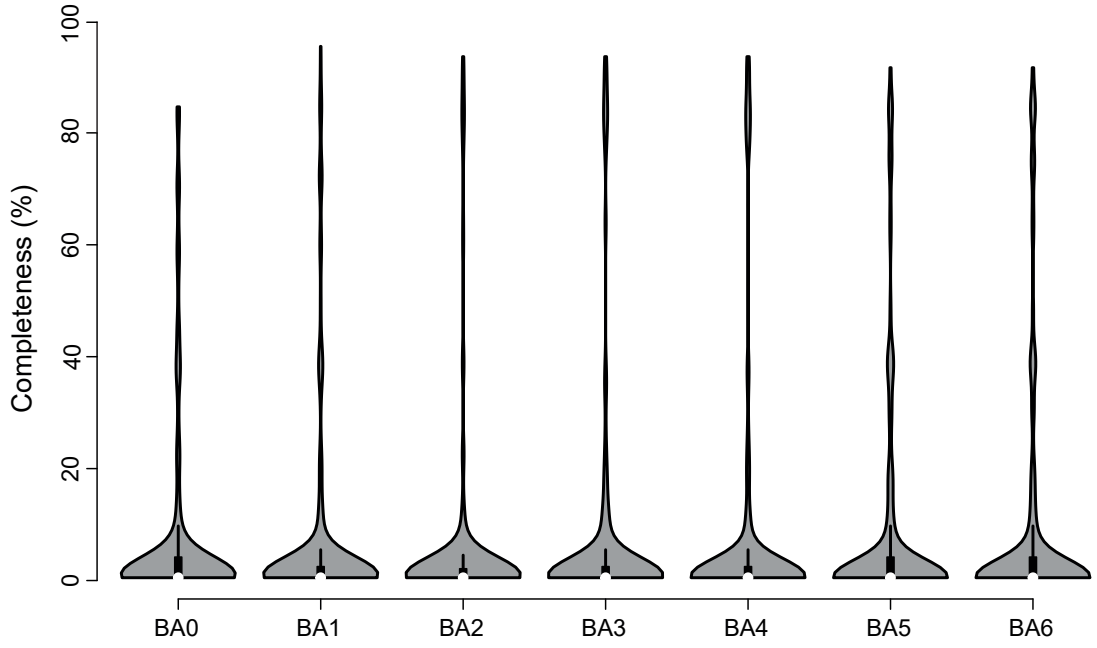


Figure B.5: Distribution of chondrichthyan skeletal completeness between the different Benthic Assemblage (BA) zones.

APPENDIX C

PATTERNS OF CHONDRICHTHYAN DIVERSITY DURING THE PALAEOZOIC

C.1 Figures and tables

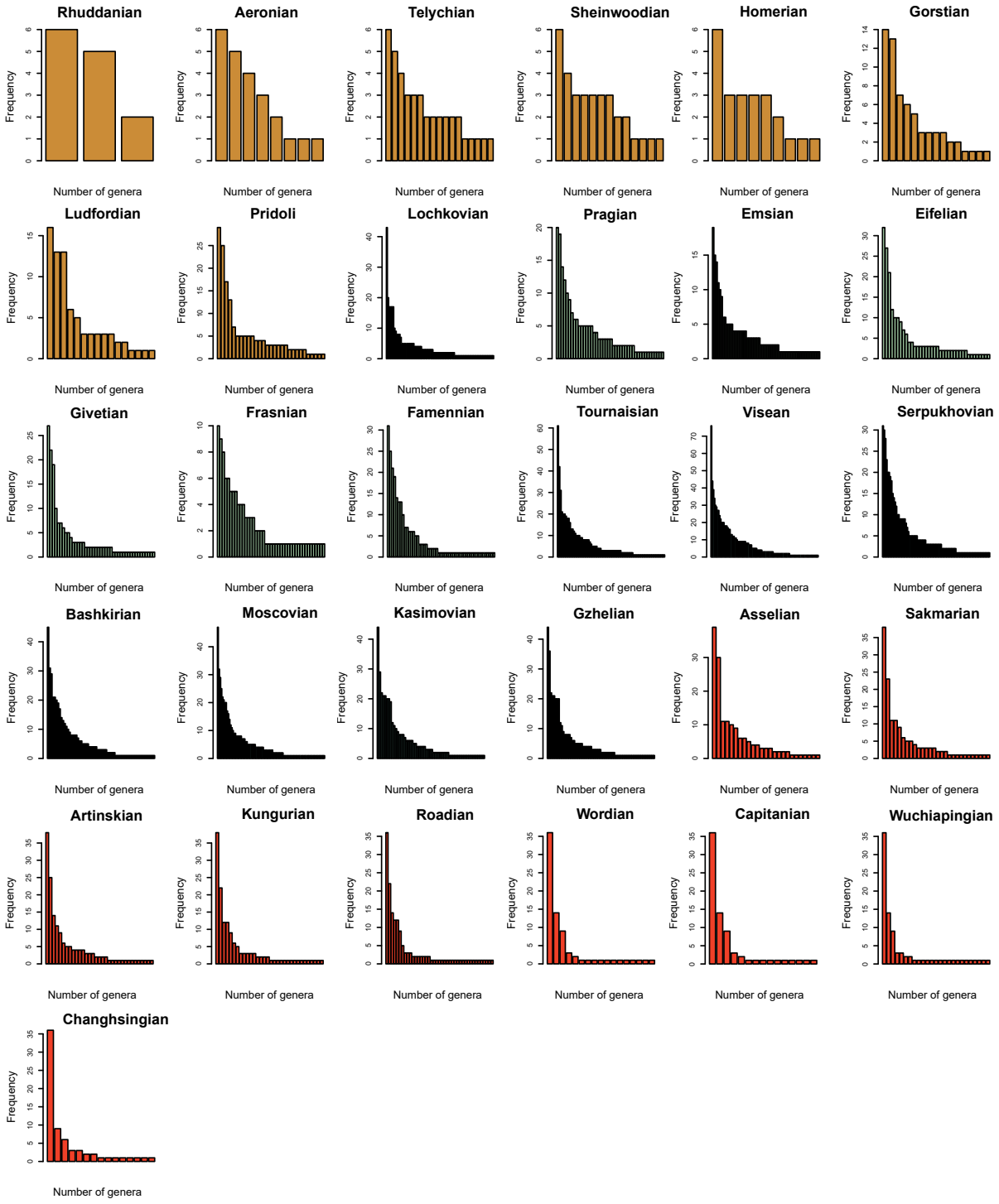


Figure C.1: Relative genus abundance of chondrichthyans for each stage of the Palaeozoic. Silurian in yellow, Devonian in turquoise, Carboniferous in blue and Permian in red.

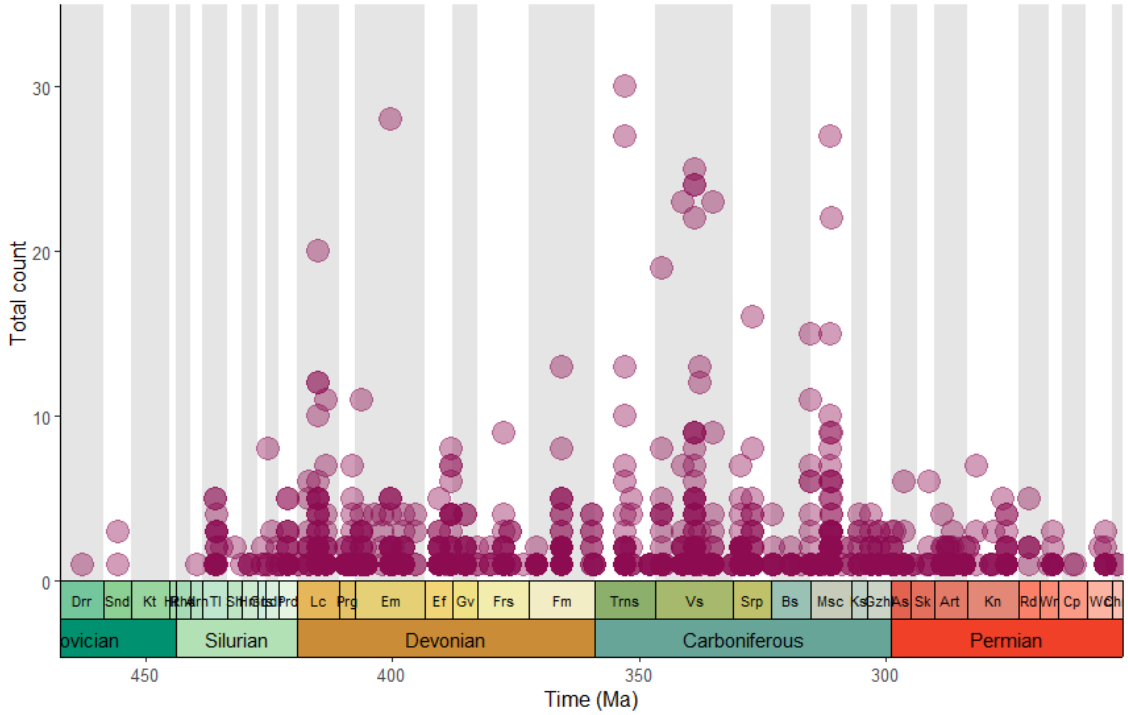


Figure C.2: Chondrichthyan local richness (alpha diversity) in the Palaeozoic after removing the three highest collections (Armagh, Alton, Illinois).

Table C.1: Metrics of diversity dynamics through time for Palaeozoic chondrichthyans.**max**, maximum age. **min**, minimum age. **mid**, midpoint. **tSing**, number of stratigraphic singleton taxa. **tOri**, number of originating taxa. **tExt**, number of taxa getting extinct. **divSIB**, sampled-in-bin diversity. **divRT**, range-through diversity. **ext2f3**, second-for-third extinction rates (based on Alroy 2015). **ori2f3**, second-for-third origination rates (based on Alroy 2015).

stage	max	min	mid	tSing	tOri	tExt	divSIB	divRT	ext2f3	ori2f3
Darriwilian	467.3	458.4	462.85	1	0	NA	1	1	NA	NA
Sandbian	458.4	453	455.7	3	0	0	3	3	NA	NA
Katian	453	445.2	449.1	0	0	0	0	0	NA	NA
Hirnantian	445.2	443.8	444.5	0	0	0	0	0	NA	NA
Rhuddanian	443.8	440.8	442.3	0	3	0	3	3	NA	NA
Aeronian	440.8	438.5	439.65	1	4	0	8	8	0	0.847298
Telychian	438.5	433.4	435.95	8	2	1	17	17	0.154151	0.287682
Sheinwoodian	433.4	430.5	431.95	2	3	4	13	13	0.693147	0.559616
Homerian	430.5	427.4	428.95	0	2	3	9	9	0.847298	0.510826
Gorstian	427.4	425.6	426.5	0	10	0	15	16	0.510826	1.466337
Ludfordian	425.6	423	424.3	1	2	1	16	19	0.080043	0.167054
Pridoli	423	419.2	421.1	5	10	4	28	32	0.367725	0.641854
Lochkovian	419.2	410.8	415	38	25	8	84	86	0.546544	1.131402
Pragian	410.8	407.6	409.2	3	5	8	40	48	0.11441	0
Emsian	407.6	393.3	400.45	14	13	16	60	64	0.693147	0.485508
Eifelian	393.3	387.7	390.5	3	7	11	38	44	0.336472	0.213574
Givetian	387.7	382.7	385.2	9	6	11	42	45	0.538997	0.223144
Frasnian	382.7	372.2	377.45	12	10	8	43	47	0.356675	0.613104
Famennian	372.2	358.9	365.55	13	13	16	50	53	1.056053	0.741937
Tournaisian	358.9	346.7	352.8	8	50	4	81	82	0.271934	1.481605
Visean	346.7	330.9	338.8	27	12	4	105	109	0.077558	0.154151
Serpukhovian	330.9	323.2	327.05	15	4	26	89	97	0.470004	0.045462
Bashkirian	323.2	315.2	319.2	3	16	4	65	75	0.067441	0.333144
Moscovian	315.2	307	311.1	28	4	6	93	100	0.093526	0.019418
Kasimovian	307	303.7	305.35	2	2	1	60	70	-0.01739	0.016529
Gzhelian	303.7	298.9	301.3	6	2	43	70	75	1.645156	0.074108
Asselian	298.9	293.52	296.21	0	9	3	25	35	0.143101	0.526093
Sakmarian	293.52	290.1	291.81	1	4	0	28	37	0	0.117783
Artinskian	290.1	283.5	286.8	1	3	5	33	40	0.167054	0.167054
Kungurian	283.5	272.95	278.225	2	2	17	32	38	0.955511	0.09531
Roadian	272.95	268.8	270.875	3	4	3	22	26	0.287682	0.559616
Wordian	268.8	265.1	266.95	0	2	1	16	22	0	0
Capitanian	265.1	259.1	262.1	0	0	8	15	21	0.628609	-0.11778
Wuchiapingian	259.1	254.14	256.62	0	4	3	17	17	NA	0.693147
Changhsingian	254.14	251.902	253.021	1	NA	14	15	15	NA	NA

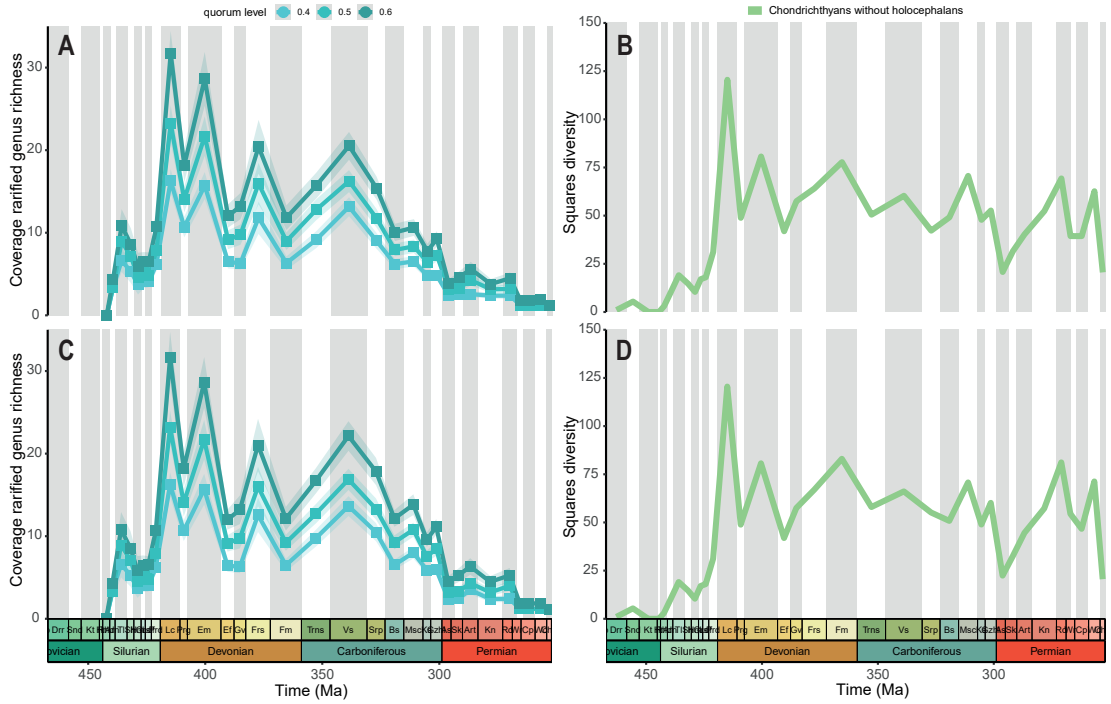


Figure C.3: Chondrichthyan subsampled genus diversity with Holocephali/Euchondrocephali excluded. A and C, coverage-standardised diversity at different quorum levels. B and D, squares diversity. A and B, total group Holocephali as per most recent phylogenies. C and D, Euchondrocephali sensu Ginter *et al.* 2010.